National Research
Council Canada

Conseil national
de recherches Canada

Eleventh Machinery Dynamics Seminar

Onzième séminaire sur la dynamique des machines

Toronto
October 1990

Toronto
Octobre 1990

SIR WILLIAM ALEXANDER
VARMINT DATABASE SYSTEM
File
Default
Quit
Help
Select MACHINE
Selected Machine
Edit MACHINE Data
Reading Schedule
COMPONENTS
Add
Modify
Delete
OK
Cancel

Selected Machine: A S/W P/P INB82

Sold by:

Publication Sales and Distribution
National Research Council Canada
Ottawa, Ontario
Canada K1A 0R6

Price: $40.00

DSS: NR15-44/1990
ISBN: 0-660-55825-4
NRCC: 32002

Vendu par :

Centre et diffusion des publications
Conseil national de recherches Canada
Ottawa (Ontario)
Canada K1A 0R6

Prix : 40,00$

MAS: NR15-44/1990
ISBN: 0-660-55825-4
CNRC : 32002

Proceedings	Compte rendu
Eleventh Machinery Dynamics Seminar	**Onzième séminaire sur la dynamique des machines**

The Westbury Hotel	L'Hôtel Westbury
Toronto, Ontario	Toronto (Ontario)
October 1-2, 1990	les 1 et 2 octobre 1990

Sponsored by:	Sous l'égide du:
National Research Council Canada	Conseil national de recherches Canada
Associate Committee on Propulsion	Comité associé de la propulsion
Machinery Dynamics Subcommittee	Sous-comité de la dynamique des machines

91-01514/

TABLE OF CONTENTS/TABLE DES MATIÈRES

PAGE

INTRODUCTION / AVANT-PROPOS by Robert J. Rogers

SESSION/SÉANCE 1

ROTORDYNAMICS MODELLING /MODÉLISATION DE LA DYNAMIQUE DES ROTORS

Co-Chairmen/Co-présidents: Donald L. Allen, Vibron Ltd.
William L. Cleghorn, University of Toronto

Comments On Modal Analysis of Rotors
Jorgen W. Lund, Technical University of Denmark, Lyngby, Denmark 3

Component Mode Synthesis Reduction Technique for Rotor-Bearing- Pedestal System
Tom S. Sankar and **Aliakbar Amini**, Concordia University, Montreal, Quebec 14

The Effect of Couplings and Bearings on the Critical Speeds of Machine Trains
Ronald L. Eshleman, Vibration Institute, Willowbrook, IL, USA 40

The Use of Finite Elements in Rotordynamics Analysis
William F. Eckert and **Anthony Craggs**, University of Alberta, Edmonton, Alberta 48

Simplified Prediction of Balance Sensitivity
Brian C. Howes, Scott G. Masterson, Beta Machinery Analysis Ltd., Calgary, Alberta 56

A Review of Fluid Effect Modelling in Rotor Dynamics
Anthony G. Taylor and **Anthony Craggs**, University of Alberta, Edmonton, Alberta 64

PAGE

SESSION/SÉANCE 2

MACHINERY HEALTH MONITORING/SURVEILLANCE DE L'ÉTAT DES MACHINES

Co-Chairmen/Co-présidents: Ronald J. Anderson, Queen's University
Dino Rubli, Stelco Technical Services Ltd.

Aspects of Optimal Preventive Replacement Strategies
Andrew K.S. Jardine, University of Toronto, Ontario 99

Vibration Signature Analysis Fundamentals for Machine Condition Monitoring
Ted Loewen and Frank Perricone, Ontario Hydro, Toronto, Ontario 110

Predictive Maintenance Today: The Information Management Challenge
Richard C. Hancock, Computational Systems Inc., Knoxville, TN, USA 133

The Industrial Alignment Project: New Approaches to Machinery Alignment
D.A. Bayly, H.E. Martell, K.P. Schwarz, W.F. Teskey, M.A. Chapman, J. Czompo, University of Calgary, Alberta; **S.J. Mugford, J.R. Gibbs**, Kadon Electro Mechanical Services Ltd., Calgary, Alberta 150

A Cost Effective Rotating Machinery Information Acquisition and Analysis System
Steven J. Sabin, Bently Nevada Canada Ltd., Nisku, Alberta 176

Continuous Monitoring for Automated Predictive Maintenance
Craig Cantrell, Computational Systems Inc., Knoxville, TN, USA 190

PAGE

SESSION/SÉANCE 3

MACHINERY FAULT DIAGNOSIS AND EXPERT SYSTEMS/ DIAGNOSTIC DES DÉFECTUOSITÉS DES MACHINES ET SYSTÈMES EXPERTS

Co-Chairmen/Co-présidents: Hugh R. Martin, University of Waterloo
W.H. El Maraghy, University of Western Ontario

Development in Expert Systems with Application to Dynamic Problems in Rotating Machinery
Rainer Nordmann and M. Keim, University of Kaiserslautern, West Germany 201

VARMINT an Expert System for Machine Monitoring
Robert S. Reilly, Christopher A. MacPhail, Design Maintenance Systems Inc.,
North Vancouver, British Columbia 223

Field Experience in Vibrational Behaviour of 2 Stage, Centrifugal Pumps
M.M. Osman and B. Alavi, Ontario Hydro, Toronto, Ontario 247

Update on Machinery Vibration Standards
A. Stewart Maxwell, Ontario Hydro, Toronto, Ontario 265

Vibration Troubleshooting of Two Helicopter Main Gearboxes
François Dubé, National Research Council Canada, Ottawa, Ontario 278

Condition Monitoring of Boring Tools
Zygmunt Reif, Mark Mailloux, Steve Prsa, University of Windsor, Ontario 291

AVANT-PROPOS

Au nom du Sous-comité de la dynamique des machines, je vous souhaite la bienvenue au onzième séminaire du CNRC sur la dynamique des machines. Il y a vingt ans déjà, le Conseil national de recherches du Canada, par l'entremise de son Comité associé de la propulsion, organisait le premier de ces séminaires bisannuels qui sont devenus les plus grands rassemblements réguliers de spécialistes de la vibration au Canada. Le but des différentes communications techniques et des expositions d'instruments et de logiciels est d'encourager les échanges de renseignements et d'expertises en matière de dynamique des rotors de surveillance de l'état des machines et de diagnostic des défectuosités.

Les dix-huit communications qui vous seront présentées ont été regroupées en trois séances selon leurs domaines particuliers. Les principaux conférenciers invités de ces trois séances seront nos éminents collègues J.W. Lund, A.K.S. Jardine et R. Nordmann, que nous tenons à remercier de leur participation. Leurs communications sont le fruit de longues recherches et ils s'avéreront une source de renseignements inestimable pour toute personne s'intéressant à la vibration des machines.

Au cours de la quatrième séance, qui se tiendra dans l'après-midi du 2 octobre, vous êtes invités à présenter de brefs communications (cinq minutes) sur l'état de vos travaux, de nous faire part de vos buts et de vos aspirations en matière de recherche et de nous donner vos commentaires sur le soutien administratif que l'on vous accorde. Ces discussions aideront à stimuler les efforts conjoints entre chercheurs et industriels et à orienter les activités de notre Sous-comité. Au cours des dernières années, nous avons effectué des sondages auprès des universités, collèges et industries canadiennes afin d'identifier les activités et les besoins de ces groupes en matière de dynamique des machines. Nous sommes aussi très actifs dans l'élaboration de normes sur les vibrations en collaboration avec l'Organisation internationale de normalisation (ISO).

En terminant, nous sommes heureux de vous accueillir à Toronto et au Westbury Hotel. Les préposés au comptoir d'inscription ainsi que les membres du Sous-comité se feront un plaisir de répondre à toutes vos questions. Nous espérons que l'ambiance détendue du séminaire vous plaira et vous incitera à discuter ouvertement de problèmes de vibration avec vos collègues. Nous vous invitons à nous faire part de vos commentaires et suggestions en rapport avec le présent séminaire dans l'espoir que vous continuerez de vous intéresser à nos futurs séminaires.

Robert R. Rogers
Président
Sous-comité de la dynamique des machines

Juillet 1990

INTRODUCTION

On behalf of the Machinery Dynamics Subcommittee, I welcome you to the Eleventh Machinery Dynamics Seminar. It has been 20 years since the first of these biennial seminars was initiated by the National Research Council Canada through its Associate Committee on Propulsion. The seminars are the largest regular gatherings of vibration specialists from across Canada. The aim of the technical presentations and the exhibits of instrumentation and software is to encourage the exchange of information and experience in the areas of machinery rotor dynamics, condition monitoring and fault diagnosis.

The eighteen contributed papers to the seminar are grouped into three sessions in these areas. The invited lead speakers for the sessions, J.W. Lund, A.K.S. Jardine and R. Nordmann, are distinguished experts whose contributions are greatly appreciated. The technical papers are well-prepared and should be a useful source of information to the machinery vibration community.

Participants at the seminar are encouraged to make brief (five minute) presentations of "work in progress" or comments on their needs for research, standards or management support during the fourth session in the afternoon of October 2. This discussion may encourage joint efforts between researchers and industry and will help guide the activities of the Machinery Dynamics Subcommittee. In recent years the Subcommittee has carried out surveys of Canadian universities, colleges and industry in order to identify the activities and needs of these groups in areas related to machinery dynamics. The Subcommittee is also active in the development of vibration standards through the International Standards Organization (ISO).

Finally, I would like to welcome you to Toronto and to The Westbury Hotel. The staff at the seminar registration desk, as well as the Subcommittee members, are available to answer any questions or concerns. We hope that you will take advantage of the informal nature of the seminar to discuss vibration issues with your colleagues. We look forward to any comments or suggestions about the seminar and to your continued interest in future seminars.

Robert J. Rogers
Chairman
Machinery Dynamics Subcommittee

July 1990

SESSION / SÉANCE 1

Rotordynamics Modelling/ Modélisation de la dynamique des rotors

LEAD PRESENTATION / PRÉSENTATION INAUGURALE

Comments On Modal Analysis of Rotors

by Jorgen W. Lund

COMMENTS ON MODAL ANALYSIS OF ROTORS

Jorgen W. Lund
Department of Machine Elements
Technical University of Denmark
2800 Lyngby, Denmark

ABSTRACT

On basis of calculations and experiments, the identification of the modes of a rotor, supported in fluid film bearings, is discussed. Some examples are given together with a more general discussion of the application of modal analysis for rotor systems.

BIOGRAPHICAL SKETCH

Jorgen W. Lund was employed for 11 years in the U.S. by General Electric, Boeing, and Mechanical Technology, Inc. In 1967 he returned to his native country to join the Technical University of Denmark where he now is a professor. His work has been in lubrication and bearing analysis, as well as in rotor dynamics. His best known contributions to the technical literature concern dynamic coefficients of bearings, damped natural frequencies and modes of rotor systems, rotor instability, and non-linear effects in bearings.

RÉSUMÉ

A partir de calculs et d'expériences, le professeur Lund examine l'identification des modes d'un rotor supporté par des paliers lisses à film fluide. Il en donne quelques exemples et poursuit en examinant de façon plus générale l'application de l'analyse modale pour les systèmes de rotors.

BIOGRAPHIE

Jorgen W. Lund a travaillé aux États-Unis pour la General Electric, Boeing et la Mechanical Technology Inc. pendant 11 ans. En 1967, il retournait dans son pays pour se joindre à l'Université technique du Danemark où il enseigne actuellement. Ses travaux portent sur la lubrification et l'analyse des roulements ainsi que sur la dynamique des rotors. Ses contributions les mieux connues ont trait aux coefficients dynamiques des roulements, à l'amortissement des fréquences et des modes naturels des rotors, à l'instabilité des rotors et aux effets non-linéaires présents dans les roulements.

COMMENTS ON MODAL ANALYSIS OF ROTORS

by

Jorgen W. Lund
Department of Machine Elements
The Technical University of Denmark
2800 Lyngby, Denmark

INTRODUCTION

For most practical purposes a rotor-bearing system behaves as a linear system. Thus, it can be represented by its modal parameters, i.e. the complex eigenvalues (damped natural frequencies) with associated eigenvectors (modeshapes). The present discussion is a review of the special properties of the modes and illustrates the advantages of a modal representation in many types of dynamical analysis.

SYSTEM EQUATIONS

When the rotor system is represented as a lumped parameter system the equations of motion may be written in matrix form as:

$$\underline{\underline{M}}\,\ddot{\underline{X}} + \Omega\underline{\underline{J}}\,\dot{\underline{X}} + \underline{\underline{K}}\,\underline{X} = \underline{F} - \underline{R} \qquad (1)$$

$\underline{X}$ is the displacement column vector (each lumped mass has four degrees-of-freedom: two lateral displacements and two angular displacements), $\underline{\underline{M}}$ is the symmetrical inertia matrix, $\underline{\underline{J}}$ is the skew-symmetric matrix of polar mass moments of inertia, Ω is the angular speed of rotation, $\underline{\underline{K}}$ is the symmetric stiffness matrix of the shaft, $\underline{F}$ is the vector of external excitations, and $\underline{R}$ is the vector of passive reaction forces in bearings, seals, aerodynamic interactions, etc.

The reaction forces incorporate the dynamic characteristics of the bearing pedestals, the foundation and/or the casing. In general, therefore, the reaction forces derive from a dynamic model similar to the one for the rotor.

In the absence of external excitation ($\underline{F}=\underline{0}$) the solution to the homogeneous equations is of the form:

$$\underline{X} = \underline{V}_n e^{s_n t} \qquad (2)$$

where s_n is the complex eigenvalue:

$$s_n = \lambda_n + i\omega_n \qquad (3)$$

By substituting this solution into eq.(1), the eigenvalue problem becomes:

$$(s_n^2\underline{\underline{M}} + s_n\Omega\underline{\underline{J}} + \underline{\underline{K}} + \underline{\underline{Z}}_n)\,\underline{V}_n = \underline{0} \tag{4}$$

$\underline{\underline{Z}}_n$ is the impedance matrix deriving from the reaction forces:

$$\underline{\underline{Z}}_n = \underline{\underline{Z}}(s_n) \tag{5}$$

Because of the asymmetric characteristics of bearings, seals and other interactions, $\underline{\underline{Z}}$ is not symmetric and it becomes necessary to introduce an adjoint eigenvector, $\underline{\underline{U}}_n$ ("left eigenvector"):

$$\underline{U}_n^T(s_n^2\underline{\underline{M}} + s_n\Omega\underline{\underline{J}} + \underline{\underline{K}} + \underline{\underline{Z}}_n) = \underline{0}^T \tag{6}$$

(superscript T means "transposed").

It should be noted that usually the eigenvalue problem is formulated differently by rearranging eq.(1) into a first order equation. Thereby the eigenvalue equation also becomes of first order, depending, however, on the composition of $\underline{\underline{Z}}$. For the present discussion this is of little import.

From eqs.(4) and (6) the following orthogonality relationships can be derived:

$$\underline{U}_m^T[(s_n+s_m)\underline{\underline{M}} + \Omega\underline{\underline{J}} + \frac{1}{s_n-s_m}(\underline{\underline{Z}}_n-\underline{\underline{Z}}_m)]\underline{V}_n = 0$$

$\underline{n \neq m}$ (7)

$$\underline{U}_m^T[\underline{\underline{K}}-s_n s_m\underline{\underline{M}} + \frac{1}{s_n-s_m}(s_n\underline{\underline{Z}}_m-s_m\underline{\underline{Z}}_n)]\underline{V}_n = 0$$

When, n=m, the equations define the modal norm N_n:

$$\underline{U}_n^T[2s_n\underline{\underline{M}} + \Omega\underline{\underline{J}} + (\frac{d}{ds}\underline{\underline{Z}}_n)]\underline{V}_n = N_n$$

$\underline{n = m}$ (8)

$$\underline{U}_n^T[\underline{\underline{K}} - s_n^2\underline{\underline{M}} + \underline{\underline{Z}}_n - s_n(\frac{d}{ds}\underline{\underline{Z}})_n]\underline{V}_n = -s_n N_n$$

By introducing modal coordinates q_n, the response can be expressed in a modal expansion:

$$\underline{X} = \sum_n \underline{V}_n q_n \qquad \dot{\underline{X}} = \sum_n s_n \underline{V}_n q_n = \sum_n \underline{V}_n \dot{q}_n \tag{9}$$

By substitution into eq.(1) and making use of eqs.(7) and (8), the governing equation for q_n becomes:

$$\dot{q}_n - s_n q_n = \frac{1}{N_n}\underline{U}_n^T\underline{F} \tag{10}$$

By differentiating the equation, and from the result subtracting the original equation multiplied by $\bar{s}_n$ (complex conjugate), the following equation is obtained:

$$\ddot{q}_n - 2\lambda_n\dot{q}_n + \omega_{on}^2 q_n = \frac{1}{N_n}\underline{U}_n^T(\dot{\underline{F}} - \bar{s}_n\underline{F}) \tag{11}$$

where:

$$\omega_{on} = |s_n| = \sqrt{\omega_n^2 + \lambda_n^2} \tag{12}$$

When s_n is a complex eigenvalue, then the complex conjugate $\bar{s}_n$ is also an eigenvalue whose associated eigenvectors are the complex conjugate of their counterparts for $s=s_n$. With the convention that a complex eigenvalue and its complex conjugate are only counted as one root, eq.(19) may be written as:

$$\underline{X} = \sum_n 2\mathrm{Re}\{\underline{V}_n q_n\}_{\omega_n \neq 0} + (\underline{V}_n q_n)_{\omega_n = 0} \tag{13}$$

where "Re{ }" means the real part.

THE TRANSFER FUNCTION MATRIX

A transformation of the response into the frequency domain via the Fourier transform yields:

$$\underline{X} = \underline{\underline{H}}\,\underline{F} \tag{14}$$

where $\underline{\underline{H}} = \underline{\underline{H}}(\omega)$ is the transfer function matrix. By solving eq.(11) and substituting into eq.(13), $\underline{\underline{H}}$ is found as:

$$\underline{\underline{H}} = \sum_n\left[\frac{2}{\omega_{on}^2 - \omega^2 - i2\omega\lambda_n}\left(\underline{\underline{A}}_n(i\omega - \lambda_n) - \underline{\underline{B}}_n\omega_n\right)\right]_{\omega_n \neq 0} + \left[\frac{1}{i\omega - \lambda}\underline{\underline{A}}_n\right]_{\omega_n = 0} \tag{15}$$

where:

$$\underline{\underline{A}}_n + i\underline{\underline{B}}_n = \frac{1}{N_n}\underline{V}_n\underline{U}_n^T \tag{16}$$

It is difficult to give any rules for the convergence of the series. Examples are shown in Figures 1 and 2 for a rotor with the following calculated eigenvalues at 7000 rpm:

frequency, $\frac{\omega_n}{2\pi}$, Hz	λ_n,sec^{-1}	log.decrement $\delta_n = -\frac{2\pi\lambda_n}{\omega_n}$
0	- 1282.9	
0	- 1500.8	
60.02	- 13.60	0.227
92.22	- 54.65	0.593
99.27	- 23.96	0.241
177.61	- 78.41	0.441
228.96	- 176.9	0.773
400.01	- 155.3	0.388
414.70	- 512.5	1.236

In the figures, the result obtained from a forced response calculation is compared with results from the series summation: one which uses the first four complex eigenvalues (60 to 177.6 Hz), and one which uses the first six eigenvalues (including the two critically damped roots). The forced response is marked by circles, the four mode summation by squares, and the six mode summation by triangles.

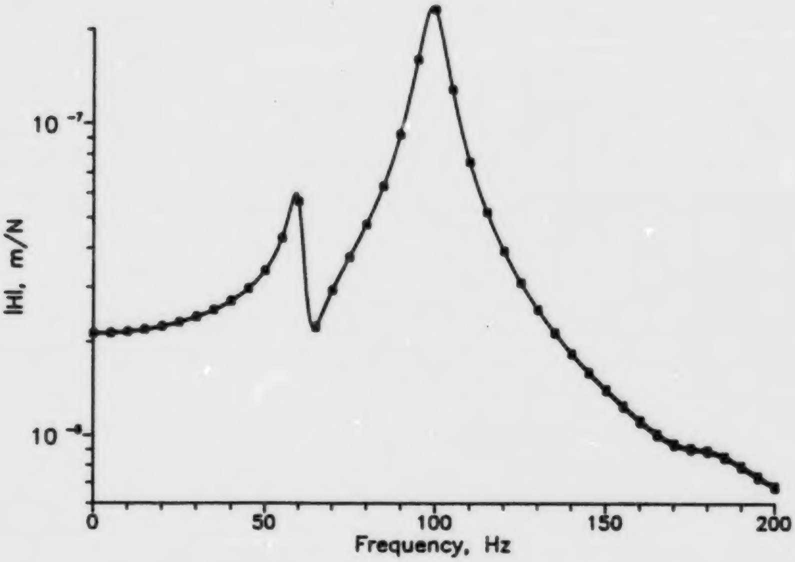

Figure 1

Fig.1 shows the transfer function between a force station and a different lateral amplitude station away from the bearings. The agreement is very close. In Fig.2 the two stations coincide and are close to a bearing. It is of particular interest that to achieve good convergence it is necessary to include the two critically damped modes.

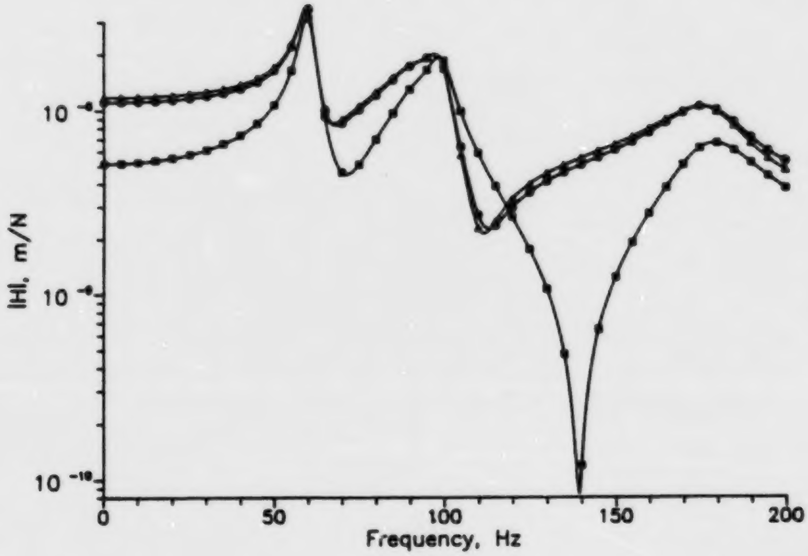

Figure 2

The results of adding the modes up to 414.7 Hz are not shown as they make little difference. This is somewhat surprising because experience from classical modal analysis seems to indicate that it is necessary to include all frequencies up to twice the desired frequency range for H. It may well be that the examples shown are not typical.

The transfer function may be measured experimentally by impacting the rotor. There are practical problems of disturbances from the synchronous frequency and its higher harmonics, and of supplying enough impact energy. Even so, results have been obtained (ref.2) of a sufficient quality to establish influence coefficients with which a rotor could be balanced succesfully. It is not clear, though, whether the experimental results, considering measurement tolerances and noise, can be curve fitted with enough accuracy to allow extraction of the eigenvalues and modeshapes with reliability.

RESPONSE TO GROUND EXCITATION

If the rotor system receives an acceleration g_x in the negative x-direction, it is equivalent to an imposed acceleration loading in the positive x-direction when it is understood that the rotor amplitudes are measured relative to the moving foundation. In the simple case where g_x is uniform along the rotor, eq.(14) can be written as:

$$\underline{X} = \underline{H}_g(\omega)\cdot g_x \qquad (17)$$

where:

$$\underline{H}_g(\omega) = \underline{\underline{H}}(\omega)\underline{\underline{M}}\cdot\underline{G} \qquad (18)$$

The vector $\underline{G}$ has a "1" for the x-amplitude at each station while all the other coordinates are zero.

If g_x is a random excitation with spectral density S_g, the resulting spectral density for the amplitude, $\underline{S}_x$, is given by:

$$\underline{S}_x = |\underline{H}_g(\omega)|^2 S_g \tag{19}$$

The mean square value of the amplitude is computed as:

$$\langle|\underline{X}|^2\rangle = \frac{1}{2\pi}\int_0^\infty \underline{S}_x d\omega = \frac{1}{2\pi}\int_0^\infty |\underline{H}_g(\omega)|^2 S_g d\omega \tag{20}$$

For white noise excitation, S_g is independent of ω such that:

$$\langle|\underline{X}|^2\rangle = \frac{1}{4\pi} S_g \int_{-\infty}^{\infty} \underline{H}_g(\omega)\cdot\bar{\underline{H}}_g(\omega) d\omega \tag{21}$$

The integral may conveniently be evaluated from the residue theorem. For a stable system where all λ_n-values are negative, only the roots from $\underline{H}(\omega)$ lie in the upper half of the ω-plane and contribute to the residues. Hence:

$$\begin{aligned}\langle|\underline{X}|^2\rangle = -S_g\sum_n \mathrm{Re}\{(\underline{A}_n^*+i\underline{B}_n^*)_{\omega_n\neq 0}\cdot\sum_m \frac{1}{(s_n+s_m)(s_n+\bar{s}_m)}[\underline{A}_m^*(s_n+\lambda_m)+\underline{B}_m^*\omega_m]_{\omega_m\neq 0} \\ + \frac{1}{2}\left[\frac{\underline{A}_m^*}{s_n+\lambda_m}\right]_{\omega_m=0}\} + \frac{1}{2}(\underline{A}_n^*)_{\omega_n=0}\cdot\sum_m \frac{1}{(\lambda_n+s_m)(\lambda_n+\bar{s}_m)}[\underline{A}_m^*(\lambda_n+\lambda_m)+\underline{B}_m^*\omega_m]_{\omega_m\neq 0} \\ + \frac{1}{2}\left[\frac{\underline{A}_m^*}{\lambda_n+\lambda_m}\right]_{\omega_m=0}\end{aligned} \tag{22}$$

where:

$$\underline{A}_n^* = \underline{\underline{A}}_n\underline{\underline{M}}\underline{G} \qquad \underline{B}_n^* = \underline{\underline{B}}_n\underline{\underline{M}}\underline{G}$$

$\langle|\underline{X}|^2\rangle$ defines the variance of $\underline{X}$. The square root of the variance, the root-mean-square value, gives the standard deviation. If the probability distribution for g_x is Gaussian, this will also be true for the distribution of $\underline{X}$ which, then, is completely defined.

As an example, Fig.3 shows the square root at the spectral density distribution for the amplitude at three locations of a compressor rotor, running at 5000 rpm. . It is excited by a random vertical acceleration with a root-mean-square value of 9.81 m/sec^2 and a uniform spectral density from 0 to 1000 Hz.

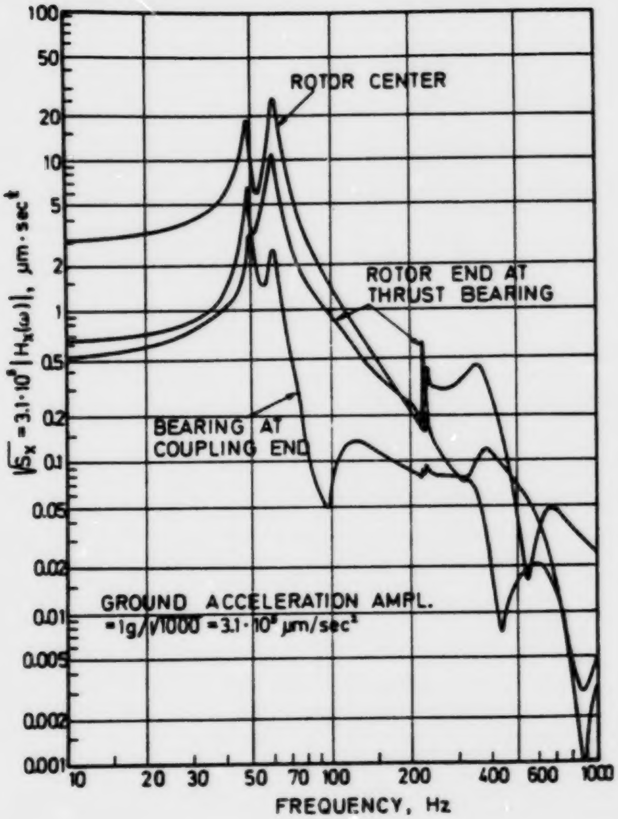

Figure 3

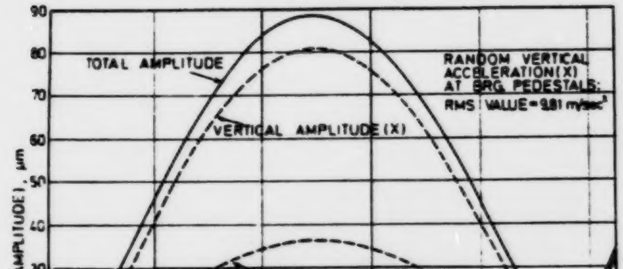

Figure 4

A direct integration of $\underline{S}_x$ over the specified frequency range according to eq.(20) yields the variance of the rotor amplitude. The square root of the variance, the rms-value, is shown for the entire rotor in Fig.4. It defines the standard deviation for the distribution of the amplitude and, by assuming the random process to be Gaussian, the probability that the amplitude exceeds this value is 31.7 per cent. Smilarly, the probabilities for exceeding twice or three times the rms-value are 4.5 per cent and 0.26 per cent, respectively.

Rather than integrating $\underline{S}_x$ directly to obtain Fig.4, eq.(22) can be employed instead. With the rotor operating at 5000 rpm there are 16 eigenvalues below 1000 Hz, namely 12 complex eigenvalues and four real roots. The result is in close agreement with the direct integration.

RESPONSE TO RANDOM MASS UNBALANCE

Probably the most common source of rotor excitation is mass unbalance where the local mass center is offset from the axis of rotation by an eccentricity, e. If e has the components e_c and e_s along orthogonal directions, fixed in the rotating shaft, the unbalance forces from a mass m become:

$$\begin{aligned} f_x &= \Omega^2 m(e_c\cos(\Omega t)-e_s\sin(\Omega t)) \\ f_y &= \Omega^2 m(e_c\sin(\Omega t)+e_s\cos(\Omega t)) \end{aligned} \qquad (23)$$

or in complex notation:

$$f_x = \Omega^2 me \qquad f_y = -i\Omega^2 me \qquad e = e_c+ie_s \qquad (24)$$

The resulting amplitude response is:

$$\underline{X} = \Omega^2\underline{H}_e \qquad (25)$$

where:

$$\underline{H}_e = \underline{\underline{H}}(\Omega)\underline{\underline{M}}\cdot\underline{E} \qquad (26)$$

$\underline{E}$ is the complex vector of mass eccentricities.

If the eccentricities are statistically determined with the same probability distribution, zero mean value, and common variance $<|e|^2>$, but otherwise uncorrelated, the corresponding variance of the amplitude becomes:

$$<|\underline{X}|^2> = \Omega^4|\underline{H}_e^*|^2<|e|^2> \qquad (27)$$

$\underline{H}_e^*$ is obtained from eq.(26) with $\underline{E}$ replaced by a vector which has a "1" at each unbalance location. In terms of root-mean-square values:

$$\frac{1}{\text{rms}(|e|)}\cdot\text{rms}(|\underline{X}|) = \Omega^2|\underline{H}_e^*| \qquad (28)$$

If the probability distribution is Gaussian, the rms-value gives the standard deviation.

An example is shown in Fig.5 for a compressor rotor. The unabalance is confined to the components mounted on the shaft, namely 8 impellers located between the bearings, the coupling outboard one bearing, and the thrust collar outboard the other bearing. These ten components account for 54 per cent of the total rotor mass.

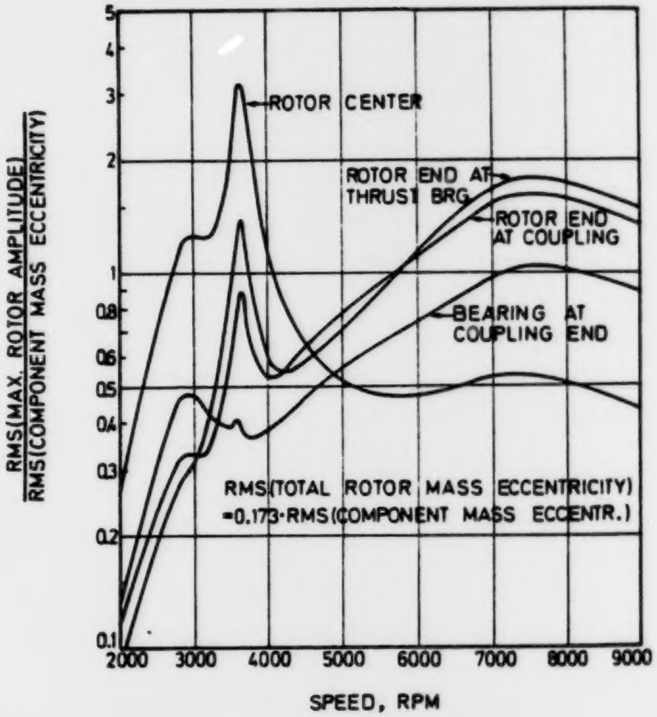

Figure 5

Strictly speaking the result shows the standard deviation for the unbalance response of a large number of rotors of identical design, manufactured and balanced to the same tolerances. In some loose sense of terminology it can be said to represent the maximum expected response of any particular rotor at a confidence level of 68 per cent. On the other hand, it provides a systematic method of depicting a rotor's sensitivity to unbalance. Three critical speeds are clearly showing up: the 1st, with forward whirl, at 2750 rpm (δ=0.86); the 1st, with backward whirl, at 3637 rpm (δ=0,21); and the 3rd, with forward whirl, at 6840 rpm (δ=1.12). (the second critical speed at 4180 rpm is heavily damped with δ=2.27). Furthermore, the resonance peaks seem evenly weighted which otherwise presents a problem in a general response analysis because an unbalance distribution can not be resolved into modal components as is possible in a "classical" system.

DISCUSSION AND CONCLUSION

Other examples of the application of modal analysis can be given. An obvious case is that of a transient response calculation where, by introducing modal coordinates, the many degrees-of-freedom become decoupled, and the troublesome higher frequencies can be eliminated by a suitable truncation. This is especially important when a numerical time stop integration is required as, for example, when $\underset{\sim}{F}$ contains non-linearities.

Because of the gyroscopic moments and the speed dependency of the various dynamic coefficients in bearings, seals, etc., the eigenvalues and the modes will change with the rotational speed. At any particular speed, the lowest natural frequency may differ markedly from that which is otherwise recognized as "the first critical speed".

If a rotor is prone to instability it will, with rare exceptions, be the lowest mode with forward whirl which exhibits self-excitation. For that mode it may be illuminating to perform an energy dissipation calculation to identify the sources of negative damping as a guide in devising corrective measures.

As part of a machinery vibration monitoring program it is common practice to obtain the frequency spectrum of the measured response, and a time sequence produces the well-known waterfall diagram which has proven a valuable tool in supervising the performance, or in a diagnosis. It is usually found that there are enough sources of disturbance to excite many of the damped natural frequencies, but in addition a number of "spurious" frequencies will invariably show up, originating from unforeseen resonances somewhere in the supporting structure, or from nearby auxiliary machinery. Thus, to interprete the measured results a preknowledge of the damped natural frequencies of the rotor by itself is very useful for identification purposes.

Today the calculation of a rotors eigenvalues and modes is readily performed, even on a PC. In view of the important insight such information provides, this type of calculation ought to replace the conventional critical speed calculation.

REFERENCES

1. J.W.Lund, "Response Characteristics of a Rotor with Flexible, Damped Supports". IUTAM Symposium "Dynamics of Rotors", Lyngby, Denmark, 1974. Springer-Verlag 1975.

2. J.Tonnesen and J.W.Lund, "Impact Excitation Tests to Determine the Influence Coefficients for Balancing Lightly Damped Rotors". Jrnl. of Engineering for Power, Trans. ASME, October 1988, pp.600-604.

COMPONENT MODE SYNTHESIS REDUCTION TECHNIQUE FOR ROTOR-BEARING-PEDESTAL SYSTEM

RÉSUMÉ

Puisque de nombreux modèles éléments finis comportent tellement de degrés de liberté qu'il est impossible de les traiter à l'aide des plus gros des ordinateurs modernes, il faut élaborer des méthodes pour l'analyse des sous-structures dans les modèles aux éléments finis; une telle analyse en est venue à prendre le nom de "Reduction Modale". Un programme machine numérique appelé SETSA a été mis au point à partir de la technique de réduction susmentionnée pour estimer rapidement les fréquences critiques du système. Le programme SETSA peut traiter n'importe quel nombre de paliers ainsi que leurs flexibilités. Il peut déterminer les fréquences naturelles du système de même que les réactions à toute excitation donnée, dans des conditions de support avec ou sans amortissement.

BIOGRAPHIE

Dr. T.S. Sankar occupe, depuis 1968, le poste de Professeur Titulaire au Département de Génie Mécanique de l'Université Concordia. Il en été le directeur durant les années 1976 à 1987. Dr. Sankar est reconnu internationalement pour sa recherche sur les systèmes mécaniques mettant une emphase particulière sur la dynamique, la fiabilité, les vibrations, la robotique, et les matériaux composés. Il reçoit de la part des deux gouvernements, provincial et fédéral, des subventions majeures à la recherche et a obtenu de nombreux contrats industriels de recherche. Il a dirigé sous sa tutelle 26 candidats à la maîtrise et 10 candidats de doctorat. Il a écrit plus de 250 articles scientifiques qui ont paru dans des journaux avec comités d'évaluation ou qui ont été présentés aux principales conférences dans le domaine. Présentement Vice Président Senior de la Société Canadienne de l'Ingénierie Mécanique, il tient des postes dans l'exécutif de plusieurs sociétés incluant les comités techniques de l'A.S.M.E. et les commission de la Fédération Internationale pour la Théorie des Machines et Mécanismes. Il a été Directeur de Sous-comité de Dynamique des Machines de 1984 à 1987.

M. Aliakbar Amini a obtenu sa maîtrise en génie mécanique, avec spécialisation en dynamique des rotors, de l'Université Concordia en mars 1990. Il possède également un baccalauréat en génie mécanique de l'Université Concordia. Ses domaines de recherche englobent la dynamique dans les systèmes mécaniques, l'analyse des contraintes et les applications à éléments finis.

COMPONENT MODE SYNTHESIS REDUCTION TECHNIQUE FOR ROTOR-BEARING -PEDESTAL SYSTEM

A. Amini and T.S. Sankar
Department of Mechanical Engineering
Concordia University
Montreal, P.Q., Canada

BIOGRAPHY

Dr. T.S. Sankar is a full Professor in the Department of Mechanical Engineering at Concordia University and was the Chairman of the Department during 1976-1987. Dr. Sankar is internationally recognized for his research in the area of mechanical systems with special emphasis on dynamics, reliability, vibrations, robotics, and composite materials. He holds major research grants from the Governments of Canada and Quebec, as well as numerous industrial grants and contracts. He has supervised 26 M.Eng. and 10 Ph.D. theses and has authored over 250 scientific papers in referred journals and major conferences. Presently the Senior Vice President of the Canadian Society of Mechanical Engineering, he holds executive positions in many learned societies including the ASME technical committees and the commissions of the International Federation for the Theory of Machines and Mechanisms. He was the past Chairman of the Machinery Dynamics Sub-committee during 1984 to 1987.

Mr. Aliakbar Amini completed his M.Eng. in Mechanical Engineering specializing in rotor dynamics at Concordia University in March 1990. He also obtained his B.Eng. in Mechanical Engineering at Concordia. His research interests include dynamics for mechanical systems, stress analysis and finite element applications.

Component Mode Synthesis Reduction Technique
For
Rotor-Bearing-Pedestal System

A. Amini, Graduate Assistant

T.S. Sankar, Professor

Department of Mechanical Engineering, Concordia University
Montreal, Quebec

ABSTRACT

Since many finite element models contain so many degrees of freedom that they cannot be directly handled on the largest of modern computers. It is, therefore, desirable to develop methods for analyzing substructures of a finite element model and one such analysis has come to be known as component mode synthesis (CMS). A digital Computer program **SETSA** was developed based on aforementioned reduction technique for quick estimation of critical frequencies of the system. Program **SETSA** can handle any number of bearings and their flexibilities. It can yield natural frequencies of the system as well as responses against any prescribed excitation for both damped and undamped support conditions.

1. INTRODUCTION

Due to the increasing demand for improved performance of high speed rotating machinery in various fields such as those used in process equipment, auxiliary power machinery, helicopter technology and nuclear applications, the engineer is faced with the problem of designing a unit capable of smooth operation under various conditions of speed and load. In many of these applications of rotor-bearing systems, achieving an acceptable performance with stable, low level amplitude of vibration is extremely difficult.

Finite element techniques are convenient and widely used to model complex rotor-bearing systems consisting of several disks, impellers or mechanical couplings. The finite element method may need a large number of degrees of freedom and require the solution of a large order set of linear equations. In addition to this, the solution of these equations may require the use of time consuming algorithms which may not be economically feasible. With component mode synthesis reduction method the size of the finite element matrices can be reduce considerably without affecting the dynamic characteristics of the system results.

Component mode synthesis has been extensively developed over the past 25 years. The trend in structural analysis towards the modeling of structural systems by component mode synthesis or substructure coupling started by considering the dynamic analysis of lightly damped system with symmetric property matrices. The development of the component mode synthesis technique was first credited to Hurty [1,2]. The technique was highly suitable for the analysis of structural system with redundant interfaces. The structure may be divided into several components. The displacement of the components is defined in terms of generalized coordinates that are related to specified sets of normalized displacement modes such as rigid-body, constraint and normal modes.

Hurty's method [2], later modified by Craig and Bampton [3], was formulated for lightly damped symmetric coefficient second order component mode system. Hurty neglected the damping term in his analysis and this resulted in real eigenvalue and eigenvector. The full modal transformation method suggested by Craig and Bampton is a superposition of fixed boundary mode plus component constraint mode.

Robin [4], Kuhar and Stahle [5], and Hintz [6] improved the component modal representation by suggesting many different procedures which permit valuable information from truncated high frequency modes to be incorporated into the retained mode in an approximated way. For example, Robin included free boundary modes and residual effects including inertial and dissipative contribution; whereas, Kuhar and Stahle (5) introduced dynamic transformation into the formulation. He believed that fixed boundary plus constrained modes tend to have the best convergence.

Complex modal analysis to the second order system was first developed by Hasselman and Kaplan [7]. The analysis accounted for any arbitrary constant coefficients which lead to complex eigenvalues and eigenvectors. Since he did not include constraint modes in their study, Therefore, contrary to Craig and Bampton [3] it does not provide a full modal transformation.

Glasgow [8] presented a significant study on complex mode synthesis allowing for a full modal transformation. The modal synthesis is valid for a broad range of second order constant coefficient differential equations which may involve general nonsymmetric velocity and/or displacement dependent terms. The equations of motion were solved for whirl mode, stability and general forced motion response.

Zheng and others [9] extending the Meirovitch [10] analysis and reviewed the gyroscopic mode synthesis including such aspects as the effect of nonlinearity and asymmetricity of bearings, gyroscopic moments of shafts and disks, and damping. Gong and others [11], neglected lateral damping and gyroscopic effect to analyze the dynamics of large steam turbine-generator rotor-bearing-foundation system. The fluid film bearing was used as a connector between the rotor and foundation.

The objective of the present investigation is to develop an efficient method to analyze the dynamic response of rotor-bearing-pedestal system based on component mode synthesis reduction method. The digital computer program **SETSA** (12) is then employed to provide a quick estimation of natural frequencies of the system. A detailed parametric analysis of Jeffcotte's rotor supported on flexible pedestal is also studied which this analysis will be presented in the next publication.

2. Component Mode Synthesis

The successful design of structures requires a comprehensive study of dynamic analysis before the structure is placed in its operating environment. A vital part of this effort is the modal analysis of structural finite element models. In the classical approach, it is usual to determine normal modes and auxiliary static analysis directly from the finite element model. However, modern structural systems have become very complex and major components are often manufactured by different organizations. It is, therefore, often difficult to assemble an entire finite element model in a timely manner. In addition, many finite element models may contain so many degrees of freedom that they cannot be directly handled on the largest of modern computers. For these reasons, it is desirable to develop methods for analyzing substructures of a finite element model. Such an analysis has come to be known as component mode synthesis in dynamic analysis and substructuring in static analysis.

Component mode synthesis allows for significant reduction in the size of the overall system problem while retaining the essential dynamic characteristics. The coordinates of the component are classified as boundary coordinates if they are common to two or more components and interior coordinates if they do not interface with any other component. It is desirable that component mode synthesis techniques for the dynamic analysis of structures have the following characteristics:

The **constrained normal mode** is found by fixing all boundary coordinates and determining the free vibration modes of the constrained component. It is these modes that provide for the reduction of the number of degrees of freedom system.

The **constraint modes** are determined by giving each of the boundary coordinates a unit displacement, in turn, fixing all other boundary coordinates and allowing the internal coordinates to displace.

When the constraint modes and constrained normal modes are obtained then each component is transformed in terms of its constrained normal mode and assembled into a lower order set of system equation. This reduced order set of system equation is then used to obtain system free and forced response.

3. Analytical Development

The analytical development here will cover the complete development of the system equations of motion using component mode synthesis. This technique allows each component to be restructured in terms of two types of component modes, namely constraint modes (static) and constrained normal mode (dynamic). It is the constrained normal mode which is responsible for the reduction size matrices of the system. By this method the influence of pedestal flexibility on rotor critical speed will be analyzed. The typical rotor-bearing to be simulated as illustrated in Fig.1 is modeled as an assemblage of discrete disks, rotor segments with distributed mass and elasticity, and discrete bearings. The rotor can be divided into several components, each component may be composed of several finite elements. It is often difficult to assemble the entire finite element model in a timely manner.

Utilizing the component mode synthesis technique, each component is analyzed separately, and the size of the component matrices is reduced by mode truncation. The reduced size of all the components are then assembled to form the system assembly, which is economically feasible and easy to handle. The finite element equation of motion, constant coefficient of component (κ) can be written as:

$$\underset{\sim}{M}^{(K)} \ddot{\tilde{X}}^{(K)} + \underset{\sim}{C}^{(K)} \dot{\tilde{X}}^{(K)} + \underset{\sim}{K}^{(K)} \tilde{X}^{(K)} = \tilde{F}^{(K)}(t) \qquad (1)$$

To establish component mode development, first the displacement vector $\tilde{X}$ is partitioned into boundary $\tilde{X}^B$ and interior $\tilde{X}^I$ coordinates. The superscript (κ) is omitted for simplicity. Then the coordinate reordering transformation $\underset{\sim}{\alpha}$ is applied to the equation (1) such that:

$$\tilde{X} = \underset{\sim}{\alpha}\, \tilde{X}_p \qquad (2)$$

where

$$\tilde{X}_p = \begin{Bmatrix} \tilde{X}_p^B \\ \tilde{X}_p^I \end{Bmatrix} \qquad (3)$$

Substituting equation (2) into equation (1) and pre-multipling by $\underset{\sim}{\alpha}^T$ to obtain:

$$\begin{bmatrix} \underset{\sim}{M}^{BB} & \underset{\sim}{M}^{BI} \\ \underset{\sim}{M}^{IB} & \underset{\sim}{M}^{II} \end{bmatrix} \begin{Bmatrix} \ddot{\tilde{X}}_p^B \\ \ddot{\tilde{X}}_p^I \end{Bmatrix} + \begin{bmatrix} \underset{\sim}{C}^{BB} & \underset{\sim}{C}^{BI} \\ \underset{\sim}{C}^{IB} & \underset{\sim}{C}^{II} \end{bmatrix} \begin{Bmatrix} \dot{\tilde{X}}_p^B \\ \dot{\tilde{X}}_p^I \end{Bmatrix} +$$

$$\begin{bmatrix} \underset{\sim}{K}^{BB} & \underset{\sim}{K}^{BI} \\ \underset{\sim}{K}^{IB} & \underset{\sim}{K}^{II} \end{bmatrix} \begin{Bmatrix} \tilde{X}_P^B \\ \tilde{X}_P^I \end{Bmatrix} = \underset{\sim}{\alpha}^T \begin{Bmatrix} \tilde{F}_P^B \\ \tilde{F}_P^I \end{Bmatrix} \tag{4}$$

or

$$\underset{\sim}{M}_p \ddot{\tilde{X}}_p + \underset{\sim}{C}_p \dot{\tilde{X}}_p + \underset{\sim}{K}_p \tilde{X}_p = \tilde{F}_p(t) \tag{5}$$

The component mode development can proceed directly using first or second order form. Though the two techniques are equivalent, it is usually more convenient to write the equations of motion in first order, or state space form. In the following formulation the first order development is adopted in detail.

3.1. First Order Development

The displacement vector of equation (4) can be used to construct the related state vector. Using this state vector the component equation of motion (5) can be written in first order form as follows:

$$\begin{bmatrix} \underset{\sim}{0} & \underset{\sim}{M}_p \\ \underset{\sim}{M}_p & \underset{\sim}{C}_p \end{bmatrix} \dot{\tilde{h}} + \begin{bmatrix} -\underset{\sim}{M}_p & \underset{\sim}{0} \\ \underset{\sim}{0} & \underset{\sim}{K}_p \end{bmatrix} \tilde{h} = \begin{Bmatrix} \tilde{0} \\ \tilde{F}_p \end{Bmatrix} \tag{6}$$

where the state vector is written as follows:

$$\tilde{h} = \begin{Bmatrix} \dot{\tilde{X}}_p \\ \tilde{X}_p \end{Bmatrix} = \begin{Bmatrix} \dot{\tilde{X}}_p^B \\ \dot{\tilde{X}}_p^I \\ \tilde{X}_p^B \\ \tilde{X}_p^I \end{Bmatrix} \tag{7}$$

For simplicity the subscript p will be omitted and by using $\underset{\sim}{\bar{\alpha}}$ transformation to equation (6), all boundaries and interior terms can be collected such that:

$$\tilde{h} = \underset{\sim}{\bar{\alpha}}\, \tilde{y} \tag{8}$$

where

$$\underset{\sim}{\bar{\alpha}} = \begin{bmatrix} \underset{\sim}{I} & \underset{\sim}{0} & \underset{\sim}{0} & \underset{\sim}{0} \\ \underset{\sim}{0} & \underset{\sim}{0} & \underset{\sim}{I} & \underset{\sim}{0} \\ \underset{\sim}{0} & \underset{\sim}{I} & \underset{\sim}{0} & \underset{\sim}{0} \\ \underset{\sim}{0} & \underset{\sim}{0} & \underset{\sim}{0} & \underset{\sim}{I} \end{bmatrix} \tag{8a}$$

and

$$\tilde{y} = \begin{Bmatrix} \tilde{y}^B \\ \tilde{y}^I \end{Bmatrix} = \begin{Bmatrix} \dot{\tilde{X}}^B \\ \tilde{X}^B \\ \dot{\tilde{X}}^I \\ \tilde{X}^I \end{Bmatrix} \qquad (8b)$$

Substituting equation (8) into (6) and premultiplying by $\underset{\sim}{\alpha}^T$ the equation (6) will become:

$$\begin{bmatrix} \underset{\sim}{A}^{BB} & \underset{\sim}{A}^{BI} \\ \underset{\sim}{A}^{IB} & \underset{\sim}{A}^{II} \end{bmatrix} \begin{Bmatrix} \dot{\tilde{y}}^B \\ \dot{\tilde{y}}^I \end{Bmatrix} + \begin{bmatrix} \underset{\sim}{B}^{BB} & \underset{\sim}{B}^{BI} \\ \underset{\sim}{B}^{IB} & \underset{\sim}{B}^{II} \end{bmatrix} \begin{Bmatrix} \tilde{y}^B \\ \tilde{y}^I \end{Bmatrix} = \begin{Bmatrix} \tilde{Q}^B \\ \tilde{Q}^I \end{Bmatrix} \qquad (9)$$

or

$$\underset{\sim}{A}\,\dot{\tilde{y}} + \underset{\sim}{B}\,\tilde{y} = \tilde{Q} \qquad (9a)$$

3.2. Constraint Mode

Constraint mode is obtained by unconstraining the interior coordinates and by allowing a unit displacement to boundary coordinates in turn with all the other boundary coordinates fixed. The constraint modes are included to treat redundancies in the interconnection system. These modes will exist only if the system of constraints on the component is indeterminate. The number of constraint modes is equal to the number of redundant constraints. The constraint mode can be developed by considering the static problem of equation (4); disregarding subscript P for simplicity, the static mode is shown as follows:

$$\begin{bmatrix} \underset{\sim}{K}^{BB} & \underset{\sim}{K}^{BI} \\ K^{IB} & K^{II} \end{bmatrix} \begin{Bmatrix} \tilde{X}^B \\ \tilde{X}^I \end{Bmatrix} = \underset{\sim}{\alpha}^T \begin{Bmatrix} \tilde{F}^B \\ \tilde{0} \end{Bmatrix} \qquad (10)$$

The interior coordinates can be obtained by considering the second row of the above equation which can result:

$$\underset{\sim}{K}^{IB}\tilde{X}^B + \underset{\sim}{K}^{II}\tilde{X}^I = 0 \qquad (11)$$

or

$$\tilde{X}^I = \underset{\sim}{\psi}\,\tilde{X}^B \qquad (12)$$

$$\underset{\sim}{\psi} = -\left(\underset{\sim}{K}^{II}\right)^{-1}\underset{\sim}{K}^{IB} \qquad (12a)$$

The displacement constraint mode can be shown as:

$$\begin{Bmatrix} \tilde{X}^B \\ \tilde{X}^I \end{Bmatrix} = \begin{bmatrix} \underset{\sim}{I} \\ \underset{\sim}{\psi} \end{bmatrix} \tilde{X}^B \qquad (13)$$

and the velocity constraint mode is:

$$\begin{Bmatrix} \dot{\tilde{X}}^{B} \\ \dot{\tilde{X}}^{I} \end{Bmatrix} = \begin{bmatrix} \underset{\sim}{I} \\ \underset{\sim}{\psi} \end{bmatrix} \dot{\tilde{X}}^{B} \tag{14}$$

Then the component constraint mode in state space form can be constructed using equations (13) and (14) such that:

$$\tilde{y}^{B} = \begin{Bmatrix} \dot{\tilde{X}}^{B} \\ \tilde{X}^{B} \end{Bmatrix} \tag{15}$$

and

$$\tilde{y}^{I} = \begin{Bmatrix} \dot{\tilde{X}}^{I} \\ \tilde{X}^{I} \end{Bmatrix} \tag{16}$$

Collecting the boundary and interior coordinates together such that:

$$\tilde{y} = \begin{Bmatrix} \tilde{y}^{B} \\ \tilde{y}^{I} \end{Bmatrix} = \begin{Bmatrix} \dot{\tilde{X}}^{B} \\ \tilde{X}^{B} \\ \dot{\tilde{X}}^{I} \\ \tilde{X}^{I} \end{Bmatrix} = \begin{bmatrix} \underset{\sim}{I} & \underset{\sim}{0} \\ \underset{\sim}{0} & \underset{\sim}{I} \\ \underset{\sim}{\psi} & \underset{\sim}{0} \\ \underset{\sim}{0} & \underset{\sim}{\psi} \end{bmatrix} \begin{Bmatrix} \dot{\tilde{X}}^{B} \\ \tilde{X}^{B} \end{Bmatrix} \tag{17}$$

or

$$\tilde{y} = \begin{Bmatrix} \tilde{y}^{B} \\ \tilde{y}^{I} \end{Bmatrix} = \begin{bmatrix} \underset{\sim}{I} \\ \underset{\sim}{\Psi} \end{bmatrix} \tilde{y}^{B} \tag{17a}$$

where

$$\underset{\sim}{\Psi} = \begin{bmatrix} \underset{\sim}{\psi} & \underset{\sim}{0} \\ \underset{\sim}{0} & \underset{\sim}{\psi} \end{bmatrix} \tag{17b}$$

3.3. Constraint Normal Mode

The constraint normal mode of the component defines the displacement relative to the connections. It describes the motion of the interior coordinates with all constraints fixed. The constrained normal mode is often called the "fixed-constraint normal mode" or simply the "normal mode" for brevity. It is obtained by setting all boundary coordinates in equation (9) to zero and obtaining the free vibration response. It is this constraint normal mode that is used for the reduction of the system matrices. Considering equation (9) and setting the boundary coordinates to zero, the remaining terms can be written as:

$$\underset{\sim}{A}^{II}\dot{\tilde{y}} + \underset{\sim}{B}^{II}\tilde{y} = \tilde{0} \tag{18}$$

Assuming the solution of the above equation in the form:

$$\tilde{y} = \tilde{y}_0 \, e^{\lambda t} \tag{19}$$

and substituting this into equation (18) and simplifying results in:

$$\left(\lambda \, \underset{\sim}{A}^{II} + \underset{\sim}{B}^{II}\right)\tilde{y}_0 = \tilde{0} \tag{20}$$

or

$$\left(\left(\underset{\sim}{B}^{II}\right)^{-1}\underset{\sim}{A}^{II} + \frac{1}{\lambda}\underset{\sim}{I}\right)\tilde{y}_0 = \tilde{0} \tag{20a}$$

or

$$\left(\underset{\sim}{D} - \hat{\alpha} \, \underset{\sim}{I}\right)\tilde{y}_0 = \tilde{0} \tag{20b}$$

where

$$\underset{\sim}{D} = -\left(\underset{\sim}{B}^{II}\right)^{-1}\underset{\sim}{A}^{II} \tag{20c}$$

$$\hat{\alpha} = \frac{1}{\lambda} \tag{20d}$$

For nontrivial solution the coefficient of the determinate (20b) must vanish, therefore:

$$\left|\underset{\sim}{D} - \hat{\alpha} \, \underset{\sim}{I}\right| = 0 \tag{21}$$

The solution of the above equation provides 2n eigenvalues λ_i and corresponding 2n displacement right eigenvectors $\tilde{U}_i$ where n is the number of component coordinates in second order form of equation (1). The 2n eigenvectors can be shown as:

$$\tilde{Y}_i = \begin{Bmatrix} \lambda_i \tilde{U}_i \\ \tilde{U}_i \end{Bmatrix} \quad \text{where} \quad i=1,\ldots 2n \tag{22}$$

or in matrix form as:

$$\underset{\sim}{Y} = \begin{bmatrix} \underset{\sim}{U}\underset{\sim}{\mathring{\Lambda}} \\ \underset{\sim}{U} \end{bmatrix} \tag{23}$$

Therefore, the interior coordinates can be written in terms of these constrained normal modes of the above eigenvector expression so that:

$$\tilde{y}^I = \sum_{i=1}^{2n} \tilde{Y}_i \tilde{\eta}_i \tag{24}$$

or in matrix form:

$$\tilde{y}^{I} = \begin{bmatrix} \underset{\sim}{U}\underset{\sim}{\mathring{\Lambda}} \\ \\ \underset{\sim}{U} \end{bmatrix} \tilde{\eta} = \underset{\sim}{Y}\ \tilde{\eta} \tag{25}$$

3.4. Superposition of Component Modes

To obtain the complete modal transformation of the component physical coordinates, it is necessary to superpose the two modes, namely the constraint mode and the constrained normal mode, together to form a full modal transformation so that:

$$\tilde{y} = \begin{Bmatrix} \tilde{y}^{B} \\ \\ \tilde{y}^{I} \end{Bmatrix} = \begin{bmatrix} \underset{\sim}{I} & \underset{\sim}{0} \\ \\ \underset{\sim}{0} & \underset{\sim}{Y} \end{bmatrix} \begin{Bmatrix} \tilde{y}^{B} \\ \\ \tilde{\eta} \end{Bmatrix} \tag{26}$$

Therefore, the superposition of equations (26) and (17a) will give:

$$\tilde{y} = \begin{Bmatrix} \tilde{y}^{B} \\ \\ \tilde{y}^{I} \end{Bmatrix} = \begin{bmatrix} \underset{\sim}{I} & \underset{\sim}{0} \\ \\ \underset{\sim}{\Psi} & \underset{\sim}{Y} \end{bmatrix} \begin{Bmatrix} \tilde{y}^{B} \\ \\ \tilde{\eta} \end{Bmatrix} \tag{27}$$

or

$$\tilde{y} = \underset{\sim}{\beta}\ \tilde{q} \tag{28}$$

where

$$\underset{\sim}{\beta} = \begin{bmatrix} \underset{\sim}{I} & \underset{\sim}{0} \\ \\ \underset{\sim}{\Psi} & \underset{\sim}{Y} \end{bmatrix} \tag{28a}$$

3.5. Mode Truncation

The purpose of mode truncation is to eliminate the excessive unknown degrees of freedom, and hence to reduce the size of the system matrices without affecting the dynamic characteristics of the final system. Therefore all degrees of freedom of the system can be extensively reduced by retaining the low frequency mode and truncating a number of higher constrained normal modes determined from the free vibration analysis of interior coordinates. This can be considered as one of the most important aspects of the component mode synthesis technique. Based on the literature survey, researchers have not as of yet found any systematic way for mode truncation to guarantee convergence. One can, therefore, conclude that it is necessary to base mode truncation on prior experience.

At this stage, the entire degrees of freedom of the component can be reduced by eliminating the insignificant mode. Truncation can be established by partitioning $\underset{\sim}{Y}$ of constrained right vector and $\tilde{\eta}$ vector of modal coordinates in equation (25) such that:

$$\underset{\sim}{Y} = \left[\underset{\sim}{Y}_R \;\vdots\; \underset{\sim}{Y}_T\right] \tag{29}$$

and

$$\tilde{\eta} = \left\{\begin{array}{c} \tilde{\eta}_R \\ \hline \tilde{\eta}_T \end{array}\right\} \tag{30}$$

Substituting the retained part of equation (29) and equation (30) into equation (27) results in the truncated modal transformation matrix β_R as shown below:

$$\tilde{y} = \begin{bmatrix} \underset{\sim}{I} & \underset{\sim}{0} \\ \underset{\sim}{\Psi} & \underset{\sim}{Y}_R \end{bmatrix} \begin{Bmatrix} \tilde{y}^B \\ \tilde{\eta}_R \end{Bmatrix} \tag{31}$$

or

$$\tilde{y} = \beta_R \, \tilde{q} \tag{32}$$

where

$$\beta_R = \begin{bmatrix} \underset{\sim}{I} & \underset{\sim}{0} \\ \underset{\sim}{\Psi} & \underset{\sim}{Y}_R \end{bmatrix} \tag{32a}$$

and

$$\tilde{q} = \begin{Bmatrix} \tilde{y}^B \\ \tilde{\eta}_R \end{Bmatrix} \tag{32b}$$

The final truncated reduced component equation of motion is obtained by substituting equation (32) into equation (9a) and premultiplying by β_R^T to obtain:

$$\beta_R{}^T \underset{\sim}{A} \, \beta_R \dot{\tilde{q}} + \beta_R{}^T \underset{\sim}{B} \, \beta_R \tilde{q} = \beta_R{}^T \tilde{Q} \tag{33}$$

or

$$\bar{A} \, \dot{\tilde{q}} + \bar{B} \, \tilde{q} = \tilde{P} \tag{34}$$

In order to assemble each truncated component with its adjacent component at interface, it is necessary to apply the $\underset{\sim}{k}$ transformation to the equation (34). This will assure connectivity between the two component coordinates. This transformation could have been avoided if proper care had been taken when constructing the modal transformation right vector (28a), since it would not have otherwise eased the computational efficiency. Therefore, the final $\underset{\sim}{k}$ reordering transformation to the truncated component is adopted such that:

$$\tilde{q} = \underset{\sim}{k} \, \tilde{q}_R \tag{35}$$

substituting the above equation into equation (34) and premultiplying by $\underset{\sim}{k}^T$, the final reduced component can be written as:

$$\underset{\sim}{\mathcal{A}}\,\dot{\tilde{q}}_R + \underset{\sim}{\mathcal{B}}\,\tilde{q}_R = \tilde{\mathcal{P}}_R \tag{36}$$

Finally the response of the system in generalized coordinates $\tilde{q}_R$ can be back transformed to obtain the relative physical coordinate through the transformation of equations (35), (32) and (8), which combined together results in:

$$\tilde{h} = \begin{Bmatrix} \dot{\tilde{X}}_P^B \\ \dot{\tilde{X}}_P^I \\ \tilde{X}_P^B \\ \tilde{X}_P^I \end{Bmatrix} = \bar{\underset{\sim}{\alpha}}\ \underset{\sim}{\beta}_R\ \underset{\sim}{k}\ \tilde{q}_R \tag{37}$$

from the bottom half of equation (37) and (2) the original coordinates $\tilde{X}^{(\kappa)}$ can be determined.

3.6. System Equation of Motion

When all the components are analyzed by the aforementioned formulation and the truncated component equations are obtained, the truncated components are then assembled together to form the complete truncated system equation. If the system has only one component then the equation (36) will be the final system assembly. The next step is to include fluid film properties at bearing locations. The bearing has four degrees of freedom (two translations and two rotations) into which the fluid film damping and stiffness will be added the $\underset{\sim}{\mathcal{A}}$ and $\underset{\sim}{\mathcal{B}}$ of equation (36) respectively.

To incorporate pedestal into the system assembly, it is necessary to transform the pedestal properties into 2n form as cited earlier in equation (6), and then increase the size of the matrices of equation (36) (d.o.f of one pedestal in 2n form multiply by the number of pedestals) to accommodate the pedestal influence on the vibration response of the rotor. The pedestal properties are then added to the assembly and the fluid film bearing is used as a connector between the pedestal and rotating assembly as clearly shown in Fig.2 and Fig.3.

To formulate the system assembly, assume κ to be the number of truncated components. The system coordinate vector $\tilde{y}_s$ can be shown in terms of boundary and interior coordinates as:

$$\tilde{y}_S = \begin{Bmatrix} \tilde{y}_S^B \\ \tilde{\eta}_R^{(1)} \\ \tilde{\eta}_R^{(2)} \\ \vdots \\ \tilde{\eta}_R^{(K)} \end{Bmatrix} \tag{38}$$

The geometric constraint $\underset{\sim}{\chi}^{(K)}$ is then related to the component's coordinate vector to the system vector by the following expression:

$$\tilde{q}_R^{(K)} = \underset{\sim}{\chi}^{(K)} \tilde{y}_S \tag{39}$$

and by rewriting the equation (36) for κth component results in:

$$\underset{\sim}{\mathcal{A}}^{(K)} \dot{\tilde{q}}_R^{(K)} + \underset{\sim}{\mathcal{B}}^{(K)} \tilde{q}_R^{(K)} = \tilde{\mathcal{P}}_R^{(K)} \tag{40}$$

The system assembly can be obtained by substituting the transformation matrix of equation (39) into equation (40), premultiplying by $(\underset{\sim}{\chi})^T$ and sum over all components. Hence:

$$\underset{\sim}{\mathcal{A}}_S \dot{\tilde{y}}_S + \underset{\sim}{\mathcal{B}}_S \tilde{y}_S = \tilde{\mathcal{P}}_S \tag{41}$$

where

$$\underset{\sim}{\mathcal{A}}_S = \sum_{K=1}^{N} (\underset{\sim}{\chi}^{(K)})^T \underset{\sim}{\mathcal{A}}_R^{(K)} \underset{\sim}{\chi}^{(K)} \tag{41a}$$

$$\underset{\sim}{\mathcal{B}}_S = \sum_{K=1}^{N} (\underset{\sim}{\chi}^{(K)})^T \underset{\sim}{\mathcal{B}}_R^{(K)} \underset{\sim}{\chi}^{(K)} \tag{41b}$$

$$\tilde{\mathcal{P}}_S = \sum_{K=1}^{N} (\underset{\sim}{\chi}^{(K)})^T \tilde{\mathcal{P}}_R^{(K)} \tag{41c}$$

where N is the number of components.

3.7. System Solution

The equation (41) can be decoupled by using the orthogonality property between normal modes if $\underset{\sim}{\mathcal{A}}_S$ and $\underset{\sim}{\mathcal{B}}_S$ were symmetric. Since $\underset{\sim}{\mathcal{A}}_S$ and $\underset{\sim}{\mathcal{B}}_S$ are not symmetric due to pedestal and bearing influence, decoupling the system equation of motion by conventional normal mode analysis is no longer possible. Therefore, it is necessary to use the biorthogonality principle between the right and the left eigenvectors of the system to decouple the system equations of motion. Right eigenvectors are the modes of the original system and the left eigenvectors are those of the transposed system. Right eigenvectors $\underset{\sim}{Y}_s$ are obtained by considering the free vibration of the system equation (41). The left eigenvectors $\underset{\sim}{Z}_s$ are obtained by considering the free vibration of the transpose of system equation (41). Right and left eigenvectors can be obtained by the same precedures as cited earlier in equations (19) to (23).

The left eigenvectors $\underset{\sim}{Z}_s$ and the right eigenvectors $\underset{\sim}{Y}_s$ can be used to decouple the system equations of motion by considering the following transformation:

$$\tilde{y}_s = \left[\underset{\sim}{Y}_s\right] \tilde{q} \tag{42}$$

substituting the above equation into equation(41) and premultiplying by Z_s^T to obtain:

$$\underset{\sim}{Z}_s^T \underset{\sim}{\mathcal{A}}_s \underset{\sim}{Y}_s \dot{\tilde{q}} + \underset{\sim}{Z}_s^T \underset{\sim}{\mathcal{B}} \underset{\sim}{Y}_s \tilde{q} = \underset{\sim}{Z}_s^T \tilde{\mathcal{P}}_s \tag{43}$$

$$\left[\ \underset{\sim}{\mathring{N}}\ \right] \dot{\tilde{q}} + \left[\ \underset{\sim}{\mathring{M}}\ \right] \tilde{q} = \underset{\sim}{Z}_s^T \tilde{\mathcal{P}}_s \tag{44}$$

Then both sides of the equation are multiplied by the inverse of $\underset{\sim}{\mathring{N}}$ which results in the final system equation of motion.

$$\dot{\tilde{q}} = - \underset{\sim}{\mathring{\Lambda}}_s \tilde{q} + \tilde{\zeta} \tag{45}$$

where

$$\tilde{\zeta} = \underset{\sim}{\mathring{N}} \underset{\sim}{Z}_s^T \tilde{\mathcal{P}}_s \tag{45a}$$

Any prescribed ground motion can now be applied to the system and the result can be back transformed to the original coordinates.

The computer program based on the above mathematical development is tested with the use of one detailed example in the following section to provide a clear insight into the accuracy and limitations of the method. In the following example the natural frequency of the rotor is calculated and the variation of error against different levels of mode truncation is described.

4. Example Analysis

The example discussed here is a simply supported Lund [13] rotor shown in Fig.4. The rotor has a diameter of 4 inches and a length of 50 inches with a modulus of elasticity of 30×10^6 psi. First the entire rotor is considered as a single component. Then the same rotor is divided into 2, 3, and finally 4 components. Each component consists of some equal length finite elements as shown in Fig.4a,b,c,d. The rotor is modeled with four degrees of freedom per station. The degrees of freedom in each station are represented by two translations and two rotations in Z and Y directions. The total number of degrees of freedom in each case is $(N+1)*4$, where N is the number of elements. The rotor supports are assumed to be rigid and unyielding against translational displacements; however, rotation about the two bending axes is permitted. The rotor is modeled symmetric about its mass center. The natural frequencies of the system are obtained by eliminating the rows and columns of those coordinates associated with translation in support points.

The computer **SETSA** simulation is performed for each rotor configuration and for different levels of mode truncation. The result of the simulations are then tabulated and recorded in increasing order of frequency of the rotor which can be seen in Tables 1, 2, 3 and 4. The percentage of error of each frequency resulting from different levels of mode truncation based on Table 2 are recorded in Table 5. A plot of this results vs number of mode retained is shown in Fig.5. Finally a plot of number of mode retained vs natural frequency of the rotor is shown in Fig.6.

5. Discussion of Results

It can be seen from the results presented in Tables 1, 2, 3 and 4 that the accuracy monotonically decrease by increasing the levels of mode truncation. It is also observed that as the finite element in each component become finer the results become more accurate (Tables 3 and 4). From the results presented in Table 5, Fig.5 and Fig.6 it is evident that the accuracy monotonically increases with increasing the number of components chosen for the analysis. When a fewer number of components and/or elements are utilized, only the higher mode frequency is affected more by the truncations. However, the lower mode frequencies are not significantly affected by truncation. The calculated result obtained by this method is in accord with those achieved by Lund [13]. The accuracy of the method and the computer program **SETSA** is thus established.

6. ACKNOWLEDGMENT

The investigation reported here was supported by a grant from the National Science and Engineering Council of Canada awarded to the second author of this paper.

REFERENCES

1. Hurty, W. C., "Vibration of Structural System by Component Mode Synthesis", ASCE: journal of Engineering Mechanical Divisions, 86, August, 1960, pp.51-69.
2. Hurty, W. C., "Dynamic Analysis of Structural Systems Using CMS", AIAA journal, 3 (4), 1965, p.678.
3. Craig, R. R., Mervyn C. C. and Bampton., "Coupling of Substructures for Dynamic Analysis", AIAA journal, 6 (7), July, 1968, p.1313.
4. Rubin, S., "Improved C.M. Representation for Structural Dynamic analysis," AIAA Journal, 13 (8), Aug. 1975, p.995.
5. Kuhar,E. J. Stahle, Stahle, C. V., "Dynamic Transformation Method for Modal Synthesis", AIAA Journal, 12 (5),1974
6. Hintz, R. M., "Analytical Methods in Component Modal Synthesis", AIAA Journal, 13 (8), Aug. 1975, pp.1007-1016.
7. Hasselman, T. K. and Kaplan, "Dynamic Analysis of Large System by Complex Mode Synthesis", ASME: Journal of Dynamic System, Measurement and Control, 96 (3), Sept. 1974, pp.327-333.
8. Glasgow, D. A., "Analysis of Rotor Bearing System Using Component Mode Synthesis", PhD Dissertation ,Arizona State University, 1981.
9. Meirovitch, L., "A New Method of Solution of the Eigenvalue Problem for Gyroscopic Systems", AIAA journal, 12 (10), 1974, pp.1337-1342.
10. Zheng, Z. C. et, al., "Gyroscopic Mode Synthesis in the Dynamic Analysis of a Multi-Shaft Rotor-Bearing System", Department of Engineering Mechanics, Tsinghua University, beijing, Shenyang Aero Engine Research Institute, Shenyang, 1985.
11. Gong, H., Chang, H. Y., Huang, H. Y., and Zheng, C. H., "Dynamic Analysis and Experiments of Rotor-Bearing Foundation System for Large Steam Turbine-Generator Set", Shanghai Power Plant Equipment Research Institute Tsinshva University Beijing.
12. Amini, Aliakbar, "Parametric Study of Rotor-Bearing-Pedestal System using Component Mode Synthesis", Master Thesis, Department of Mechanical Engineering Concordia University, Feb. 1990.
13. Lund, J. W., "Stability and damped critical speed of a flexible in fluid film bearings", jornal of Engineering for Industry, May, 1976, pp.509-517.

List of Figures and Tables

Fig.1	Typical system configuration
Fig.2	Component assembly matrix including fluid film and pedestal properties.
Fig.3	Component assembly matrix including fluid film and pedestal mass properties.
Fig.4	Lund rotor composed of a) one component b) two components c) three components and d) four four components.
Fig.5	Influence of mode truncation on the rotor criticals.
Fig.6	Error at different levels of mode truncation.
Table 1	Natural frequency of one component assembly at different levels of mode truncation Lund rotor.
Table 2	Natural frequency of two component assembly at different levels of mode truncation Lund rotor.
Table 3	Natural frequency of three component assembly at different levels of mode truncation Lund rotor.
Table 4	Natural frequency of four component assembly at different levels of mode truncation Lund rotor.
Table 5	Error at different levels of mode truncation.

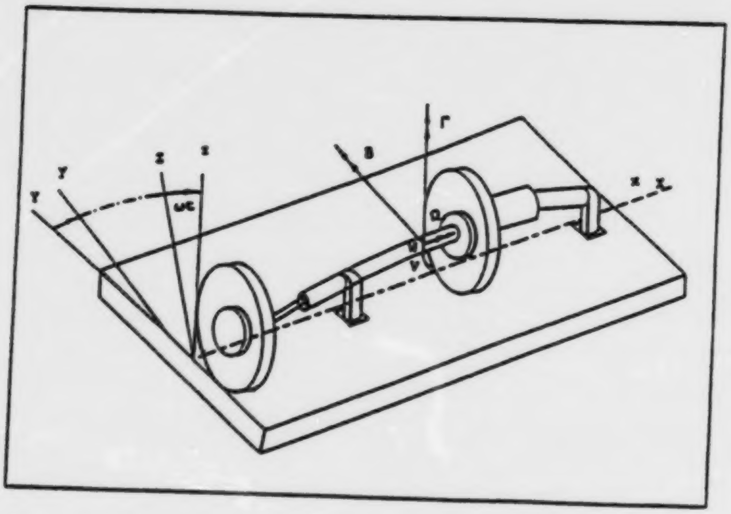
Y
Y
Z
z
ωt
B
Γ
Ω
u
v
x
X

Fig. 1 Typical system configuration

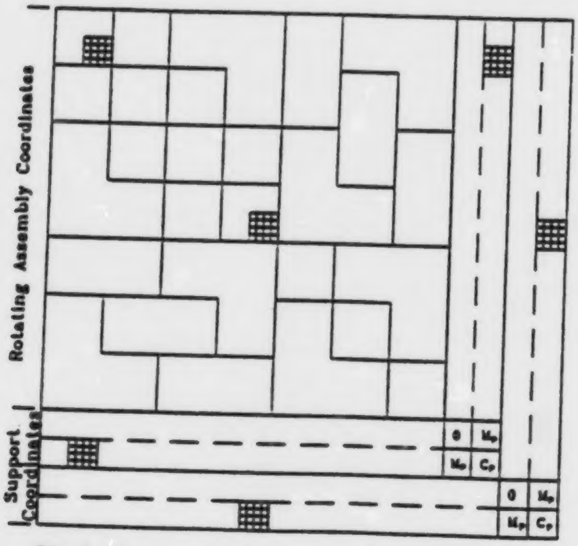
Rotating Assembly Coordinates
Support Coordinates
Support Coordinates
0
M_p
M_p
C_p
0
M_p
M_p
C_p

Fig. 2. Three components assembly matrix

Legend

▦ Bearing fluid film damping

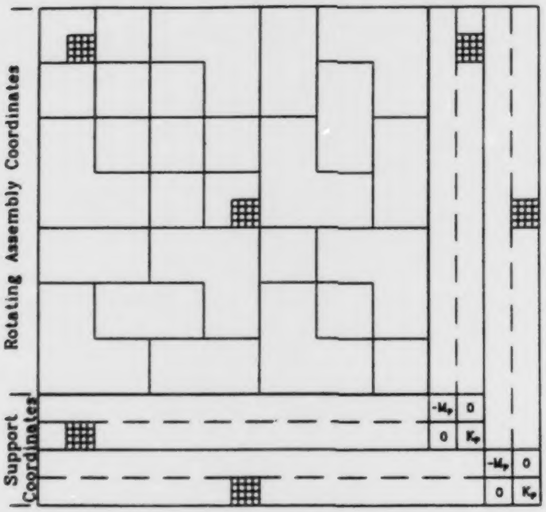
Rotating Assembly Coordinates
Support Coordinates
$-M_p$
0
0
K_p
$-M_p$
0
0
K_p

Fig. 3. Three components assembly matrix

Legend

▦ Bearing fluid film stiffness

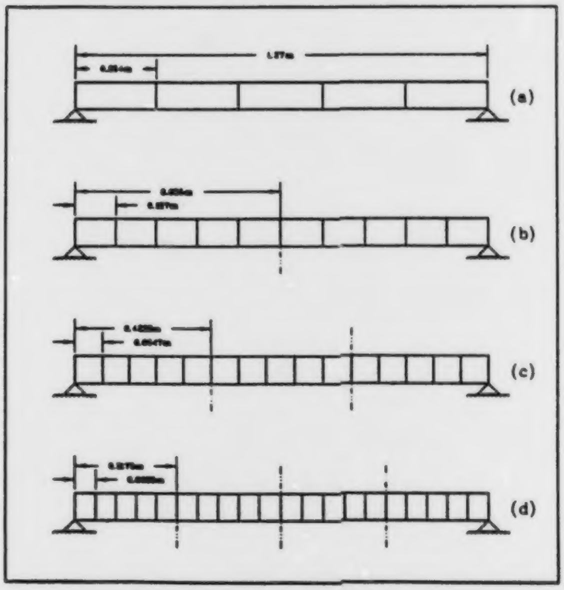
1.27m
0.254m
(a)
0.635m
0.127m
(b)
0.4233m
0.0847m
(c)
0.3175m
0.0635m
(d)

Fig. 4. Simply supported undamped Lund rotor composed of: a) one component, b) two component, c) three component and d) four component assembly.

Table 1

Natural Frequencies of One Component Assembly
at Different Levels of Mode Truncation

No.	Retain 4 Mode	Retain 8 Mode	Retain 12 Mode	Retain 20 Mode	Retain All Mode
1	126.864	126.864	126.855	126.855	126.855
2	641.096	505.186	505.186	504.849	504.835
3	1546.611	1546.615	1130.324	1128.645	1128.521
4	---------	2850.855	2850.855	1999.210	1995.453
5	---------	---------	4525.956	3119.284	3111.106
6	---------	---------	---------	6517.288	4748.115
7	---------	---------	---------	8073.554	6279.373
8	---------	---------	---------	---------	8410.807
9	---------	---------	---------	---------	11030.337
10	---------	--------	---------	---------	14091.646

Lund rotor

Table 2

Natural Frequencies of Two Component Assembly
at Different Levels of Mode Truncation

No.	Retain 4 Mode	Retain 8 Mode	Retain 12 Mode	Retain 20 Mode	Retain All Mode
1	126.860	126.852	126.8497	126.849	126.849
2	504.525	504.525	504.4824	504.481	504.481
3	1156.426	1125.603	1125.2418	1124.732	1124.692
4	2503.101	1977.040	1977.0402	1975.581	1975.504
5	4112.930	3166.255	3046.9970	3043.671	3043.305
6	5851.553	5851.553	4321.1765	4315.612	4315.145
7	----	8104.688	6013.3910	5789.229	5780.586
8	----	10356.494	10356.494	7448.477	7431.932
9	----	----	13073.519	9267.640	9254.835
10	----	----	15687.175	11962.114	11922.512

Lund rotor

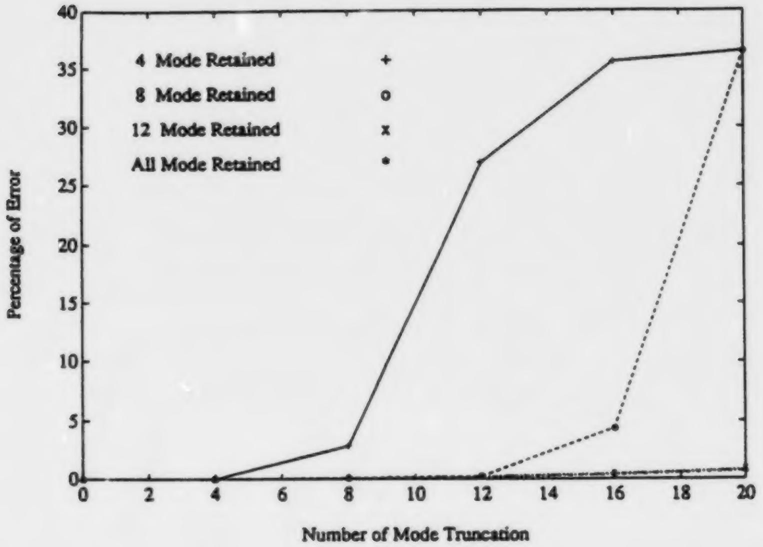

Fig. 5. Error at Different Level of Mode Truncation

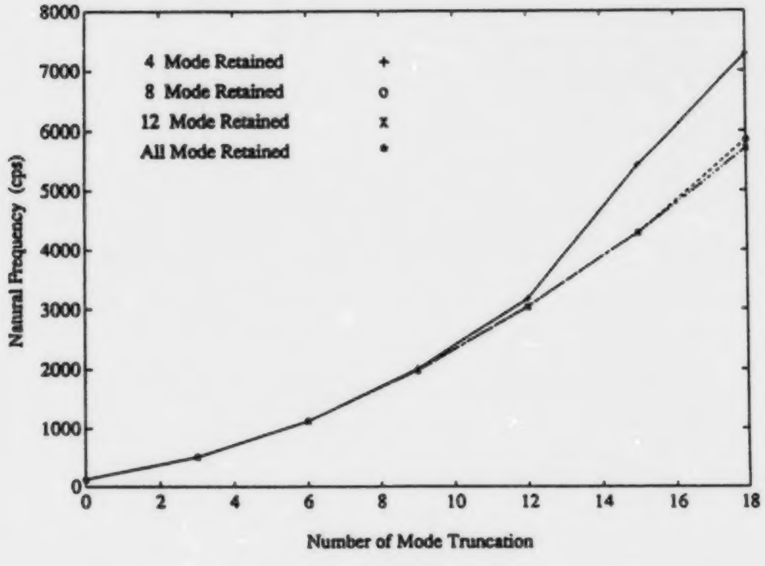

Fig. 6 Influence of Mode Truncation on N.F of the Rotor

Table 3

Natural Frequencies of Three Component Assembly at Different Levels of Mode Truncation					
No.	Retain 4 Mode	Retain 8 Mode	Retain 12 Mode	Retain 20 Mode	Retain All Mode
1	126.850	126.849	126.848	126.848	Size of matrices exceeded the computer capacity
2	504.645	504.468	504.445	504.438	
3	1124.335	1124.335	1124.216	1124.212	
4	2004.106	1973.675	1973.641	1972.966	
5	3169.379	3039.555	3036.034	3034.020	
6	5422.612	4292.800	4292.800	4288.749	
7	7280.533	5861.691	5722.816	5718.428	
8	--------	7697.238	7320.881	7305.872	
9	--------	--------	9047.626	9032.991	
10	--------	--------	--------	12881.762	

Lund rotor

Table 4

Natural Frequencies of Four Component Assembly at Different Levels of Mode Truncation					
No.	Retain 4 Mode	Retain 8 Mode	Retain 12 Mode	Retain 20 Mode	Retain All Mode
1	126.848	126.848	126.848	Size of matrices exceeded the computer capacity	Size of matrices exceeded the computer capacity
2	504.477	504.444	504.432		
3	1125.007	1124.240	1124.166		
4	1972.734	1972.734	1972.465		
5	3066.721	3033.196	3033.188		
6	4402.052	4287.346	4286.428		
7	6007.132	5721.932	5711.647		
8	9182.582	7289.425	7289.425		
9	--------	9153.271	8993.439		
10	--------	11198.397	10817.150		

Lund rotor

Table 5

Error at Different Levels of Mode Truncation				
No.	% Error 4 Mode Retain	% Error 8 Mode Retain	% Error 12 Mode Retain	% Error 20 Mode Retain
1	0.00939	0.00282	0.000938	0.000638
2	0.01836	0.01836	0.009805	0.009610
3	2.86960	0.1278	0.0956	0.05035
4	26.9020	0.2319	0.2319	0.15795
5	35.597	4.386	0.4550	0.3455
6	36.51	36.517	0.8106	0.6807

Lund rotor

NOMENCLATURE

$\underset{\sim}{A}$	Partitioned coefficient matrix first order form
$\underset{\sim}{\mathcal{A}}$	First order modally transformed coefficient matrix
B	Rotor station rotational degree of freedom xz
$\underset{\sim}{B}$	Partitioned coefficient matrix first order form
$\underset{\sim}{\mathcal{B}}$	First order modally transformed coefficient matrix
$\underset{\sim}{C}$	Damping matrix
$\underset{\sim}{D}$	Matrix of dynamical eigenvalue problem
$\underset{\sim}{\hat{D}}$	System matrix of dynamical eigenvalue problem
E	Modulus of elasticity
$\tilde{F}$	Force vector in second order form
$\tilde{g}$	System modal synthesis state vector
$\tilde{h}$	State vector before partitioning
$\underset{\sim}{I}$	Identity matrix
$\underset{\sim}{K}$	Stiffness matrix
$\underset{\sim}{k}$	Reordering transformation matrix
ℓ_1, ℓ_2	Disk location
ℓ	Element length
$\tilde{M}$	Mass matrix
$\underset{\sim}{\mathring{M}}$	Diagonal matrix of biorthogonality
N	Number of elements
$\underset{\sim}{\mathring{N}}$	Diagonal matrix of biorthogonality
$\tilde{\mathcal{P}}$	Modally synthesized force vector
$\tilde{q}$	Synthesized mode state vector
$\tilde{Q}$	Partitioned force vector
t	Time, thickness
$\underset{\sim}{U}$	Matrix of constrained right vector
V	Absolute lateral displacement coordinate in y direction
W	Absolute lateral displacement coordinate in z direction
$\tilde{x}$	Physical displacement coordinates
$\tilde{y}$	State vector partitioned
$\underset{\sim}{Y}$	Constraint matrix left vector
y_0	Right eigenvector
z_0	Left eigenvector
$\underset{\sim}{Z}$	Constrained matrix left vector

$\bar{\alpha}$	Second reordering transformation matrix applied to first order form
$\hat{\alpha}$	Inverse of eigenvalue, damping exponent of system eigenvalue
α	First reordering transformation matrix applied to second order equation.
$\underset{\sim}{\beta}$	Modal transformation matrix right vector
$\underset{\sim}{\gamma}$	Component transformation matrix
Γ	Rotor station rotational degree of freedom xy
$\tilde{\zeta}$	Vector of modal force
$\tilde{\eta}$	Vector of modal coordinate
λ	Eigenvalue
$\underset{\sim}{\hat{\Lambda}}$	Diagonal matrix of eigenvalue first order form
ρ	Density
$\underset{\sim}{\psi}$	Displacement static constraint matrix
$\underset{\sim}{\Psi}$	Displacement constraint matrix first order form
ω	Whirl speed
Ω	Spin speed

Subscripts

B	Bending
d	Disk
P	Partitioned, Pedestal
R	Retained
r	Rotational
S	System
t	Translational
T	Truncated

Superscripts

B	Boundary
e	Element
i	Index
I	Interior
k	Index, kth component
T,T	Transpose

L'EFFET DES ACCOUPLEMENTS ET DES PALIERS SUR LA VITESSE CRITIQUE DES MACHINES MONTÉES EN SÉRIE

par

Ronald L. Eshleman, Ph.D., P.E.
Vibration Institute
Willowbrook, Illinois 60514, USA

RÉSUMÉ

Ce document traite de l'effet des accouplements et des paliers sur la vitesse critique des machines montées en série en prenant pour exemple la pompe d'alimentation d'une chaudière actionnée par un moteur dont la plage de fonctionnement comprend deux vitesses critiques. Une modélisation informatisée, validée par des essais a été utilisée pour déterminer quels changements devaient être apportés pour amener les vitesses critiques hors de la plage des vitesses de fonctionnement. Les deux vitesses critiques ont été augmentées en changeant les accouplements et les paliers de l'entraînement de la pompe.

MOTS CLÉS

Accouplements, paliers, pompes d'alimentation de chaudières, moteurs, vitesses critiques

BIOGRAPHIE

Ronald L. Eshleman est directeur du Vibration Institute et agit comme consultant auprès de l'industrie. Ses champs de compétence comprennent la conception et la mise au point de machines ainsi que le diagnostic et la correction des défectuosités. Il utilise différentes techniques de réduction des vibrations pour régler une foule de problèmes concernant les machines et les structures. Il détient un doctorat de l'Illinois Institute of Technology. Il est membre de l'ASME, a travaillé comme réviseur technique à la revue **Shock and Vibration Digest** depuis son lancement en 1969 et a écrit un grand nombre d'articles sur les vibrations.

THE EFFECT OF COUPLINGS AND BEARINGS ON THE CRITICAL SPEEDS OF MACHINE TRAINS

by

Ronald L. Eshleman, Ph.D., P.E.
Vibration Institute
Willowbrook, Illinois 60514, USA

ABSTRACT

The effect of couplings and bearings on the critical speeds of machine trains is discussed. A case history of a motor driven boiler feed pump with two critical speeds in the operating speed range is provided as an example. A computer model, validated by testing, was used to determine the changes required to eliminate the critical speeds from the operating speed range. Both critical speeds were raised by changing the couplings and the feed pump drive bearings.

KEY WORDS: COUPLINGS, BEARINGS, BOILER FEED PUMPS, MOTORS, CRITICAL SPEEDS

BIOGRAPHICAL SKETCH

Ronald L. Eshleman is Director of the Vibration Institute and a vibration consultant to industry. His areas of expertise include the design and development of machinery as well as fault diagnosis and correction. He has used vibration control techniques to solve a variety of machine and structural problems. Eshleman holds a Ph.D. from Illinois Institute of Technology. He is a member of ASME, has served as Technical Editor of the **Shock and Vibration Digest** since it was first published in 1969, and has published many technical papers in the vibration field.

INTRODUCTION

It is common knowledge that a machine's bearings, pedestals, and foundation affect its lateral critical speeds. However, the effects of coupling it to adjacent machines is often not considered in the machine train design. This paper is concerned with the change in critical speeds of a unit in a coupled 4000 Hp motor driven boiler feed pump drive train. It shows the effects of shim pack and gear couplings on the unit's critical speeds which were raised out of the operating speed range with a coupling change. The effects of bearing type and clearances on critical speeds are shown for the pump drive.

BACKGROUND INFORMATION

Upon commissioning, the boiler feed pump drive unit shown schematically in Figure 1 was experiencing high radial vibration, Figure 2 (up to 6 mils - pk to pk), at high flow rates (up to 750,000 lb./hr.). Since the flow rate increases with pump speed, the increasingly high vibration was associated with the speed of the drive and the pump. The motor runs

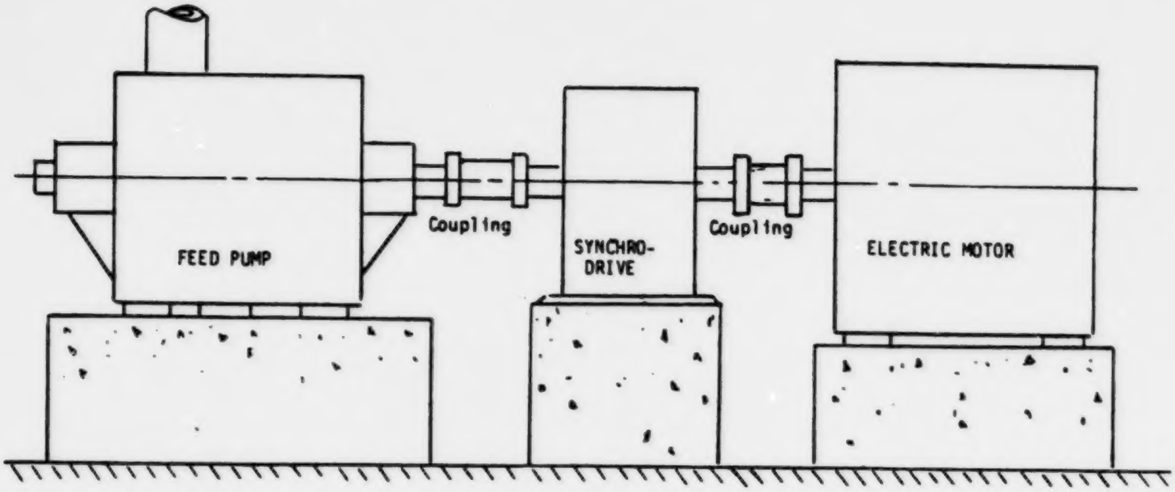
FEED PUMP
Coupling
SYNCHRO-DRIVE
Coupling
ELECTRIC MOTOR

Figure 1. Schematic Arrangement of Boiler Feed Pump Train

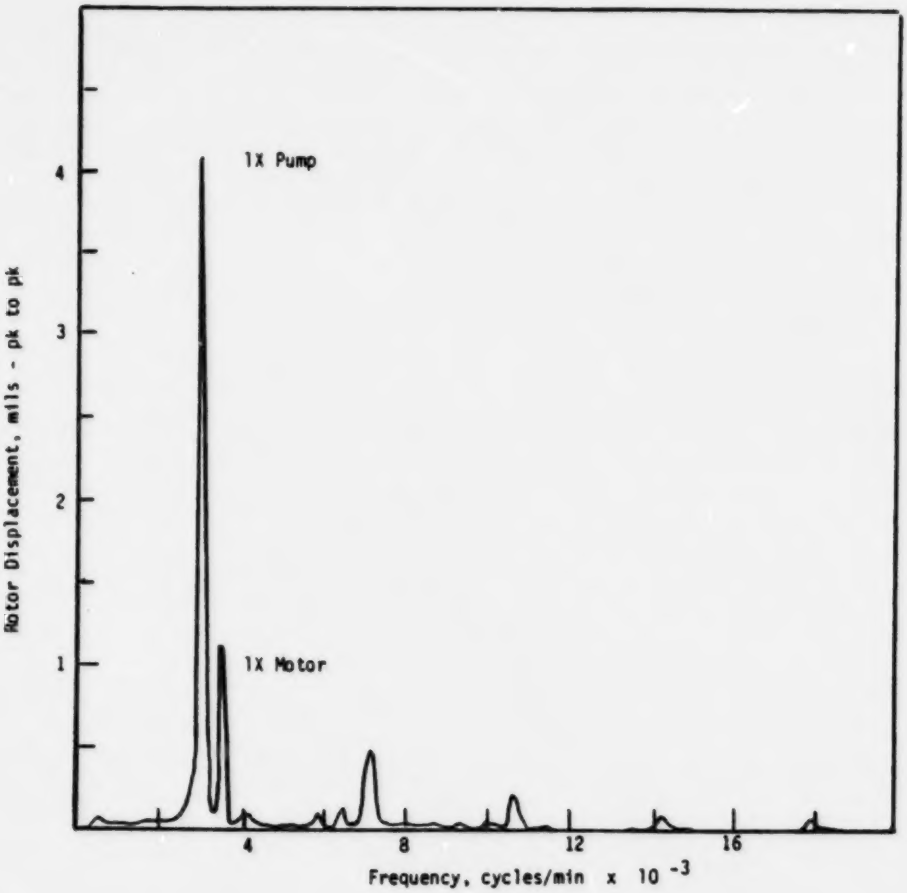

Figure 2. Spectrum of Vibration on Input to Synchro Drive prior to Modification

at a nominal speed of 3600 RPM. The boiler feed pump unit consists of a 4000 Hp, two-pole induction motor driving an eleven stage boiler feed pump through a variable speed drive (Synchro-Drive). Shim pack couplings were used throughout the train. Permanently mounted X-Y proximity probes were used to monitor the vibrations. After repeated attempts to balance the drive, a vibration engineering study was commissioned to determine the source of the excessive vibrations.

FIELD TESTING

Coast down tests were conducted on the output shaft of the Synchro Drive. Figure 3 shows a bode plot of the shaft vibrations, measured with a proximity probe on coast down. Three critical speeds are shown during the coast down -- 2120 RPM, 2900 RPM, and 3450 RPM. The distinct phase changes at the two latter speeds associate these critical speeds with the Synchro Drive. The peak at 2120 RPM is associated with the motor and is not a problem. However, the critical speeds at 2900 RPM and 3450 RPM are within the operating speed of the Synchro Drive; and, therefore, are the cause of the excessive operating vibrations. The Synchro Drive had uncoupled critical speeds in excess of 4400 RPM. Coupling of the unit had dropped two of its critical speeds into the operating speed range.

MODEL STUDY

A math model (Figure 4) of the boiler feed pump drive train was developed. This model included the motor armature on its two plain sleeve bearings; the motor-Synchro Drive coupling (shim pack); the Synchro Drive with its two input shaft elliptical bearings, center guide roller bearing, and output elliptical bearings; and the Synchro Drive - pump shim pack coupling. The pump input stiffness was modeled with radial and angular springs since it was stiff compared to the drive.

It was found that the input bearings of the Synchro Drive were soft in the vertical direction. This had the effect of lowering the third critical speed (3550 RPM) into the system operating speed range (Figure 5). New stiffer bearings were recommended that raised the third critical to 4550 RPM. However, the second critical speed remained at 2980 no matter how much the bearing stiffness was raised.

Figure 6 shows a critical speed map with varied output bearing stiffness with the higher input bearing stiffness. It shows that substantially decreasing the output bearing stiffness will lower the third critical speed but not the second critical speed. Figures 5 and 6 show that the bearing change removes the third critical speed from the operating speed range but leaves the second critical at a speed of 3000 RPM which severely limits the operational versatility of the feed pump. This limited the pump service so that it could not be operated in a range between 250,000 lb./hr. and 550,000 lb./hr.

The next alteration of the unit, to change the second critical speed, was

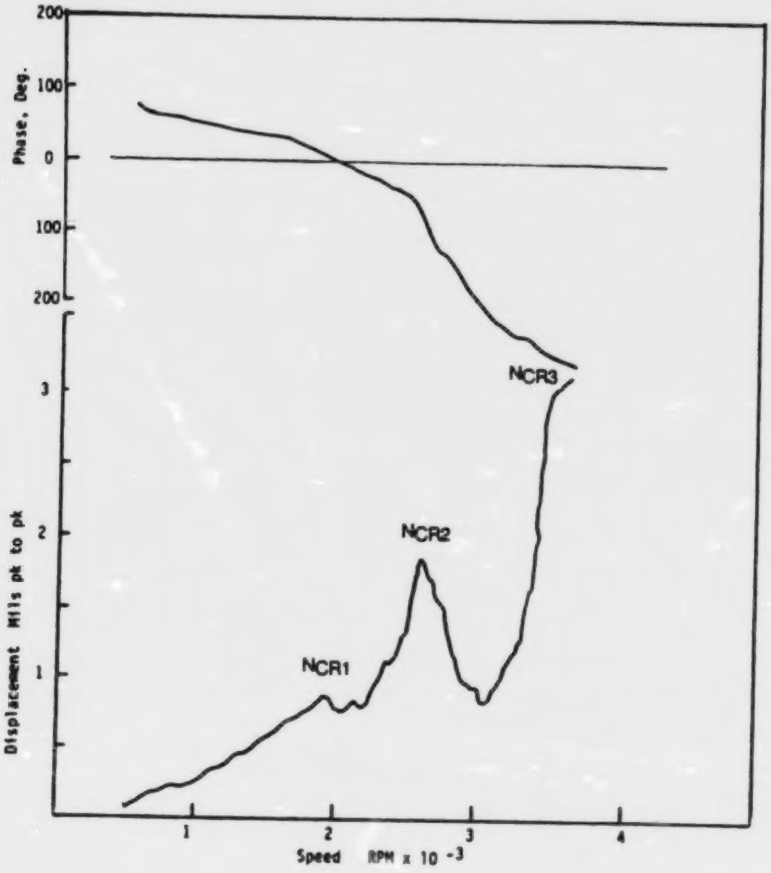

Figure 3. Boiler Feed Pump Coast Down - Drive Output

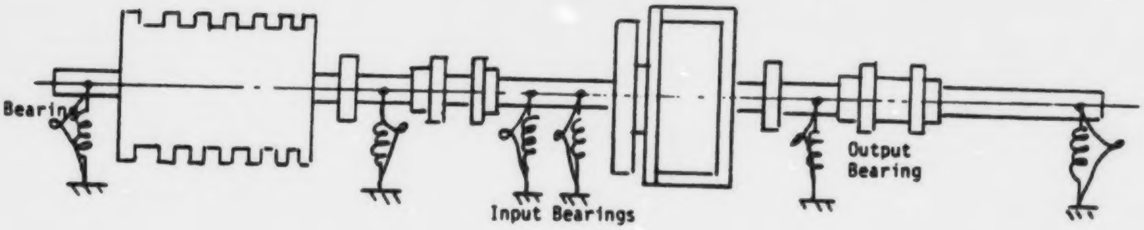
Bearing
Input Bearings
Output Bearing
Motor
Coupling
Fluid Drive
Coupling
Pump

Figure 4. Boiler Feed Pump System Model

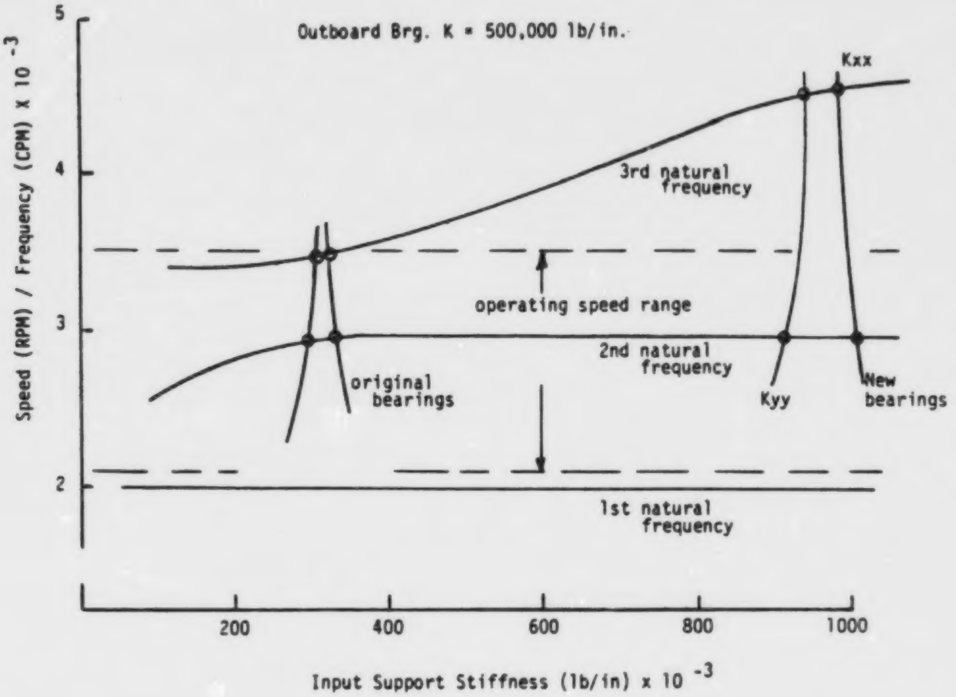

Figure 5. Critical Speed Map of Synchro Drive - Input Bearing

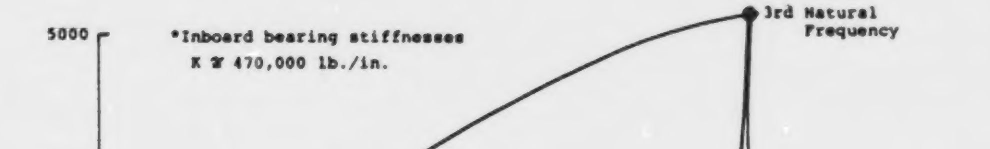

Figure 6. Stiffness - Critical Speed Map - Boiler Feed Pump with Thomas Couplings

on the couplings. It had been shown earlier* that gear couplings tend to flexurally uncouple two machines and raise the critical speeds. The Synchro Drive input and output couplings were modeled as gear couplings and new critical speeds were calculated. The critical speed map, Figure 7, shows that both the second and third critical speeds have been raised substantially -- to 3950 RPM and 5500 RPM, respectively. Thus the gear couplings yield more end restraint under load and effectively raise the critical speed.

DISCUSSION OF RESULTS

After the bearing change, critical speeds were changed as predicted -- the third critical was removed from the operating speed range, and the second was raised to about 2980 RPM. The gear coupling change was bypassed in favor of reconditioning the Synchro Drive.

The Synchro Drives were returned to the factory for reconditioning. At completion of reconditioning, the shop tests revealed a vibration level of 1.5 mils pk to pk at 3500 RPM. The units were subsequently placed in service and vibration levels of 4 to 5 mils pk to pk at 3000 RPM were observed upon startup -- not acceptable by any means. The high vibration level occurred due to the proximity to the second critical speed.

Finally, the gear couplings were installed -- raising the second critical speed out of the operating speed range (Figure 7). The vibration was lowered to 1 mil pk to pk at 3500 RPM -- design problem solved.

However, it was found later, as predicted by Figure 7, that if the output bearing stiffness is allowed to decrease, the second critical speed will drift down toward the operating speed range. As a result, high vibration is observed on the input shaft (Figure 8) at the frequency of the output shaft. Thus there is a great sensitivity in the unit to output bearing wear or installation of a bearing with excessive clearance.

CONCLUSION

This case history illustrates the fact that system critical speeds may not be equal to component critical speeds. For the motor they were equal; for the Synchro Drive the criticals were greatly changed by the overhung elastically connected couplings (shim pack). In this case, the gear couplings uncoupled the system in the lateral modes and provided end restraint because of angular friction due to application of load. Thus, couplings often do make a difference in lateral vibration problems.

In addition, it was shown that bearing clearances are vitally important in the design and operation of turbomachinery.

---

*Eshleman, R.L. and Eubanks, R.A., "Effects of Axial Torque on Rotor Response: An Experimental Investigation," ASME Paper No. 70WA-DE14, ASME, NY, 1970.

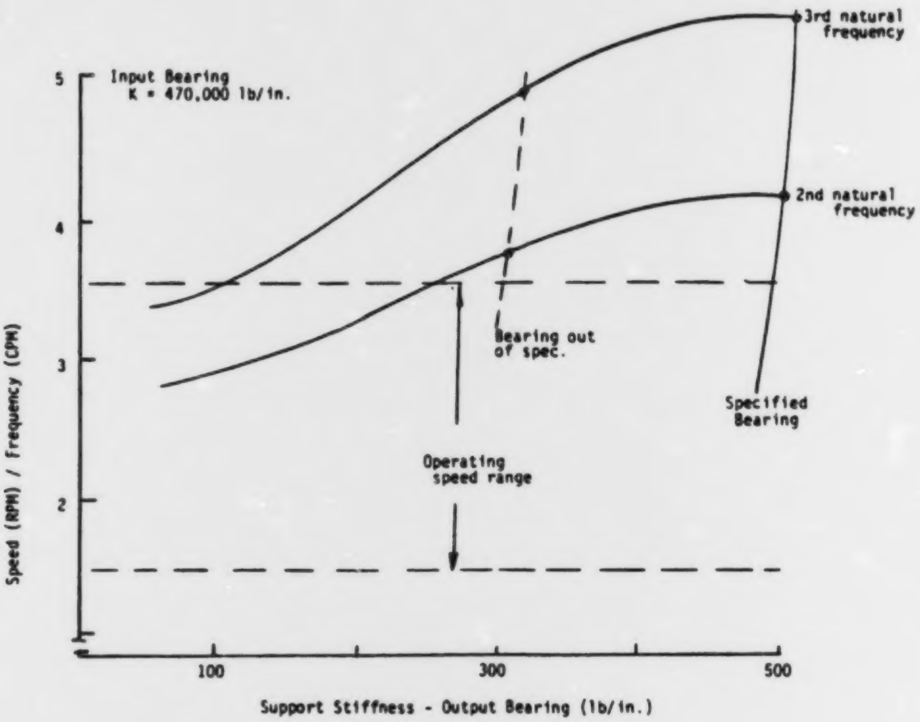

Figure 7. Critical Speed Map - Boiler Feed Pump Train with Gear Couplings

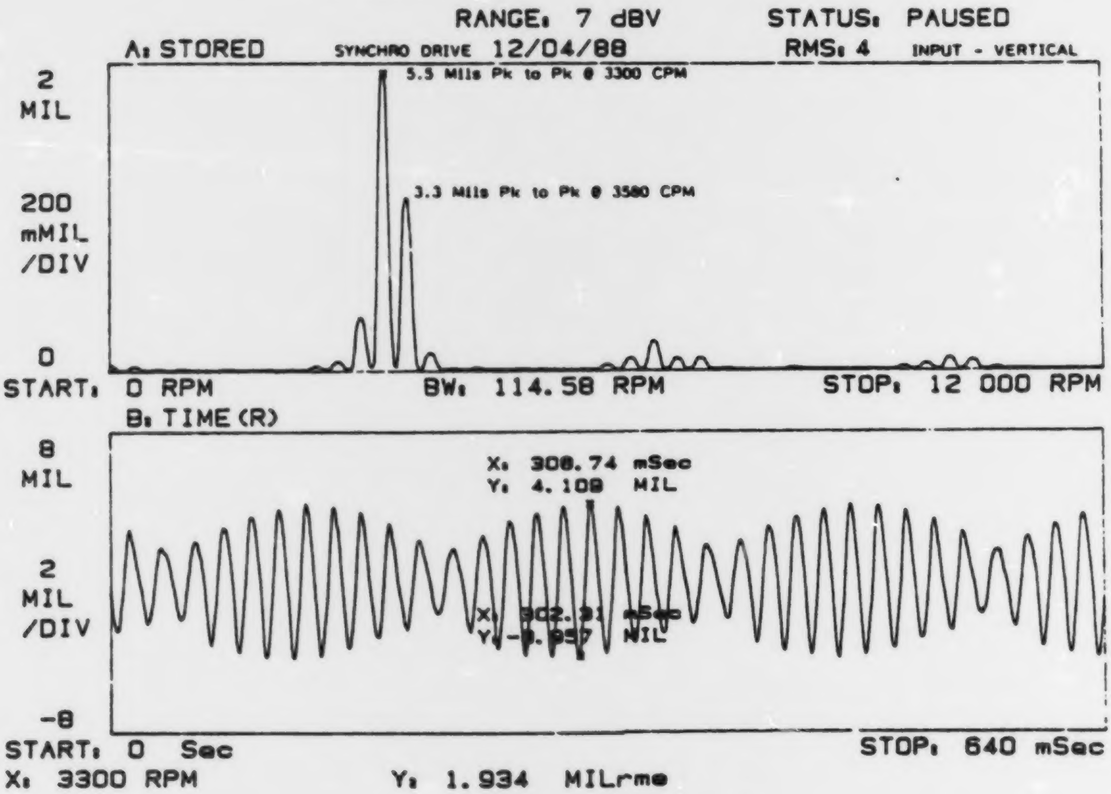

Figure 8. Vibration - Drive Input Vertical

THE USE OF FINITE ELEMENTS IN ROTORDYNAMICS ANALYSIS

W.F. Eckert
A. Craggs

University of Alberta
Edmonton, Alberta
Canada
T6G 2E1

ABSTRACT

Shaft elements based on beam theory are limited in accuracy when used to model discontinuities in shaft sections such as abrupt changes in diameter. Beam theory requires that plane sections remain plane when the shaft or beam is in bending, however at a sharp change in diameter this is clearly not the case. Three dimensional elements are better at representing these changes in shaft section, but at the expense of simplicity and matrix size. Results comparing the two types of elements for modelling shafts will be presented.

KEY WORDS

finite element method, isoparametric element, axisymmetric element

BIOGRAPHICAL SKETCH

William Eckert is currently a Doctorate student at the University of Alberta. He obtained a B.Sc. in Mechanical Engineering from the University of Alberta in 1979, prior to working for Imperial Oil Limited as a mechanical design engineer and a machinery specialist for seven years.

Anthony Craggs is a Professor of Mechanical Engineering at the University of Alberta.

RÉSUMÉ

Les éléments d'arbre basés sur la théorie de poutre possèdent une précision limitée lorsqu'ils sont utilisés pour modeler les sections d'arbre avec changement abrupt de diamètre. La théorie de poutre exige que les sections planes demeurent planes quand l'arbre ou la poutre est sous flexions, cependant cela n'est pas le cas pour transition abrupte de diamètre. Les éléments tri-dimensional sont supérieurs pour la représentation de ces changements dans les sections d'arbre, mais cela est au dépends de la simplicité et de la dimension de la matrice. Des résultats comparant les deux genres d'éléments utilisés pour modeler les arbres seront présentés.

MOTS CLÉS

Éléments finis, éléments isoparamétriques, éléments axisymmétriques

BIOGRAPHIE

William Eckert prépare actuellement son diplôme Ph.D. à l'Université de l'Alberta. Il a reçu son diplôme B.Sc. en mécanique à l'Université de l'Alberta 1979, avant d'être employé comme ingénieur mécanicien et spécialiste en machines tournantes pendant sept années chez Imperial Oil Limited.

Anthony Craggs est Professeur au département de Mechanical Engineering à l'Université de l'Alberta.

INTRODUCTION

Finite element models are essential in the design and vibration analysis of rotating machines. The elements most commonly used are the Euler and Timoshenko beam elements. These beam elements are based on simple bending theory, which assumes that any transverse plane remains plane during bending.

The Euler model is the simplest to formulate and there are many practical situations where it gives excellent agreement with measurements. This is usually where the shaft is fairly uniform, long, and mounted in short bearings. On the other hand, if the span of the shaft is only an order of magnitude or less different from its diameter then shear deformation and rotatory inertia play an important role, and the beam element formulated from Timoshenko theory is the most appropriate. However, both models need some empirical modification when there are many step changes of section.

At abrupt diameter changes in a shaft the assumption of plane sections remaining plane is not true. The transverse plane at the step change in diameter distorts during bending, resulting in reduced stiffness near the discontinuity. Sanderson and Kitching [1] measured this decrease in stiffness for the case of static bending. As a result normal beam elements do not accurately model step changes in shaft diameter, and therefore can give poor predictions when used to calculate the critical speeds of typical machine shafts.

In an effort to improve the modelling of shafts, Geradin and Kill [2], and Stephenson, Rouch, and Arora [3] have devised and tested a subparametric three dimensional axisymmetric element. This element treats the shaft as an elastic solid, and as a result correctly models step changes in diameter. This paper extends that work by using an isoparametric three dimensional axisymmetric elements in comparison to beam elements.

ELEMENT FORMULATION

The element used in this work is a cubic isoparametric axisymmetric element that allows nonsymmetric loads, and bending of the element in the r-z plane. The element geometry is shown in Figure 1. All twelve nodes are used to define the element geometry, as well as defining the element deflections. Therefore, a single element can be used to model uniform, tapered or smoothly varying diameter changes. The previous element used four nodes to define the geometry, while defining the deflections at twelve nodes, and could model uniform or straight tapered shaft sections.

The strain energy for an element of elastic material can be written as follows:

$$\text{Strain Energy} = \frac{1}{2}\iiint \{\varepsilon\}^{T}\{\sigma\}\,\text{dvol} \tag{1}$$

where $\{\varepsilon\}$, $\{\sigma\}$ are the elastic strain and stress vectors respectively. Substituting into (1) the stress-strain relationship (2), results in equation (3).

$$\{\sigma\} = [D]\{\varepsilon\} \tag{2}$$

$$\text{S. E.} = \frac{1}{2}\iiint \{\varepsilon\}^{T}[D]\{\varepsilon\}\, r\, dr\, dz\, d\theta \tag{3}$$

[D] and $\{\varepsilon\}$ are the three dimensional elasticity matrix and the strain vector for cylindrical coordinates, and are given by (4) and (5).

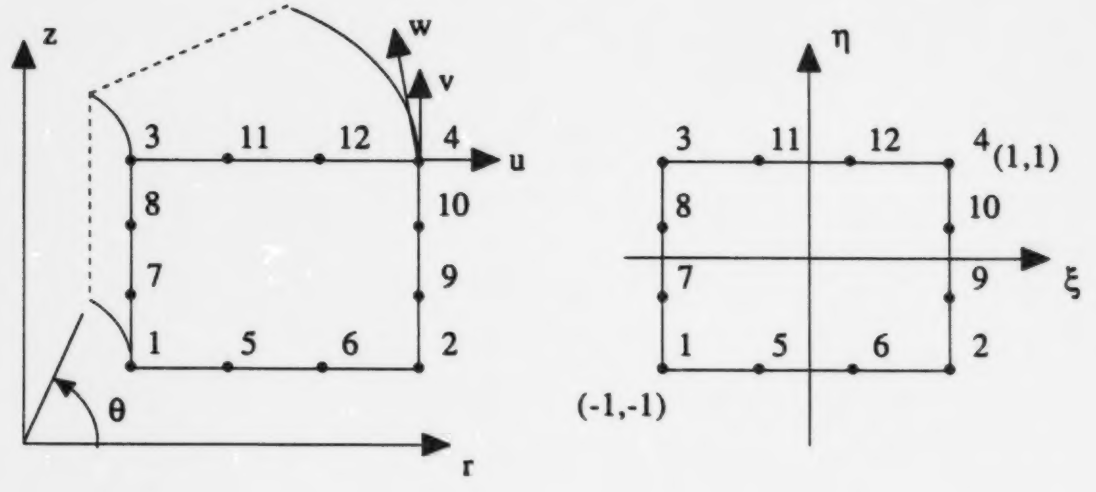

(a) Element Coordinates (b) Local Coordinates

Figure 1. Cubic Isoparametric Axisymmetric Element

$$[D] = \frac{E\,(1-\nu)}{(1+\nu)\,(1-2\nu)} \begin{bmatrix} 1 & \frac{\nu}{(1-\nu)} & \frac{\nu}{(1-\nu)} & 0 & 0 & 0 \\ \frac{\nu}{(1-\nu)} & 1 & \frac{\nu}{(1-\nu)} & 0 & 0 & 0 \\ \frac{\nu}{(1-\nu)} & \frac{\nu}{(1-\nu)} & 1 & 0 & 0 & 0 \\ 0 & 0 & 0 & \frac{(1-2\nu)}{2\,(1-\nu)} & 0 & 0 \\ 0 & 0 & 0 & 0 & \frac{(1-2\nu)}{2\,(1-\nu)} & 0 \\ 0 & 0 & 0 & 0 & 0 & \frac{(1-2\nu)}{2\,(1-\nu)} \end{bmatrix} \tag{4}$$

$$\{\varepsilon\} = \left\lfloor \frac{\partial u}{\partial r},\ \frac{\partial v}{\partial z},\ \left(\frac{u}{r} + \frac{1}{r}\frac{\partial w}{\partial \theta}\right),\ \left(\frac{\partial u}{\partial z} + \frac{\partial v}{\partial r}\right),\ \left(\frac{1}{r}\frac{\partial u}{\partial \theta} + \frac{\partial w}{\partial r} - \frac{w}{r}\right),\ \left(\frac{1}{r}\frac{\partial v}{\partial \theta} + \frac{\partial w}{\partial z}\right) \right\rfloor^{T} \tag{5}$$

To allow for bending of the axisymmetric element, theta dependent cosine and sine terms are included in the displacements (u = radial displ., v = axial displ., and w = tangential displ.) as given in (6). These relationships allow the calculation of the displacement at any point inside the element cross section, and represents in-plane bending only. Note that $\lfloor N \rfloor$ is the transposed vector of the shape (serendipity) functions, and is dependent on the local coordinates ξ and η. The vectors $\{u_e\}$, $\{v_e\}$, and $\{w_e\}$ are the unknowns representing the nodal displacements.

$$u = \lfloor N \rfloor \{u_e\} \cos\theta,\ v = \lfloor N \rfloor \{v_e\} \cos\theta, \text{ and } w = \lfloor N \rfloor \{w_e\} \sin\theta \tag{6}$$

The axial and radial positions (7) at any point in the element are given by the same shape functions resulting in a isoparametric element.

$$r = \lfloor N \rfloor \{r_e\}, \text{ and } z = \lfloor N \rfloor \{z_e\} \tag{7}$$

Using the displacement equations (6), the strain vector (5) can be rewritten as equation (8):

$$\{\varepsilon\} = [B] \left\{ \begin{matrix} \{u_e\} \\ \{v_e\} \\ \{w_e\} \end{matrix} \right\} = [B]\{\delta_e\} \tag{8}$$

where:

$$[B] = \begin{bmatrix} \lfloor N_r \rfloor \cos\theta & 0 & 0 \\ 0 & \lfloor N_z \rfloor \cos\theta & 0 \\ \frac{1}{r}\lfloor N \rfloor \cos\theta & 0 & \frac{1}{r}\lfloor N \rfloor \cos\theta \\ \lfloor N_z \rfloor \cos\theta & \lfloor N_r \rfloor \cos\theta & 0 \\ -\frac{1}{r}\lfloor N \rfloor \sin\theta & 0 & (\lfloor N_r \rfloor - \frac{1}{r}\lfloor N \rfloor)\sin\theta \\ 0 & -\frac{1}{r}\lfloor N \rfloor \sin\theta & \lfloor N_z \rfloor \sin\theta \end{bmatrix} \tag{9}$$

The strain energy equation (3) can now be rewritten, transforming from element to local coordinates using the Jacobian matrix, [J]:

$$\text{S. E.} = \frac{1}{2}\{\delta_e\}^T \left(\int_0^{2\pi}\int_{-1}^{1}\int_{-1}^{1} r[B]^T[D][B]\,\|J\|\, d\xi\, d\eta\, d\theta \right) \{\delta_e\} \tag{10}$$

Since:

$$\int_0^{2\pi} \cos^2\theta\, d\theta = \int_0^{2\pi} \sin^2\theta\, d\theta = \pi, \text{ and } \int_0^{2\pi} \cos\theta \sin\theta\, d\theta = 0 \tag{11}$$

the theta dependent terms can be analytically integrated and the stiffness matrix can be written:

$$[K] = \pi \int_{-1}^{1}\int_{-1}^{1} r(\xi,\eta)[B]^T[D][B]\,\|J\|\, d\xi\, d\eta \tag{12}$$

where the Jacobian relates the derivatives with respect to r and z to ξ and η (13).

$$[J] = \begin{bmatrix} \frac{\partial r}{\partial \xi} & \frac{\partial z}{\partial \xi} \\ \frac{\partial r}{\partial \eta} & \frac{\partial z}{\partial \eta} \end{bmatrix} \quad \text{and} \quad \begin{Bmatrix} \frac{\partial}{\partial r} \\ \frac{\partial}{\partial z} \end{Bmatrix} = [J]^{-1} \begin{Bmatrix} \frac{\partial}{\partial \xi} \\ \frac{\partial}{\partial \eta} \end{Bmatrix} \qquad (13)$$

To derive the mass matrix the virtual work expression (14) can be written:

$$-\partial W = \partial\{\ddot{\delta}_e\}^T \left(\int_0^{2\pi} \int_z \int_r \rho\, [A]^T [A]\, dr\, dz\, d\theta \right) \{\ddot{\delta}_e\} \qquad (14)$$

where:

$$[A] = \begin{bmatrix} \lfloor N \rfloor \cos\theta & 0 & 0 \\ 0 & \lfloor N \rfloor \cos\theta & 0 \\ 0 & 0 & \lfloor N \rfloor \sin\theta \end{bmatrix} \qquad (15)$$

Using equations (11), and the transformation from element to local coordinates allows the mass matrix to be written as:

$$[M] = \pi\, \rho \int_{-1}^{1} \int_{-1}^{1} r(\xi,\eta)\, [A]^T [A]\, \|J\|\, d\xi\, d\eta \qquad (16)$$

The stiffness (12) and mass (16) matrices are only for in-plane bending. For out-of-plane bending the $\sin\theta$ and the $\cos\theta$ terms in equations (6) are replaced by $\cos\theta$ and $\sin\theta$ terms respectively. The resultant matrices for out-of-plane bending are the same as (12) and (16), and are uncoupled from the in-plane bending.

RESULTS

For long slender beams or shafts of uniform cross-section, the three dimensional axisymmetric element compares well in calculated natural frequencies to the Euler beam formulation. However, in this situation the added complexity and larger matrices of the axisymmetric element are a disadvantage, and the beam elements are quite adequate. Also for short stubby beams of uniform cross-section (an example would be a short shaft section between two bearings) the Timoshenko beam element is more than adequate. When the shaft is stubby and has a number of step changes in diameter, the beam elements are inaccurate. In this paper two test cases are presented that illustrate the advantage or difference between the simple bending theory formulation, and the full elastic solid formulation for shafts of this last type.

Case I

The first shaft modelled is shown in Figure 2. The cantilevered shaft is short and stubby, and has a hollow overhung section. The material is steel with an elastic modulus of 30 x 10^6 psi and a density of 0.283 lbs/cu. in. The axisymmetric model had 7 elements with a total of 168 degrees of freedom (DOF). However, the model was statically condensed to reduce the size of matrices before solving the eigenvalue problem. The number of retained DOF are shown in the column headings of Table 1. The beam element model consisted of 28 elements with all 56 DOF retained, and of 56 elements with all 112 DOF retained. The first six calculated critical speeds are shown in Table 1.

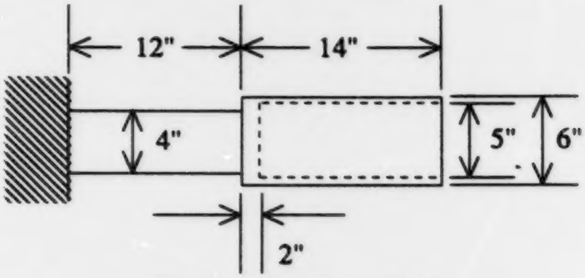

Figure 2. Cantilever Shaft

Table 1. First Six Critical Speeds (Natural Frequencies) in RPM

Timoshenko 56 DOF	Timoshenko 112 DOF	Axisymmetric 54 DOF	Axisymmetric 108 DOF
11561	11557	13134	12822
66690	66683	64792	64628
188131	187985	190021	185819
289884	289400	275109	266643
423057	421610	410398	387730
542514	539599	507354	478886

As can be seen, doubling the degrees of freedom of the Timoshenko model shows that the critical speeds, for this model, have converged. However, the axisymmetric model indicates lower critical speeds, especially for the higher modes. This effect is expected as the step change in diameter has been shown to reduce the effective stiffness of the shaft. Since the axisymmetric element correctly models this effect, it produces a more accurate representation of the shaft critical speeds. The first critical speed of the axisymmetric element appears to be higher than the beam element model. This apparent error is an artifact of the static condensation process. Using a component mode procedure rather that static condensation would improve the first critical calculated.

Case II

The second configuration of shaft modelled is shown in Figure 3. The shaft is simple supported with a increased diameter in the center section. The material properties were the same as Case I. Again the short length and heavy diameter would indicate that the Timoshenko beam element is the best choice for this situation. The axisymmetric model consisted of 4 elements with 102 DOF, and the beam element model consisted of 24 elements with 48 DOF. The first six calculated natural frequencies in rpm are given in Table 2.

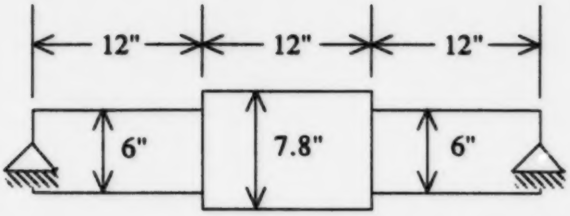

Figure 3. Simply Supported Stepped Shaft

Table 2. Calculated Critical Speeds in RPM

Timoshenko 48 DOF	Axisymmetric 102 DOF
22978	22037
78950	74053
171233	157517
257843	216917
364290	314403
472299	397183

Again the solid axisymmetric element results in much lower critical speeds due to the effect of the step changes in diameter. Here, the lowest critical speed is accurate because no static condensation was used. For this configuration of shaft the Timoshenko element would be the method most likely to be used. However, the results show that the beam element predicts critical speeds that are in considerable error.

CONCLUSION

The higher order axisymmetric element has proven to give more accurate predictions of shaft critical speeds for shafts of typical design. However, this element has some disadvantages, in that it requires more computer memory, and numerical integration to form each element. For uniform shaft sections, the beam element formulations are acceptable. But most rotating machine shafts have fairly heavy cross sections to the span length ratios, and incorporate a number of shaft diameters. For these shaft designs, the results indicate that the plane sections remain plane assumption causes unacceptable errors. Therefore, the three dimensional axisymmetric solid element should be the element of choice for accurate modelling of the dynamic properties. If necessary the Euler, Timoshenko and axisymmetric elements can be combined to model a shaft.

REFERENCES

[1] N. Sanderson and R. Kitching, "Flexibility of Shafts with Abrupt Changes of Section", *Int. J. Mech. Sci.*, Vol. 20, 1978, pp. 189-199.

[2] M. Geradin and N. Kill, "A New Approach To Finite Element Modelling Of Flexible Rotors", *Eng. Compt.*, Vol. 1, March 1984, pp. 52-64.

[3] R.W. Stephenson, K.E. Rouch, and R. Arora, "Modelling Of Rotors With Axisymmetric Solid Harmonic Elements", *Journal of Sound and Vibration*, 131, 1989, pp. 431-443.

[4] O.C. Zienkiewicz, "The Finite Element Method In Engineering Science", McGraw-Hill, 1971, pp. 263-267.

SIMPLIFIED PREDICTON OF BALANCE SENSITIVITY

Brian C. Howes, M.Sc., P.Eng.
Scott G. Masterson, B.Sc.

Beta Machinery Analysis Ltd.
300, 1615 - 10 Avenue S.W.
Calgary, Alberta
T3C 0J7

RÉSUMÉ

Il est possible d'estimer la première et la seconde vitesses critiques d'un rotor à l'aide de mesures pendant un ralentissement.

En combinant la connaissance des vitesses critiques à la géométrie et au poids du rotor, il est possible d'estimer la sensibilité au déséquilibre statique et dynamique.

Le rotor devrait fonctionner dans la zone "rotor rigide", par opposition à la zone "rotor flexible".

BIOGRAPHIE

Brian C. Howes, M. Sc., ing., est ingénieur en chef à la Beta Machinery Analysis Ltée, à Calgary (Alb.), et, depuis 1972, il a participé activement au dépannage des machines à mouvement tant rotatif qu'alternatif. C'est l'un des experts les plus en vue en analyse des vibrations.

G. Scott Masterson est également ingénieur de projet chez Beta Machinery Analysis Ltée.

SIMPLIFIED PREDICTION OF BALANCE SENSITIVITY

Brian C. Howes, M.Sc., P.Eng.
Scott G. Masterson, B.Sc.

Beta Machinery Analysis Ltd.
300, 1615 - 10 Avenue S.W.
Calgary, Alberta
T3C 0J7

ABSTRACT

It is possible to estimate the first and second critical speeds of a rotor by making use of measurements during a coast-down.

Combining the knowledge of the critical speeds with the geometry and weight of the rotor, it is possible to estimate the sensitivity to static and dynamic unbalance.

The rotor should be operating in the "rigid rotor" region as opposed to the "flexible rotor" region.

BIOGRAPHICAL SKETCH

Brian C. Howes, M.Sc., P.Eng., is the Chief Engineer at Beta Machinery Analysis Ltd. in Calgary, Alberta, and has been involved in machinery troubleshooting for both rotating and reciprocating equipment since 1972. He is one of the foremost experts in vibration analysis.

Scott Masterson is also a Project Engineer with Beta Machinery Analysis Ltd.

INTRODUCTION

This paper describes a technique for balancing machines at speeds between their first and second shaft criticals in a single run.

When a machine has no balancing history, conventional balancing procedures will often require two or three trial weight runs to determine sensitivities and to balance the rotor. Unfortunately, costly down-time often prevents the completion of such a job.

The method of STATIC - DYNAMIC BALANCING uses the following assumptions to simplify the problem:

1. The rotor and its supports are approximately symmetrical about the centre of mass.
2. Two plane balancing is being performed.
3. Static and dynamic components of vibration are being considered as opposed to the "raw" vibration.
4. The machine approximates a rigid rotor/flexible bearing system. (Refer to Figure 1).

The experimental technique requires the collection of "as found" and "coast-down" vibration data. These data, along with some of the physical characteristics of the machine, will enable a calculation of both the static and dynamic balance sensitivities of the system. Some sample calculations will follow.

The reasoning behind this type of balancing is that a two plane balance problem can be effectively reduced to two single plane problems that can be solved simultaneously in one run.

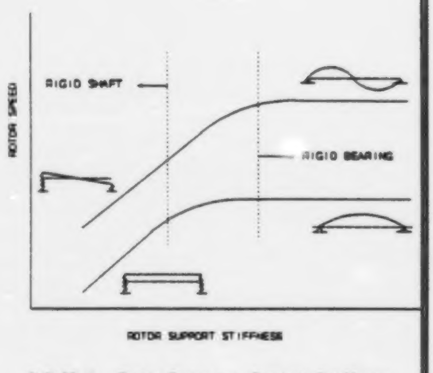

FIGURE 1 Rotor Speed vs Support Stiffness

PROCEDURE

Static - Dynamic balancing proceeds as follows:

1. Collect "As Found" vibration data.
    - Proximity probes give the best results for rigid pedestals.
    - Shaft absolute (Shaft stick) data is more appropriate when pedestal vibration is significant.
2. Obtain displacement amplitude and phase data from the coast-down.
3. After performing runout subtraction, resolve the "as found" and coast-down data into static and dynamic components. (Refer to: Rotor Balancing by Static-couple Derivation, John M. Csokmay).
4. Construct Bode or Nyquist plots of both the static and dynamic components of the rundown.
5. Determine the first (static) critical from coast-down data, and ensure that the operating speed is below the second (dynamic) critical.
6. Estimate the total rotating mass.
7. Calculate the theoretical static and dynamic balance sensitivities. (See calculations that follow procedure.)
8. Calculate both the static and dynamic masses required at each balance plane from the sensitivities.
9. Determine the angles by which the high spots lag the heavy spots from the two coast down plots. Locate the light spot for both static and dynamic unbalances on each balance plane.
10. Vectorially sum the masses required at each balance plane and attach the two resultant masses at the required locations.

CALCULATING STATIC AND DYNAMIC BALANCE SENSITIVITIES

This method operates under the premise that both static and dynamic (couple) unbalances are independent and have separate balance sensitivities. These sensitivities are calculated as follows:

Static Sensitivity

The force from static unbalance mass, m_s, rotating at a radius, r, and speed, w

Equals:

The force of the entire rotating mass, M rotating about an eccentric distance, e_s at speed, w.

Or:

$$(m_s)(r)(w)^2 = (M)(e_s)(w)^2$$

The static sensitivity can be given in the following terms:

$$S_s = (m_s)(r)/(e_s) = M$$

Static Sensitivity: (continued)

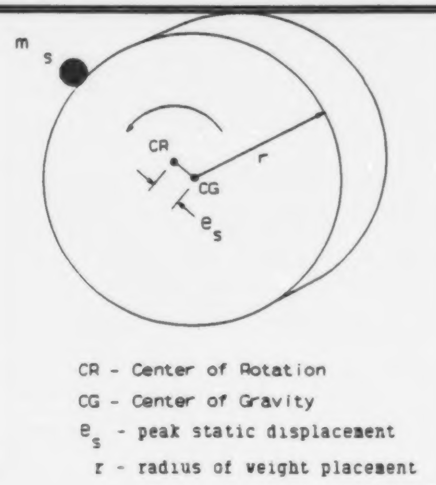
m
s
CR
CG
e
s
r
CR - Center of Rotation
CG - Center of Gravity
e_s - peak static displacement
r - radius of weight placement

Figure 2 Static Unbalance

Dynamic Sensitivity: (See Figure 3)

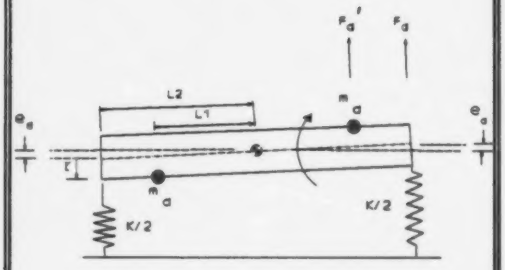
F_d'
F_d
L2
L1
m_d
e_d
e_d
r
m_d
K/2
K/2

Figure 3 Dynamic Unbalance

The force from the dynamic unbalance mass, m_d rotating at a radius, r and speed, w

Equals:

The dynamic force opposing the stiffness, K at each bearing.

The total bearing stiffness is calculated as follows:

$w_c = (K / M)^{1/2}$

$K = M w_c^2$

But the stiffness at a bearing is K/2

The dynamic force at the bearing opposing this stiffness is:

$F_d = K/2\ (e_d) = 0.5\ M(e_d)(w_c)^2$

The force from the dynamic unbalance mass at each balance plane is:

$F_d' = (m_d)(r)w^2$

But the dynamic forces at the bearings are reduced by the ratio of L_1/L_2:

$F_d = F_d'\ (L_1/L_2)$

Let: $c = (L_1/L_2)$

$F_d = c\ (m_d)(r)w^2$

Equating Forces:
$c\ (m_d)(r)w^2 = 0.5\ M\ (e_d)w_c^2$

The dynamic sensitivity is then:

$$S_d = (m_d)(r)/(e_d) = \frac{M\ w_c^2}{2\ c\ w^2}$$

Where:

M = total rotating mass
e_s = peak static component of displacement at bearing
e_d = peak dynamic component of displacement at bearing
m_s = total static mass
m_d = dynamic mass at each balance plane
r = radius of balance weights
w = rotational speed at which es is measured
w_c = first critical speed
S_s = static balance sensitivity
S_d = dynamic balance sensitivity
L_1 = distance from balance plane to centre of mass
L_2 = distance from bearing to centre of mass
c = ratio of L_1/L_2
F_d = dynamic force at each bearing
F_d' = dynamic force at each balance plane
K = combined bearing stiffnesses

EXAMPLE 1:

SAMPLE BALANCE CALCULATIONS FOR A 30 MW GENERATOR

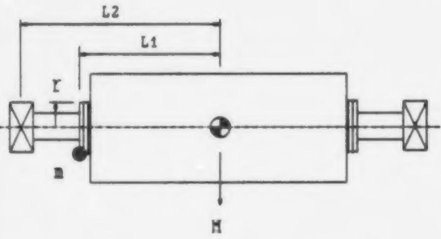

Figure 4 Generator Rotor

Total rotor mass: M = 11,800 kg
Operating Speed: w = 3600 rpm
1st Critical Speed: w_c = 1350 rpm
Radius for Balance Weights: r = 14 "
L_1/L_2 ratio: c = 0.67

Estimate of Balance Sensitivities:

Static Sensitivity:

$S_s = (m_s)(r)/(e_s) = M$
S_s = 11,800 kg in/in pk
= 416 oz-in/mil pk
= 208 oz-in/mil p-p

This is the total sensitivity.

104 oz-in/mil p-p will be required at each balance plane.

(manufacturers rated static sensitivity
is 200 oz-in/mil p-p total)

Dynamic Sensitivity:

$$S_d = (m_d)(r)/(e_d) = \frac{M\, w_c^2}{2\, c\, w^2}$$

$$S_d = \frac{(11{,}800 \text{ kg})(1350)^2}{2(.67)(3600)^2}$$

S_d = 1240 kg in/in pk
= 43.7 oz-in/mil pk
= 21.8 oz-in/mil p-p

This is the sensitivity at each bearing. 21.8 oz-in/mil p-p will be required at each balance plane.

(manufacturers rated dynamic sensitivity
is 14-21 oz-in/mil p-p)

Figures 5 and 6 demonstrate the static and dynamic components of the generator coast-down vibration. Data have been taken with proximity probes, and slow roll corrected. The angles by which high spots lag the heavy spots can be found from the total phase changes over the coast-down.

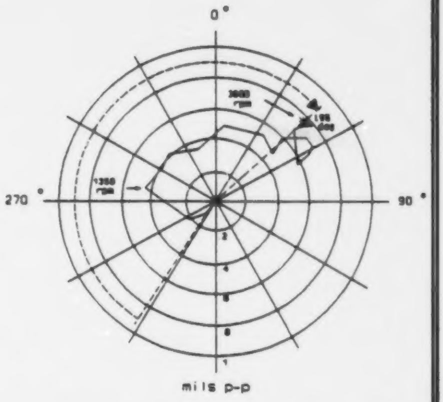

Figure 5 Static Component of Generator Coast-Down

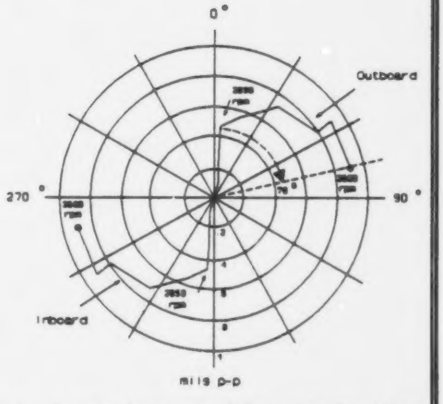

Figure 6 Dynamic Component of Generator Coast-Down

EXAMPLE 2: COAL DRYER EXHAUST FAN

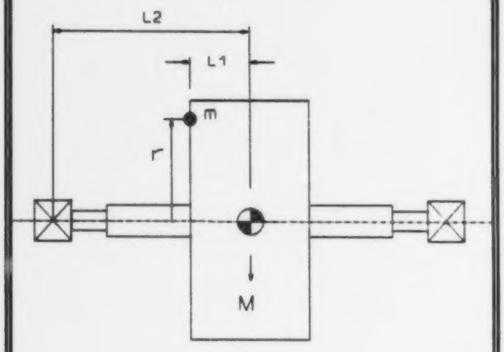

Figure 7 Dryer Exhaust Fan Rotor

Machine Layout

Total Rotor Mass M = 10,200 Kg
Operating Speed w = 1190 RPM
First Critical Speed w_c = 880 RPM
Radius for Balance Wts. r = 48"
L_1/L_2 Ratio c = .22

Estimate of Balance Sensitivities

Using the same calculations as Example 1, the following sensitivities are obtained:

Estimated
Static Sensitivity: S_s = 180 oz-in/mil p-p

Estimated
Dynamic Sensitivity: S_D = 224 oz-in/mil p-p

Estimate of Balance Weight Placements

Figures 8 and 9 show static and dynamic rundown plots. The static lag angle (high spot lags heavy spot) is about 130° and the dynamic lag angle is about 75°.

The static and dynamic weights should be placed opposite the respective heavy spots.

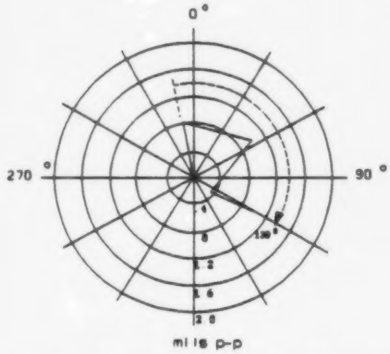

Figure 8 Static Component of Fan Coast-Down

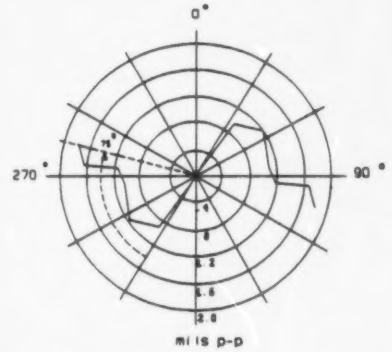

Figure 9 Dynamic Component of Fan Coast-Down

Actual Balance Sensitivities

A. As Found Case Vibrations:

Fan Outboard	1.91 mils p-p, 118°
Fan Inboard	.80 mils p-p, 227°

Resolved As Found Case Vibrations:

Static Component	=	0.90 mils p-p, 143°
Outboard Dynamic Component	=	1.14 mils p-p, 99°
Inboard Dynamic Component	=	1.14 mils p-p, 279°

B. Attach Balance Weights

These balance weights were determined from previously known overall sensitivities before the rotor mass was known.

Total Static Weight	=	101 g
Dynamic Weight	=	123 g per side

Vibration after placement of balance weights:

Static Component	=	.38 mils p-p, 179°
Outboard Dynamic Component	=	.30 mils p-p, 348°
Inboard Dynamic Component	=	.30 mils p-p, 168°

C. Weight Effect Vectors, T.

ie: T = Effect of Weights =
(Trial weight vibration) - (As found vibration)

T_{Static} = .38, 179° - .90, 143°
= 0.63 mils p-p, 302°

$T_{Dynamic\ Outboard}$ = .30, 348° - 1.14, 99°

= 1.28 mils p-p, 292°

D. Calculation of Actual Sensitivities:

Static Sensitivity, $S_S = M_s r/T_{Static}$

= 101g x 48"/.63 mils p-p

= 7695 g-in/mil p-p

S_s = 271 oz-in/mil p-p

Dynamic Sensitivity, $S_d = M_d r/T_{Dynamic}$

= 123 g x 48"/1.28 mils p-p

= 4613 g-in/mils p-p

S_d = 163 oz-in/mils p-p

EXAMPLE 3: ROTOR MODEL

Here is an example of a non-symmetrical rotor with a very flexible shaft. The layout is shown in Figure 10.

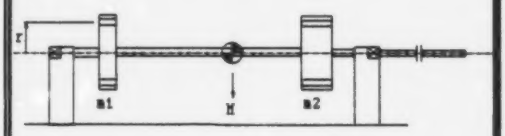

Figure 10 Rotor Model

$M = 1612$ g
$m_1 = 629$ g
$m_2 = 816$ g

$w = 5000$ rpm
$w_c = 3500$ rpm
$r = 1.2"$
$c = .66$

Estimated and actual sensitivities are as follows:

Static Sensitivity:

Estimated, $S_s = .0284$ oz-in/mil p-p
Actual, $S_s = .0177$ oz-in/mil p-p

Dynamic Sensitivity:

Estimated, $S_D = .0102$ oz-in/mil p-p
Actual, $S_D = .0289$ oz-in/mil p-p

The discrepancies between actual and estimated values result from the fact that the shaft is neither rigid or symmetrical.

It should be noted that there are additional sources of dynamic unbalance when the balance weights at a plane are not symmetrically applied.

Table 1 summarizes the estimated and actual sensitivities of the three examples presented.

TABLE 1 STATIC AND DYNAMIC BALANCE SENSITIVITIES - ESTIMATED VS. ACTUAL

CASE STUDY	$\frac{w/w_{c1}}{w/w_{c2}}$	STATIC SENSITIVITY			DYNAMIC SENSITIVITY		
		ACTUAL oz-in/mpp	ESTIMATED oz-in/mpp	ACT/EST	ACTUAL oz-in/mpp	ESTIMATED oz-in/mpp	ACT/EST
Rotor Model 1.6 kg Rotor 5000 rpm	1.43 .71	.0177	.0284	.62	.0289	.0102	2.83
Generator 11,800 kg 3600 rpm	2.67 < 1	200	208	.96	14 - 21	21.8	.64 - .96
Dryer Exhaust Fan 10,000 kg 1190 rpm	1.35 < 1	271	180	1.5	163	224	.73

This type of modal balancing enables a good first estimate of balance sensitivities when the rotor is rigid and symmetrical about its center of gravity. The degree to which the rotor becomes flexible and non-symmetrical determines the variation between the estimated and actual sensitivities.

References: Csokmay, J. M.,
"Rotor-Balancing by Static-Couple Derivation."
IRD Mechanalysis, Inc. Columbus, Ohio

A REVIEW OF FLUID EFFECT MODELLING IN ROTOR DYNAMICS

Anthony G. Taylor, Anthony Craggs
University of Alberta
Edmonton, Alberta T6G 2G8

October, 1990

The analysis of the behaviour of turbomachinery by commissioning engineers and 'trouble-shooting' specialists in rotor-dynamics has been, to a large extent experiential. However, the prediction and analysis of some of these problems at the design stage has proved very difficult in spite of the great many academic and industrial papers written since the early 20's. In many instances, for non-critical machinery, little attempt has been made to predict the vibrational behaviour at the design stage. This article is a review of the methods of rotor-dynamics analysis used to - date, with emphasis on the fluid modelling.

Key Words: rotordynamics, instability, whirl, whip

Biographical Note

Anthony Taylor is an engineer who has worked in vibration analysis and acoustics for about 20 years, most recently as a field engineer for Bently Nevada Canada Ltd., Nisku, Alberta. He has B.Eng. and M.Eng. degrees from the Universities of Sheffield (England) and Toronto respectively and is presently pursuing a Ph.D. at the University of Alberta. Anthony Craggs is a professor in the Mechanical Engineering department at the University of Alberta.

RÉSUMÉ

L'analyse du comportement des machines tournantes par ingénieurs et spécialistes en dynamiques des rotors, a été basée fortement dans l'expérience pratique. Cependant, la prédiction des problèmes, au stage de dessin reste toujours très difficile malgré un grand nombre d'articles académiques et industriels qu'on publie depuis les années vingt. Souvent, pour des machines non-critiques, une telle analyse n'est jamais faite. Cet article est une revue des méthodes d'analyse utilisées, en soulignant l'influence des forces dues aux fluides.

MOTS CLÉS

Dynamiques, machines tournantes, instabilité, tourbillon, fouettement

BIOGRAPHIE

Anthony Taylor est analyste de vibration et de l'acoustique depuis vingt ans, le plus récemment chez Bently - Nevada Canada Ltée, Nisku, Alberta. Il détient des diplômes de B.Eng. et M.Eng. des Universités de Sheffield (Angleterre) et Toronto respectivement et prépare actuellement son Ph.D. à l'Université de l'Alberta. Anthony Craggs est professeur au département de génie mécanique à l'Université de l'Alberta.

1 Introduction

In Jeffcott's much cited 1919 paper [1], the response of a simple rotor with a weightless shaft and pinned - pinned bearings was analyzed. The behaviour of such a system, as set out by Jeffcott, is essentially as taught today in industry seminars on balancing, including the expressions 'critical speed' and 'heavy spot', which he probably coined.

Jeffcott made no assumption about the frequency of precession that would be caused by simple unbalance, but proved that for this axi - symmetric system, it would indeed be synchronous with rotation. He derived the frequency of maximum unbalance response and the amplitude at that speed for a given level of viscous damping.

The addition to the model of oil - film bearings and seals, working fluids, a support structure which is usually of non - symmetric stiffness and a rotor which may have non - axi - symmetric properties and internal hysteretic damping, introduces major complexities to the mathematics and various mechanisms of unstable vibration. Some simplifying assumptions can be made. For instance for machine trains where a process steam turbine or motor drives a compressor through a gear coupling or other flexible coupling, it is generally assumed that coupling of lateral vibration between machines is negligible.

This has been shown in most cases to be a reasonable assumption, but the problem remains very difficult. However where machines are coupled with solid couplings or are strongly coupled (from a vibrational point of view) through the structure, e.g. as in vertical pump - sets, this assumption cannot be made.

The inability to accurately predict rotordynamic phenomena, particularly instability problems, has resulted in many very expensive retro - fits [2] and in the writer's own consulting experience, the total replacement of a process steam turbine [3]. Modelling the solid, elastic parts of the rotor and support structure is amenable to standard methods such as the lumped mass / transfer matrix approach for beam structures such as shafts. The Raleigh-Ritz method has been used for many years for coupling several admissible functions (i.e. shapes which satisfy the boundary conditions such as mode shapes) [4] in order to analyze the elastic vibrations of structures, and more recently, finite element methods have become common for determining the natural frequencies and mode shapes of the structures.

The motion-dependent forces generated in the fluids were first modelled for rotating equipment in the late 40's. In contrast, the motion dependent aerodynamic forces, responsible for wing divergence and flutter, have been incorporated into aeroelastic analyses since well before World War II. Theodorsen's detailed paper[5] in 1935 derived the oscillatory aerodynamic forces using potential flow theory. The expressions for these forces were, in turn, incorporated into the mathematical model of the airplane structure, from which flutter and divergence 'critical speeds' could be derived.

In rotating equipment, the counterparts of flutter; oil whirl and oil/aerodynamic whip, have been well characterized and can be readily identified with appropriate instrumentation. The term 'whirl' is used widely but with various interpretations. The most common usage, which will be used in this review, refers to the precessional motion of a rotor or of a journal within a bearing, at some circular frequency, which may be the same as the rotor rotational frequency (synchronous whirl), subsynchronous i.e. at a frequency below that of rotation speed, or supersynchronous. To further characterize the precessional frequency, it may be subharmonic i.e. at a frequency equal to an exact fraction of rotation speed or harmonic, equal to an exact multiple of rotation speed and which is therefore phase-locked to any whirl component at rotational speed frequency. There is not universal agreement on the terminology, particularly of 'synchronous' and 'harmonic'. However, the above meanings seem to be the most widely used.

The term 'swirl' has been coined and is generally applied to the motion of the fluid rather than that of a rotor. Also 'subrotative' is sometimes used for subharmonic. 'Oil-whirl' or 'journal-whirl' as Newkirk and Taylor described it [6] is a self-excited instability which can occur at any speed below the first lateral rotor / bearing / structure 'critical speed' which is characterized by a precessional frequency equal to typically 43%- 48% of rotation speed and which therefore tracks rotation speed [7, 8]. The writer has on one occasion, seen evidence of some oil whirl above the first critical. Charles Jackson, experienced field engineer, author of [9] and numerous papers confirms this (private communication) and Muszynska, [10] develops an analytical mechanism for it, but it is rare and seems, at least at present, to be of little consequence.

'Whip' prefaced by 'oil', 'aerodynamic', 'steam', or 'gas' depending on the swirling fluid driving the motion is characterized by a precessional frequency essentially equal to that of the first critical speed (natural frequency) and which can occur when rotation speed exceeds approximately twice the first critical frequency. That is to say, this frequency is essentially constant for increasing rotor speed and the instability can occur at a speed such that this natural frequency is a lower eigenvalue of the system than the oil whirl frequency. There are other causes of 'resonant whip', which will be discussed below (Subsection 2.4). Oil-whirl is an instability localized to a bearing and can cause severe damage to the bearing although in many instances does not. The rotor motion generally involves no excitation of the elastic modes of the rotor, the entire rotor moving as a rigid body with the journals. Whip involves a natural mode of the rotor/bearing system and can cause severe damage to bearings, seals or the rotor. However, there are many machines operating with a small amount of whip. That is, vibration signals show a persistent component of vibration at the first rotor/bearing natural frequency (critical) with no deleterious effects. This suggests that there are 'degrees' of instability. That is to say that although the presence of some subsynchronous vibration at a natural frequency implies self excitation, the amplitude is self limiting.

Although Newkirk made the distinction between oil-whirl and whip in 1925 on the basis of experiments and Robertson confirmed this analytically in 1933 [11], the low frequency tracking phenomenon seems to have been absent from later studies by Newkirk [12], Lund [13] (his results show it but it is not discussed) and the very detailed work by Gunter [14]. In these later studies, attention was confined to the conditions necessary for whirl or whip at speeds exceeding the first critical speed only.

From the point of view of the industrial 'end-user' of turbo- machinery, a precise understanding of the dynamics of the machine is rather academic, except in so far as knowing what is to be the 'fix' and in assigning liability for the problem, e.g. the pump or the motor manufacturer. In order to protect the end user, many standards have been developed which can be used for specifying acceptance levels of vibration (American Petroleum Institute, International Association for Standardization - I.S.O., Hydraulic

Institute etc.).

These standards specify vibration limits, either seismic i.e. on the machine casing (usually bearing housing) vibration relative to ground, or shaft displacement relative to the bearing housing. In the case of the A.P.I. Standards, which are widely used on this continent, detailed acceptance procedures are set out for proving a machine on the test stand. This has in the past included a limit on the crest factor or 'Q' value of the resonance peak in vibration measured when passing through the 'critical speeds' during a run-down of the machine. This is usually defined today as the ratio of the resonant frequency to the bandwidth at the 3 dB down point, i.e. at an amplitude equal to 0.707 times the peak value.

This gave a measure of protection in effectively demanding a minimum level of damping in the lateral bending modes, thereby limiting the response due to residual unbalance and, hopefully, the sensitivity of those modes to instability. Recently this provision has been removed, to the regret of some specialists in the field, but presumably because of the possible use of 'anti- swirl' devices which can eliminate 'whip' even in a machine with a high 'Q'. The writer has experience of such an installation [15] in which an anti - swirl seal system [16] was used most successfully.

Unfortunately, such test procedures do not guarantee a trouble- free machine because the loading conditions can rarely be simulated adequately on the test stand and the properties of the machine foundation are unlikely to be the same as the field installation. There has been considerable progress in the modelling and understanding of fluid induced forces in turbomachinery in the last few years, particularly with respect to instability. However, the theories developed do not represent all machinery configurations or operating conditions.

The fluid effects in large, slowly rotating machinery, of both vertical and horizontal configurations do not appear to have been modelled. Also the assumption of small perturbations of a rotor within a seal or bearing, about a mean eccentricity position is generally if not universally made. In machines such as large induced or forced draft fans and large motors it is not unusual to see a shaft orbit 60-70 % of the bearing clearance with no deleterious effects. In hydraulic turbine-generator sets and large vertical pumpsets, clearances are large and so is the shaft-relative motion. Clearly, the small perturbation assumption and the consequent constant film pressure assumption made in calculating bearing stiffness and damping coefficients are questionable in so far as predicting instability is concerned.

This article is an over - view of the types of analysis that have been carried out over many years, into the vibrational behaviour of rotating machinery. This is prior to the undertaking of additional research at the University of Alberta.

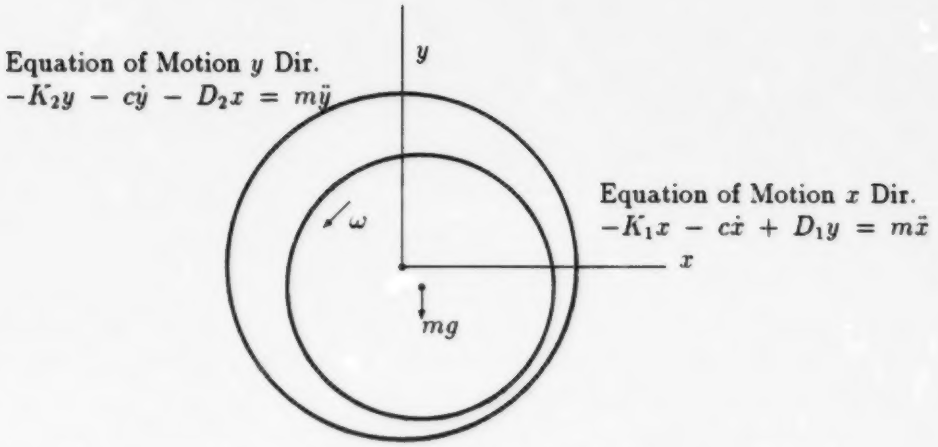
Equation of Motion y Dir.
$-K_2 y - c\dot{y} - D_2 x = m\ddot{y}$
y
Equation of Motion x Dir.
$-K_1 x - c\dot{x} + D_1 y = m\ddot{x}$
ω
x
mg

Figure 1: Equations of Motion of Centre of Mass of Simple Rotor - Notation

2 Literature Review

2.1 Instabilities (Whirl / Whip), Bearing Coefficients

Hagg, [17] in his abstract, groups oil whirl and whip together, but notes that the 'upper limit of whirling frequency has been found to be one half rotational frequency in the general case'; this limit being reached for the case of an unloaded bearing. This therefore does not include the 'tracking' oil whirl phenomenon but only the essentially constant frequency 'whip' instability. Hagg sets up the equations of motion for a single bearing (rigid rotor) as:

$$m\frac{d^2x}{dt^2} + c\frac{dx}{dt} + K_1 x - D_1 y = 0 \tag{1}$$

$$m\frac{d^2y}{dt^2} + c\frac{dy}{dt} + K_2 y + D_2 x = 0 \tag{2}$$

or

$$\begin{bmatrix} m & 0 \\ 0 & m \end{bmatrix}\left\{\begin{array}{c} \ddot{x} \\ \ddot{y} \end{array}\right\} + \begin{bmatrix} c & 0 \\ 0 & c \end{bmatrix}\left\{\begin{array}{c} \dot{x} \\ \dot{y} \end{array}\right\} + \begin{bmatrix} K_1 & -D_1 \\ +D_2 & K_2 \end{bmatrix}\left\{\begin{array}{c} x \\ y \end{array}\right\} = \left\{\begin{array}{c} 0 \\ 0 \end{array}\right\} \tag{3}$$

where: x and y are lateral displacements of the mass centre, m is the mass of the rotor, c is the viscous damping coefficient (axisymmetric), K_1 and K_2 are the direct stiffness coefficients in the x and y directions and D_1 and D_2 are the cross - coupling stiffness coefficients, see Figure 1.

This comes from considering a small perturbation in position of the journal so that the pressure field remains unchanged. The cross - coupling stiffness terms arise from geometry changes only. Assuming a solution of the form $x = A_1 e^{\lambda t}$, $y = A_2 e^{\lambda t}$ and applying Routh's stability criterion to the characteristic equation in λ^4, a necessary and sufficient condition for stability is obtained:

$$(K_1 - K_2)^2 + 2c^2\left(\frac{K_1}{m} + \frac{K_2}{m}\right) > 4D_1 D_2 \tag{4}$$

or using a notation more commonly used today:

$$(K_{xx} - K_{yy})^2 + 2c^2\left(\frac{K_{xx}}{m} + \frac{K_{yy}}{m}\right) > -4K_{xy}K_{yx} \tag{5}$$

which demonstrates the destabilizing nature of large cross- coupling terms. This analysis does not yield any cross-coupling terms which arise due to coriolis effect of the rotor translation and simultaneous precession. The latter effect is considered by Hagg in an analysis of a centred (unloaded) bearing for which the equations of motion in terms of polar coordinates ϵ, shaft radial displacement from the journal equilibrium position (bearing centre in this case) and θ, precession angle:

$$m\frac{d^2\epsilon}{dt^2} - m\epsilon\left(\frac{d\theta}{dt}\right)^2 + B\Omega\epsilon\cos\gamma + c\frac{d\epsilon}{dt} = 0 \tag{6}$$

$$m\epsilon\frac{d^2\theta}{dt^2} + 2m\frac{d\epsilon}{dt}\frac{d\theta}{dt} + D\epsilon\frac{d\theta}{dt} - B\Omega\epsilon\sin\gamma = 0 \tag{7}$$

where:

$B\Omega\epsilon$ = the bearing resultant force at angle γ to the horizontal.
Ω = rotational speed ($B = K/\Omega$), C, D =damping coefficients.

which are non-linear equations unless $d\theta/dt$, the precessional velocity, is assumed constant. Then applying Routh's criterion to the resulting characteristic equation, Hagg derives the stability criterion: $4K/m > \Omega$ or $\omega_n = \Omega/2$ or the speed should not exceed twice the first lateral critical speed for stability. This is the now well known criterion for the *possible* onset of oil whip. As a means of avoiding oil whip, Hagg investigated, analytically and experimentally, the behaviour of tilt-pad bearings which were just becoming popular at the time. Hagg's procedure was to use Reynolds' equation for laminar incompressible flow between plates. The pressure is integrated over the pad with boundary condition of zero pressure at each end of the pad. The work done per cycle of precession by the rotor on the oil film is then derived. This work is set equal to that done by viscous drag for circular precession at eccentricity ϵ with precession frequency ω. i.e. $= 2\pi\epsilon^2\omega$ resulting in a viscous damping coefficient:

$$c = \frac{n\mu}{2\eta^3}\left(\frac{l^3w^3}{l^2 + w^2}\right)$$

where: l = length of pad, w = width of pad, η = radial clearance, μ = absolute viscosity, n = number of pads. This would give a direct damping coefficient only C_{xx} or C_{yy}. Because coriolis is not considered, no cross-coupled damping coefficients are derived. However, for tilt-pad bearings these are usually very small. Hagg reasons that for instability to occur, the work done per cycle of displacement, by the oil film pressures due to journal rotation, must be greater than the damping energy, or work done on the oil film by the vibrating rotor. For the tilt-pad bearing, the work done by the principal bearing force during one complete cycle is shown to be approximately zero. This ignores the small frictional force so that the journal force on a pad can be considered to act always through the pivot point of the pad. This is not the case for a cylindrical sleeve bearing so that this work is not zero in the latter case. Hence the tilt-pad bearing should be resistant to instability, which of course it is and was so demonstrated by Hagg's experiments. Reference [18] extended the previous study to include shaft flexibility. The stability criterion was experimentally modified to:

$$(K_1 - K_2)^2 + \frac{2}{m}\left(\frac{B_1^2 K_1}{1 + K_1/K_s} + \frac{B_2^2 K_2}{1 + K_2/K_s}\right) > 4D_1 D_2 \tag{8}$$

where the damping coefficient of the previous formula has been separated into B_1 and B_2 for x and y directions and K_s is the shaft flexibility.

Using the above stability criterion and the expression for film pressure:

$$p = \left(\frac{R}{c}\right)^2 \mu N \alpha e^{\beta}\left(\frac{\epsilon}{c}\right)$$

where: R = radius, c = clearance, ϵ = eccentricity, μ = absolute viscosity, α and β are dimensionless constants, and e = base of natural logarithms. This expression was deduced by Hagg from data produced by Needs [19] using an electrical analogue simulation of a one dimensional Reynold's equation for a 120°, partial arc bearing. From this the stiffness and damping coefficients were derived and a flexible rotor stability criterion was obtained: by holding cN_c^2/g constant and varying:

$$\left\{\left[(R/c)^2 \mu n/p\right], cN/g\right\}$$

each crossing of the stability boundary is determined.

This resulted in a very practical family of curves for a simple rotor with fluid film bearings where the first lateral mode only is considered (the most common case in practise).

The above criterion was verified with an electrical analogue to within 10% accuracy and an experimental rig consisting of a small steam turbine was used to check the theory for several partial arc bearings as well as full cylindrical sleeve bearings, as well as a full cylindrical sleave bearing with a circular central groove. The results agreed fairly well quantitatively with theory and qualitatively well with field experience, in terms of the trends in stability for changes in bearing clearance and oil viscosity for different speed ranges of operation and the effect of shaft flexibility.

The effect of oil film properties on the unbalance response of rotors was investigated by Hagg and Sankey [20]. However, in this case the effective stiffness and damping coefficients were experimentally determined at rotation speed. In these experiments, only direct stiffness and damping coefficients were determined.

2.2 Derivation of Bearing Coefficients - Laminar Flow

In order to derive stiffness and damping coefficients for hydrodynamically lubricated bearings, some form of Reynolds' equation is generally used. This implicitly assumes that inertia forces are negligible, i.e. the Reynolds number is sufficiently low that viscous

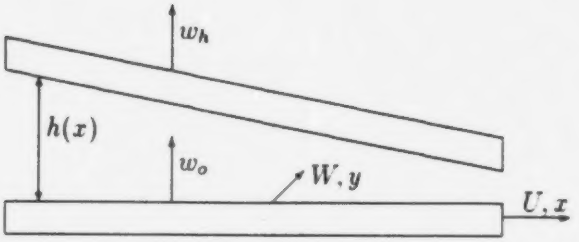

Figure 2: Slipper Bearing

forces are dominant and that laminar, Couette flow prevails (there are no Taylor vortices) [21] - the Taylor number:

$$T_a = U_i d/\nu\sqrt{d/R_i} < 41.3$$

where: U_i = peripheral velocity of inner cylinder, d = gap width, R_i = radius of inner cylinder, ν = kinematic viscosity.

Reynolds' equation for a slipper bearing can be expressed as [22, 23]:

$$\frac{\partial}{\partial x}\left(h^3\rho\frac{\partial p}{\partial x}\right) + \frac{\partial}{\partial y}\left(h^3\rho\frac{\partial p}{\partial y}\right) = 6\mu\left[\frac{\partial}{\partial x}(h\rho U) + \frac{\partial}{\partial y}(h\rho W)\right] + 12\mu\rho(w_h - w_o) \qquad (9)$$

Where: μ = dynamic viscosity, p = pressure, ρ = density, U, W are velocities of the boundary in the x and z directions.
For incompressible flow this becomes:

$$\frac{\partial}{\partial x}\left(h^3\frac{\partial p}{\partial x}\right) + \frac{\partial}{\partial y}\left(h^3\frac{\partial p}{\partial y}\right) = 6\mu\left[\frac{\partial}{\partial x}(hU) + \frac{\partial}{\partial y}(hW)\right] + 12\mu(w_h - w_o) \qquad (10)$$

Sternlicht [24] used this form of Reynolds' equation with $(w_h - w_o) = V'$ the squeeze film velocity around the bearing, using an iterative finite difference method. This yields the eight coefficients of the equation of motion:

$$\begin{bmatrix} m & 0 \\ 0 & m \end{bmatrix}\begin{Bmatrix} \ddot{x} \\ \ddot{y} \end{Bmatrix} + \begin{bmatrix} B_{xx} & B_{xy} \\ B_{yx} & B_{yy} \end{bmatrix}\begin{Bmatrix} \dot{x} \\ \dot{y} \end{Bmatrix} + \begin{bmatrix} K_{xx} & K_{xy} \\ K_{yx} & K_{yy} \end{bmatrix}\begin{Bmatrix} x \\ y \end{Bmatrix} =$$

$$\begin{Bmatrix} G\cos(\omega t + \phi) \\ G\sin(\omega t + \phi) \end{Bmatrix} \qquad (11)$$

The damping cross - coupling terms B_{xy} and B_{yx} are stated to be negligible. The above form of Reynolds' equation can be modified to a more convenient expression for a rotor. The local velocity at A, Figure 2, tangent to the surface at A is U where

$$U = \omega R - \dot{x}_j\cos\theta - \dot{z}_j\sin\theta h = c(1 + \varepsilon\cos\theta), \quad \varepsilon = e/c$$

If W = 0 and $w_o = 0$ then ignoring second order terms:

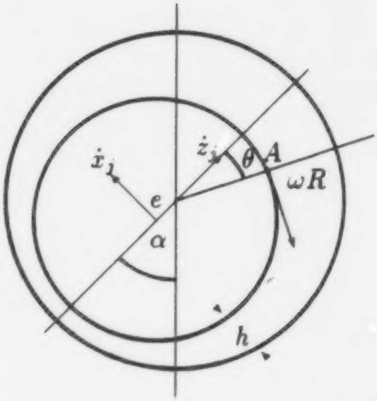

Figure 3: Journal Precessing in Bearing Annulus: x,y,z are local coordinates at angle θ. The journal has components of precessional velocity $\dot{x}_j$, $\dot{z}_j$ and constant angular velocity ω.

$$\frac{\partial}{\partial x}\left(h^3\frac{\partial p}{\partial x}\right)+\frac{\partial p}{\partial y}\left(h^3\frac{\partial}{\partial y}\right)=6\mu\left[R\omega\left\{1-2\frac{\dot{\alpha}}{\omega}\right\}\frac{\partial h}{\partial x}\ +\ 2\dot{e}\cos\theta\right] \tag{12}$$

This is Lund and Sternlicht's starting point [25].

Their procedure was then to derive expressions for radial and tangential forces in terms of the eccentricity ratio ε, attitude angle α, the squeeze film velocity $\dot{\epsilon}$ the non - dimensionalized precessional velocity $\dot{\alpha}/\omega$, ω, the bearing geometry and oil viscosity. They then expand these expressions (which involve integration around the oil film, carried out numerically) in a Taylor series for a perturbation from the equilibrium position. Retaining first order terms only and returning to a non - rotating frame of reference the coefficients of dx, $d\dot{x}$, dy, $d\dot{y}$ become the stiffness and damping coefficients in the inertial frame i.e.

$$dF_x = -K_{xx}dx - C_{xx}d\dot{x} + K_{xy}dy + C_{xy}d\dot{y} \tag{13}$$

$$dF_y = K_{yx}dx - C_{yx}d\dot{x} + K_{yy}dy + C_{yy}d\dot{y} \tag{14}$$

The stiffness and damping coefficients so derived are functions of the geometry of the bearing, the eccentricity, the attitude angle and the time derivatives of the latter two. Lund and Sternlicht eliminate the term $\partial f/\partial\left(\frac{\dot{\alpha}}{\omega}\right)$ stating that as the Taylor expansion is about an equilibrium position where $\dot{\alpha}$ and $\dot{\varepsilon}$ both equal zero, that $\partial f/\partial\left(\frac{\dot{\alpha}}{\omega}\right)$ = zero.

However, this does not follow. In fact, if it did, then by the same reasoning the similar term; $\partial f/\partial\left(\frac{\dot{\varepsilon}}{\omega}\right)$ would also be zero. If, however, it is reasoned that $\dot{\alpha}$ is merely constant i.e. a constant precession rate (or zero as is the case for the equilibrium position) then the result in the paper follows, without any condition (other than the 'small' assumption implicit in the linearization) on $\dot{\varepsilon}$. Therefore the stiffness and damping coefficients so derived are valid at the given eccentricity ratio i.e. for small deflections from that position.

In order to use standard analytical procedures for unbalance response and stability calculations, it was necessary to reduce the coefficient matrices to 'equivalent' diagonal matrices i.e. eliminating the cross - coupling terms. As these terms are not always equal and are usually opposite in sign (in Lund and Sternlicht's analysis they are of equal magnitude but opposite sign), this transformation cannot be achieved by a rotation of coordinate axes to find a set of principal axes. Using the response of a simple rotor with bearings having direct stiffness and damping coefficients only, Lund and Sternlicht obtained equivalent diagonal matrices. This equivalence was therefore dependent on the rotor configuration and, further was only valid for one lateral bending mode. It was essentially equivalent to a modal method of analysis with one mode only. For many rotors, operating well below the second lateral mode (critical speed), this model would suffice.

Lund extended this analysis [26] to the more complicated geometry of the tilting - pad bearing. The same basic theory as above was used and applied to each pad. Overall coefficients were then derived by summing over the pads. The cross - coupling terms were found to be ignorable (except at pad resonance). This is as Hagg had found and is the major reason for adoption of this design, as it indicates a greatly reduced tendency to instability.

The pad resonance derives from the rotational motion of the individual pads resulting in a 'critical mass', (an unfortunate use of the phrase), i.e. the mass of the pad for which this oscillatory motion becomes resonant for a given rotational speed, oil viscosity and pad geometry. Lund used the bearing coefficients for oil film bearings in [13] in which he modelled a complete rotor, including bearing, aerodynamic effects and hysteretic friction in the rotor.

In the introduction to [13] it is stated that the calculated 'criticals' on the basis of rigid bearings, is often borne out on the test stand in-spite-of flexible fluid film bearings because of the stiffening effect of the damping in the bearings. This may have reflected experience restricted to a certain class of machines or the characteristics of the particular test stand. It has been the writers experience that many compressor sets in the petrochemical industry and turbine- generator sets, that the name plate critical speed(s) are often removed from that determined by measurement of vibration signals during start-ups and run-downs, by several hundred R.P.M..

Lund also states that 'the true critical' is the damped natural frequency rather than the undamped natural frequency, often calculated at that time. In industry and in rotor dynamics trouble - shooting particularly, the speed of maximum unbalance response is generally regarded as the 'critical'. This is, after all, what is measured in the field and what matters to the user.

The term 'critical' is perhaps an unfortunate one in that many 'criticals' are so heavily damped as to be most uncritical but some operators still accelerate madly through that speed range incurring other system problems. Donald E. Bently coined the term 'balance resonance' which is more appropriate but not widely used. In practical terms the speed of maximum unbalance response and the damped natural frequency are very close. Lund's analysis of a simple rotor in plain bearings shows a pair of roots, (eigenvalues) which appear to 'track' rotation speed at a fraction of approximately 0.5 over most of the speed range. This pair of forward or backward modes are regarded by Lund as the 'first' modes, distinct from the rotor 'critical'. At instability it is the first mode which goes unstable and at a frequency $\approx 0.5\times$ rotor speed. Lund makes the point that this is not the first critical which has become unstable. However this result looks very like that of Muszynska [7], i.e. that the 'tracking' eigenvalue is the 'oil whirl' mode and when the rotor speed rises above twice the first 'critical speed', this critical now becomes the lower of the two eigenvalues and becomes unstable (or may do so in the absence of sufficient external damping).

One may also reason that the 'tracking mode' has begun to couple with the rotor critical as their frequencies approach, resulting in two new coupled modes. In such a case, as with aircraft flutter, one of the two modes generally goes less stable (the one with inherently less damping such as a bending mode) while the other goes more stable. Lund's model for the rotor was derived from the lumped mass transfer matrix method, analogous to that of Myklestad's or Prohl, [27, 28] incorporating frequency - dependent hysteretic damping and oil - film coefficients as described above. In his analysis Lund retains all the backward precession modes (sometimes ignored by other writers) and in fact notes that it is the first backward mode which, for that rotor, had the greatest unbalance response and was therefore, in practical terms the first critical of the rotor.

In an analysis of the same rotor, using tilting - pad bearings, to prevent oil whip instability, Lund also included the effect of floating ring seals, behaving essentially as unloaded bearings and thereby creating a destabilizing mechanism. In fact they were shown to cause an instability within the speed range of the machine which did not occur without the inclusion of the seal in the model. Unfortunately this lesson had to be re-learned in the design of the space shuttle fuel pumps - below. Details of the seal model were not given in the paper, but it is presumed that the same laminar, incompressible flow was assumed, permitting the use of Reynolds's equation.

In Prohl's paper, referred to above [28], the rotor was discretized into an equivalent system of disks and massless shaft sections. Vibration is assumed to be planar (no damping is included) and the bearings are considered isotropic. Stiffnesses, both angular and linear are assumed independent of speed. The equations of motion for an arbitrary section of shaft yields the shear force and moment at the station 'n' in terms of those at station 'n-1', the elastic properties of the beam element and the unbalance force on the element. The bending moment, shear force, rotation (in the plane of the shaft) and lateral displacement at a point on the rotor is then a linear function of these quantities, along the rotor up to that point, for a given speed.

Using a two step tabular process, firstly a unit shear force is assumed at one end, moment $= 0$, and the deflections and rotations are derived along the rotor. Then similarly for a unit moment and zero shear at one end the deflections and rotations are derived along the rotor.

This is essentially a means of deriving a dynamic 2x2 flexibility matrix for the rotor from one end to the other. For a critical speed the moment at the end must be zero. Therefore, the procedure is repeated for increments of speed to determine these speeds. This is therefore a series of steady - state analyses.

Lund and Orcutt, some 20 years later [29] improved upon Prohl's method by including non - isotropic bearings with unequal cross - coupling terms stiffness and damping coefficients. This therefore resulted in elliptical shaft orbits and the inability to determine principal axes. Because of the low viscosity lubricant used in the particular machine analyzed, the flow regime was turbulent and the coefficients had to be derived accordingly (see below). To accommodate damping, displacements along the rotor are represented in complex form as are the bearing stiffness and damping coefficients i.e. they were represented as complex impedances:

$$Z_{xx} = K_{xx} + i\omega B_{xx} \qquad Z_{xy} = K_{xy} + i\omega B_{xy} \quad etc.$$

The beam element relationships are derived in a manner similar to Prohl. Lund and Orcutt developed the theory for using distributed mass and moment of inertia, but did not use it in the paper as it was considered an unnecessary complication.

In carrying out the calculation of shear and bending moment for each speed increment (with appropriate changes in bearing coefficients), Lund and Orcutt extended the analysis by setting the bending moment to zero at the rotor end and thereby derived the displacements and rotations along the rotor for each speed i.e. a complete unbalance response. This analysis therefore also provided the orbit shapes along the rotor at all speeds and whether the modes being excited were forward or backward precession.

Lund and Saibel recognized [30] that in many machines, instabilities are self - limiting, the orbits reaching a 'limit cycle'. They used the method of averaging [31] which gives approximate solutions to non-linear equations. The method yields first order approximations of the whirl orbit shape for given bearing coefficients, which are, in turn functions of the eccentricity ratio ϵ. The stability of the orbit shape is examined by considering a variation of the shape in order to produce linearized equations in small variations of the orbit parameters and applying Routh's criterion to these equations (similar to Tondl's procedure, Subsection 2.4). This therefore permitted one to examine the severity of the instability, although, as the authors point out, one would not deliberately design a machine to run in this way.

Lund [32] also developed a modal method for rotor - bearing systems including damping. The normal procedure for decoupling equations of motion using the normal modes of a system, requires that the mass and stiffness matrices be symmetric. To permit such a method to be used for the case involving the non - symmetric cross - coupling terms generated by fluid - film bearings (and seals), it was necessary to develop an othogonality criterion for non - symmetric matrices.

Lund sets up a complex eigenvalue problem for free vibration of the rotor / bearing system, which can be solved for its eigenvalues which occur as complex conjugate pairs, and an associated set of eigenvectors. Then replacing the coefficient matrices by their transposes and reversing the direction of rotation (mathematically in the gyroscopic term of the element equation of motion), a second complex eigenvalue problem is set up. This has the same complex eigenvalues as the first analysis but for non - symmetric matrices, yields a different set of eigenvectors (complementary or left eigenvectors). These two sets of eigenvectors permit the decoupling of the equations of motion of the rotor.

2.3 Turbulent Flow Bearing Coefficients

Although, for most bearings with normal lubricants, the assumption of laminar flow is justifiable, this is not always the case. In pump sets, where the pumpage, often water, may be used as the lubricant, the flow in the bearing annulus can be turbulent. In addition the flow through the inter-stage seals may also be turbulent.

Ng and Pan [33] developed a lubrication equation for turbulent flow of the same form as Reynolds' equation for laminar flow. Their starting point was the expression for the time averaged Navier - Stokes (momentum) equation which in indicial form[1] can be expressed as:

$$\frac{\partial}{\partial t}\left[\overline{\rho}\,\overline{u_i} + \overline{\rho' u_i'}\right] + \left[\overline{\rho}\,\overline{u_j}\,\overline{u_i}\right]_{,j} + \left[\overline{\rho}\overline{u_i' u_j'}\right]_{,j} =$$

$$- \overline{p}_{,i} + \left[\overline{\tau_{ij}} - \overline{u_j}\overline{\rho' u_i'} - \overline{\rho' u_j'}\,\overline{u_i'} - \overline{\rho' u_j' u_i'}\right]_{,j}$$

where ρ is density, u_i, u_j are the ith and jth components of velocity (i and j take values 1,2,3), the overbar denotes the time averaged quantity and the primes denote a perturbation in the quantity from the mean, the $_{,i}$ and $_{,j}$ denotes partial differentiation with respect to the ith and jth components of displacement x_i, x_j, p is pressure and τ is the viscous shear stress. For incompressible steady flow, ignoring the mean flow inertia terms, this reduces to :

$$\overline{\tau_{ij}}_{,j} - (\rho\overline{u_i' u_j'})_{,j} = \overline{p}_{,i}$$

where $-\rho\overline{u_i' u_j'}$ is the Reynolds' stress $= \tau_{ij}'$
Therefore:

$$(\overline{\tau_{ij}} + \tau_{ij}')_{,j} = -\overline{p}_{,i}$$

But,

$$\tau_{ij}' = \varepsilon\rho\overline{u_i}_{,j}$$

where ε is the 'eddy diffusivity'.

Therefore:

$$\tau_{ij}' = \mu\left(\frac{\varepsilon}{\nu}\right)\overline{u_i}_{,j}$$

$$\tau_{ij} = \mu\overline{u_i}_{,j} + \mu\left(\frac{\varepsilon}{\nu}\right)\overline{u_i}_{,j}$$

or

$$\tau_{ij} = \mu\left(1 + \frac{\epsilon}{\nu}\right)\overline{u_i}_{,j} = \overline{p}_{,i} \qquad (15)$$

Ng and Pan make use of Reichardt's formula for ϵ/ν, with constants determined by their own experiments, and the relationship:

$$\tau_{ij,j} = p_{,i}$$

to integrate Equation 15 to obtain the velocity profile across the annular channel.

---

[1] Ng and Pan did not use indicial notation. The writer has done so for compactness to set up the starting point in Ng and Pan's paper.

After some considerable manipulation, an equation having the same form as the Reynolds' lubrication equation is obtained. The integration procedure assumes that the flow field can be represented as a small perturbation of 'turbulent Couette' flow. This permitted Ng and Pan's colleague, F.K. Orcutt at Mechanical Technology Inc., to develop bearing coefficients for turbulent flow for tilting - pad bearings[34].

A rigorous treatment of turbulent flow in an annulus was carried out by Yamada [35]. This work concerns only situations when the Reynolds number is sufficiently high that Taylor vortices (a pattern of vortices about stationary circumferential axes) are no longer formed, i.e. the flow is completely turbulent. Yamada examines theoretically and experimentally, flow in the annulus between concentric cylinders, including axial and circumferential components of velocity and assuming turbulent 'law of the wall' velocity profiles. Thus the velocity distribution in the axial direction obeys a law of the form:

$$v = v_0 \left(\frac{2y}{s}\right)^{\frac{1}{n}}$$

where s = radial clearance, y = distance from the wall, v_0 = max velocity (at the mid point), n = constant to be determined by experiment.

Also, the frictional resistance coefficient is of the form

$$\lambda = cR_e^{-\alpha}$$

where R_e = axial Reynolds' number, $= v_{mean}s/\nu$, ν is the kinematic viscosity and c, α are constants. For the circumferential direction with turbulent flow, the same power law results. The circumferential velocity u at radial position y is:

$$u = \frac{u_1}{2}\left(\frac{2y}{s}\right)^{\frac{1}{n}}$$

for

$$0 \leq \frac{s}{2}$$

and

$$u_1 - u = \frac{u_1}{2}\left[2\frac{(s-y)}{s}\right]^{\frac{1}{n}}$$

for

$$\frac{s}{2} \leq y \leq s$$

where u_1 is the circumferential velocity of the inner cylinder $= r\omega$, the outer cylinder remaining stationary.

Using $n = 7$ (7th. power law) and c, α deduced from experiment in the above expressions result in a friction factor for combined axial and circumferential flow:

$$\lambda = 0.26R_e^{-0.24}\left[1 + \left(\frac{7}{8}\right)^2\left(\frac{R_\omega}{2R_e}\right)^2\right]^{0.38} \qquad (16)$$

for which the general expression is:

$$\lambda = cR_e^{-\alpha}\left[1 + \left(\frac{n}{n+1}\right)^2\left(\frac{R_\omega}{2R_e}\right)^2\right]^{\frac{1-\alpha}{2}}$$

where R_ω is the Reynolds' number for circumferential flow. Yamada indicates that for pipe flow using a 7th. power law $u/U = (y/R)^{\frac{1}{n}}$ with $n = 7$, Blazius' equation is obtained, viz $\lambda = 0.27R_e^{-0.25}$. However, Blazius formula was actually deduced to be $\lambda = 0.3164R_e^{-0.25}$ for smooth pipes [23, 36]. But Blazius defined R_e as $(v_{mean}d/n$ for the pipe. Thus for the limiting case of the annulus becoming a pipe, the clearance $s \rightarrow r_2$ in which case Yamada's $R_e(axial)$ becomes $v_{mean}r_2/\nu = v_{mean}\frac{d}{2}/\nu$; i.e. $R_e(Blazius) = 2R_e(Yamada)$. This indeed leads to the two expressions being equivalent.

Therefore using Blazius' rule, the case of concentric cylinders with a 7th. power law would result in a friction factor for combined axial and circumferential flow:

$$\lambda = 0.27\, R_e^{-\frac{1}{4}}\left[1 + \left(\frac{7}{8}\right)^2\left(\frac{R_\omega}{2\,R_e}\right)^2\right]^{\frac{3}{8}} \tag{17}$$

which is very close to that derived by Yamada. In Black et al's papers, discussed below, this latter expression was used to derive stiffness, damping and inertia coefficients for turbulent flow through seals. Black [37] makes the same assumption as Ng and Pan, that turbulent flow in the annulus can be considered a perturbation superimposed on a 'mean Couette flow'. Then for axial flow through the annulus the pressure gradient is:

$$\frac{dp}{dz} = -2\frac{\lambda_a}{c}\frac{1}{2}\rho w^2$$

where w is the mean axial velocity, c is the radial clearance and λ_a is the axial friction coefficient.

Black takes his expression for λ_a from Yamada's paper (the Blazius' law version) expressing it as:

$$\lambda_a = 0.079R_e^{-0.25}\left[1 + \left(\frac{7}{8}\right)\left(\frac{R_r}{R_e}\right)^2\right]^{0.375}$$

The difference between this and Yamada's form, above, is because
$\lambda(Yamada) \equiv 4\lambda(Black)$. Also $R_e(Black) = 2R_e(Yamada)$ i.e. Black's usage was consistent with that of Blazius.

Using the stress law $\tau = 1/8\lambda\rho U^2$ where ρ = density, U = shaft peripheral velocity, Black derives a linearized expression for circumferential pressure distribution in terms of the local clearance for the eccentric journal, shaft peripheral speed, mean velocity increment due to the pressure gradient and the local (around the journal) rotational Reynold's number. Having expressions for axial and circumferential pressure gradient, in terms of mean axial velocity and circumferential, pressure induced, mean perturbation velocity, these velocities are eliminated from the continuity equation for an incompressible fluid at the angular position corresponding to the local clearance. A pressure field equation is thus derived which has the same form as Reynolds' equation for the laminar régime.

The rest of their paper was concerned with the load bearing capabilities of a bearing which had a substantial axial flow component, as a function of Sommerfeld number and bearing clearance. However, Black concludes that stiffness and damping coefficients would depend solely on journal position.

In his almost simultaneous and widely referenced paper, [38] effective fluid stiffness damping and inertia coefficients are derived for a centred shaft, executing small vibrations within an annular seal.

Starting with the integral form of the continuity equation for an incompressible fluid subject to the squeeze action of the shaft within the seal, and the linear momentum equation along the annular passage, Black postulates small deviations about the average axial fluid velocity due to the perturbations in lateral shaft position and derives a lateral force [2]:

$$F_y = -\epsilon k(D) y$$

where D is the operator d/dt. $k(D)$ can be approximated by:

$$k(D) = \mu_0 + \mu_1 T D + \mu_2 T^2 D^2$$

where:

$$T = \frac{L}{V}, \quad \epsilon = \frac{\pi}{6\lambda}\left(\frac{\sigma}{1.5 + 2\sigma}\right) RP, \quad \sigma = \frac{\lambda L}{y_0}$$

where: λ = friction coefficient, y_0 = radial clearance, P = pressure differential across the seal, R = seal radius.

Therefore, the coefficients $\epsilon\mu_0$, $\epsilon\mu_1 T$ $\epsilon\mu_2 T^2$ can be considered stiffness, damping and inertia coefficients for the fluid, which were added to the corresponding terms for the rotor to derive an expression for the unbalance response in the normal fashion. Black extended the analysis to include speed dependent pressure drop across the seal, resulting in an increase of damping coefficient with speed and a 'negative fluid mass' effect. In order to investigate fluid whip instability, Black considers fully developed 'turbulent Couette flow' within the annular space, in the circumferential direction i.e. mean fluid rotation velocity equal to half the shaft speed $\omega/2$. Then considering a frame of reference rotating at $\omega/2$, expressions are developed for the radial component of the fluid forces in the rotating frame. These are transformed to the inertial frame and the equation of motion for free vibration is so derived. The stability boundary is then determined by inspecting the complex eigenvalues and finding the condition for a quasi - stable solution.

The frequency of precession given by this analysis is:

$$\Omega = \frac{\omega}{2}$$

where

$$\omega = 2\sqrt{\frac{s + \epsilon\mu_0}{m}}$$

where s and m are respectively the shaft stiffness and mass, i.e. the precession is at a frequency equal to a half shaft rotation speed, when the rotation speed is a little higher than twice the rotor critical speed.

Black further considers the case for speed dependent pressure drop across the seal and includes external viscous damping to develop a stability boundary for a centrifugal pump. Black and Jensen [39] extended the study above to include circumferential pressure - induced flow which is the dominant effect in a bearing. However, in the seal application this is assumed small compared with the axial flow. This resulted in a modification to the μ_0, μ_1, μ_2 coefficients as a function of the length/radius ratio of the seal.

---

[2] We use Black's notation here for easy cross - reference. See later definitions of D

In [39] the concept of 'rotary receptance' r/F is introduced for an unbalanced journal (or subject to some rotating force F) producing a precession radius r. The integral forms of the continuity and momentum equations are used, allowing for circumferential and axial flow for an incompressible fluid. The friction head loss per unit length along the seal is assumed, as in the previous study, proportional to velocity squared and Yamada's [35] coefficient of friction is used. The friction coefficient is assumed constant within the annulus and average velocities are used in the momentum equation (the radial velocity profile across the fluid gap is not accounted for).

The differential equation for pressure perturbation distribution with respect to non - dimensionalized axial position and time is derived as a function of radial journal perturbation and the constants of the seal. Then assuming a harmonic variation in pressure and radial position perturbation, and integrating around the seal, the radial force is found in terms of a complex dynamic stiffness and the radial displacement amplitude. The components of the dynamic stiffness can then be resolved into hydraulic 'inertia', 'damping' and 'stiffness' components in terms of the μ_0, μ_1 and μ_2 parameters, derived in the previous study, [38].

Evaluation of the differential equation for a practical range of seal parameters permitted a modification to the μ's due to fluid circulation, so that the modified values may be used in the matrix formulation of the equations of motion for fluid in the seal annulus:

$$\begin{Bmatrix} F_y \\ F_x \end{Bmatrix} = \frac{-\pi RP}{\lambda} \begin{bmatrix} \left(\mu_0 - \frac{1}{4}\mu_2\omega_s^2T^2\right) & \frac{1}{2}\mu_1\omega_s T \\ -\frac{1}{2}\mu_1\omega_s T & \left(\mu_0 - \frac{1}{4}\mu_2\omega_s^2T^2\right) \end{bmatrix} \begin{Bmatrix} y \\ x \end{Bmatrix}$$

$$+ \begin{bmatrix} \mu_1 T & \mu_2\omega_s T^2 \\ -\mu_2\omega_s T_2 & \mu_1 T \end{bmatrix} \begin{Bmatrix} \dot{y} \\ \dot{x} \end{Bmatrix} + \begin{bmatrix} \mu_2 T^2 & 0 \\ 0 & \mu_2 T^2 \end{bmatrix} \begin{Bmatrix} \ddot{y} \\ \ddot{x} \end{Bmatrix} \tag{18}$$

Finally Black and Jensen [39] investigated the case of high eccentricity of the journal within the seal. The perturbation about the steady - state position was still assumed small but the axial and circumferential Reynolds' numbers and friction factors were allowed to vary around the annulus. The stiffness characteristics were then evaluated by a numerical solution and only showed significant differences from the centred journal for high eccentricity ratios. This assumes that, under the conditions of high eccentricity, the 'turbulent Couette flow' assumption for the velocity profile is still valid. The results of [39] show that the velocity and acceleration terms arising from the fluid in the seals, strongly control the displacement response, to the extent of totally suppressing the first lateral mode 'critical' of the pump rotor and the onset of 'whip' instability. This is in agreement with several field investigations the writer has carried out on water and petro - chemical pump - sets, in which the first 'critical' was undetectable on run - ups or shut - downs.

2.4 Internal Friction

The phenomenon of instability induced by internal damping, has been the subject of considerable analysis, [40, 41, 42, 14, 43], perhaps because of its counter - intuitive aspect. To the field engineer, it is a phenomenon which typically occurs in machines such as compressors which have 'stacked' rotors, which, if not very precisely assembled, can generate internal friction damping i.e. within the rotor rather than externally applied through, for instance, the viscous damping of a fluid film bearing. Although internal damping instability is not a common occurrence, it can be very severe and sudden when it does occur.

In 1924 Kimball [40, 41] demonstrated that the presence of internal friction (viscous or coulomb), leads to a tangential disturbing force which is at approximately the first resonant frequency (critical speed) of the rotor. The direction of this disturbing force is such as to promote whirling i.e. in the direction of rotation, when the rotation speed is above the first resonance, and so as to suppress whirling when rotation speed is below the first resonance.

Ehrich [42] showed that the unstable mode need not necessarily be the fundamental mode but is generally the mode closest to one half rotation speed. This does not agree with [40, 43, 14]. However, the re-excitation of the first mode 'whip' due to fluid - induced forces occurs at speeds above twice the first (or other) critical speed frequency. It is therefore possible that where internal damping is insufficient to cause instability below twice the first critical, the combined destabilizing effects of fluid whip and internal damping cause instability at a speed in the vicinity of twice the first critical.

Both Gunter and Tondl examine several different configurations to evaluate the behaviour of internal damping. The case of a simple 'Jeffcott' rotor with internal viscous damping can be very easily analyzed to demonstrate the principle. Referring to Figure 4,

$$z = x + iy \qquad \text{and} \qquad \zeta = \xi + i\eta$$

is the complex displacement of the centre of the rotor referred to an inertial reference frame, and referred to a frame of reference rotating at the rotor speed respectively. Therefore the transformation between the two systems is:

$$z = \zeta e^{i\omega t}$$

For a simple horizontal unbalanced rotor with its centre of gravity ε from the geometric centre, we have an equation of motion referred to the inertial frame [43]:

$$m\ddot{z} + c\dot{z} + kz = mg + m\varepsilon\omega^2 e^{i\omega t}$$

Transforming this to the rotating frame, and adding a term for internal damping P_v:

$$m(\ddot{\zeta} + 2i\omega\dot{\zeta} - \omega^2\zeta) + c(\dot{\zeta} + i\omega\zeta) + k\zeta - P_v = mge^{-i\omega t} + m\varepsilon\omega^2 \qquad (19)$$

For simple viscous damping $P_v = -h\dot{\zeta}$ and we can return to the inertial frame to get:

$$\ddot{z} + D\dot{z} + \delta(\dot{z} - i\omega z) + \Omega^2 z = g + \varepsilon\omega^2 e^{i\omega t}$$

where:

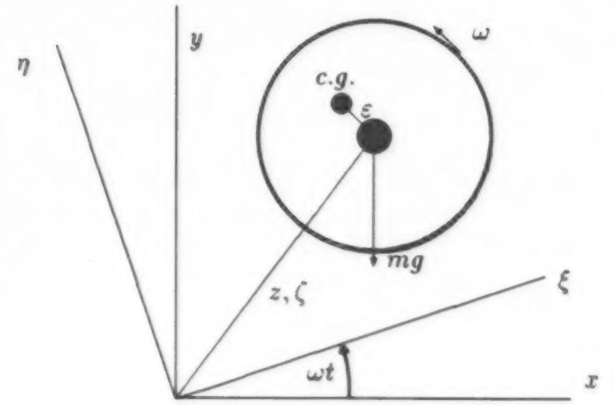

Figure 4: Simple Rotor with Internal Friction

$$D = c/m, \qquad \delta = h/m, \qquad \Omega^2 = k/m$$

[3] This is a linear homogeneous ordinary differential equation, which has a solution:

$$z = Z_1 e^{i\lambda_1 t} + Z_2 e^{i\lambda_2 t} + Z_\varepsilon e^{i\omega t} + Z_g$$

The first two terms are solutions of the complementary function and the second two are a particular solution which describe the rotor response due to unbalance and the rotor weight.

$$Z_\varepsilon = R_\varepsilon e^{-i\phi} \qquad \text{and} \qquad Z_g = R_g e^{\psi}$$

where

$$R_\varepsilon = \frac{\varepsilon\omega^2}{\sqrt{[(\Omega^2 - \omega^2)^2 + D^2\omega^2]}}$$

and

$$\tan\phi = \frac{D\omega}{\Omega^2 - \omega^2}$$

also:

$$R_g = \frac{g}{\sqrt{\Omega^4 + \delta^2\omega^2}}$$

and

$$tan\psi = \frac{\delta\omega}{\Omega^2}$$

Therefore the particular solution demonstrates that the internal friction has the effect of deflecting the deflection due to gravity, an angle ψ and reduces the magnitude of the deflection due to gravity. The unbalance produces the response of a circular orbit of radius R_ε at a circular frequency ω. The $\lambda_{1,2}$ are the roots of the characteristic equation:

---

[3] Tondl used k for damping coefficient, c for stiffness coefficient and κ for (damping coefficient)/m. The writer has used k for stiffness coefficient, c for damping coefficient, which is the usual convention, and D for c/m

$$\lambda^2 - i\lambda(D + \delta) - \Omega^2 + i\delta\omega = 0 \tag{20}$$

i.e.

$$\lambda_{1,2} = \frac{1}{2}i(D + \delta) \pm \sqrt{[\Omega^2 - \frac{1}{4}(D + \delta)^2 - i\delta\omega]}$$

One of these eigenvalues (the positive square root) corresponds to the forward precessing mode and the other to the backward precessing mode. The backward mode solution will disappear with time.

Using the Routh - Hurwitz criterion on Equation 20 yields the necessary and sufficient condition for stability:

$$\omega < \Omega\left(1 + \frac{D}{\delta}\right) \tag{21}$$

Note that Ω is the undamped natural frequency. This very simple condition illustrates well the effect of the ratio of external to internal damping on stability.

The analysis for the case of internal hysteretic damping is rather more complex. Starting with Equation 19, Tondl [43] uses:

$$P_v = -h\,(max|\zeta|)\frac{\dot{\zeta}}{|\dot{\zeta}|}$$

Changing to polar coordinates ρ and ϕ in the rotating frame of reference:

$$\zeta = \rho e^{i\phi}$$

and equating real and imaginary parts, two coupled equations in ρ and ϕ are obtained:

$$\ddot{\rho} - \rho\dot{\phi}^2 - 2\rho\omega\dot{\phi} + (\Omega^2 - \omega^2)\rho + D\dot{\rho} + \frac{\delta(max|\rho|)\dot{\rho}}{\left|\sqrt{\dot{\rho}^2 + \rho^2\dot{\phi}^2}\right|} = g\cos(\omega t + \phi) \tag{22}$$

$$\rho\ddot{\phi} + 2\dot{\rho}\dot{\phi} + 2\omega\dot{\rho} + D(\omega + \dot{\phi}) + \frac{\delta(max|\rho|)\rho\dot{\phi}}{\left|\sqrt{\dot{\rho}^2 + \rho^2\dot{\phi}^2}\right|} = -g sin(\omega t + \phi) \tag{23}$$

A particular solution of Equation 22 and Equation 23 is an orbit of radius $\rho = R$ and a precessional velocity $\dot{\phi} = -\omega$. This is satisfied by $\phi = -\omega t + \phi_0$, where R and ϕ_0 are constants defined by:

$$R\Omega^2 = g cos\phi_0, \qquad \delta(R) = g\sin\phi_0$$

This represents the static condition under the gravity and hysteretic friction loading - see Figure 5.

A perturbation is postulated: $\rho \rightarrow (\rho_0 + r)$ and $\phi \rightarrow \phi_0 + \psi$ where r and ψ are small. Then after some considerable manipulation and retaining only first order terms, two differential equations are derived in terms of these perturbations.

$$\ddot{r} + \left(D + \frac{\delta(R)}{R\omega}\right)\dot{r} + \Omega^2 r + \delta(R)\psi = 0 \tag{24}$$

and

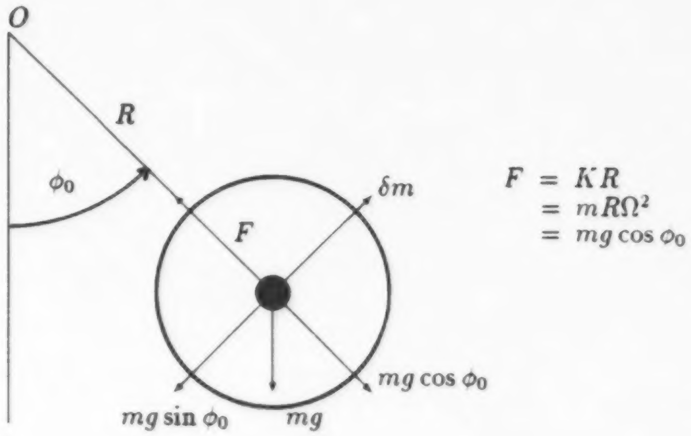

Figure 5: Static Deflection Under Gravity and Friction Loading

$$R\ddot{\psi} + DR\dot{\psi} + R\Omega^2\psi - \delta'(R)r = 0 \tag{25}$$

where δ' is $\partial\delta/\partial R$. Assuming a solution of the form $r = r_0 e^{\lambda t}$ and $\psi = \psi_0 e^{\lambda t}$ results in a characteristic equation:

$$\lambda^4 + \lambda^3\left(2D + \frac{\delta}{R\omega}\right) + \lambda^2\left[2\Omega^2 + D\left(D + \frac{\delta}{R\omega}\right)\right]$$

$$+ \lambda\left(2D + \frac{\delta}{R\omega}\right)\Omega^2 + \Omega^4 + \frac{\delta\delta'}{R} = 0 \tag{26}$$

Applying the Routh - Hurwitz criterion, as above results in the necessary and sufficient condition for stability at all speeds:

$$\delta\delta' < D^2R\Omega^2 \tag{27}$$

which is again in the form of the ratio of internal damping to external damping.

2.5 Space Shuttle Turbo - Pumps

D.W. Childs has published numerous papers from 1969 until quite recently on the rotordynamic analyses of the liquid hydrogen and liquid oxygen fuel turbopumps of the U.S. space shuttle main engine. The history of the development of these pumps illustrates most strongly, the influence of the fluid forces on the dynamics of rotating machines and the difficulty in adequately modelling these forces.

In [44] Childs developed an elegant procedure for analyzing a rotating elastic body using body - fixed axes. The initial application for this had been spin - stabilized spacecraft. The formulation requires an inertial coordinate system $\{x, y, z\}$; a body - fixed coordinate system $\{x_0, y_0, z_0\}$ moving with the rotating undeformed body, with the origin coincident with the centre of mass of the undeformed rotating body; a set of n coordinate systems $\{x_i, y_i, z_i\}$ with origins at the centres of mass of each of the n elastically connected bodies; and finally a fourth set of n coordinate systems $\{\tilde{x}_i, \tilde{y}_i, \tilde{z}_i\}$ with origins at the elastically displaced centres of mass of the n elastically connected rigid bodies.

Thus, the position of a particle in the i'th rigid body with respect to the $\{x_i, y_i, z_i\}$ system, is determined by the elastic deformation of the $\{\tilde{x}_i, \tilde{y}_i, \tilde{z}_i\}$ system and its position within that system. The transformation from the $\{x_i, y_i, z_i\}$ system to the $\{x_0, y_0, z_0\}$ system is a simple translation for each i.

Childs sets up the equations of motion for the individual rigid bodies with respect to the inertial frame and defines the angular motion of the $\{x_0, y_0, z_0\}$ system via Newton's 2nd law applied to the whole rotor. The equations of motion of the i'th rigid body are then restated using the kinematic relationships in a form that includes the elastic deformations and their rates of change relative to an observer in the body (vehicle) - fixed coordinate system $\{x_0, y_0, z_0\}$.

The assumptions of linear theory are made that the deformations can be stated in terms of a reference undeformed configuration and that deflections are linear functions of the applied loads. This implies that the orthogonal transformation of vectors from the $\{x_0, y_0, z_0\}$ to the $\{\tilde{x}_i, \tilde{y}_i, \tilde{z}_i\}$ system, becomes the identity matrix for small values of the Euler angles, (the set of three consecutive rotations which define the angular position in space) i.e. that changes in loads due to changes in geometry are negligible.

The applied loads can be expressed as the product of a stiffness matrix (banded) premultiplying a deflection vector consisting of the linear and angular deformations of the n discrete rigid bodies. This permits the elimination of internal forces in the equations of motion by substitution of the stiffness matrix coefficients and deflections in the $\{x_0, y_0, z_0\}$ system. The result is then a set of differential equations of motion in the body - fixed coordinate system:

$$[M]\left\{\hat{\ddot{x}}\right\}_0 + [C]\left\{\hat{\dot{x}}\right\}_0 + [K]\{x\}_0 = \{F\}_0 - \{P\}_0 - \{S\}_0$$

Where $\{x\}_0$ is a vector of linear and angular elastic deformations. The $\hat{}$ denotes as seen by an observer moving with the $\{x_0, y_0, z_0\}$ coordinate system. Also $\{\hat{x}\}_0 = \{x\}_0$ for small angular deflections. $\{F\}_0$ is a vector of applied forces and moments at the i'th mass, $\{P\}_0$ is a vector containing terms involving the linear acceleration of the centre of mass of the whole vehicle in the inertial frame and $\{S\}_0$ contains terms in $\boldsymbol{\Omega} \times \boldsymbol{\Omega}$ and $\boldsymbol{\Omega}$, where $\boldsymbol{\Omega}$ is the angular velocity of the whole body, i.e. these are angular inertia terms of the body in the inertial frame. Having set up the equations of motion, modal coordinates are used and modal damping introduced via a modal damping matrix.

In [45, 46] the above method of analysis is applied to the space shuttle fuel pumps. Bearing constraints are introduced by means of spring stiffnesses at the bearing locations. Two bending modes were used in the response analysis, derived from an independent eigenvalue analysis. External damping was accounted for by direct (no cross - coupling) damping coefficients at the bearings i.e. due to damping in the roller bearings only.

In [46] it was predicted that the first 'rigid body' mode of the rotor would be unstable for a damping coefficient ξ at speeds above 51000 RPM. This was not considered a problem as the normal maximum operating speed was 30000 RPM (this was given as 37500 RPM in later references). No fluid forces were included in this analysis. The type of stability analysis used involved examining the response of the coupled bending modes and the frequency of the whirl mode as a function of time, during a simulated run - up for a given level of hysteretic modal damping.

In [47] the model was improved considerably by including seal forces as stiffness, damping and inertia matrices derived using the formulation of Black (above). The structural response and stability analyses carried out in [47, 48] bare a close resemblance to those used for aircraft structural vibration response due to propeller unbalance and flutter respectively. For both the response and stability analyses, a set of normal modes of the system are required. these are derived from a set of admissible functions by use of the Rayleigh - Ritz method. These admissible functions consisted of free - free elastic bending modes of the rotor, calculated separately plus 'rigid - body' modes of the rotor on its elastic bearing / support structure.

Generally in turbomachinery, the mode which becomes unstable is a forward precessing mode [49, 50], although there is some evidence that backward modes can be unstable for rotors [2]. This appears to be most likely in the case of overhung rotors. A backward whirl mode was the least damped mode in whirl flutter calculations carried out by the writer for the De Havilland Dash - 7 aircraft. In [46] backward whirl modes appear to have been ignored, which was probably alright for the hydrogen pump, but the oxygen pump has overhung impellers and it would have been safer to include these modes.

Childs predicted [47] 'a serious rotordynamic instability problem' for the fuel (hydrogen) pump involving a re - excitation of the first bending forward precession mode. He also found via parametric studies that the stability was increased if support stiffness asymmetry was increased. This was also the case for the Dash - 7 analysis and it is understood from contacts with Kraftswerkunion (Federal Republic of Germany) engineers, that they have used this as a means of controlling instabilities in steam turbines. In the Dash - 7 instance it was reasoned that asymmetry decoupled lateral and vertical modes thus making the excitation of a whirl mode less likely.

The prediction of an instability problem was correct [48] resulting in hardware damage on the test stand and a research program to improve seal design [51] to control this instability. Hirs' method of deriving seal coefficients [52] was used for this work [51, 53].

A similar analysis was carried out on the oxygen pumps [47, 54]. In this case the transient response calculation predicted a potentially excessive lateral rotor displacement and consequent rub. However it showed that instability was possible but unlikely. It was reasoned that although the results predicted instability for $\xi = 0.02$ that because the rotor is essentially solid, the ξ would be lower than this. Also the analysis predicted instability at a speed only a little higher than the frequency of the unstable mode, which was considered unlikely because classical 'whip' usually occurs when the rotation speed is above approximately twice the frequency of the unstable mode. This is of course not the case for internal friction (above).

However, the first mode did prove unstable [55]. In addition vibration became excessive at high speed, associated with excitation of the second lateral bending mode (critical speed) of the rotor system. This second mode at 32500 CPM is very close to the 30380 RPM full power level speed required for circumpolar orbital missions of the space shuttle. This was a very undesirable situation, the more so because this mode is lightly damped. The above results led to considerable research into seal optimization to control instability, including [56, 57, 58] on helically grooved seals, seals with various surface roughnesses and sawtooth seals respectively for turbulent flow.

These pumps are very high speed, of an unusual structural design and have highly unusual working fluids. However the problems they posed were essentially similar to those in their more prosaic industrial counterparts. The analyses carried out to make these machines fully operational can be extremely useful for other applications.

2.6 Finite Element Analysis for Bearings

Most of the work on the derivation of bearing coefficients used the method of finite differences until the 1970's when the finite element method was first applied to fluid mechanics problems. The variational calculus approach is most commonly used in fluid mechanics. The finite element representation of a bearing lubrication problem using Reynolds' equation is described in [59] and [60]. Both direct and variational approaches are described in the paper.

The variational statement for the incompressible Reynolds' differential lubrication equation is that the pressure field minimizes the functional $I(p)$ and satisfies the pressure and flow boundary conditions (unless the pressure boundary conditions are specified on the whole boundary):

$$I(p) = \int\!\!\int_A \left[\left(\frac{\rho h^3}{24\mu} \boldsymbol{\nabla} p - \rho h \overline{\boldsymbol{U}} - \frac{\rho h^3 \boldsymbol{B}}{12\mu} \right) \cdot \boldsymbol{\nabla} p + \left(\frac{\partial(\rho h)}{\partial t} + \rho v_d \right) p \right] dA + \int_{S_q} \rho Q p \, ds \qquad (28)$$

Where ρ = density (constant), h = film thickness, $\overline{\boldsymbol{U}}$ is the average velocity of the two bearing surfaces, $\boldsymbol{B}$ is the body force, μ = the absolute viscosity, v_d is the leakage velocity through a porous bearing, A = area, Q = is the leakage flow at the boundary and S_q is the segment of boundary over which there leakage flow is specified.

This functional representation can be shown to be equivalent to the differential equation form of Reynolds' equation :

$$\boldsymbol{\nabla}\cdot\left(\frac{\rho h^3}{12\mu}\boldsymbol{\nabla} p\right) = \boldsymbol{\nabla}\cdot\left(\rho h\overline{\boldsymbol{U}} + \frac{\rho h^3}{12\mu}\boldsymbol{B}\right) + \frac{\partial(\rho h)}{\partial t} + \rho v_d \tag{29}$$

subject to the flow boundary condition :

$$Q = \rho \boldsymbol{q} \cdot \boldsymbol{n} \equiv h\left(\rho\overline{\boldsymbol{U}} + \frac{\rho h^2}{12\mu}\boldsymbol{B} - \frac{\rho h^2}{12\mu}\boldsymbol{\nabla} p^*\right)\cdot\boldsymbol{n} \tag{30}$$

where p^* is some distribution of p which satisfies the Reynolds' equation. This boundary condition is that the average flow normal to the boundary corresponds with that specified.

Body forces can usually be ignored for a bearing. Therefore for a non - porous bearing Equation 28 can be re-stated as:

$$I(p) = \int\!\!\int_A \left\{\frac{\rho h^3}{24\mu}\left[\left(\frac{\partial p}{\partial x}\right)^2 + \left(\frac{\partial p}{\partial y}\right)^2\right] - \rho h\left[U_x\frac{\partial p}{\partial x} + U_y\frac{\partial p}{\partial y}\right] + \frac{\partial(\rho h)}{\partial t}p\right\} dA$$
$$+ \int_{S_q}\left[q_x \boldsymbol{n}_x + q_y \boldsymbol{n}_y\right] p\, ds \tag{31}$$

or

$$I(p) = \int\!\!\int_A \left\{\frac{\rho h^3}{24\mu}\left(\frac{\partial p}{\partial x_j}\right)\left(\frac{\partial p}{\partial x_j}\right) - \rho h U_j\frac{\partial p}{\partial x_j} + \frac{\partial(\rho h)}{\partial t}p\right\} dA + \int_{S_q} q_j \boldsymbol{n}_j\, p\, ds \tag{32}$$

(sum on j).

This is the form of the equation used by Allaire et al. [61]. The field variables within an element can be expressed as a function of the nodal values of the element, using an interpolation function which is some function of the geometrical coordinates. This results in an expression of the form:

$$p_k(\chi_i) = \{N(\chi_i)\}^T\{p\}_{k(nodes)} = N_i\, p_{i(nodes)} \qquad \text{(sum on } i\text{)} \tag{33}$$

The $\{N(\chi_i)\}$ are referred to as a normal or cardinal basis and k is the element number ($i = 1$ to r where $r =$ number of nodes per element). χ_i are functions of the spacial coordinates local to the element x_j where for a 2 - dimensional element, $j = 1,2$ i.e. (x,y) coordinates. Similarly expressions can be set up for the other field variables, which in this case are U_x, U_y and $\partial h/\partial t$. The interpolation functions need not be the same for all field variables.

The natural basis is determined as follows for (for example) a 2 - dimensional quadrilateral element with a linear interpolation function:

$$\begin{aligned} p_k(\chi_i) &= a_1 + a_2x_1 + a_3x_2 + a_4x_1x_2 \\ &\quad \text{where } \chi_i = a_1,\ a_2x_1,\ a_3x_2,\ a_4x_1x_2 \text{ for } i = 1 \text{ to } 4 \end{aligned}$$

and the a_i are constants. Therefore for node 1 letting $x_j = x_{j1}$:

$$p_1 = a_1 + a_2 x_{11} + a_3 x_{21} + a_4 x_{11} x_{21} \tag{34}$$

and similarly for the other nodes, 2, 3, 4. Hence:

$$\left\{ \begin{array}{c} p_1 \\ p_2 \\ p_3 \\ p_4 \end{array} \right\}_k = \left[\begin{array}{cccc} 1 & x_{11} & x_{21} & x_{11}x_{21} \\ 1 & x_{12} & x_{22} & x_{12}x_{22} \\ 1 & x_{13} & x_{23} & x_{13}x_{23} \\ 1 & x_{14} & x_{24} & x_{14}x_{24} \end{array} \right]_k \left\{ \begin{array}{c} a_1 \\ a_2 \\ a_3 \\ a_4 \end{array} \right\}_k \tag{35}$$

or

$$\{p\}_k = [T]_k \{a\}_k$$

Therefore :

$$\{a\}_k = [T]_k^{-1} \{p\}_k$$

Then :

$$p_k(\chi_i) = \{1 \;\; x_1 \;\; x_2 \;\; x_1 x_2\}_k \, [T]_k^{-1} \, \{p\}_k$$

Therefore the normal basis is given by :

$$\{N_k(\chi_i)\}^T = \{1 \;\; x_1 \;\; x_2 \;\; x_1 x_2\}_k [T]_k^{-1} \text{ for element } k \text{ i.e. no sum on } k$$

For the general case, (any interpolation function) and dropping the k and χ for simplicity we can write for a given element:

$$\begin{aligned} p &= \{N\}^T \{p\} = N_i p_i \\ U_x &= \{N\}^T \{U_x\} = N_i U_{x_i} \\ U_y &= \{N\}^T \{U_y\} = N_i U_{y_i} \\ \dot{h} &= \{N\}^T \{\dot{h}\} = N_i \dot{h}_i \end{aligned} \tag{36}$$

The above uses the same $\{N\}$ for all the field variables (actions). Now

$$\frac{\partial p}{\partial x} = \left\{ \frac{\partial N}{\partial x} \right\}^T \{p\} = \{p\}^T \left\{ \frac{\partial N}{\partial x} \right\} \tag{37}$$

$$\frac{\partial p}{\partial y} = \left\{ \frac{\partial N}{\partial y} \right\}^T \{p\} = \{p\}^T \left\{ \frac{\partial N}{\partial y} \right\} \tag{38}$$

If we now substitute these approximate expressions for p, U_x, U_y, $\dot{h}$, $\partial p/\partial x$, $\partial p/\partial y$ in Equation 32 and then minimise this equation by setting its derivative $\partial I/\partial\{p\}^T = 0$ we obtain:

$$[K_p]\{p\} = \{q\} - [K_{U_x}]\{U_x\} - [K_{U_y}]\{U_y\} - [K_h]\{\dot{h}\} \tag{39}$$

where :

$$
\begin{aligned}
K_{p_{ij}} &= -\int\!\!\int_A \frac{\rho h^3}{12\mu}\left[\frac{\partial N_i}{\partial x}\frac{\partial N_j}{\partial x} + \frac{\partial N_i}{\partial y}\frac{\partial N_j}{\partial y}\right] dA \\
K_{U_x\,ij} &= \int\!\!\int_A \rho h \frac{\partial N_i}{\partial x} N_j \, dA \\
K_{U_y\,ij} &= \int\!\!\int_A \rho h \frac{\partial N_i}{\partial y} N_j \, dA \\
K_{\dot{h}\,ij} &= -\int\!\!\int_A \rho N_i N_j \, dA \\
q_i &= \int_{S_q} Q N_i \, dS
\end{aligned}
$$

The [K]'s are known as 'fluidity' matrices. They are influence coefficient matrices for the various 'actions'. The element matrices can now be assembled into system or 'global' matrices by matching the pressures at the element nodes and the corresponding flows on the right hand side of Equation 39. This set of equations has the same form as the element equations 39 except that it now consists of square matrices $n \times n$ and vectors $1 \times n$, where n is the total number of system nodes.

The pressure boundary conditions permit the modification of $[K_p]$ and flow boundary conditions are automatically taken care of on the right hand side of Equation 39. Then we have a set of algebraic equations to solve for the nodal pressures p instead of the differential equations we started out with. Hence for given surface velocities, film thickness, density and squeeze rate, we can determine the pressure distribution.

Allaire et al. [61] used the fluidity approach to calculate pressure distribution using triangular elements and linear interpolation functions for pressure within the elements. They assumed ρ, h, U_x, U_y and $\dot{h}$ all constant within each element. It was determined that aligning the element diagonals approximately in line with the direction of the pressure gradient optimized the accuracy and reduced computing time. Also, varying the grid spacing in the circumferential direction directly as the film thickness helped reduce computing time. Allaire et al. considered the use of quadrilateral elements but concluded that the improved accuracy over triangular elements could simply be offset by increasing the number of triangular elements. Huebner and Thornton [60] consider the quadrilateral element preferable. Calculating the pressure field as above presumes we know the values of the film thickness h. This depends on the load, i.e. we have to determine the equilibrium position. For given bearing surface velocities, the bearing develops a film thickness profile corresponding to a pressure profile which can support the load. Therefore, an iterative calculation is required to determine h around the bearing at equilibrium.

Allaire et al. carried out numerical differentiation with respect to the inertial displacements and velocities x, y, $\dot{x}$ and $\dot{y}$ to produce curves of bearing coefficients versus Sommerfeld number. These could then be used in bearing stability calculations as described above in the earlier studies and for unbalance response and critical speed calculations. In fact, the University of Virginia set up a joint University - industry program to make a suite of computer codes available to designers and users of rotating machinery.

2.7 Discussion

Much of the excellent work on bearing and seal coefficient stiffness and damping coefficient determination, makes assumptions about the mean journal position and shaft precessional motion, which are frequently not satisfied in the field.

The 'D.C.' or mean shaft position can be very easily determined from the D.C. voltage change from eddy - current non contact probes on the run - down of a machine. This position is often considerably removed from the ideal location which would be determined by the load due to the rotor weight and / or process fluid forces alone. Some machine misalignment frequently preloads the shaft and thereby displaces its position. Temperature and load variations can further change the position.

The motion (or orbit) of the shaft (the A.C. component of displacement) within the bearing can be quite complex, having several major frequency components. However, for a stable machine the most common orbit shape consists of a synchronous, elliptical orbit with small components at other frequencies superimposed.

When a shaft orbit becomes unstable such as during oil whirl or whip, the subsynchronous component of the orbit, which may be minor or dominant is generally elliptical and close to circular. Given that in either case, the orbit can be a significant fraction of the diametral clearance, it is reasonable to suppose that such orbits would have a significant effect on the pressure profile and therefore of the observed stiffness and damping coefficients of the bearing.

The trends in turbomachinery design in recent years are to lighter, higher speed, higher load rotors. The elastic / hydrodynamic behaviour of rotors has therefore become of major importance at the design stage.

There is a present need for an analytical procedure which could build upon the approach of [30] and make use of finite element methods and modern computing power. It should be feasible to create a model, in which fluid film stiffness and damping coefficients vary cyclically with precession of the journal and which comprises finite element models of the fluid film bearings, rotor and support structure. This would permit calculation of unbalance response for large orbits and determination of the sensitivity of self - excited vibration.

References

[1] H.H. Jeffcott 'The lateral Vibration of Loaded Shafts in the Neighbourhood of a Whirling Speed - The Effect of Want of Balance' *Phil. Mag. and J. of Sc. Vol 37 1919 pp 304 -314*

[2] J.C. Wachel 'Rotordynamic Instability Field Problems' *N.A.S.A.- C.P. 2250 Texas A and M May 10-12 1982*

[3] A.G. Taylor, Unpublished Consulting Report *Bently Nevada Canada Ltd.*

[4] R.L. Bisplinghoff, H. Ashley, R.L. Halfman 'Aeroelasticity' *Addison - Wesley 1955*

[5] T. Theodorsen 'General Theory of Aerodynamic Instability and the Mechanism of Flutter' *N.A.C.A. Rpt. No. 496 1935*

[6] B.L. Newkirk, H.D. Taylor 'Shaft Whipping Due To Oil Action in Journal Bearings' *General Electric Review Aug 1925 Vol XXVIII No 8*

[7] A. Muszynska 'Whirl and Whip - Rotor / Bearing Instability Problems' *J.S.V. (1986) 110(3) pp 443 -462*

[8] A.G. Taylor 'Computer - Aided Diagnosis of Machinery Instability Problems - Several Case Histories' *Ninth Machinery Dynamics Seminar, National Research Council of Canada, Montréal 1986*

[9] C. Jackson 'The Practical Vibration Primer'*Gulf Publishing Co. 1985*

[10] A. Muszynska 'Multi - Mode Whirl and Whip in Rotor/Bearing Systems' *The Second International Symposium on Transport Phenomena, Dynamics, and Design of Rotating Machinery, Honolulu, Hawaii, April, 1988*

[11] D. Robertson 'Whirling of a Journal in a Sleeve Bearing' *Phil. Mag. S.7 Vol No 96 Jan 1933 P.113*

[12] B.L. Newkirk, J.F. Lewis 'Oil Film Whirl - An Investigation of Disturbances Due to Oil Films in Journal Bearings' *Trans. ASME Jan. 1956 pp 21 -27*

[13] J.W. Lund 'Stability and Damped Critical Speeds of a Flexible Rotor in Fluid - Film Bearings' *J. Eng. for Ind. May 1974*

[14] E.J. Gunter 'Dynamic Stability of Rotor - Bearing Systems' *N.A.S.A. Sp.- 113 1966*

[15] A.G. Taylor, Unpublished Consulting Report *Bently Nevada Canada Ltd.*

[16] 'Edward H. Miller, G.E. Co. 'Rotor Stabilizing Labyrinth Seal for Steam Turbines' *U.S. Pat. 4,420,161 Dec. 13, 1983*

[17] Hagg A.C., 'The Influence of Oil-Film Journal Bearings on the Stability of Rotating Machines'*J.of App. Mechs. Sept. 1946*

[18] Hagg A.C., Warner P.C. 'Oil Whip of Flexible Rotors'*Trans. ASME Oct. 1953*

[19] S.J. Needs 'Effects of Side Leakage in 120 - Degree Centrally Supported Journal Bearings' *Trans. A.S.M.E. APM - 56-16 pp. 721-732*

[20] A.C. Hagg, G.O. Sankey 'Some Dynamic Properties of Oil Film Journal Bearings With Reference to the Unbalance Vibration of Rotors' *J. of App. Mechs. June 1956*

[21] G.I. Taylor 'Stability of a Viscous Liquid Contained Between Two Rotating Cylinders.'*Phil. Trans. Royal . Soc. Vol. CCXXIII (223) Ser. A Feb. 8, 1923*

[22] A. Cameron 'The Principles of Lubrication' *Longmans 1966*

[23] H. Schlichting 'Boundary Layer Theory' *Mc Graw Hill 1979*

[24] B.Sternlicht 'Elastic and Damping Properties of Cylindrical Journal Bearings' *J. Bas. Eng. June 1957 p.101*

[25] J.W. Lund, B. Sternlicht 'Rotor-Bearing Dynamics with Emphasis on Attenuation' *J. Bas. Eng. Dec. 1962p. 491*

[26] J.W. Lund 'Spring and Damping Coefficients for the Tilting-Pad Journal Bearing' *A.S.L.E. Trans. 7 Pp. 342- 353 (1964)*

[27] N.O. Myklestad 'A New Method of Calculating Natural Modes of Uncoupled Bending Vibration of Airplane Wings and Other Types of Beams' *J. of Aero. Sc. Apr. 1944*

[28] M.A. Prohl 'A General Method for Calculating Critical Speeds of Flexible Rotors' *J. of App. Mech. Sept. 1945*

[29] J.W. Lund, F.K. Orcutt 'Calculations and Experiments on the Unbalance Response of a Flexible Rotor' *J. of Eng. for Ind. Nov. 1967 pp 785 - 796*

[30] J.W. Lund, E. Saibel 'Oil Whip Whirl Orbits of a Rotor in Sleeve Bearings' *J. of Eng. for Ind. Nov. 1967*

[31] N.N. Boboliubov, Y.A. Mitropolsky 'Asymptotic Methods in the Theory of Non-Linear Oscillations' *Gordon and Breach Science Publishers / Hindustan Publishing Corpn. India (translation from the russian) 1961*

[32] J.W. Lund 'Modal Respose of a Flexible Rotor in Fluid - Film Bearings' *J. of Eng. for Ind. May 1974 pp. 525 - 533*

[33] C.W. Ng, C.H.T. Pan 'A Linearized Turbulent Lubrication Theory' *J. Bas. Eng. Sept. 65 p.675*

[34] F.K. Orcutt 'The Steady - State and Dynamic Characteristics of the Tiltpad Journal Bearing in Laminar and Turbulent Flow Regimes' *J. Lub. Tech. Trans. A.S.M.E. July 1967*

[35] Y. Yamada 'Resistance of a Flow Through an Annulus with an Inner Rotating Cylinder' *Bul. Jap. Soc. Mech. Eng. V.18 May 1962*

[36] F.W. White 'Viscous Fluid Flow' *Mc Graw Hill 1974*

[37] H.F. Black 'Empirical Treatment of Hydrodynamic Journal Bearing Performance in the Super - Laminar Régime' *J. Mech. Eng. Sc. Vol. 12 No. 2 1970*

[38] H.F. Black 'Effects of Hydraulic Forces in Annular Pressure Seals on the Vibration of Centrifugal Pump Rotors' *J. Mech. Eng. Sc. Vol. 11 No. 2 1969*

[39] H.F. Black, D.N. Jensen 'Dynamic Hybrid Bearing Characteristics of Annular Controlled Leakage Seals' *Proc. Inst. Mech. Engrs. 1969-1970 Vol. 184 Pt3N pp. 92-100*

[40] A.L. Kimball 'Internal Friction Theory of Shaft Whirling' *General Electric Review Vol. XXVII No. 4 April 1924*

[41] A.L. Kimball 'Measurement of Internal Friction in a Revolving Deflected Shaft' *General Electric Review Vol. XXVIII NO. 8 Aug.1925*

[42] F.F. Ehrich 'Shaft Whirl Induced by Rotor Internal Damping' *J. App. Mechs. June 1964 pp. 279 - 282*

[43] A. Tondl 'Some Problems of Rotor Dynamics' *Publishing House of the Czechoslovak Academy of Sciences, Prague - Chapman & Hall London*

[44] D.W. Childs 'Simulation models for flexible spinning bodies' *Simulation, June 1969 pp. 291 - 296*

[45] D.W. Childs 'A Simulation Model for Flexible Rotating Equipment' *J. of Eng. for Ind. Feb.1972 pp.201 - 209*

[46] D.W. Childs 'A Rotor Fixed Modal Simulation Model for Flexible Rotating Equipment'*J. of Eng. for Ind. May 1973 pp. 659 - 669*

[47] D.W. Childs 'SSME Turbopump Technology Improvement via Transient Rotordynamic Analysis - Final Report'*NASA - CR - 144165 Dec. 1975*

[48] D.W. Childs 'The Space Shuttle Main Engine High - Pressure Fuel Turbopump Rotordynamic Instability Problem'*J. of Eng. for Power Trans. ASME Vol. 100, Jan. 1978*

[49] D.E. Bently 'Forced Subrotative Speed Dynamic Action of Rotating Machinery'*ASME Petroleum Mech. Eng. Conf. Dallas, Texas Sept. 1974*

[50] J. S. Alford 'Protecting Turbomachinery From Self Excited Rotor Whirl '*J. Eng. for Power Oct. 1965*

[51] D.W. Childs'Rotordynamic Analysis for the HPFTP (High Pressure Fuel Turbopump) of the SSME (Space Shuttle Main Engine) - Final Report'*NASA - CR - 161620 July 1980*

[52] G.G. Hirs 'A Bulk Theory for Turbulence in Lubricant Films'*J. Lub. Tech. Apr. 1973*

[53] D.W. Childs 'Dynamic Analysis of Turbulent Angular Seals Based on Hirs' Lubrication Equation'*NASA - CR - 161620 July 1980*

[54] D.W. Childs 'Transient Rotordynamic Analysis for the Space - Shuttle Main Engine High Pressure Oxygen Turbopump' *NASA - CR - 140455 N74 34003. also synopsis in J. Spacecraft and Rockets Vol. 12 NO.1 Jan. 1975*

[55] D.W. Childs, D.S. Moyer 'Vibration Characteristics of the HPOTP (High - Pressure Oxygen Turbopump) of the SSME (Space Shuttle Main Engine)'*J. Eng. for Gas Turbines for Power Vol. 107 Jan. 1985*

[56] Chang-Ho Kim, D.W. Childs 'Analysis for Rotordynamic Coefficients of Helically - Grooved Turbulent Annular Seals' *J. Trib. Trans. ASME Jan. 1987, Vol. 109 p.136*

[57] D.W. Childs, Chang-Ho Kim 'Analysis and Testing for Rotordynamic Coefficients of Turbulent Annular Seals With Different, Directionally - Homogeneous Surface - Roughness Treatment for Rotor and Stator Elements' *J. Trib. July 1985 Trans. ASME Vol. 107 P.296*

[58] D. Childs, F. Garcia 'Test Results for Sawtooth- Pattern Damper Seals: Leakage and Rotordynamic Coefficients' *J. Trib. Trans. ASME Vol. 109 Jan. 1987*

[59] J.F. Booker, K.H. Huebner 'Application of Finite Element Methods to Lubrication: An Engineering Approach' *J. Lub. Tech. Trans. ASME Oct. 1972 pp.313-323*

[60] K.H. Huebner, E.A. Thornton 'The Finite Element Method for Engineers' *Wiley 1983*

[61] P.E. Allaire, J.C. Nicholas, E.J. Gunter 'Systems of Finite Elements for Finite Bearings' *J. Lub. Tech. Trans. ASME April 1977*

SESSION / SÉANCE 2

Machinery Health Monitoring/
Surveillance de l'état des machines

LEAD PRESENTATION / PRÉSENTATION INAUGURALE

Aspects of Optimal Preventive Replacement Strategies

by Andrew K.S. Jardine

ASPECTS OF OPTIMAL PREVENTIVE REPLACEMENT STRATEGIES

Andrew K.S. Jardine
Professor and Chairman

Department of Industrial Engineering
Faculty of Applied Science and Engineering
University of Toronto
Toronto, Ontario
Canada M5S 1A4

ABSTRACT

Review of optimal preventive replacement strategies under hard-time maintenance, covering age- and block-replacement. The move towards condition based maintenance (CBM). The possible role of proportional hazards modelling (PHM) to efficiently interpret data emanating from CBM procedures such as oil analysis and vibration monitoring. Applications discussed cover the use of PHM in maintenance decision making within the military (aircraft engines) rail operations (locomotive engines) and the mining industry (haul trucks) where inspections include engine oil analysis. The potential for using the PHM procedure to identify cost effective replacement decisions when inspection is through vibration monitoring will be explored.

BIOGRAPHY

Andrew K.S. Jardine obtained his BSc and MSc degrees in Mechanical Engineering from the University of Strathclyde. His 1973 PhD thesis in Production Engineering from the University of Birmingham is entitled "Maintenance Decision Making". Since 1986 he has been Professor and Head of the Department of Industrial Engineering at the University of Toronto. Among many industrial and academic activities, he has been a maintenance management advisor from time to time for firms such as British Steel, Imperial Chemical Industries, Allied Breweries, Canada Cement Lafarge, Unilever, J.D. Irving Equipment, Canada Starch, Polysar and Ontario Hydro. His research work is concerned with the development and application of mathematical models for engineering decision making, with particular emphasis on equipment maintenance and replacement. In recent years he has published a number of papers related to equipment reliability and maintenance which use statistics from machinery health monitoring in making maintenance decisions.

RÉSUMÉ

Étude des stratégies optimales de remplacement préventif à utiliser lors des visites régulières d'entretien et couvrant le remplacement de pièces usées ou de vie limitée. L'évolution vers l'entretien basé sur l'état. Le rôle que pourrait jouer la modélisation des risques proportionnels dans l'interprétation efficace des données provenant des procédures d'entretien basé sur l'état comme l'analyse de l'huile et le contrôle des vibrations. Les applications examinées couvrent l'utilisation de la modélisation des risques proportionnels dans la prise de décisions sur l'entretien du matériel dans les domaines militaire (moteurs d'aéronef), ferroviaire (moteurs de locomotives) et minier (camions remorques) où les inspections comprennent l'analyse de l'huile du moteur. La possibilité d'utiliser la procédure de modélisation des risques proportionnels pour déterminer des remplacements rentables lorsque l'inspection se fait par contrôle des vibrations sera traitée.

BIOGRAPHIE

Andrew K.S. Jardine a obtenu son baccalauréat et sa maîtrise en génie mécanique de l'Université de Strathclyde. Sa thèse de doctorat en techniques de production déposée en 1973 à l'Université de Birmingham s'intitule "Maintenance Decision Making". Depuis 1986, M. Jardine est professeur et chef du Département de génie industriel à l'Université de Toronto. Ses activités industrielles et universitaires sont nombreuses; il a été notamment conseiller en gestion de maintenance pour des entreprises telles British Steel, Imperial Chemical Industries, Allied Breweries, Canada Ciment Lafarge, Unilever, J.D. Irving Equipment, Canada Starch, Polysar et Ontario Hydro. Ses recherches ont trait à l'élaboration et à l'application de modèles mathématiques de décision, surtout en matière de maintenance et de remplacement des équipements. Ces récentes années, il a publié un certain nombre d'articles portant sur la fiabilité et la maintenance des équipements ainsi que sur la prise de décision en maintenance fondée sur des statistiques de contrôle d'état.

INTRODUCTION

Maintenance is often viewed as Cinderella activity within an organization. Given that the cost of caring for equipment is often a very significant element in the cost of a product or service, then surely the maintenance activity should be viewed positively as a profit contributing element in an organization's operation.

The purpose of this paper firstly is to draw attention to the easily used age - and block - replacement strategies for components subject to preventive replacement, and focus on the Weibull analysis of failure data. The possible benefit that proportional hazards modelling can play to assist maintenance management interpret efficiently data emanating from a condition based maintenance scheme (such as oil analysis or vibration monitoring) is then presented.

COMPONENT PREVENTIVE REPLACEMENT

There are two common preventive replacement strategies used for replacing components (such as bearings, pumps, switches etc.) on a preventive basis. One is termed a block (or constant interval) policy, the other an age-based policy. Many other strategies are possible, and an extensive survey of a variety of maintenance models is given by Valdez-Flores and Feldman (1).

The block (or constant interval) policy (See Fig. 1).

Preventive replacements are made at constant intervals, of length t_p, with failure replacements occurring whenever necessary.

If C_p = total cost of a preventive replacement, C_f = total cost of a failure replacement, $H(t_p)$ = the expected number of failure replacements in the interval (O, t_p), and $C(t_p)$ = the total cost/unit time for a preventive replacement interval of length t_p, then

$$C(t_p) = \frac{C_p + H(t_p)C_f}{t_p} \qquad (1)$$

The above mathematical model relates the preventive replacement interval t_p to total cost/unit time, $C(t_p)$. The cost conflicts associated with this problem are illustrated in Fig. 2 where it can be seen that what is sought is the best balance between money spent on preventive replacements and money saved through a reduction of failure replacements.

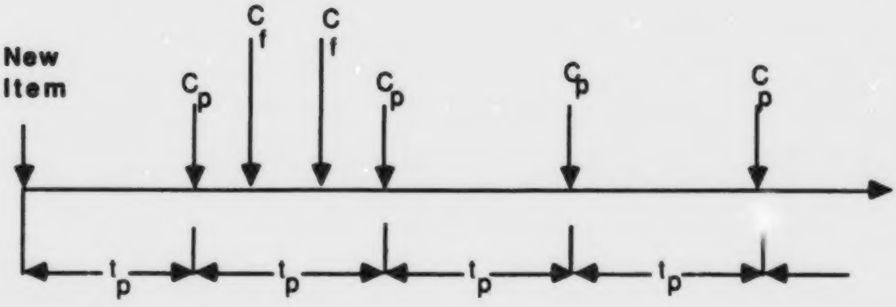

Fig.1 The constant interval preventive replacement policy.

The best value of t_p is obtained by differentiating the right-hand side of eqn. (1) with respect to t_p and setting the result to zero.

This gives

$$t_p h(t_p) - H(t_p) = C_p/C_f$$

where $h(t_p)$ is the derivative of $H(t_p)$ and is termed the renewal density. $H(t_p)$ is often called the renewal function and is discussed in detail by Cox (2).

In practice $H(t_p)$ is often quite a difficult quantity to obtain and various approximation methods are used to obtain good estimates. One such approach is to solve the recurrence relation

$$H(T) = \sum_{i=0}^{T-1}[1 + H(T-i-1)] \int_{i}^{i+1} f(t)dt; \quad T \geq 1$$

with $H(0) = 0$ and where $H(T)$ is the expected number of failures in T time intervals. For fuller details see Jardine (3, pp. 82 - 85), where a numerical example illustrating the solution of the above is also provided.

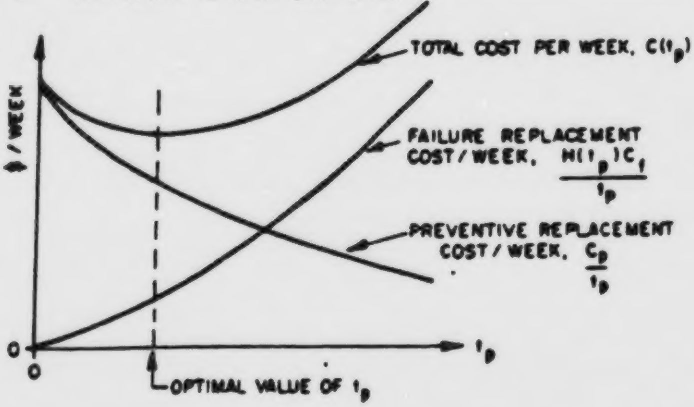

Fig. 2. Preventive replacement cost conflicts

Age-Based Policy

This policy is illustrated in Fig. 3, where it is noted that the replacement cycle is either classed as "good" (since the item is replaced on a preventive basis) or "failed" (since the operating time is terminated by a failure replacement). In this case t_p is the running time that always occurs before an item is replaced under preventive conditions, whence $C(t_p)$ the total cost per unit time is given by the expression

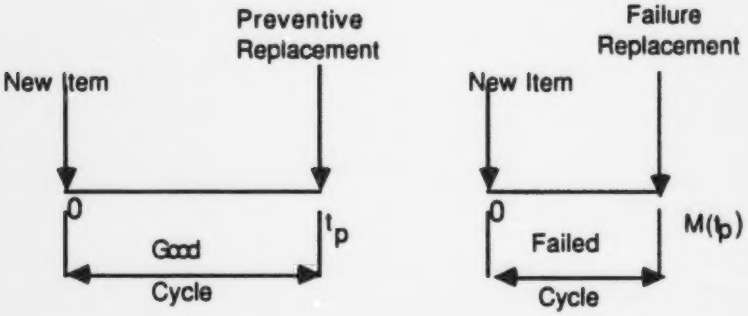

Fig: 3. The age-based preventive replacement policy.

$$C(t_p) = \frac{C_pR(t_p) + C_f[1 - R(t_p)]}{t_pR(t_p) + M(t_p)[1 - R(t_p)]} \qquad (2)$$

where $R(t_p)$ is the probability of the item operating successfully from new for a duration of length t_p. $M(t_p)$ is the mean time to failure of those items that fail before the scheduled preventive replacement age, t_p, i.e.

$$M(t_p) = \left[\int_0^{t_p} t \,.\, f(t)\, dt\right] /[1 - R(t_p]$$

where $f(t)$ is the failure distribution of the item. C_p and C_f are as defined for the constant interval policy.

The optimal value of t_p is obtained by setting $C'(t_p) = 0$, which gives the optimal age as being when

$$[f(t_p)/R(t_p)] \int_0^{t_p} R(t)dt + R(t_p) - 1 = \frac{C_p}{C_f - C_p}$$

As was the case for the constant interval policy a numerical example illustrating the solution of eqn. (2) is provided by Jardine [3].

For preventive replacement of a component to be a worthwhile strategy it is necessary that two conditions are met:

(1) The total cost associated with a failure replacement must be greater than the total cost of a preventive replacement. In practice this condition is usually met since, for example, a failure may be unexpected and considerable time may elapse between notification of the failure and eventual part replacement. On the other hand, a preventive replacement is planned, the spare part is available and production losses are, therefore, kept to a minimum.

(2) Wearout of the item must be occurring. With increasing item use there must be an increasing probability of failure. Because of the flexibility of the Weibull distribution it is often used to model an equipment's failure pattern. The Weibull probability distribution is given by the expression

$$f(t) = \frac{\beta}{\eta}\left(\frac{t}{\eta}\right)^{\beta-1} \exp[-(t/\eta)^{\beta}] \text{ for } t \geq 0$$

an important feature of which is the shaping parameter β. If failure data are analyzed and the β value that describes the failures is greater than unity then wear-out of the item is occurring. (The symbol η is termed the characteristic life and is the time at which there is a 63.2% probability of the item having previously failed.) Reference [4] discusses how β can, in practice, be determined.

It must be stressed that if either of the two necessary conditions is not met then the best replacement procedure is that of replace-only-on-failure - "R-O-O-F." The tacit assumption is often made that as an item is used there is an increasing probability of it failing and thus preventive replacement must be a worth-while strategy. This is not necessarily the case and correct statistical analysis of failure data must be used in order to confirm or reject the hypothesis that the item in fact exhibits wear-out characteristics.

For the Weibull distribution the failure rate, r(t) is:

$$r(t) = \frac{\beta}{\eta}\left(\frac{t}{\eta}\right)^{\beta-1}$$

PROPORTIONAL HAZARDS MODELLING:

Recent developments in estimating the reliability of equipment have focused on Cox's proportional hazards model [5]. The essential change here is that rather than estimate the reliability of equipment based only on its age t, it might be preferable to base a reliability estimate not only on age but also on concomitant information, such as that gleaned through vibration monitoring or SOAP (Spectrometric Oil Analysis Programs). Pottinger and Sutton [6] stated in their paper:

"Much condition-monitoring information tells us something is not quite right, but it does not necessarily inform us what margins remain for exploitations before real risk, and particularly real commercial risk, occurs."

It is to address this concern that the use of a proportional hazards model is useful. Essentially the procedure is to modify r(t), the failure rate, by multiplying it by a function g(z(t)) with z(t) being the concomitant variable (or covariate or explanatory variable as it is sometimes called). Thus the modified (or extended failure rate) is

$$r(t,z(t)) = r(t)g(z(t)),$$

which is the proportional hazards model. A common form for g(z(t)) is

$$g(z(t)) = e^{\gamma z(t)}$$

where γ is the regression coefficient. Cox's proportional hazards model effectively is a multiple regression model that can handle censored data.

Note: A censored observation is one where it is known how long an item has operated successfully, but at the time of data collection, it has not yet failed but has been 'suspended' or 'censored' while in service. In statistical analysis of failure data, censored observations frequently occur since censorings occur, for example, if items are replaced under preventive replacement or in reliability testing when the testing has to stop due to a time constraint, yet some items on test have not failed.

If required, γ and z(t) can be made vectors if more than one covariate should be incorporated into the hazard model.

Table 1 is taken from a paper by Jardine and Anderson [7] and illustrates use of the proportional hazards model to estimate the reliability of jet engines on the Boeing 707 aircraft. The background to the analysis is that the 707 engines are subject to routine SOAP inspections. On the basis of the readings obtained of metal deposits found in the engine oil, a decision is made on whether or not to remove the engine before its scheduled life.

TABLE 1

Estimated failure rate (failures/item/flight hour) at premature overhaul

Number	Flight hours	Fe	Ag	Failure rate (all overhauls)	Failure rate (valid overhauls)
1	1177	5	6	0.435	0.452
2	1166	2	6	0.1190	0.0951
3	846	12	2.4	0.0681	0.0415
4*	1263*	8	1	0.01270	0.00541
5*	924*	2	3	0.00251	0.00082
6	771	8	0	0.00080	0.00018
7*	567*	8	1	0.00074	0.00017
8*	719*	2	2.5	0.00062	0.00015

*denotes doubtful overhaul

Essentially, "trends and averages" of metal deposits are obtained through the regular analysis of oil samples, in much the same manner as reported by Morrow [8] when undertaking condition based maintenance through vibration monitoring. If the metal deposit readings are 'high' the engine is removed from the aircraft and overhauled. This is an expensive business and the purpose of the proportional hazards model analysis is to combine objectively information on flying hours, level of silver (Ag) deposits in oil in parts per million and level of iron (Fe) deposits in parts per million. The final column of Table 1 indicates the results obtained. It is interesting to note that on four occasions, it was found during overhaul that 'nothing was wrong with the engine.' Clearly the aircraft engineer erred in the side of safety; but what is promising is that the statistical analysis also predicted a low hazard rate. This result for failure rate estimation was obtained from the model:

$$r(t,\ z(t)) = \frac{5.335}{3255.19}\left(\frac{t}{3255.19}\right)^{4.335} \quad x \exp[0.506z_1(t) + 1.25z_2(t)]$$

where

t = flight hours

z_1 = iron deposits in parts per million,

z_2 = silver deposits in parts per million,

and the 'baseline' failure rate, i.e. assuming there was no effect of the covariates iron and silver, was Weibull with

$$r(t) = \frac{\beta}{\eta}\left(\frac{t}{\eta}\right)^{\beta-1}$$

$$= \frac{5.335}{3255.19}\left(\frac{t}{3255.19}\right)^{4.335}$$

Use of the proportional hazards model relating to sonar domes within the U.S. Navy is reported by Ascher [9]. Recent papers dealing with proportional hazards modelling include Bendell [10], and Ansell and Phillips [11] with quite a full discussion of P.H. modelling being given by Kalbfleisch and Prentice [12]. Jardine et al [13] report on the possible role that proportional hazards modelling could play to assist in improving maintenance decisions associated with Canadian Pacific Rail's diesel engines which undergo scheduled major overhaul at intervals of approximately four years. Between these overhauls the condition of an engine is monitored by a series of physical tests and spectroanalysis carried out on samples of lubricating oil. At present the results of these tests are interpreted by the combination of skilled oil-analyst technicians and an expert system. The success rate of this is over 70 per cent, where success is defined to mean that the oil-analyst/expert system recommends that the engine should be scheduled for maintenance and it does indeed subsequently show evidence of an imminent failure. The paper reports an examination of the method of proportional hazards modelling to determine whether or not PHM could improve on the accuracy of the oil-analyst/expert system in determining the risk of failure of a diesel engine.

Within the mining industry oil analysis is often performed on haul truck transmissions and engines. When visiting a large open pit mine the author asked the maintenance manager about the success rate of the spectroscopic oil analysis program. The response was "About 65%." Thus, on 35% of occasions, either the oil analysis report suggests that the equipment is in need of repair then subsequently nothing is identified as being defective, or a signal is given that the equipment is in a good state of repair, yet shortly thereafter a failure occurs. As was the case with the C.P. Rail situation it seems that there is scope for improving the reliability of conclusions being drawn from interpretation of oil analysis data, and perhaps the PHM approach can assist.

CONDITION-BASED MAINTENANCE VIA VIBRATION MONITORING

In a recent article in the McLean Hunter publication IMRON (Industrial Maintenance Repair and Overhaul News) [14] it is stated that "medium sized plants typically report savings between $350,000 and $500,000 per year as a result of using vibration control as part of a predictive maintenance program - often called condition monitoring - on rotating machinery. Some firms achieve double those savings, or more, simply by a different management approach in two primary areas: rather than using vibration control strictly to predict imminent machine failures, they increase equipment life by lowering vibration levels, and they expand the role of technicians in their vibration programs".

As indicated in the previous section of this paper, it seems that there is significant scope for improving equipment maintenance decisions when the equipment is subject to a regular oil analysis program.

Informal comments from plant engineers also suggest the same is true for equipment that is regularly monitored through vibration monitoring procedures. Rather than using the "trending and averaging" approach [8] , perhaps proportional hazards modelling can assist maintenance management interpret reliably the fairly extensive records available through vibration monitoring of their equipment.

CONCLUDING REMARKS

If dedicated effort is put into the use of quantitative procedures to assist maintenance management there will be major enhancements in the quality of decision making in maintenance. So often organizations are data rich, but information poor.

ACKNOWLEDGEMENT

Much of the material presented in this paper has appeared in the papers Unit Replacement, A.K.S. Jardine., Terotechnica, 2, (1981), 51-58 and Equipment Reliability and Maintenance, A.K.S. Jardine and J.A. Buzacott, European Journal of Operational Research, Vol. 19, No. 3(1985) 285-296

REFERENCES

1. Valdez-Flores C., and Feldman, R.M., *A Survey of Preventive Maintenance Models for Stochastically Deteriorating Single-Unit Systems*, Naval Research Logistics, Vol. 36(1989).

2. Cox, D.R., Renewal Theory, Wiley, 1962.

3. Jardine, A.K.S., 1973. *Maintenance, Replacement and Reliability*, Pitman. Reprinted edition is available from Canadian Scholars' Press Inc. 339 Bloor Street West, Suite 220 Toronto Ontario M5S 1W7 Canada

4. Kapur, K.C., and Lamberson, L.R., *Reliability in Engineering Design*, Wiley, New York, 1977.

5. Cox, D.R., *Regression models and life tables (with discussion)*, Journal of the Royal Statistical Society, Series B 34 (1972) 187-220.

6. Pottinger, K., and Sutton, A., *Maintenance management - An art or a Science*, Maintenance Management International 3 (4) (1981) 251-256.

7. Jardine, A.K.S., and Anderson, P.M. *Use of concomitant variables for reliability estimation*, Proceedings of the 8th Symposium on Advances in Reliability Technology, Bradford University, 1984. Also appeared in Maintenance Management International 5, (1985), 135-140.

8. Morrow, R.S., *Computer Aided Machinery Health Monitoring Using Trending and Averaging of Vibrations*, Proceedings, Ninth Machinery Dynamics Seminar, National Research Council, Montreal, September, 1986.

9. Ascher, H., *Regression analysis of repairable system reliability in electronic systems effectiveness and life cycle costing*, NATO ASI *Series*, Springer, Berlin 1983, 119-133.

10. Bendell, A, *Proportional hazards modelling in reliability assessment, Reliability Engineering*, II 175-183 (1985).

11. Ansell, J.I., and Phillips, M.J., *Practical problems in the statistical analysis of reliability data*, Appl. Statist., 38, (2), 205-247 (1989).

12. Kalbfleisch, J.D. and Prentice, R.L., *The Statistical Analysis of Failure Time Data*, Wiley, New York, 1980.

13. Jardine, A.K.S., Ralston, P, Reid, N and Stafford, J., *Proportional Hazards Analysis of Diesel Engine Failure Data.*, Quality and Reliability Engineering International, Vol. 5, (1989) 207-216.

14. IMRON, *Why Machine Monitor*, 11, March 1990.

FONDEMENTS DE L'ANALYSE DES SIGNATURES DE VIBRATIONS POUR LA SURVEILLANCE DE L'ÉTAT DES MACHINES

T. Loewen et F. Perricone
Ontario Hydro Research Division
Toronto, Ontario

RÉSUMÉ

Cette communication décrit les avantages qui peuvent être tirés de programmes d'entretien préventif des usines basés sur l'information fournie par les systèmes de surveillance de l'état des machines. Les caractéristiques des systèmes de surveillance comme la capacité de détecter et de diagnostiquer précocement des pannes de machine sont présentées.

L'accent est mis sur le traitement et l'analyse des signaux de vibrations ainsi que les aspects du matériel qui sont critiques pour obtenir des données fiables.

BIOGRAPHIES

Ted Loewen est superviseur de la Section de la dynamique des équipements d'usine de la Division de recherche d'Ontario Hydro à Toronto. Il a oeuvré dans le domaine de l'analyse et du contrôle des vibrations des machines tournantes pendant plus de 15 ans. Il détient un B. Sc. et une M.A. Sc. en génie mécanique des universités du Manitoba et de Waterloo respectivement.

Frank Perricone est chef du groupe de la dynamique des machines et des structures de la Section de la dynamique des équipements d'usine de la Division de recherche d'Ontario Hydro à Toronto. Il a travaillé à la mise en service et au dépannage des problèmes de vibration du matériel tournant et des systèmes de conduites de centrales ainsi qu'à la mise au point de systèmes de contrôle des vibrations. Il détient un B.A. Sc. et une M.A. Sc. en génie mécanique des universités de Toronto et de Waterloo respectivement.

VIBRATION SIGNATURE ANALYSIS FUNDAMENTALS FOR MACHINE CONDITION MONITORING

T. LOEWEN AND F. PERRICONE
ONTARIO HYDRO RESEARCH DIVISION

ABSTRACT

This paper outlines benefits which can be derived from plant predictive maintenance programs based on information provided by machinery condition monitoring systems. The monitoring system requirements such as the capability to detect and diagnose machinery faults at an early stage are presented.

The emphasis of the paper is on a discussion of vibration signal processing and analysis as well as hardware considerations which are critical to obtaining reliable data.

AUTHORS

Ted Loewen is supervisor of the Plant Equipment Dynamics Section of the Ontario Hydro Research Division in Toronto. Mr. Loewen has been active in rotating equipment vibration analysis and vibration monitoring for more than 15 years. Mr. Loewen has a B.Sc and M.A.Sc in mechanical engineering from Universities of Manitoba and Waterloo respectively.

Frank Perricone is a Unit Head of the Machine and Structural Dynamics group in the Plant Equipment Dynamics Section of the Ontario Hydro Research Division in Toronto. His areas of work have included commissioning and troubleshooting vibration problems of power plant rotating equipment and piping systems as well as developing vibration monitoring systems. Mr. Perricone holds B.A.Sc and M.A.Sc degrees in mechanical engineering from Universities of Toronto and Waterloo respectively.

VIBRATION SIGNATURE ANALYSIS FUNDAMENTALS FOR MACHINERY CONDITION MONITORING

INTRODUCTION

There are significant financial rewards to industrial plants which can minimize plant downtime as well as maintenance expenditures. Predictive or on condition maintenance can contribute towards both of these objectives. This has led to an increasing interest in predictive maintenance. Important aspects of predictive maintenance are the "tools" and methods used to detect and diagnose equipment faults requiring maintenance.

Vibration analysis of equipment is commonly used to provide information required for predictive maintenance programs. The selection of instrumentation and software based microprocessor equipment for vibration data collection and analysis has greatly expanded. Consideration of some vibration signature fundamentals is important in selection of suitable equipment and proper application of existing equipment. This will contribute to obtaining reliable data on which to make important maintenance decisions.

PREDICTIVE MAINTENANCE

The optimum approach to maintenance would be to do only (but all of) the required maintenance at an opportune time which is the goal of a predictive maintenance program. With this maintenance strategy, maintenance is carried out only when the condition of the machine dictates that a corrective action should be taken. To make this possible requires a monitoring system which can provide accurate diagnostic information on the condition of the machinery.

The major benefits of a predictive maintenance program are:

Reduced Maintenance Costs

Faults are identified at an early stage reducing the probability of a catastrophic machine failure. Manpower, parts and equipment can be planned for with the early knowledge of the repair and maintenance requirements. Manpower requirements can be scheduled well in advance allowing the optimum use of personnel. Maintenance costs are also reduced because the average time between overhauls can be increased. Early identification of a fault often allows a problem to be corrected during scheduled outages avoiding the high cost associated with emergency repairs.

Since machine faults are identified at an early stage of machine deterioration, secondary damage resulting from primary faults can be minimized. Thus, costly maintenance repairs can be reduced significantly.

Maintenance costs can also be reduced since the quality of maintenance work can be checked immediately after it is completed reducing the risk of placing a unit back on-line with improperly corrected faults or a newly introduced deficiency.

Increased Plant Availability

An on condition monitoring program provides continuous information on the status of the plant machinery. This information when properly used by various departments of a company can be used to maintain a high level of machine availability. There would be fewer times when a fault goes undetected which could result in extensive damage. The net result would be less damage, shorter repair times and a significant reduction in unplanned shutdowns.

The planning function can also be enhanced because of improved trending or monitoring of developing faults. When a fault is detected, a machine operation can sometimes be modified to keep the system on line longer. When a shutdown is necessary, the shutdown can often be planned for off peak load periods.

A predictive maintenance program can also provide more information on the machine's characteristics which could be used in identifying and correcting design deficiencies. This could assist in the design of more reliable machines and fewer shutdowns for repairs.

Improved Personnel Safety

The lead time provided by a condition monitoring system enables the machine to be stopped safely before an unsafe condition occurs which could result in personnel injury. Personnel safety is enhanced because unnecessary maintenance and work done on an emergency basis is significantly reduced.

REQUIREMENTS FOR EFFECTIVE MONITORING FOR PREDICTIVE MAINTENANCE

To implement an effective machinery predictive maintenance program requires a monitoring system that has the following capabilities:

- detects developing defects at an early stage

- provides diagnostic information which permits identification of specific faults so that repairs and overhauls can be directed at specific known deficiencies

- trends parameters related to machinery condition to assist in maintenance planning

Vibration Monitoring - A Proven Machine Condition Indicator

All operating machinery vibrates and its vibration characteristics have long been recognized as an important indicator of its condition. Machinery vibration depends on the forces acting on the various components and the dynamic characteristics of the system. Machinery faults generally result in greater or new forces and/or a change in the machine's dynamic characteristics. The analysis of machine vibration can identify the faults or changes in a machine's condition.

However, a complicating factor is that the machinery forces and dynamic characteristics may also be affected by changes in process and/or environmental conditions. Thus it is desirable to monitor both vibration and process conditions so that the differences in process can be taken into account when assessing changes in vibration. This will greatly minimize false alarms.

Monitoring Overall Vibration Level

In industry, it has been a common practice to monitor only overall vibration levels. If the vibration levels are monitored continuously, the system may be used to provide protection by shutting down the machine if the overall vibration levels exceed preset alarm levels. However, monitoring only the overall vibration levels is not adequate for predictive maintenance since early detection and diagnostic information are not provided.

Monitoring overall vibration levels will generally only detect defects at an advanced stage. The reason for this is that the overall vibration signal level is generally dominated by the unbalance frequency component and thus not sensitive to changes in other frequency components unless the changes or defect size become very large.

As an example, if the vibration velocity level of a machine is 10 mm/s due to unbalance

(1xrpm component) and 1 mm/s due to misalignment (2xrpm component), the overall vibration level would be $\sqrt{10^2+1^2} = 10.05$ mm/s. If the misalignment component increases by a factor of 2, the overall level would only have increased to $\sqrt{10^2+2^2} = 10.20$ mm/s. Thus a significant change (ie 100% increase) in the misalignment would have only resulted in a minor effect on the overall vibration level. Therefore the increased misalignment would neither have been detected or diagnosed.

Monitoring of overall levels is not sensitive to detecting developing faults until the vibration component associated with the fault is the highest component. Since it is necessary to detect faults at an early stage for a successful predictive maintenance program, a mandatory requirement is to include a frequency analysis capability into the monitoring strategy. Of equal significance is that the vibration frequencies can provide diagnostic information about unbalance, misalignment, gear fault, rolling element bearing faults, looseness, impacting, resonances, critical speeds, rubs, instabilities, electrical faults, etc.

DIGITAL SAMPLING AND FREQUENCY ANALYSIS FUNDAMENTAL CONCEPTS

As outlined in the previous section, a frequency analysis capability is a mandatory ingredient for a successful predictive maintenance program. Fortunately, numerous spectrum analysis instrumentation and PC based data acquisition systems are available and are widely used. With the wide range of signature analysis equipment available, it is important to consider their technical characteristics to ensure that reliable data is obtained and that the data is correctly interpreted.

The following sections outline some fundamentals of digital sampling and frequency

analysis which are intended to provide some basic signal processing concepts which are of practical importance to the use of vibration instrumentation such as FFT analyzers, digital sampling PC computer based data acquisition cards and vibration monitoring equipment.

Digital Sampling

Since most vibration signals do not possess a mathematical or analytical expression, they must first be digitized and then analyzed by means of numerical algorithms on a digital computer. There are two common errors that can be encountered when sampling a signal. They are:

1. - quantization
2. - aliasing

Signal Quantization

A quantization error can occur because a signal can not be digitized with infinitesimal accuracy but instead only with discrete levels. The actual value or amplitude of the digitized waveform is rounded off to the nearest digital level which is determined by the number of bits in the A/D. The following table summarizes the resolution accuracy that can be achieved with 8 to 16 bit A/D converters.

NUMBER OF BITS FOR THE A/D CONVERTER	RESOLUTION
8	1/256
10	1/1024
12	1/4096
14	1/16384
15	1/32768
16	1/65536

For example, suppose that an instrument has an 8 bit A/D with a measuring voltage range of 10 volts. The maximum signal resolution that can be achieved with that instrument is 10 volts / 256 which is 39.06 millivolts. Whereas for a 16 bit A/D, the maximum signal resolution would be 10 volts /65536 which is 0.15 millivolts.

For dynamic signals, a 12 bit A/D converter will perform an acceptable task when proper signal conditioning and amplification are provided. When a higher accuracy and a large dynamic range are required, a 14-16 bit A/D converter should be considered. However, precautions should be taken to ensure that the bus noise of the instrument or computer is lower than the resolution of the A/D system and that associated signal processing components such as anti-aliasing filters have specifications which are compatible with the capabilities of the A/D system.

The Effect Of Undersampling - Aliasing

One major pitfall to avoid when digitizing continuous signals is aliasing. It occurs when the continuous waveform is undersampled. Some familiar cases illustrate the effect of aliasing.

Everyone has seen the aliasing phenomenon on television or at the movies. In the old western movies, as the cartwheels turn faster and faster, they appeared to slow down and then stop. If the speed increased, the stagecoach wheels seemed to go backward, stop, and go forward a number of times. Similarly, the same phenomenon could be observed with airplane propellers as their rotating speed increased. This aliasing effect occurred because the sampling speed of the camera was not sufficient for the high rotating speed of the cartwheels or the airplane propellers.

The rule governing proper sampling is referred to as the Shannon's Sampling Theorem, which states that the sampled time signal must not contain components at frequencies above half the maximum sampling rate (the Nyquist or folding frequency). If the sampling rate is less than twice the highest frequency component, then aliasing frequencies will occur. These frequency peaks are indistinguishable from the energy contributed by the true signal and therefore the sampling process has actually created a false signal (i.e an "alias", or "false name").

The following figure shows an example of the aliasing phenomenon. In this example, ten cycles of a high frequency signal (100 kHz) are shown in the data window. It is assumed that the signal is sampled 12 times in the ten cycles as illustrated by the dots. This sampling rate corresponds to a sampling frequency of 120 kHz. Thus the Nyquist frequency is 60 kHz.

Since the sine wave frequency is higher than the Nyquist frequency, an alias frequency is expected. The sine wave which passes through the dots represents the alias frequency. In this case it is 20 kHz. If this was a vibration measurement, the vibration spectrum would show a false 20 kHz frequency component which was not in the original signal.

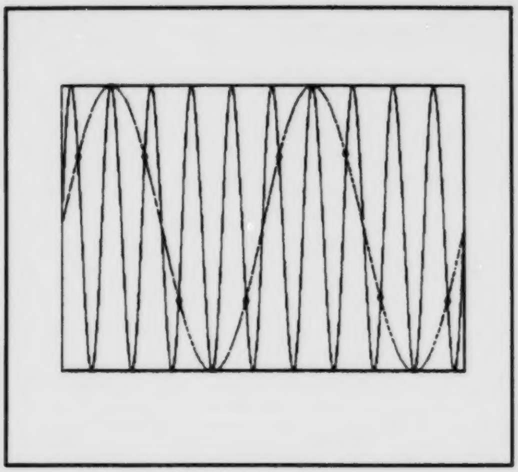

In general, the alias frequency (f_a) of a signal frequency sampled at a rate of (f_r) is given as:

$$f_a = f_r - f \quad when \ \frac{f_r}{2} < f < f_r$$

For the example above,

$$f_a = 120\,kHz - 100\,kHz = 20\,kHz$$

In the above example, the 100 kHz frequency exists between the Nyquist frequency $(f_r/2)$ and the Nyquist rate (f_r) . Aliasing can also occur when the signal contains frequencies well above the Nyquist rate. For example, a faulty signal conditioning system could inject a high frequency noise in the order of 100 kHz on a vibration signal where the maximum frequency of interest is only 200 Hz. In this case a low frequency alias would also occur due to the noise. The general formulae for determining aliasing frequencies are:

$$f_a = \left\{ kf_r - f \ \ when \ \ (k-\frac{1}{2})f_r < f < kf_r \right\}$$

and

$$f_a = \left\{ f - kf_r \ \ when \ \ kf_r < f < (k+\frac{1}{2})f_r \right\}$$

where

$$k = 1,2,3,.......$$

An anti-aliasing filter is required to reduce aliasing problems. Essentially, it is a low pass filter that attenuates frequencies above its cutoff frequency but passes those below its cutoff. This filter must precede any sampling process.

Unfortunately, the construction of a brickwall anti-aliasing filter that passes all frequencies below its cutoff and completely attenuates all frequencies above its cutoff is not possible. The characteristics of a typical non ideal anti-aliasing filter is shown in the figure below.

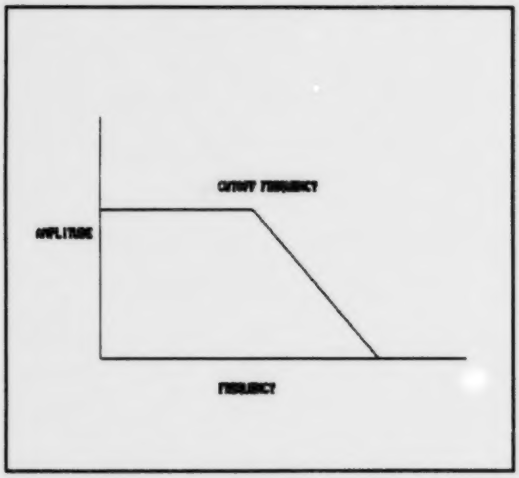

The filter passes all frequencies almost perfectly below the cutoff frequency, while above the cutoff frequency attenuation increases with frequency. This rate of increasing attenuation is called the filter rolloff and is usually expressed in decibels (dB) per octave. Theoretically, a brickwall filter has an infinite rolloff.

The following are practical guidelines to be used when choosing a low pass filter and sampling rate:

- **establish the highest frequency of interest in the signal**
- **specify the required alias suppression**
- **choose the sampling rate and the filter rolloff to provide the required aliasing suppression**

There is a tradeoff between the sampling rate and the filter rolloff which needs to be considered when choosing an anti-aliasing filter and sampling rate. A less expensive anti-aliasing filter system can be used with a higher sampling rate. This requires a more expensive A/D and the acquisition and processing of much more data. The extra data requires more computer memory capacity and more time for data analysis. On the other hand, a very steep rolloff filter could be very expensive, in particular if a large data acquisition system is contemplated. Lastly, a steep rolloff filter introduces more phase shift which could be important if waveform fidelity is the biggest concern.

Fourier Analysis - The Basis For Frequency Analysis

The mathematical basis of frequency analysis is the Fourier transform. From a mathematical point of view, the Fourier transform changes information in the time domain into the frequency domain. The most important concept in Fourier analysis is that a time signal, such as the voltage signal output from a vibration transducer, can be expressed as a summation of sinusoidal components of different frequencies, phase angles and magnitudes.

The basis for frequency analysis is the fourier integral.

$$X(f) = \int_{-\infty}^{\infty} x(t) e^{-j2\pi ft} dt$$

The fourier integral takes a continuous input time function $x(t)$ and transforms it to a continuous output function of frequency $X(f)$.

Since:

$$e^{-j\theta} = \cos\theta - j\sin\theta$$

The Fourier integral can be also written as:

$$X(f) = \int_{-\infty}^{\infty} x(t)(\cos(2\pi ft) - j\sin(2\pi ft))dt$$

If a signal $x(t)$ is represented by a sequence of samples $x[n]$ then the Discrete Fourier Transform (DFT), which is much better adapted to digital computations, is defined as:

$$X(f_k) = \sum_{n=0}^{N-1} x[n]\ e^{-j2\pi nk/N}$$

where N = the number of samples (length of the sequence $x[n]$)

$x[n]$ = the input time samples

$X\left[f_k\right]$ = the output discrete frequencies

Of all the DFT properties, the following two properties are the most important to consider when applying the DFT.

Frequency Resolution

When a DFT is performed, an error in the amplitude and frequency will occur unless a frequency component in the original signal coincides exactly with a computed analysis line. The output of the DFT is a set of discrete frequencies $X\left[f_k\right]$ (often referred to as bins or lines since they appear as bins or lines on a spectrum analyzer) spaced at $1/(Nt_s)$. The sampling interval is t_s and the discrete frequencies range from 0 (DC component) to the Nyquist frequency which is half of the sampling frequency. Frequencies in the original signal which exist between the DFT bin frequencies, will be represented only at the DFT frequency bin locations. In general, two harmonics separated by less than $2/(Nt_s)$ cannot be resolved. When high frequency resolution is required, the data block collection time Nt_s must be increased. A large DFT can be applied directly to the larger sampled sequence or a special zoom algorithm can be utilized which uses a smaller DFT on a repetitive basis.

The following table summarizes the relationships among the important sampling parameters when using a DFT:

CHOOSE DESIRED SAMPLING PARAMETER	CHOSEN PARAMETER AUTOMATICALLY FIXES THE VALUE OF THE PARAMETER BELOW, BECAUSE OF THE RELATIONSHIP IN PARENTHESES	THEN MAKE EITHER OF THE REMAINING TWO PARAMETERS (CAN'T BE BOTH) AS CLOSE AS POSSIBLE TO THE DESIRED VALUE BY CHOOSING N* IN THE RELATIONSHIPS SHOWN
Δt	$F_{max}\left[F_{max}=\frac{1}{2\Delta t}\right]$	$T\,[\,T=N\Delta t]$ $\Delta f\left[\Delta f=\frac{1}{N\Delta t}\right]$
F_{max}	$\Delta t\left[\Delta t=\frac{1}{2F_{max}}\right]$	$T\,[\,T=N\Delta t]$ $\Delta f\left[\Delta f=\frac{1}{N\Delta t}\right]$
Δf	$T\left[T=\frac{1}{\Delta f}\right]$	$\Delta t\left[\Delta t=\frac{T}{N}\right]$ $F_{max}\left[F_{max}=\frac{N}{2}\cdot\Delta f\right]$
T	$\Delta f\left[\Delta f=\frac{1}{T}\right]$	$\Delta t\left[\Delta t=\frac{T}{N}\right]$ $F_{max}\left[F_{max}=\frac{N}{2}\cdot\Delta f\right]$

***N, THE DATA BLOCK SIZE, IS ALWAYS A POWER OF 2**

For example, assume that a frequency measurement is required with a 0.5 Hz frequency resolution and a 4 kHz Nyquist frequency bandwidth. What is the minimum collection time and the minimum number of time samples?

- the required frequency resolution is 0.5 Hz ($\Delta f = 0.5$ Hz)

- the minimum collection time T is 1/0.5 = 2 seconds

- the minimum number of time samples for a 4 kHz bandwidth is 16,000 samples which is obtained using $F_{max} = \frac{N}{2} \cdot \Delta f$

In most hardware and software systems, the FFT (Fast Fourier Transform) is used instead of the DFT (Discrete Fourier Transform). The FFT is an efficient algorithm for calculating the DFT. The FFT algorithm takes advantage of the circular properties of the DFT in significantly reducing the number of computations that are required. The development of the algorithm in June 1967 by Cooley and Tukey reduced the computation of the DFT of an N-point time series from N^2 operations to $N \log_2 N$ operations. For a typical case, such as for a 1024 sample transform, the reduction factor in computation time is more than 100.

Periodicity of the DFT Processed Signal

A necessary requirement for the DFT, which is often overlooked, is that the sampled signal must be periodic with the period Nt_s equal to the total data collection time. If a DFT is performed on a signal which does not fulfill this requirement (as in most cases), then "leakage" occurs which results in spurious frequency components. This effect is commonly referred to as leakage because power from discrete frequency components is "leaked" into adjacent bands.

For most cases, a non-periodic sampled sequence will occur because a block of a continuous signal must be first "time windowed". A time window "slices" the data into a section for analysis as shown in the figures below.

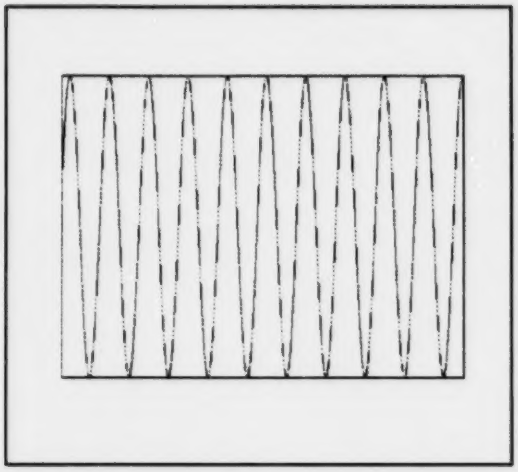

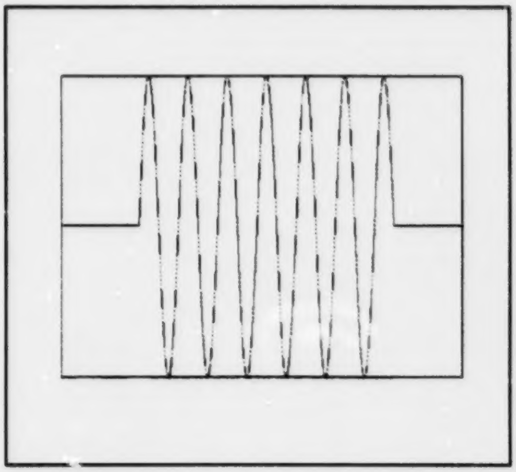

When a continuous time record is cut into a section for analysis, two significant effects occur concurrently:

- there will be a noticeable widening at the bases of the spectral components

- the magnitudes of the frequency components will not be correct

An example of the leakage phenomenon is shown in the following figures.

Figure L1 shows a time window which contains 10 cycles of a 97.65625 Hz sine wave with a peak magnitude of 1.0 volt. Since this signal is periodic in the time window, no "leakage"

will occur. Figure L2 shows the FFT of the signal. Note the sharpness of the frequency component and that the magnitude is 1.0 volt.

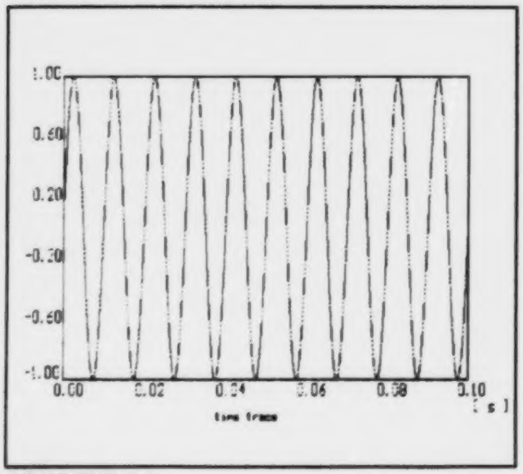

FIGURE L1

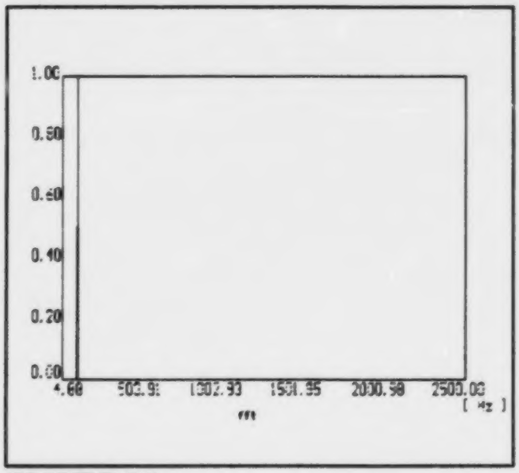

FIGURE L2

Figure L3 shows a 105 Hz sine wave with a magnitude of 1 volt in the same data window. In this case, the time data window contains 10.752 cycles and therefore the signal is not periodic in the time window. Figure L4 shows the FFT of the signal. Due to the leakage effect, the base of the 105 Hz frequency component has widened significantly and the magnitude has reduced to 0.64 volt.

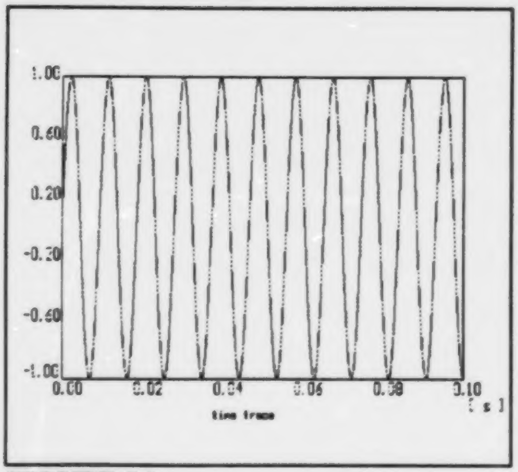

FIGURE L3

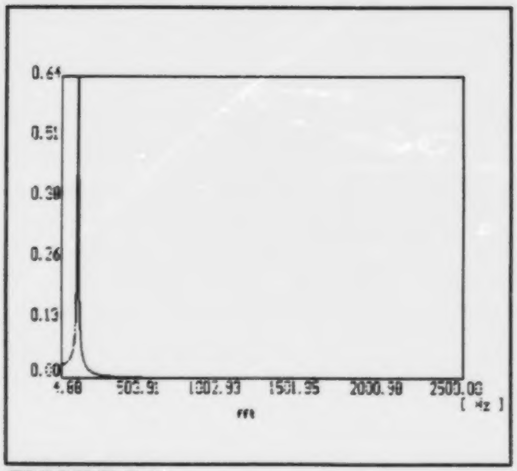

FIGURE L4

Leakage can be alleviated by applying a smoothing window or by forcing the sampled sequence to be periodic in the analysis window.

A smoothing window can be applied to the sampled sequence to smooth the signal discontinuities at the beginning and the end of the sampled sequence as illustrated by the following three figures.

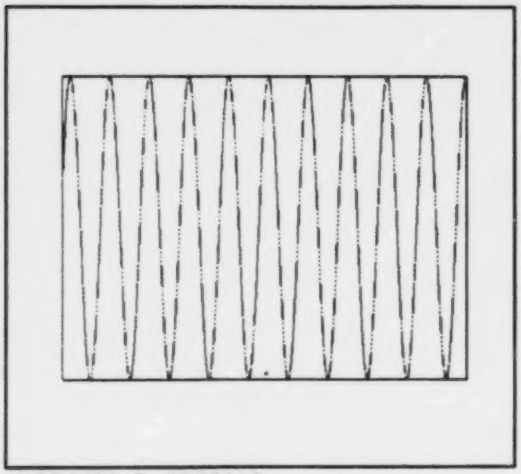

ORIGINAL SIGNAL

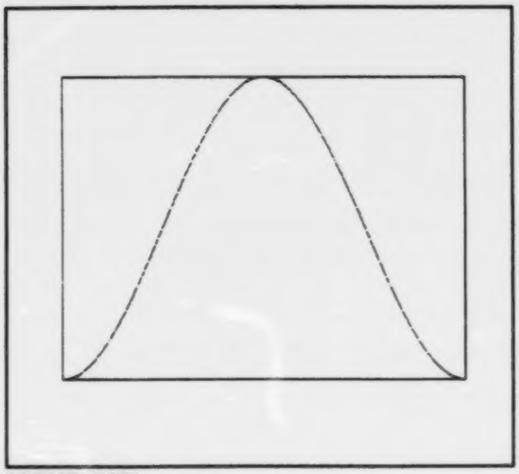

WINDOW

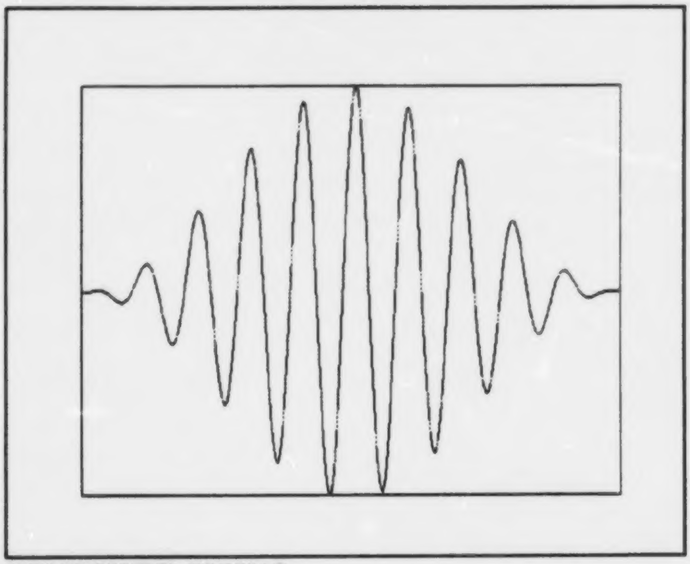

WINDOWED SIGNAL

The normal process is to multiply the window and the signal in the time domain. However, it is more efficient to apply windows by convolution in the frequency domain.

When windows are applied, they alter system performance. Ideally, it is desirable to minimize the effects of the windows. To that extend, many types of windows, each with their own particular characteristics, have been developed. A discussion on the various windows is beyond the scope of this paper. Further information is available in a classic paper on the subject by F.J. Harris.

Another method of controlling leakage is to force the sampled sequence to be precisely periodic. This can be accomplished by tying the digital sampling process to the speed of a machine or process and therefore forcing the number of periods to be an integer. For rotating machinery this can be accomplished by controlling the sampling process with a phase marker and obtaining an integer number of samples at equally spaced intervals around the shaft revolution cycle. This is referred to as order analysis.

CONCLUSIONS

A predictive maintenance program can assist in minimizing plant downtime and maintenance expenditures. This program requires monitoring of the equipment condition to be effective. The monitoring must be sensitive to incipient faults to provide adequate time for maintenance planning. Diagnostic information to identify the cause of the fault is also required to enable defect specific maintenance.

One tool which has emerged as a proven machine condition indicator is vibration analysis. With the wide range of vibration analysis equipment available, it is important to consider their technical characteristics to ensure that reliable data is obtained and that the data is correctly interpreted.

REFERENCES

Cooley, J. W., and J. W. Tukey, "An Algorithm for the Machine Calculation of Complex Fourier Series," Math. Computations, 19, April 1965

Harris, F. J., "On the Use of Windows for Harmonic Analysis With the Discrete Fourier Transform", Proc. IEEE 66, 51-83, January 1978

Elliott, D. F., Handbook of Digital Signal Processing - Engineering Applications, Academic Press Inc., San Diego, California, 1987

Ramirez, R. W., The FFT - Fundamentals and Concepts, Prentice-Hall Inc., Englewood Cliffs, N.J.,1985

Stanley, W. D., Dougherty, G. R., Dougherty, R., Digital Signal Processing, Reston Publishing Company Inc., Reston, Virginia, 1984

Perricone, F., Loewen, T., "Vibration Monitoring", Ontario Hydro NGD Fourth Maintenance Conference, January, 1990

PREDICTIVE MAINTENANCE TODAY: THE INFORMATION MANAGEMENT CHALLENGE

RICHARD C. HANCOCK
COMPUTATIONAL SYSTEMS, INC.
KNOXVILLE, TENNESSEE, U.S.A. 37932

ABSTRACT

Predictive maintenance, defined as the ability to monitor machinery condition non-invasively and determine maintenance requirements based on condition status, has become a key component in many industries' efforts to gain a competitive edge. Oil analysis (tribology), thermography, motor current analysis, and vibration analysis are some of the technologies commonly included in the predictive maintenance effort. At present, the huge amount of data available can overwhelm maintenance technicians and managers. Developments in automated problem detection, automated diagnostics, and interfaces between these different technologies are helping make the available information more manageable and productive.

BIOGRAPHY

Richard C. Hancock was employed for 10 years by Energy Industries, Inc., a U.S. manufacturer of reciprocating compressor packages for natural gas production and transmission. His work there involved applications engineering and marketing, and he has been involved with machinery condition monitoring at CSI since for the last 2 years. He completed an undergraduate degree in 1972 at the University of Georgia.

RAPPORT SUR L'ÉTAT DE LA MAINTENANCE PRÉVENTIVE OU LE DÉFIT DE LA GESTION DE L'INFORMATION

Richard C. Hancock
Computational Systems Inc.
Knoxville, Tennessee
U.S.A. 37932

RÉSUMÉ

La maintenance préventive, que l'on définit comme étant la possibilité de contrôler l'état d'une machine sans intervention directe et de déterminer ses besoins en matière d'entretien en se basant sur les rapports fournis par un ordinateur, est devenue un des éléments importants dans la stratégie d'un grand nombre d'entreprises pour devenir plus compétitives. La tribologie, la thermographie, le contrôle des moteurs selon les moyens conventionnels, et l'analyse des vibrations sont quelques unes des technologies qui font désormais partie des méthodes de maintenance préventive. Dans l'état actuel des choses, les techniciens et gestionnaires en maintenance sont littéralement ensevelis sous l'énorme quantité de données disponibles. La mise au point de méthodes automatisées de détection des problèmes, d'outils de diagnostic automatisés, et de systèmes d'interface entre ces différentes technologies rendent cette information beaucoup plus utile et plus facile à gérer.

BIOGRAPHIE

Richard C. Hancock fut pendant 10 ans à l'emploi de la firme américaine Energy Industries, Inc., un fabricant de compresseurs alternatifs pour l'exploitation et le transport du gaz naturel, où il était chargé du génie appliqué et de la mise en marché; il s'occupe du contrôle de l'état des machines chez CSI depuis deux ans. Il est diplômé de l'Université de Georgie, promotion 1972.

PREDICTIVE MAINTENANCE TODAY: THE INFORMATION MANAGEMENT CHALLENGE

Industrial organizations have sought methods to improve the "run to failure" mode of machinery maintenance ever since the beginning to the industrial revolution. Preventive maintenance techniques were developed whereby timespan or service intervals are used to schedule repairs or overhauls. Over the last thirty years instrumentation has evolved that allows maintenance to be based on some measure of a machine's actual condition without removing the equipment from service. This delivers the most cost effective maintenance effort by predicting necessary repairs rather than reacting to machinery failures. Currently, technologies for oil analysis, thermal monitoring, motor current analysis, and vibration analysis are used for predictive capabilities. Of these technologies vibration analysis probably contains the most information on machine condition.

During the 1960's and 1970's the U.S. Navy, the petrochemical industry, and the nuclear power industry heavily invested in the development of predictive maintenance (PDM) vibration technology for critical equipment evaluation. Even with the great advances made during this period, instrumentation required for a PDM program in the early 1980's was quite elaborate, expensive, and heavy. This might have included dedicated tape recorders, dedicated spectrum analyzers, and graphics plotters. The time required to collect, analyze, and archive data served to limit vibration based condition monitoring to a relatively small population of critical machinery. Since most of the data evaluation was manual at this stage, the availability of experienced vibration analysis personnel was another limiting factor to the widespread usage of this form of predictive maintenance.

Advances during the late 1980's have provided lightweight data collection instruments and personal computer (PC) based information management programs that makes PDM cost effective in a much wider range of industries and plant sizes. With these systems personnel who are relatively inexperienced in vibration analysis can collect data on large numbers of machinery points, often as many as 800 points per day per man. However, evaluation of this data to determine the most appropriate maintenance action requires a higher level of experience. In many plants this level of experience is limited or non-existent. In short, the information generating component (hardware/software) of vibration-based PDM technology grew faster than the human resource for handling the data. As the technology enters the 1990's the effort is focused on solving this information management challenge. This development can be divided into two areas:

- Improved automatic problem detection methods to sort through large volumes of data collected on periodic surveys;
- Automated diagnostic "expert" programs to expedite the initial evaluation of potential problems and to help train new vibration analysts;

AUTOMATIC PROBLEM DETECTION

Currently available vibration-based PDM systems consist of an integrated hardware and software package which uses a host computer workstation for data storage and diagnostic analysis. These systems also include a portable data collector and vibration transducer (Figure 1). The transducer converts mechanical vibration into an analog electrical signal in terms of phase, frequency, and amplitude. The portable data collector temporarily stores incoming vibration signals from the transducer and processes the waveform using Fast Fourier Transform (FFT) techniques. Using database information stored in the host computer, measurement parameters for a large number of machinery points can be downloaded to the lightweight portable data collector. The vibration measurements are then made during a periodic survey and the results are uploaded to the host computer. At many plant sites, 5,000 to 7,000 points monitored monthly is typical, so the time required to manually evaluate each signature would be prohibitive. Computer based diagnostic software can certainly manipulate large volumes of data quickly. The major challenge is to approach the accuracy and consistency of an experienced vibration analyst in detecting potential problems. To achieve this efficiency and reliability, three major alarm algorithms are commonly used. These are overall alarming, envelope alarming, and selective frequency band alarming.

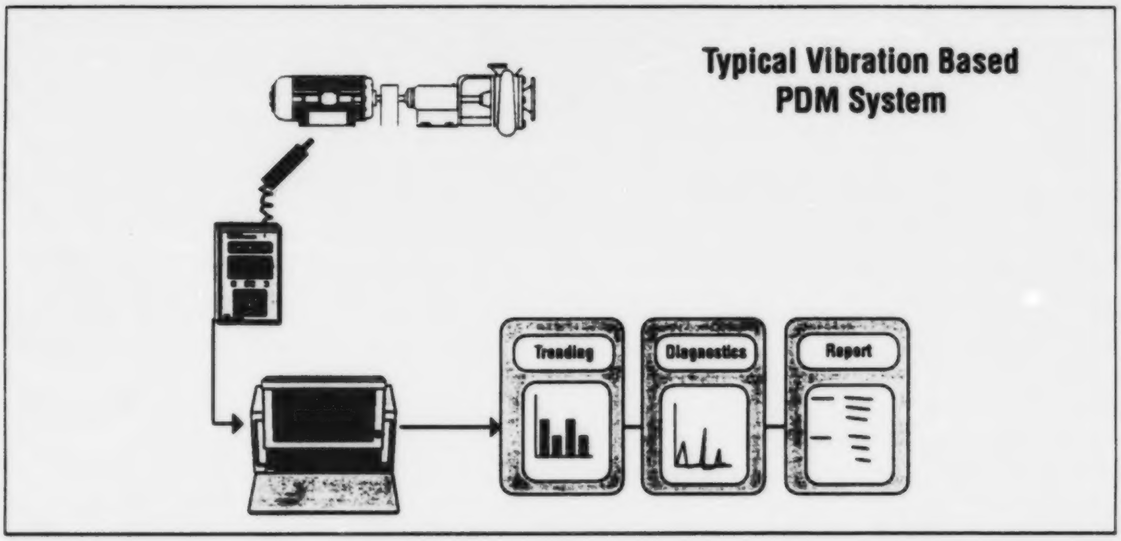

Figure 1.

Overall Alarming

Overall alarming is an algorithm which calculates the vibration energy beneath a spectral pattern and compares the energy to industrial standards for overall vibration energy, such as ISO standards, EPRI standards, API standards, etc., (see Figure 2). Overall energy is typically calculated by applying the root-mean-square (RMS) summation method to the spectral pattern. If the overall vibration energy level is in excess of an industrial standard, then alarms are triggered by the PDM diagnostic software to indicate that a significant change has taken place in the machine's condition. Unfortunately, overall alarming is considered insensitive to small changes in energy associated with bearing defects, electrical defects, gear tooth defects, and other small energy defects. If overall alarm levels are set to alarm on changes in high energy defects such as imbalance or looseness, then significant changes in low energy defects such as bearing and electrical defects will not be adequate to trigger alarms. The converse also is undesirable. If overall alarm levels are set to alarm on low energy defects, small changes in looseness or imbalance energies will cause unwarranted alarms. For these reasons, most analysts use overall alarming only to supplement more detailed alarm algorithms.

Standard	Measurement	Alert Level	Alarm level
1. Hydraulic Institute, 14th Edition	casing	0.30*	———
2. ISO 2372	casing	0.25	0.60
3. EPRI FP 754	shaft	0.50	0.80
4. API 610, 6th Edition	shaft	0.40	———
5. Rathbone Chart	casing	0.30	0.60

* Filtered reading valid 2,000 to 20,000 CPM.

Figure 2. Overall Vibration Standards Summary

Envelope Alarming

A second type of alarm algorithm, called envelope alarming, involves penetration of an "imaginary" envelope pattern drawn over the spectral pattern. Most PDM diagnostic software programs typically use constant percentage enveloping. Constant percentage envelope alarming creates an envelope pattern by applying a percent delta (% Δ) to a "baseline" spectra. In other words, the analyst will collect baseline spectra for all of his plant equipment, and then mathematically create the alarm envelope by applying a multiplication factor of 110 percent to 115 percent of the baseline spectra (see Figure 3).

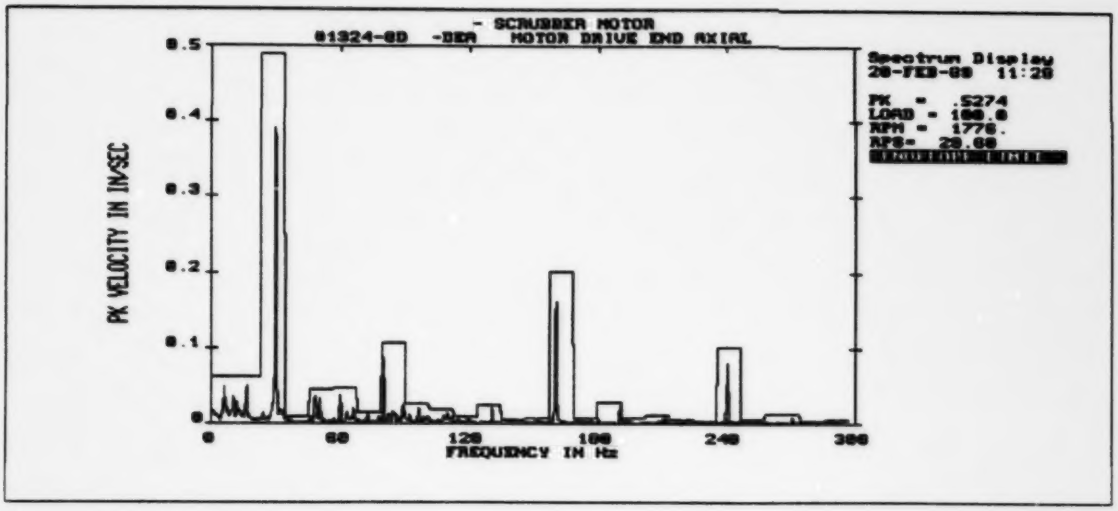

Figure 3. Constant Percentage Alarm Envelope

Unwarranted alarming is common with constant percentage envelopes primarily due to the observance that vibration levels are not typically consistent within individual spectral resolution lines. To further explain, perfectly constant machine operating speed is not achievable. Small speed variations (two to three percent) will often result in a detectable shift in rotational frequency and frequency related spectral lines. As an example, if the operating speed of a machine changes by three percent from one survey to the next, the spectral pattern would shift to the left or right by three percent, but the constant percentage alarm envelope would remain stationary. Unwarranted alarms would occur as the shifting spectral pattern penetrated the stationary envelope pattern.

A second problem is the phenomenon where spectral line amplitudes will often have small variations for a period of time and then change abruptly for no apparent reason to new levels with new variations. Although spectral line amplitude variations are typically small, their random changes cause significant false alarming of the spectral envelope, particularly in envelope areas where the original baseline area has very low amplitudes. For instance, if the baseline amplitude at a certain frequency is extremely small, the envelope pattern at that line will be "115 percent of something extremely small". Unwarranted alarming would thus occur with high regularity.

A much more powerful envelope algorithm called variable shape enveloping has been introduced. This new algorithm allows the computer to utilize three shaping criteria for each spectral bin to create the alarm envelope. The three shaping criteria are:

(1) user-defined absolute delta ([Δ]) above baseline spectra;
(2) percent delta (% Δ) above baseline spectra; and
(3) absolute full scale amplitude level([z]).

It would be best to describe the creation of a variable shaped envelope by referring to Figure 4. Note that the three individual shaping patterns are shown above a typical spectra. The resulting variable shape envelope is created by tracing the smallest of each the three shaping criteria within a spectral bin (see Figure 5). Unwarranted alarming can be virtually eliminated with variable shape enveloping because the user can "tweak" each of the three shaping criteria to his specific needs. Also, variable shape envelopes are automatically shifted left or right for variations in machine speed. The following generic shaping values appear to be a good starting point, based on current experience level:

Absolute delta [Δ] = 0.05 (protects individual faults)

Percent delta % Δ = 500 (protects small amplitude faults)

Absolute amplitude [z] = 0.3 large amplitude faults)

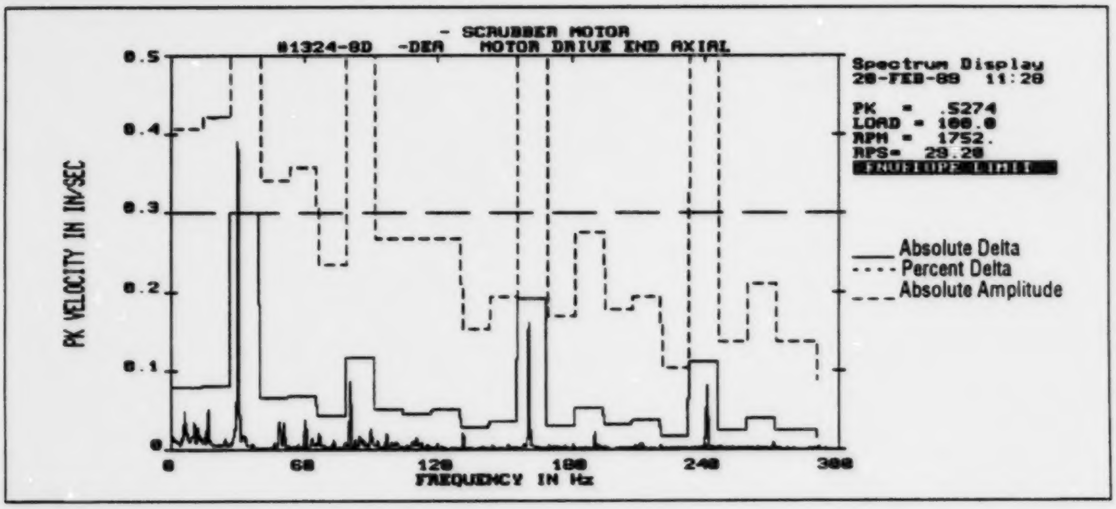

Figure 4. Variable Shaping Criteria

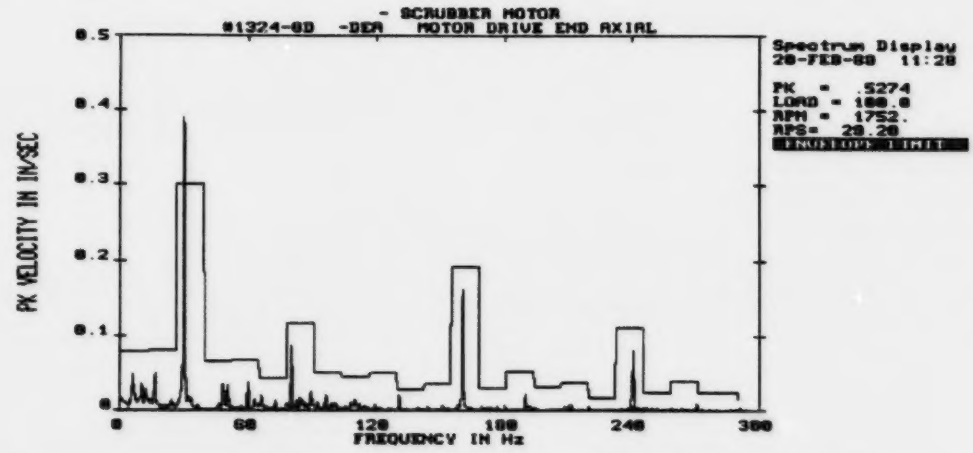

Figure 5. Smallest of Shaping Criteria

Shaping values for specific classes of machinery will be published as they become available through user's feedback. It is important to remember that envelope alarm patterns are always produced from a baseline vibration signature. What happens if the baseline signature has fault peaks? If the user is unaware that fault peaks exist, then the envelope may not alarm, and the machine may fail. The user would then be forced to repair the machine, collect a "new" baseline, and create a "new" alarm envelope.

Selective Frequency Band Alarming

The third and perhaps most powerful alarm algorithm available is selective frequency band alarming. A basic principal of vibration signature analysis is that individual mechanical faults generate vibration frequency peaks in well-defined patterns. Utilizing this principal, selective frequency band alarming allows the user to trend known fault frequencies, even before they develop. During plant database setup, the user establishes for each machine the frequency width and alarm levels for several known fault patterns. For instance, the user may establish an overall alarm level, and then individual alarm levels for imbalance, misalignment, cavitation (if a pump), bearing faults, belt deterioration (if belt driven), and motor electrical faults. Again, each of those mechanical faults (and most others) produce vibration in anticipated patterns.

An example of this type alarm system can be applied to a sleeve bearing type of machine. Sleeve bearing machines usually have a high percentage of synchronous energy and very little or no vibration content above 10xRPM. Table 1 shows recommendations for selective bands and alarm levels for general sleeve bearing machines.

Table 1
General Sleeve Bearing Machine

Fault Band	Frequency Range	Alarm Levels	Units
Overall Vibration	0-10xRPM	.35	in/sec
Subharmonic Faults	0-0.8xRPM	.10	in/sec
1xRPM Faults	0.8-1.2xRPM	.30	in/sec
2x-3xRPM Faults	1.5-3.5xRPM	.25	in/sec
3xRPM Faults	3.5-.10xRPM	.20	in/sec
Vane Pass	~3x or 5x	.10	in/sec
Phase at 1xRPM		30°	deg.

Once fault bands are established for each measurement point, incoming vibration signatures are automatically broken into individual fault bands and compared to established fault band alarm levels. Another advantage of selective frequency band alarming is that band alarming is not only performed in the analysis software, but also in the data collector. For instance, if a user receives a bearing band alarm on a general roller bearing machine while in the field, he can then collect additional and more detailed bearing band data at that time without having to return to the analysis software package to be warned of a potential problem (see Figure 6).

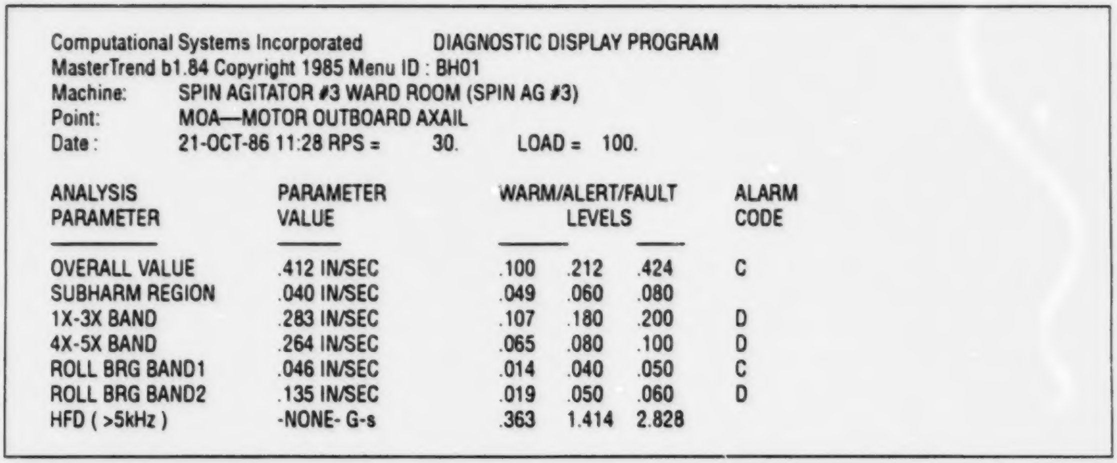

```
Computational Systems Incorporated         DIAGNOSTIC DISPLAY PROGRAM
MasterTrend b1.84 Copyright 1985 Menu ID : BH01
Machine:       SPIN AGITATOR #3 WARD ROOM (SPIN AG #3)
Point:         MOA—MOTOR OUTBOARD AXAIL
Date :         21-OCT-86 11:28 RPS =       30.      LOAD =   100.

ANALYSIS                PARAMETER              WARM/ALERT/FAULT         ALARM
PARAMETER               VALUE                       LEVELS              CODE
————————                —————                  ——————      ————

OVERALL VALUE           .412 IN/SEC            .100    .212    .424     C
SUBHARM REGION          .040 IN/SEC            .049    .060    .080
1X-3X BAND              .283 IN/SEC            .107    .180    .200     D
4X-5X BAND              .264 IN/SEC            .065    .080    .100     D
ROLL BRG BAND1          .046 IN/SEC            .014    .040    .050     C
ROLL BRG BAND2          .135 IN/SEC            .019    .050    .060     D
HFD ( >5kHz )           -NONE- G-s             .363    1.414   2.828
```

Figure 6. Alarm Menu

Selective frequency bands also can be correlated to variable speed machines. Bands will be shifted to the left or right on the frequency axis if speed changes from survey to survey. Also, bands can be set to any width (see Figure 7), meaning the user can zero in on specific fault frequencies, or broaden the band to capture a general range of faults. It is critical to realize that selective frequency band alarming uses well established industrial standards for band widths and alarm levels.

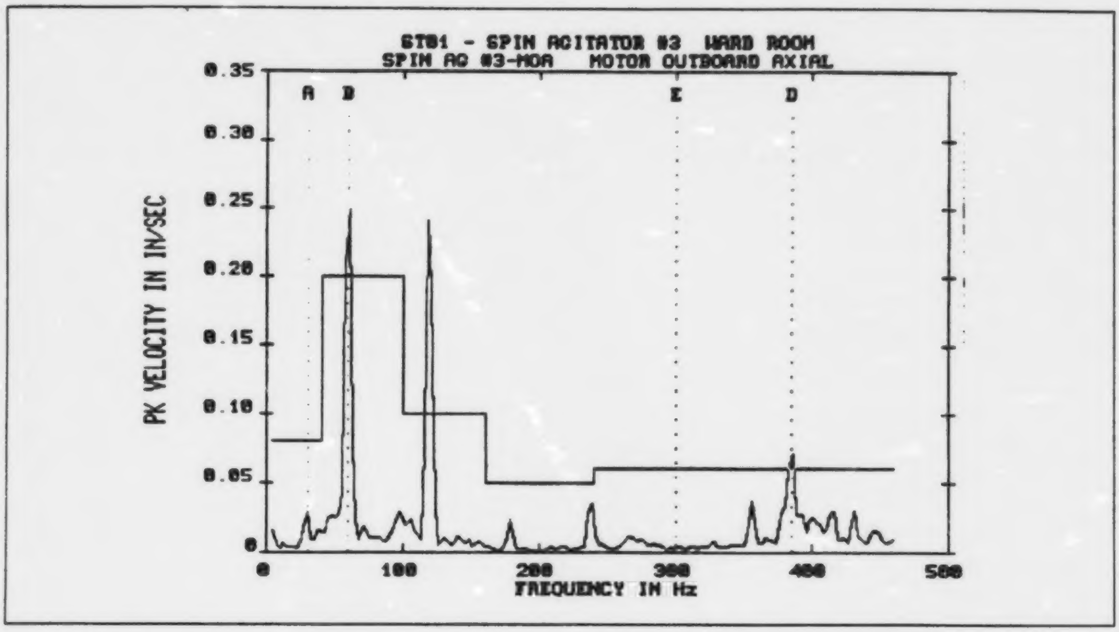

Figure 7. Different Alarm Band Widths

AUTOMATED VIBRATION DIAGNOSTICS

Several vibration analysis "expert" programs have been available during the late 1980's. Most of these emulate a diagnostic consultant by asking the user to supply information from which the most probable faults are deduced. It is necessary for the user to identify the type and construction of the machine, to manually extract significant features related to vibration characteristics of the machine, and to provide results from special tests performed on the machine. The programs then apply heuristic diagnostic rules derived from the experience of machinery analysts, with these rules stored in the host computer in a "knowledge base". A logical analysis of the input data is then performed by a software module referred to as the "inference engine". These manual interface programs have proven to be valuable tools for correctly identifying machinery faults and for accelerating the novice analyst along the learning curve. However, the process of sorting out the data for input is time consuming, and some of the required terminology may be unfamiliar to a novice, so the manual interface "experts" cannot make the most efficient use of all the data now available. These drawbacks have led to the development of automated diagnostic programs. An automated vibration diagnostics program can minimize the effort required of the user in the initial data analysis, and at the same time apply a higher level of consistency to the evaluation process. While an automated diagnostic program may be able to provide a prioritized list of the most likely faults in the machinery train it is important to remember that the results must be considered advisory information only; the recommendations presented by any automated expert program should be carefully reviewed by the personnel who bear responsibility for the final actions taken.

Usually an automated diagnostic program requires data from two sources. One contains details about the machinery train configuration, including information on measurement point locations, component types, mounting system, coupling design, and bearing descriptions. The other data source is the vibration spectra stored in a PDM database. In some cases, data from special tests such as start-up or coastdown observations can also be utilized by the automated system. An example of some of the information needed for the machinery configuration is shown in Figure 8; special tests that might be used are listed in Table 2.

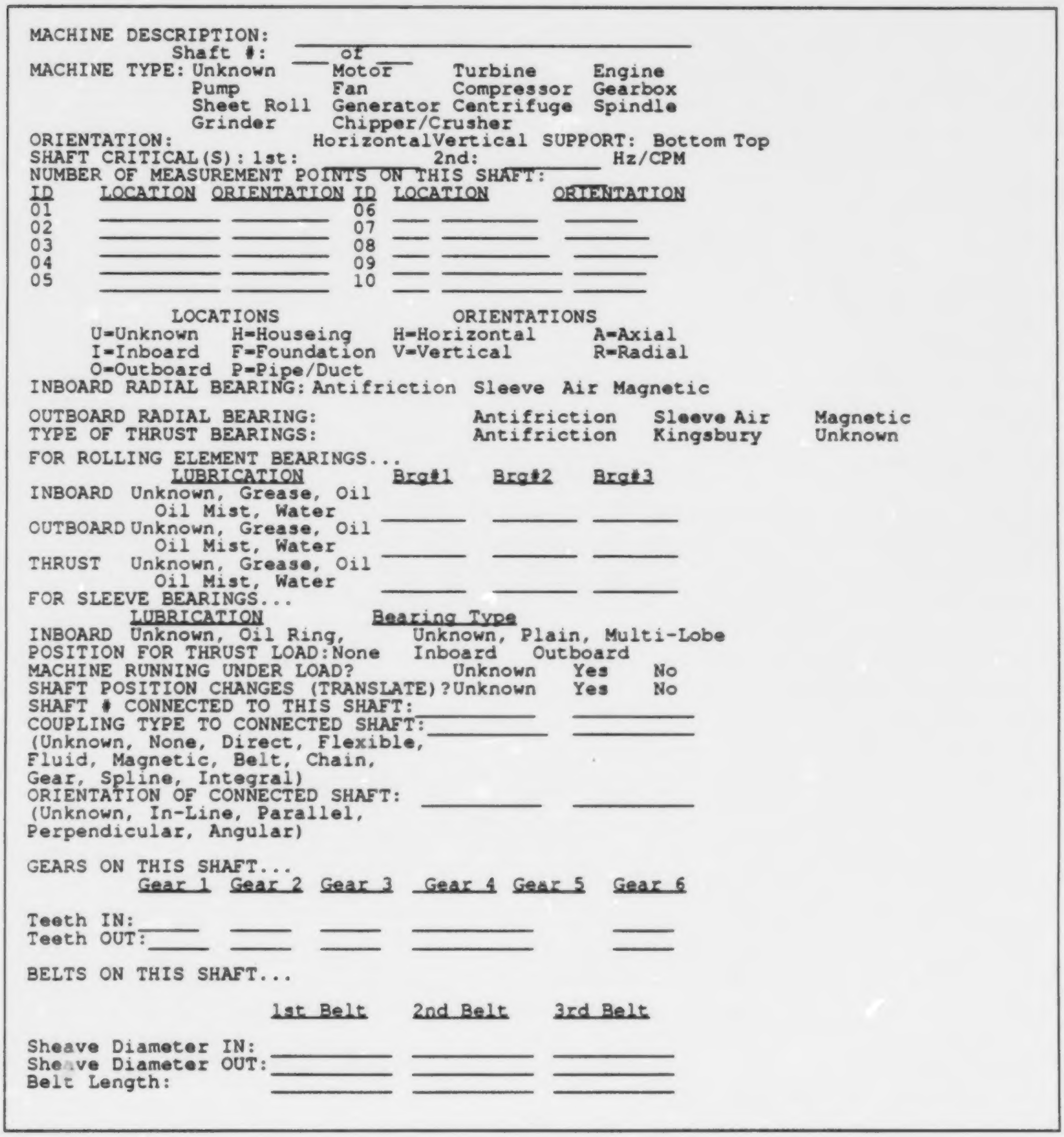

```
MACHINE DESCRIPTION:  _________________________________
             Shaft #:    ____ of ____
MACHINE TYPE: Unknown     Motor      Turbine     Engine
              Pump        Fan        Compressor  Gearbox
              Sheet Roll  Generator  Centrifuge  Spindle
              Grinder     Chipper/Crusher
ORIENTATION:            HorizontalVertical SUPPORT: Bottom Top
SHAFT CRITICAL(S): 1st: __________ 2nd: __________ Hz/CPM
NUMBER OF MEASUREMENT POINTS ON THIS SHAFT: ____
ID    LOCATION  ORIENTATION ID  LOCATION      ORIENTATION
01    ________  ________    06  __ ________   ______
02    ________  ________    07  __ ________   ______
03    ________  ________    08  __ ________   ______
04    ________  ________    09  __ ________   ______
05    ________  ________    10  __ ________   ______

            LOCATIONS                 ORIENTATIONS
     U=Unknown   H=Houseing   H=Horizontal      A=Axial
     I=Inboard   F=Foundation V=Vertical        R=Radial
     O=Outboard  P=Pipe/Duct
INBOARD RADIAL BEARING: Antifriction  Sleeve  Air  Magnetic

OUTBOARD RADIAL BEARING:           Antifriction   Sleeve Air    Magnetic
TYPE OF THRUST BEARINGS:           Antifriction   Kingsbury     Unknown
FOR ROLLING ELEMENT BEARINGS...
           LUBRICATION          Brg#1     Brg#2     Brg#3
INBOARD  Unknown, Grease, Oil
           Oil Mist, Water      _______   _______   _______
OUTBOARD Unknown, Grease, Oil
           Oil Mist, Water      _______   _______   _______
THRUST   Unknown, Grease, Oil
           Oil Mist, Water      _______   _______   _______
FOR SLEEVE BEARINGS...
         LUBRICATION         Bearing Type
INBOARD  Unknown, Oil Ring,     Unknown, Plain, Multi-Lobe
POSITION FOR THRUST LOAD:None   Inboard   Outboard
MACHINE RUNNING UNDER LOAD?          Unknown   Yes   No
SHAFT POSITION CHANGES (TRANSLATE)?Unknown    Yes   No
SHAFT # CONNECTED TO THIS SHAFT:__________  __________
COUPLING TYPE TO CONNECTED SHAFT:__________  __________
(Unknown, None, Direct, Flexible,
Fluid, Magnetic, Belt, Chain,
Gear, Spline, Integral)
ORIENTATION OF CONNECTED SHAFT:  __________  __________
(Unknown, In-Line, Parallel,
Perpendicular, Angular)

GEARS ON THIS SHAFT...
         Gear 1  Gear 2  Gear 3   Gear 4  Gear 5   Gear 6

Teeth IN: _____  _____   _____   _________         _____
Teeth OUT:_____  _____   _____   _________         _____

BELTS ON THIS SHAFT...

                     1st Belt     2nd Belt     3rd Belt

Sheave Diameter IN:  __________   __________   __________
Sheave Diameter OUT: __________   __________   __________
Belt Length:         __________   __________   __________
```

Figure 8.

Table 2. Special Test Used By Expert System

Time Waveform/Orbit Data
Closeup
Startup Data
Coastdown Data
Load/Speed Dependent Data
Phase Data
Physical Observation/Trend Data
Slow Roll Data

When the user invokes the automated program to evaluate either a single machine or a group of machines the computer extracts significant features from the stored vibration spectra. This extracted data is specific for the machine configuration being diagnosed and includes the features shown in Table 3.

Table 3. Feature Extraction

Overall RMS
Floor Energy
Total Peaks Energy (DSP, VEL, ACC)
Subharmonic Peak
1x, 2...10xRPM
>10x Synchronous

The end result can be a display of possible faults such as listed in Table 4, ranked in order of probability.

Table 4. Faults

CAVITATION
MISALIGNMENT
BEARING DAMAGE
GEAR DAMAGE
COUPLING DAMAGE
BELT DAMAGE
RUBS
UNBALANCE
CRACKED SHAFTS
OIL WHIRLS
RESONANCES

The following case history is an example of automated diagnostics applied to a bottom ash sluice pump in a fossil power plant. This machine train consists of a 900 horsepower AC induction motor driving a Byron Jackson 8x20 SDO type pump through a gear type coupling. The machine configuration details are shown in Figure 9.

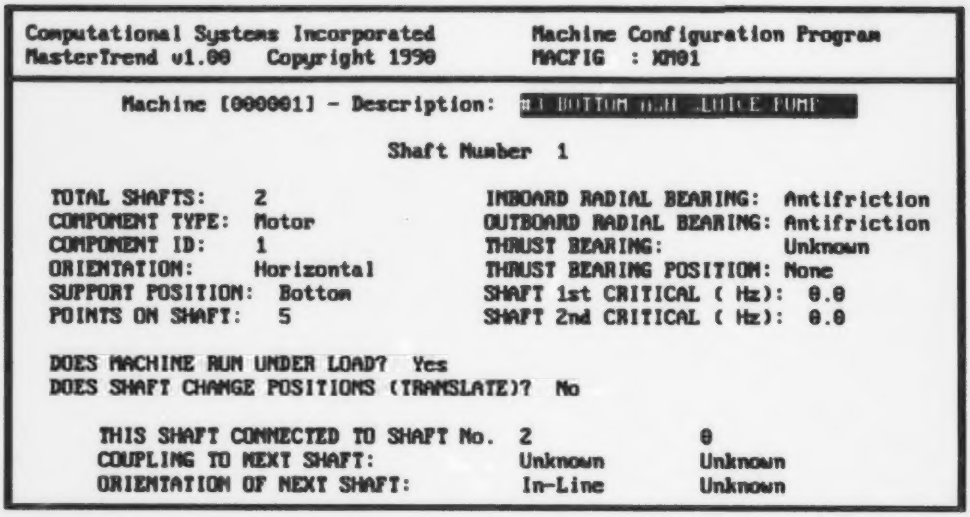

```
Computational Systems Incorporated        Machine Configuration Program
MasterTrend v1.00   Copyright 1990        MACFIG  : XM01

       Machine [000001] - Description:  #3 BOTTOM ASH SLUICE PUMP

                            Shaft Number  1

 TOTAL SHAFTS:      2                    INBOARD RADIAL BEARING:  Antifriction
 COMPONENT TYPE:  Motor                  OUTBOARD RADIAL BEARING: Antifriction
 COMPONENT ID:      1                    THRUST BEARING:          Unknown
 ORIENTATION:     Horizontal             THRUST BEARING POSITION: None
 SUPPORT POSITION:  Bottom               SHAFT 1st CRITICAL ( Hz):  0.0
 POINTS ON SHAFT:    5                   SHAFT 2nd CRITICAL ( Hz):  0.0

 DOES MACHINE RUN UNDER LOAD?  Yes
 DOES SHAFT CHANGE POSITIONS (TRANSLATE)?  No

    THIS SHAFT CONNECTED TO SHAFT No.  2            0
    COUPLING TO NEXT SHAFT:           Unknown      Unknown
    ORIENTATION OF NEXT SHAFT:        In-Line      Unknown
```

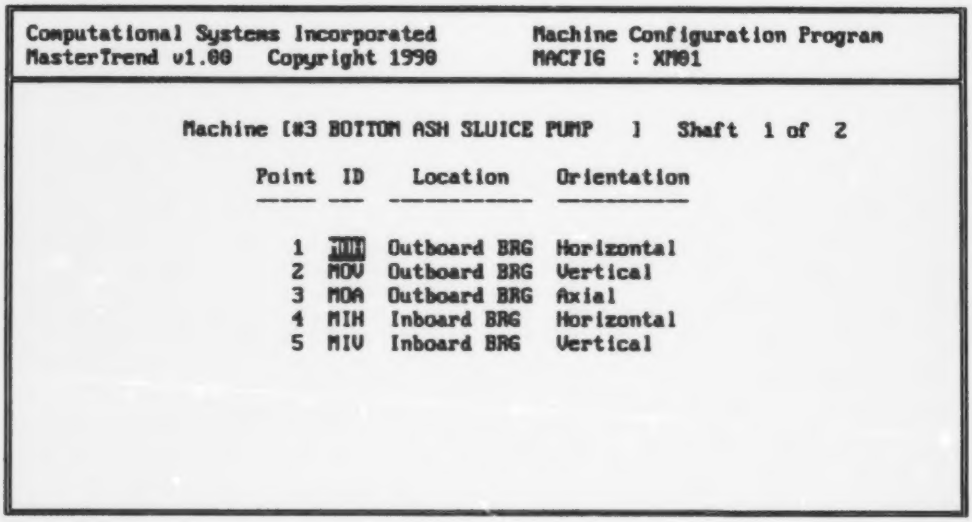

```
Computational Systems Incorporated        Machine Configuration Program
MasterTrend v1.00   Copyright 1990        MACFIG  : XM01


            Machine [#3 BOTTOM ASH SLUICE PUMP    ]   Shaft  1 of  2

                   Point  ID    Location     Orientation
                   -----  ---  -----------   -----------

                     1   MOH  Outboard BRG  Horizontal
                     2   MOV  Outboard BRG  Vertical
                     3   MOA  Outboard BRG  Axial
                     4   MIH  Inboard BRG   Horizontal
                     5   MIV  Inboard BRG   Vertical
```

Figure 9.

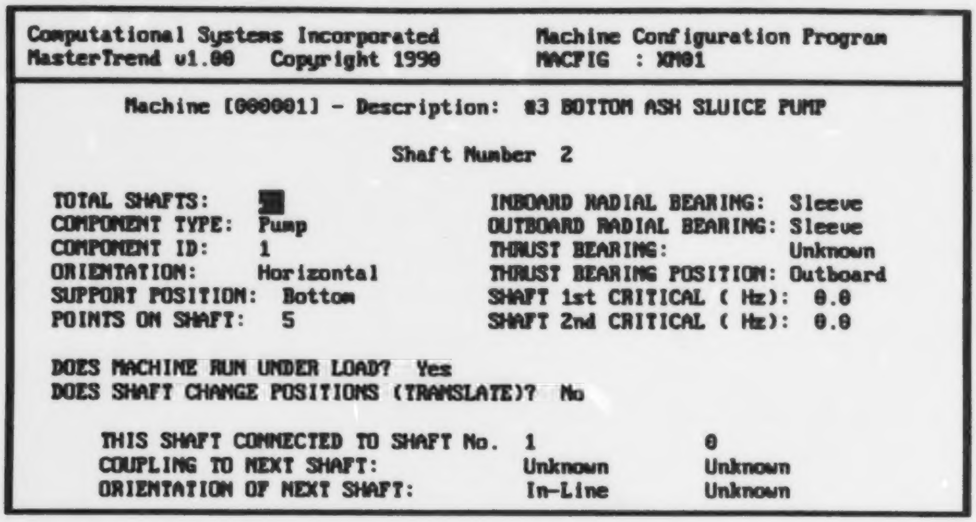

```
Computational Systems Incorporated        Machine Configuration Program
MasterTrend v1.00   Copyright 1990        MACFIG  : XM01

       Machine [000001] - Description:  #3 BOTTOM ASH SLUICE PUMP

                              Shaft Number  2

  TOTAL SHAFTS:       2                  INBOARD RADIAL BEARING:  Sleeve
  COMPONENT TYPE:     Pump               OUTBOARD RADIAL BEARING: Sleeve
  COMPONENT ID:       1                  THRUST BEARING:          Unknown
  ORIENTATION:        Horizontal         THRUST BEARING POSITION: Outboard
  SUPPORT POSITION:   Bottom             SHAFT 1st CRITICAL ( Hz):  0.0
  POINTS ON SHAFT:    5                  SHAFT 2nd CRITICAL ( Hz):  0.0

  DOES MACHINE RUN UNDER LOAD?  Yes
  DOES SHAFT CHANGE POSITIONS (TRANSLATE)?  No

     THIS SHAFT CONNECTED TO SHAFT No.  1              0
     COUPLING TO NEXT SHAFT:            Unknown        Unknown
     ORIENTATION OF NEXT SHAFT:         In-Line        Unknown
```

11:12:28

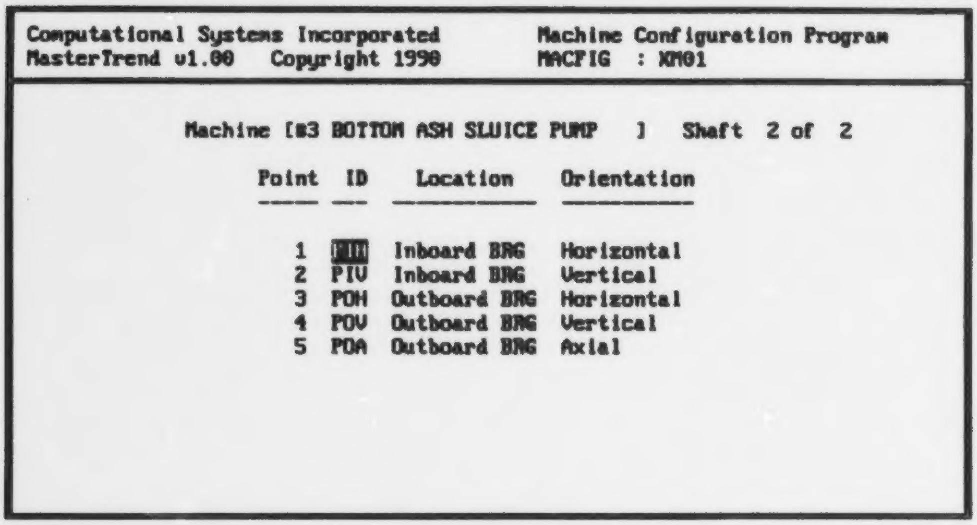

```
Computational Systems Incorporated        Machine Configuration Program
MasterTrend v1.00   Copyright 1990        MACFIG  : XM01

          Machine [#3 BOTTOM ASH SLUICE PUMP    ]   Shaft  2 of  2

                  Point  ID    Location      Orientation
                  -----  ---  -----------   -----------

                      1  PIH  Inboard BRG    Horizontal
                      2  PIV  Inboard BRG    Vertical
                      3  POH  Outboard BRG   Horizontal
                      4  POV  Outboard BRG   Vertical
                      5  POA  Outboard BRG   Axial
```

11:12:54

Figure 9 Continued.

The user selects the machine to be analyzed (Figure 10).

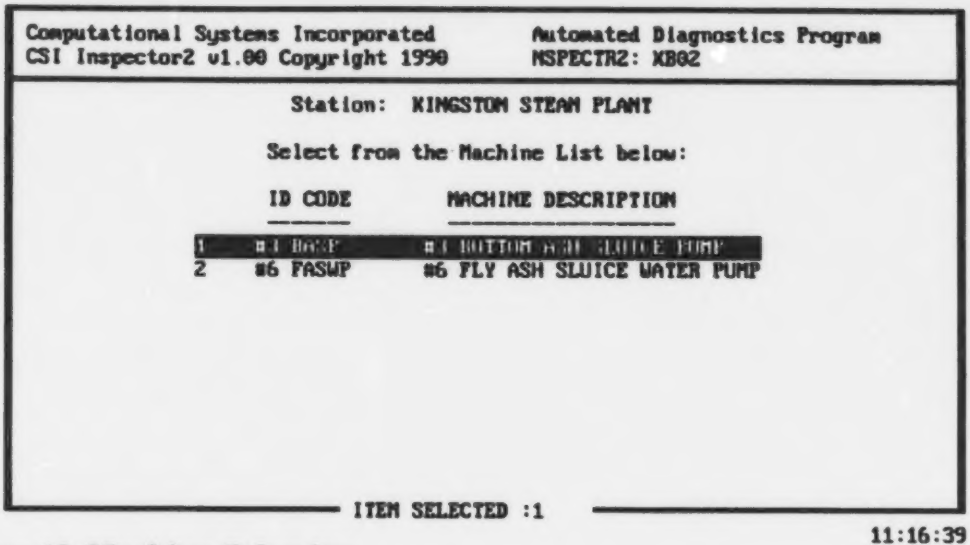

```
Computational Systems Incorporated        Automated Diagnostics Program
CSI Inspector2 v1.00 Copyright 1990       MSPECTR2: XB02

                    Station:  KINGSTON STEAM PLANT

                  Select from the Machine List below:

                  ID CODE       MACHINE DESCRIPTION
                  -------       -------------------

             1    #3 BASP       #3 BOTTOM ASH SLUICE PUMP
             2    #6 FASWP      #6 FLY ASH SLUICE WATER PUMP

------------------------- ITEM SELECTED :1 -------------------------
                                                             11:16:39
```

Figure 10. Machine Selection.

The automated diagnostic program extracts the significant feature information (Figure 11).

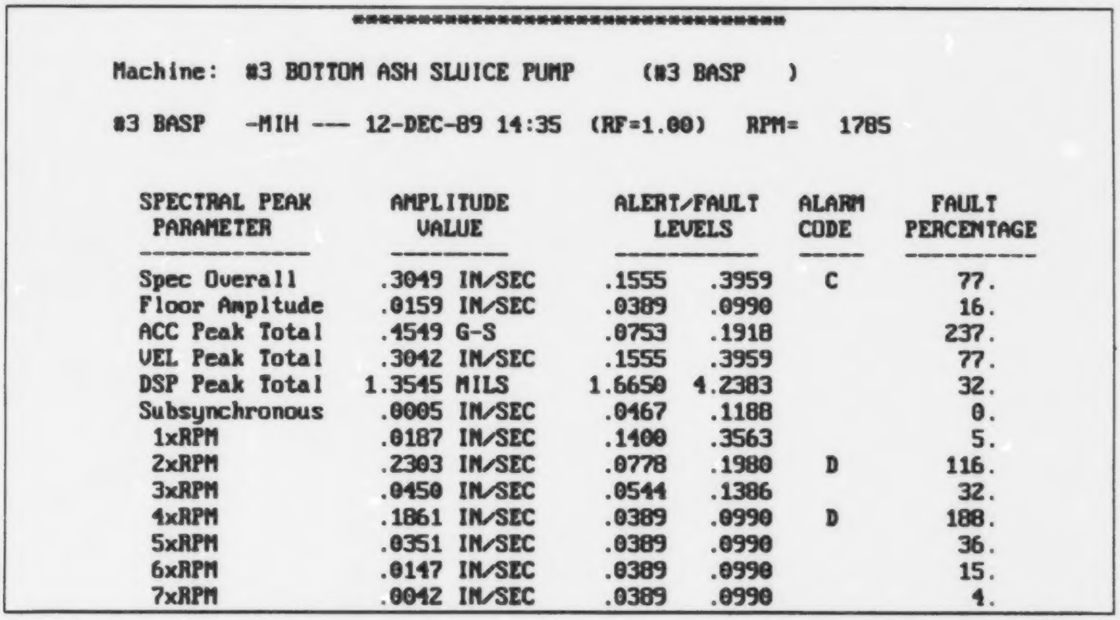

```
                ********************************

   Machine:  #3 BOTTOM ASH SLUICE PUMP      (#3 BASP    )

   #3 BASP   -MIH ---  12-DEC-89 14:35  (RF=1.00)  RPM=   1785

     SPECTRAL PEAK       AMPLITUDE         ALERT/FAULT     ALARM     FAULT
      PARAMETER            VALUE             LEVELS        CODE   PERCENTAGE
     -------------      ---------        -----------     -----   ----------
     Spec Overall       .3049 IN/SEC      .1555   .3959     C          77.
     Floor Ampltude     .0159 IN/SEC      .0389   .0990                16.
     ACC Peak Total     .4549 G-S         .0753   .1918               237.
     VEL Peak Total     .3042 IN/SEC      .1555   .3959                77.
     DSP Peak Total    1.3545 MILS       1.6650  4.2383                32.
     Subsynchronous     .0005 IN/SEC      .0467   .1188                 0.
      1xRPM             .0187 IN/SEC      .1400   .3563                 5.
      2xRPM             .2303 IN/SEC      .0778   .1980     D         116.
      3xRPM             .0450 IN/SEC      .0544   .1386                32.
      4xRPM             .1861 IN/SEC      .0389   .0990     D         188.
      5xRPM             .0351 IN/SEC      .0389   .0990                36.
      6xRPM             .0147 IN/SEC      .0389   .0990                15.
      7xRPM             .0042 IN/SEC      .0389   .0990                 4.
```

Figure 11. Feature extract screen.

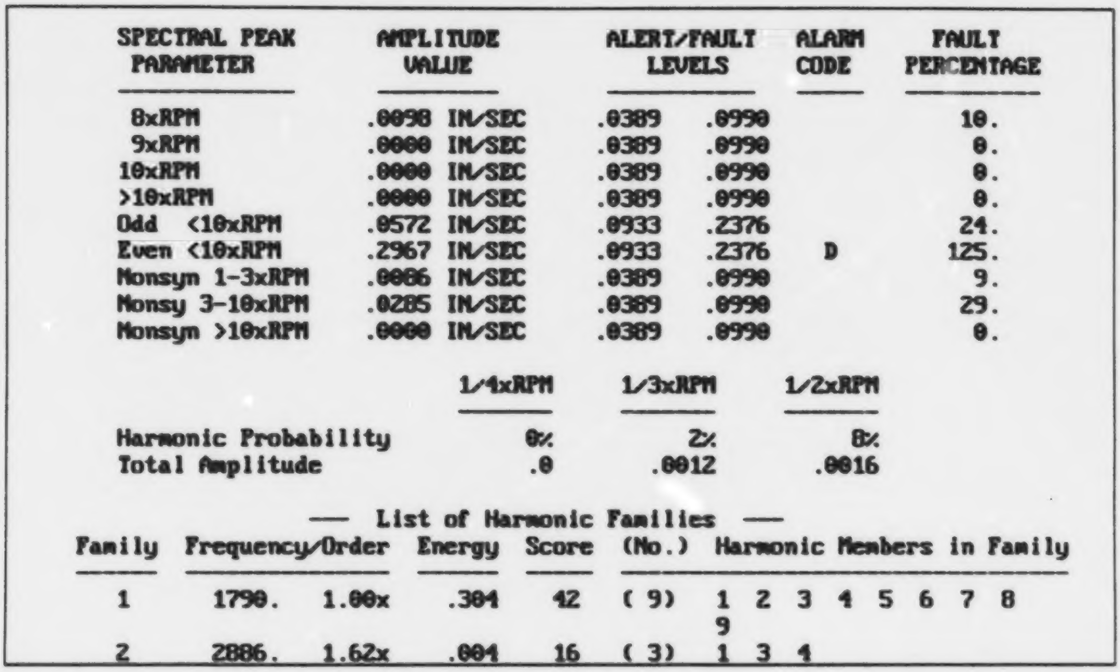

```
SPECTRAL PEAK         AMPLITUDE          ALERT/FAULT     ALARM     FAULT
 PARAMETER              VALUE               LEVELS        CODE   PERCENTAGE
_____________        __________        ____________     _____   __________
 8xRPM              .0098 IN/SEC      .0389   .0990                 10.
 9xRPM              .0000 IN/SEC      .0389   .0990                  0.
10xRPM              .0000 IN/SEC      .0389   .0990                  0.
>10xRPM             .0000 IN/SEC      .0389   .0990                  0.
Odd  <10xRPM        .0572 IN/SEC      .0933   .2376                 24.
Even <10xRPM        .2967 IN/SEC      .0933   .2376      D         125.
Nonsyn 1-3xRPM      .0086 IN/SEC      .0389   .0990                  9.
Nonsy 3-10xRPM      .0285 IN/SEC      .0389   .0990                 29.
Nonsyn >10xRPM      .0000 IN/SEC      .0389   .0990                  0.

                            1/4xRPM       1/3xRPM       1/2xRPM
                            _______       _______       _______
Harmonic Probability            0%            2%            8%
Total Amplitude                 .0         .0012         .0016

               —— List of Harmonic Families ——
Family   Frequency/Order   Energy   Score   (No.)  Harmonic Members in Family
______   _______________   ______   _____   ______________________________
  1        1790.   1.00x     .304     42    ( 9)   1  2  3  4  5  6  7  8
                                                    9
  2        2886.   1.62x     .004     16    ( 3)   1  3  4
```

Figure 11 Continued.

Spectral data can also be viewed by the user (Figure 12).

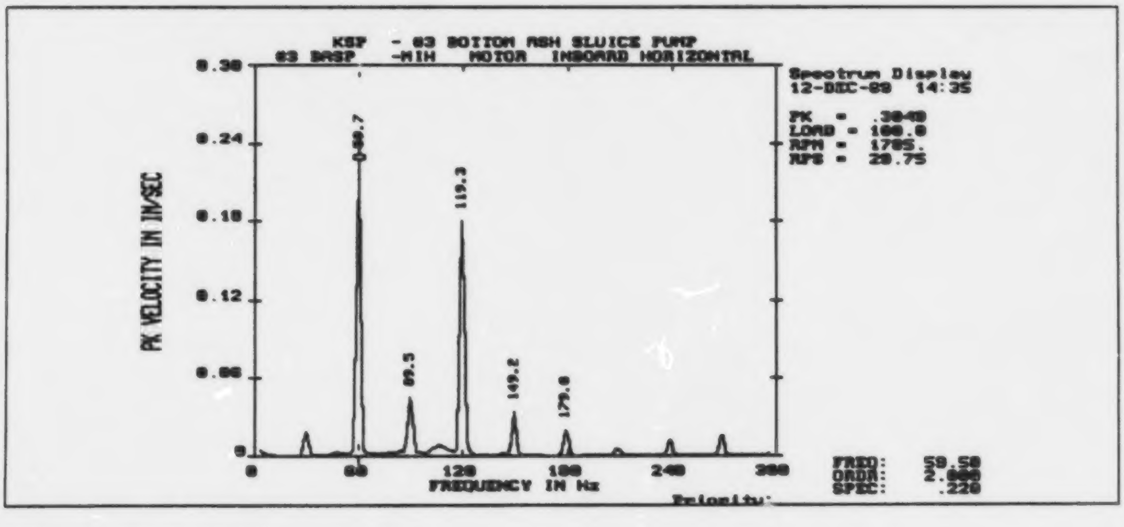

Figure 12. Spectra.

The diagnostic results are displayed (Figure 13).

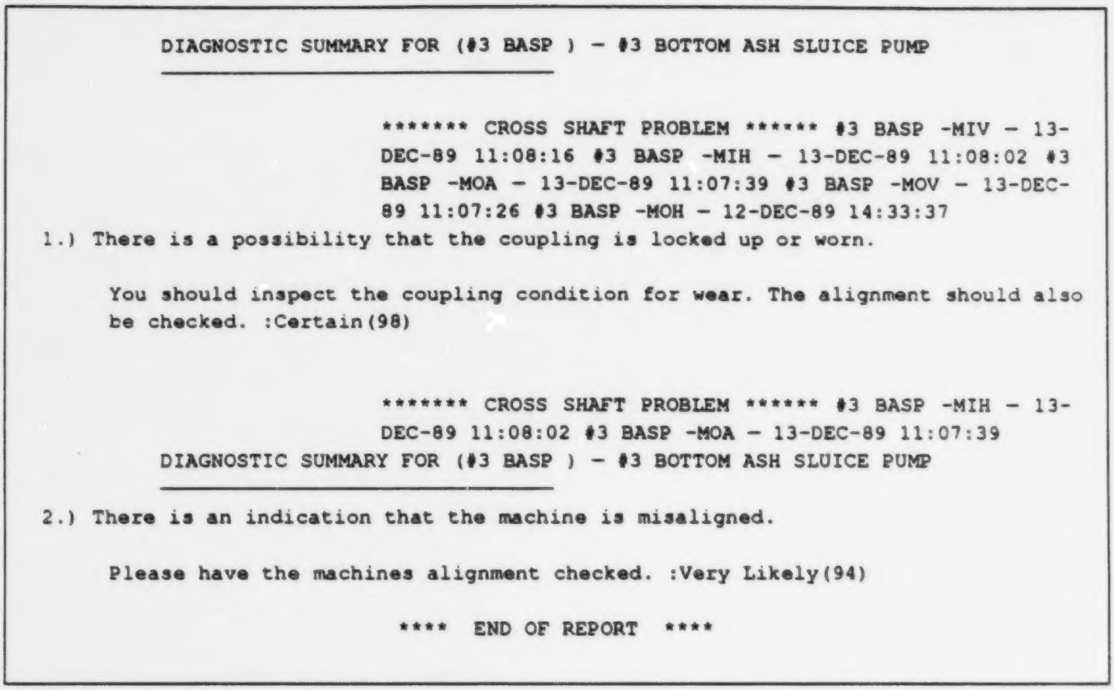

```
        DIAGNOSTIC SUMMARY FOR (#3 BASP ) - #3 BOTTOM ASH SLUICE PUMP
        ______________________________

                              ******* CROSS SHAFT PROBLEM ****** #3 BASP -MIV - 13-
                              DEC-89 11:08:16 #3 BASP -MIH - 13-DEC-89 11:08:02 #3
                              BASP -MOA - 13-DEC-89 11:07:39 #3 BASP -MOV - 13-DEC-
                              89 11:07:26 #3 BASP -MOH - 12-DEC-89 14:33:37
1.) There is a possibility that the coupling is locked up or worn.

    You should inspect the coupling condition for wear. The alignment should also
    be checked. :Certain(98)


                              ******* CROSS SHAFT PROBLEM ****** #3 BASP -MIH - 13-
                              DEC-89 11:08:02 #3 BASP -MOA - 13-DEC-89 11:07:39
        DIAGNOSTIC SUMMARY FOR (#3 BASP ) - #3 BOTTOM ASH SLUICE PUMP
        ______________________________

2.) There is an indication that the machine is misaligned.

    Please have the machines alignment checked. :Very Likely(94)

                               ****  END OF REPORT  ****
```

Figure 13. Result screen.

Typically, automated diagnostics can now provide this level of evaluation on a machinery train in two to three minutes. As experience level increases and knowledge bases are expanded to cover a wider range of machinery types, automated diagnostic programs will be a major factor for improving PDM efficiency.

SUMMARY

In large industrial facilities it is fairly common to have PDM vibration programs involving data collection on 5,000 or more machinery points each month. With programs this large the program analysts could easily be overwhelmed by the volume of data produced. Developments of more effective automatic problem detection methods and in automated diagnostic systems greatly reduce the manual effort involved and also help train new personnel.

THE INDUSTRIAL ALIGNMENT PROJECT: NEW APPROACHES TO MACHINERY ALIGNMENT

by

D.A. Bayly, H.E. Martell, K.P. Schwarz, W.F. Teskey, M.A. Chapman and J. Czompo
Department of Surveying Engineering
The University of Calgary
2500 University Drive N.W.
Calgary, Alberta Canada T2N 1N4

S. J. Mugford and J. R. Gibbs
Kadon Electro Mechanical Services Ltd.
#1, 2624 - 54 Ave. S. E.
Calgary, Alberta Canada T2C 1R5

Abstract

This paper describes the Industrial Alignment Project which has as its objective the development of improved systems and procedures for monitoring alignment changes of heavy machinery, making use of advances in inertial, photogrammetric and survey technology. The project has been jointly undertaken by The University of Calgary and 13 industrial partners with Kadon Electro Mechanical Services Ltd as principal industreial investigator. The paper outlines the overall scope of the Industrial Alignment Project and then discusses work in progress on three promising systems. One is an electronic theodolite system which can be used to measure alignment changes of large rotating shafts in near real-time and to monitor general deformation, as for instance encountered by a machine casing. Another is an inertial survey system which has been modified to allow rapid and precise azimuth transfer in confined spaces, as for instance required in the alignment of large rolls in pulp and paper mills. The third system is a digital photogrammetric camera capable of real-time monitoring of deformations in machines and structures. In all cases, expected accuracies of the systems are discussed.

Keywords

Electronic theodolites, inertial measuring unit (IMU), digital camera, statistical testing, deformation monitoring, shaft alignment.

Biographies

The alignment group at the University of Calgary consists of four professors in the Department of Surveying Engineering, a full-time project manager and a number of graduate students. Dr. K.P. Schwarz is principal investigator of the project and specialist in inertial technology. Dr. W.F. Teskey is responsible for precise engineering measurements and supervises the electronic theodolite applications. Dr. M.A. Chapman is responsible for applications in close-range photogrammetry, digital imaging and stereovision. Dr. M. Sideris is responsible for optimization and spectral analysis. H.E. Martell is project manger, inertial expert, and responsible for assessing new technologies for industrial applications. D. Bayly and J. Czompo are Ph.D. students at the U. of C. One specializes in alignment applications of coordinate analysing theodolites, the other in mathematical model development and spectral analysis methods.

The main industry partners in the alignment project are S.J. Mugford and J.R. Gibbs from Kadon Electro Mechanical Ltd. Stu Mugford is president of Kadon and a professional engineer with a background in electrical engineering. Ray Gibbs is engineering manager at Kadon and is a P.Eng with a mechanical engineering background. Both have interests in vibration analysis, alignment and repair of rotating equipment and technology transfer between university and industry.

RÉSUMÉ

Les auteurs décrivent le Projet de centrage industriel qui a comme objectif la mise au point de systèmes et méthodes améliorés pour contrôler le décentrage des matériels lourds, en faisant appel aux progrès enregistrés en technologie inertielle, photogrammétrique et géodésique. Le projet a été entrepris conjointement par l'Université de Calgary et 13 partenaires industriels avec à leur tête la société Kadon Electro Mechanical Services Ltée en tant que chercheur industriel principal. La présente étude décrit le cadre général du Projet de centrage industriel et fait ensuite état des travaux en cours concernant trois systèmes prometteurs. Le premier est un système de théodolite électronique capable de mesurer le décentrage des gros arbres tournants presque en temps réel et de contrôler la déformation générale, par exemple celle subie par le carter d'une machine. Le deuxième est un système de levé inertiel modifié pour permettre un transfert azimutal rapide et précis dans les espaces restreints, comme cela s'impose notamment dans le cas des énormes rouleaux employés dans le susines de pâtes et papiers. Le troisième système est une chambre photogrammétrique numérique capable de surveiller en temps réel les déformations subies par les machines et les constructions. Dans tous les cas, les précisions prévues des systèmes sont analysées.

MOTS-CLÉS

Théodolites électroniques, centrale inertielle (IMU), chambre numérique, essais statistiques, contrôle des déformations, centrage des arbres.

BIOGRAPHIES

Le groupe du centrage à l'Université de Calgary comprend quatre professeurs du Département d'arpentage, un directeur de projet à plein temps et un certain nombre d'étudiants diplômés. Le professeur K.P. Schwarz, spécialiste de la technologie inertielle, est le chercheur principal du projet. Le professeur W.F. Teskey est responsable des mesures techniques de précision et supervise les applications du théodolite électronique. Le professeur M.A. Chapman est responsable des applications en photogrammétrie rapprochée, en imagerie numérique et en stéréovision. Le professeur M. Sideris est chargé de l'optimisation et de l'analyse spectrale. M. H.E. Martell est à la fois directeur de projet, spécialiste en inertie et chargé d'évaluer de nouvelles technologies applicables dans l'industrie. MM. D. Bayly et J. Czompo sont étudiants au Ph. D. à l'Université de Calgary. Le premier se spécialise dans les applications au centrage des théodolites à analyse des coordonnées, et l'autre, dans les modèles mathématiques et les méthodes d'analyse spectrale.

Les principaux partenaires industriels dans le projet de centrage sont S.J. Mugford et J.R. Gibbs de Kadon Electro Mechanical Ltée. Stu Mugford, le président de Kadon, est un ingénieur spécialisé en génie électrique. Directeur de l'ingénierie chez Kadon, Ray Gibbs est ingénieur-mécanicien. Tous deux s'intéressent à l'analyse des vibrations, au centrage et à la réparation du matériel tournant, ainsi qu'au transfert technologique université-industrie.

1. Introduction

The Industrial Alignment Project is an NSERC supported research effort jointly conducted by investigators at the University of Calgary and Kadon Electro Mechanical Services of Calgary with support from 13 industry participants from the oil and gas, pipeline, cement, pulp and paper, steel and fertilizer sectors in the western provinces. The aim of this group, over the next three years, is to design and develop new systems and software capable of monitoring alignment changes in rotating machinery, deformations in machinery casings and installation and maintenance of specialized equipment. The present state of the art provides adequate alignment technology in the cold align case, via reverse indicator and laser methods for instance. However, there is still need for improvement in the hot alignment case. The many approaches to the problem of monitoring changes in the alignment of rotating shafts and deformations in casings under operating conditions include Essinger bars, Dynalign bars, optical tooling, precise levelling, vibrational analysis, Permalign, water-cooled stands and proximity probes. They do not resolve the hot alignment problem in a satisfactory manner and are also difficult to use in non-standard alignment cases such as the alignment and continuous monitoring of curved surfaces, as encountered in the setting of rollers on slab casting units.

Regular maintenance of machinery can be an expensive proposition, not only in the actual maintenance procedures, but in lost production time. Hence a methodology is needed which allows for not only good initial installation of equipment but periodic, reliable checking of machinery in the operating mode. This paper will describe the problems as we visualize them at present in the field of alignment, briefly outline the techniques available today and present in detail a description of the systems proposed for inclusion into this project.

For the purpose of coaxial alignment, existing methods depend largely on rim and face, reverse indicator or laser technology. Present monitoring techniques for shaft or casing misalignment include the utilization of Essinger bars, Dynalign bars or optical tooling devices. In cases where these systems are found to be effective we do not recommend changing the methodology . However we would like to place new emphasis on the use of electro-optical methods for continuous or periodic monitoring of changes in shaft alignment or machinery deformation. These tools include electronic theodolites, digital cameras and laser devices, including those used for alignment, distance measuring and velocity/displacement determination. Used in conjunction with powerful portable computers these can provide fast, highly accurate evaluation of data at single or multiple epochs. Optical methods are remote and normally do not require sophisticated installation and machinery shutdown, hence they are ideal for monitoring machinery alignment changes under hot (operating) conditions. Alignment of parallel shafts or, for instance, parallel rollers in the pulp and paper industry has traditionally relied on precision levelling or optical tooling units such as the Wild GAP1. Since inertial reference units can supply azimuth information from internal gyro technology without regard to line of sight these systems may have highly useful applications in confined areas where optical methods are impractical.

For those applications in which changes in shaft alignment or machinery deformation are monitored through the use of electronic theodolites, digital cameras, or laser devices, the number of deformation parameters will in general be smaller than the number of measurements. This will allow testing of the statistical significance of the deformation parameters, i.e. determine in an objective manner whether the deformations are real or only the result of measurement errors. In the aforementioned applications a number of stable reference points will usually be available in the vicinity surrounding the machine to be monitored. Again, through statistical tests, we will be able to determine which points are stable and thus avoid the situation in which movements of reference points are erroneously interpreted as alignment changes or machinery deformations.

2. Alignment Models

Alignment and monitoring problems, from an analytical point of view, may be viewed in terms of vector spaces. The use of electro-optical measuring devices lends itself naturally to ordered triples of real numbers, that is 3-dimensional coordinates in space. For applications where horizontal and vertical planes can be considered as separate entities 2-dimensional or 1-dimensional subsets may be used alone or in combination with each other. Whatever the nature of the problem, given some consistent and stable datum definition, coordinate geometry may be utilized to indicate, in meaningful ways, the co-linearity of axial shafts or trains or the parallelity of shafts or rollers. Vector fields can be fitted to pre-defined surfaces such as spheres, planes or conics, and the time dependent deformations of such surfaces can then be described by a vector displacement field.

For the alignment problem two general cases can be distinguished:

parallelity and
co-linearity.

In the first case the objective is to secure that two axes have the same direction in space, in the second case that the two axes meet in space without displacement and are parallel. Deviations from the first condition will be called misalignment, deviations from the second condition will usually be a combination of misalignment and displacement.

Parallelity is defined by the simple vector formula

$$\mathbf{b} = c\mathbf{a} \qquad (1)$$

where $\mathbf{a} = (a_x, a_y, a_z)^t$ and $\mathbf{b} = (b_x, b_y, b_z)^t$ are vectors to be aligned ($\mathbf{a} \neq \mathbf{0}$; $\mathbf{b} \neq \mathbf{0}$) and c is a constant. If $c < 0$, the two vectors have different directions; for $c > 0$ they have the same direction.

Misalignment can either be defined by means of the vector dot product or by the vector cross product. For small misalignment angles, i.e. almost parallel shafts, the second is more sensitive.

The misalignment vector can be defined as the normalized vector cross product

$$\mathbf{m}(\mathbf{a},\mathbf{b}) = \frac{\mathbf{a} \times \mathbf{b}}{|\mathbf{a}| \cdot |\mathbf{b}|} \qquad (2)$$

where $\mathbf{m}(\mathbf{a},\mathbf{b})$ is zero in case of perfect alignment. The absolute value, i.e. the length of $\mathbf{m}(\mathbf{a},\mathbf{b})$ is a function of the misalignment angle θ

$$m = |\mathbf{m}(\mathbf{a},\mathbf{b})| = \sin\theta \qquad (3)$$

while the direction of **m(a,b)** gives the axis around which we can rotate **b** to make it parallel to **a**. Furthermore m can be written as

$$m = \frac{\sqrt{(a_x b_y - a_y b_x)^2 + (a_y b_z - a_z b_y)^2 + (a_z b_x - a_x b_z)^2}}{\sqrt{a_x^2 + a_y^2 + a_z^2} \cdot \sqrt{b_x^2 + b_y^2 + b_z^2}} \,. \tag{4}$$

For small angles m = θ, approximately, thus Eq.(4) gives the misalignment angle directly from coordinate measurements.

The vector **m(a,b)** may be computed at an initial epoch - the case of initial alignment - or at multiple epochs. In the latter case results are monitored for changes in shaft orientation with respect to time. Other applications of these types of alignment problems would be rollers in pulp and paper mills, placement of footings or pre-cast parts in rectangular patterns.

It should be noted that the equations above specify directions only. They do not say whether the two shafts are co-linear or not. In fact, equations (1) to (4) typically specify the orientation of two shafts which are meant to be co-linear but deviate slightly from the ideal condition. This is, for instance, the case for two rotating shafts which are coupled to drive fans, pumps or compressors.

Besides parallelity another measure, the displacement, has therefore to be introduced to define co-linearity. For this, let us consider two lines in space representing the two shaft axes. Their direction is characterized by vectors **a** and **b**, respectively (Figure 1).

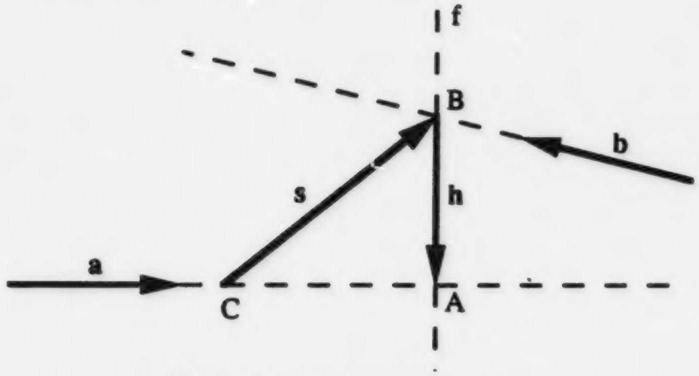

Figure 1 : Displacement vector **h**

Consider furthermore a plane f orthogonal to **a** which is intersected by the vector **a** in point A. Line **b** intersects the plane in point B. The displacement vector **h**, with respect to the reference axis **a**, is defined by a vector which points to A from B, lies in the plane f, and is given by

$$\mathbf{h} = \frac{\mathbf{a} \times (\mathbf{a} \times \mathbf{s})}{|\mathbf{a}| \cdot |\mathbf{a}|} \tag{5}$$

where s is a vector pointing to B from an arbitrary point C of line **a**. Note that **h** depends on the choice of f, i.e. the choice of the plane on which the displacement vector is computed (or measured).

Thus, the alignment process in the co-linear case can be summarized as rotating the vector **b** by **m(a,b)** about B and then reducing **h** to zero, i.e. moving **b** to coincide with **a**. On the other hand, by computing θ and $h = |\mathbf{h}|$ one can characterize the quality of a specific alignment state. If $m = 0$ and $h = 0$, the shafts are perfectly co-linear.

The alignment conditions may change after warming up, so one may want to apply an initial misalignment when the machine is down, in order to achieve good alignment when it is running. The initial (cold) values $\mathbf{h}_0$ and $\mathbf{m}(\mathbf{a}_0, \mathbf{b}_0)$ are determined in an a priori manner.

3. Operational Considerations

We have looked at the ideal case in purely formal terms. Let us review some of the methods which are used in practice and outline how they relate to the model given in the previous chapter. We will only consider the co-linearity problem because it includes the parallelity problem and is more important in practice. For a typical application of the parallelity problem, see chapter 6. We will examine a typical dial indicator method and then go on to several alignment methods which could be used with electronic theodolite systems.

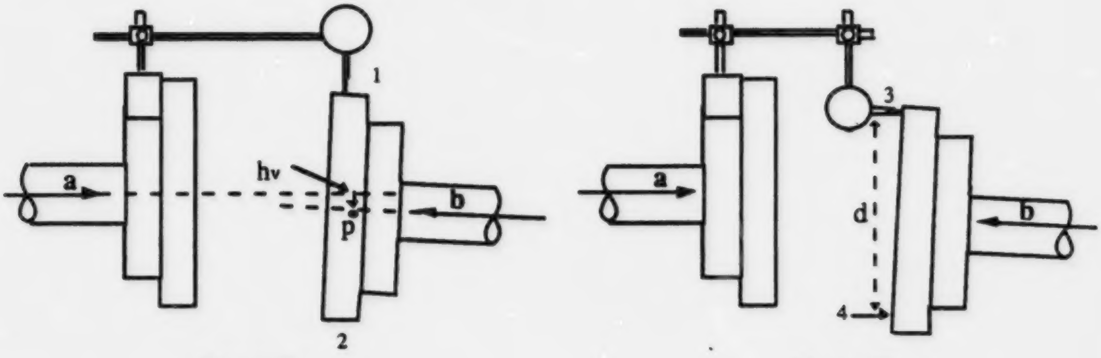

Figure 2a

Figure 2b

The general set-up for the rim and face method

Positions 1 to 4 on Figure 2 indicate where the dial indicator readings must be taken. When readings are taken in a radial direction at points 1 and 2 the offset in the measurement plane between the shaft axes is equal to one-half of the difference between the readings. The position of point P relative to the reference axis **a** thereby gives the vertical separation between the shafts. From radial readings in the plane 90 degrees to that given by points 1 and 2 the lateral separation can be computed.

How does this relate to the discussion in the previous chapter ? Obviously, the vector **h** is constrained to lie in the measurement plane orthogonal to **a** and to pass through the points 1 and 2.

Thus, the problem is reduced to two dimensions. The two components of the displacement vector are measured in horizontal and vertical directions in the measurement plane. Thus

$$\mathbf{h} = \begin{pmatrix} h_h \\ h_v \end{pmatrix}, \tag{6}$$

where the choice of the local coordinate system is essential to this simple solution. The displacement vector changes if the dial indicator readings are made in a different plane.

Additional information is required to obtain the misalignment θ between the two shafts. It is derived from either radial readings in a different measurement plane (the reverse indicator method) or axial readings as shown in figure 2b on the right hand side above and described below. θ is obtained from

$$\tan\theta = \frac{\text{reading 3 - reading 4}}{d} \quad . \tag{7}$$

Again readings are required in planes orthogonal to each other. They are nothing else but the components of the vector **m(a,b)**, i.e. misalignments in the horizontal and vertical planes. Having determined relative displacement and misalignment angle one can extrapolate back to the feet to shim the machine into the correct alignment.

Note that with these methods the vectors **a** and **b** are never explicitly determined. Relative displacements and misalignments are obtained directly from measurements which determine **h** in a specific plane and the non-orthogonality of this plane with respect to shaft **b**.

If precision electronic theodolites are employed for computation of shaft misalignments the situation is described by the vector configuration given in Figure 4. To begin however, a brief description of how these vectors are obtained in practice might be in order. The observation procedure is depicted in Figure 3.

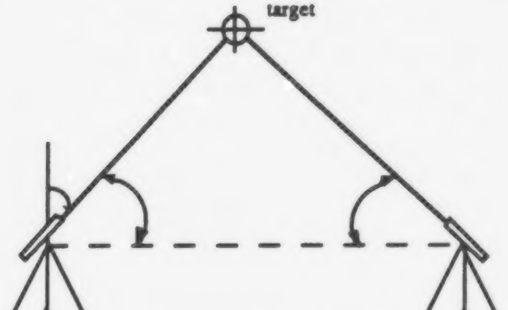

Figure 3 : Determination of unknown x, y, z

Looking at the figure above one sees that if two theodolites, placed at the endpoints of a known baseline are used to sight at the same point, the resulting intersection in the horizontal plane uniquely defines the x and y coordinates of that point with respect to the x and y coordinates of the known points at which the theodolites are placed. Furthermore, if an angle is measured in the vertical plane from at least one of those theodolites, a height difference from the theodolite to the targeted point can also be computed. Thus, the x, y and z coordinates of the point on the machine can be obtained with respect to some origin which can either be the position of one of the theodolites or some relatively stable point in the vicinity of the machine, say the footings of the building for instance. The target itself may be a precisely etched adhesive square placed on the shafts and coupling in the event the machine is shut down or the endpoint of a laser beam aimed at various points on the machine when it is running.

Figure 4 then depicts the theodolite method of resolving the lateral and vertical displacements of the two shafts relative to each other as well as the relative orientation of the shafts.

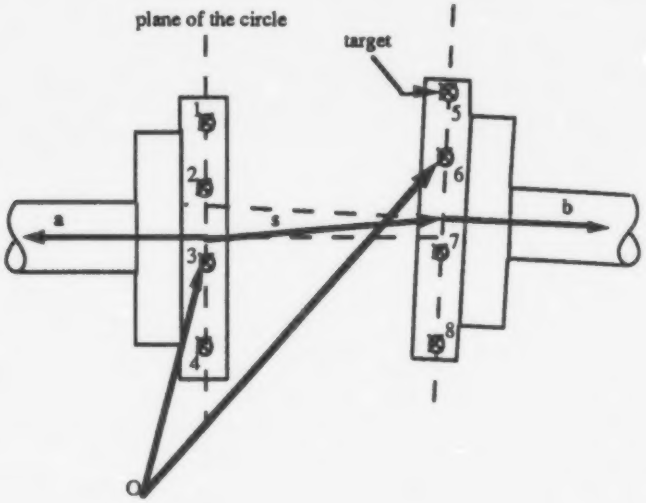

Figure 4 : Coordinate determination at n points on each coupling.

Any point on the exterior of a rotating shaft or coupling must describe a circle. The axis of each shaft, represented by **a** and **b**, will be normal to the plane inscribed by this circle and will be located at the centre point of such a circle. These points describe the position of the endpoints of the axis of each shaft in space as well as the direction of each axis, which is orthogonal to the plane; for details see chapter 6.

By defining **s** as the vector between the two circle centres this case can be directly related to the model discussed earlier, since **a** and **b** are given by this method. Thus, equations (2)-(5) can be used for misalignment and displacement computations.

Up to this point both dial indicator and theodolite methods provide much the same information on the misalignments of rotating machinery, that is, horizontal and vertical displacement as well as relative misaligment. There are some important differences, however. The first is obvious from Figure 4 - the theodolite method can be used to make additional measurements. In addition, when used with a laser beam defining the target point, it can be used while the machine is operating and can thus monitor alignment changes on a regular basis without down time. This is not possible with the dial indicator method.

Another example of alignment under operating conditions, on a much larger scale than the usual rotating shaft situation, occurs in the kiln alignment problem (Figure 5).

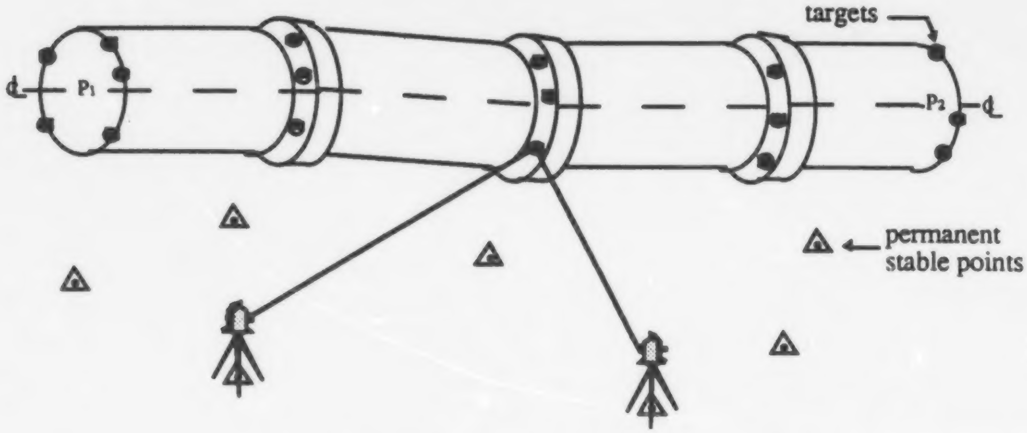

Figure 5 : Kiln Alignment

The figure above shows the top and side view of a kiln which has misalignment problems at the support rollers or excessive clearance between tire and spacer pads, for instance. It is slowly rotating. The two theodolites are being used in the same way as described in the shaft alignment case, except here the aim is to survey best fitting circles at each of the tires. Thus the kiln is considered as having n segments which may be slightly out of alignment. Each of these segments is described by a vector orthogonal to the plane of the circle and originating at its centre. Each of these vectors is close to the reference alignment vector which is represented by the vector connecting the endpoints P_1 and P_2.

The information so obtained can be used in a variety of ways to check for misalignments between the various segments of the kiln. One method would be to take all the tire centre coordinates T_i computed from the measurements and, using equation (5), reduce the displacement vectors h_i for each tire (Fig. 6) to zero.

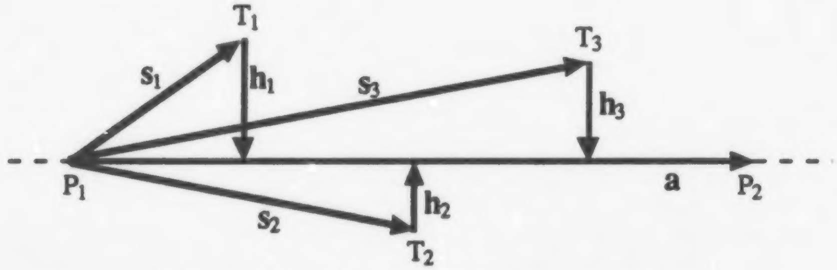

Figure 6 : Kiln Alignment Displacement Vectors

The reference axis a is determined by the two end circle centre points P_1 and P_2. The corresponding s_i vectors can be computed as vectors pointing to the tire centre points from one end centre point P_1. Further details on the kiln alignment problem are presented in chapter 6.

4. The General Deformation Problem Using the Network Approach

In other sections of this paper, detailed solutions to the shaft alignment problem and the kiln alignment problem are described. A more general problem is the determination of alignment changes in time. In this case it can not be assumed any more that the misalignment and displacement vectors are stable over the measurement period. Stabilty can only be assumed for each specific measurement epoch. In its most general form, this problem can be described as a deformation problem in time where the continuous deformation of a piece of machinery is determined by measuring deformations in a discrete network of points on the surface of the machinery. It thus is related to the problem of measuring deformations in a general three-dimensional survey network.

Close range survey network analysis relies on the theory which has been developed over the years for geodetic surveying. A brief summary will be presented here. More details can be found in surveying texts such as Davis et al. (1981), Mikhail and Gracie (1981), and Mikhail and Ackerman (1976).

Most of the common alignment methods are based on measurement of relative displacements. The surveying engineering approach is to define a coordinate system and locate targets in that system using a variety of observational types. Benefits of a coordinate system approach are listed below (see Bayly et al. (1988)) :

1. A survey network unites all of the measurements relating to a particular project, both in space and in time.

2. Pre-analysis of the survey network makes it possible to plan the survey so that it will meet cost and accuracy specifications.

3. There is flexibility in design of the network with respect to the types of measurements, and the geometry and logistics of the measurement process. (For example, survey networks are not limited to measurements made at right angles to machinery axes).

4. The coordinate system facilitates computations and allows the use of powerful, sophisticated computer software.

5. A real or virtual reference datum can be chosen, which is essential for long-term monitoring projects.

6. Target positions expressed in one coordinate system can readily be transformed to other coordinate systems.

7. There are well-developed and proven analysis techniques for dealing with systematic errors (e.g. mathematical modelling and calibration procedures); random observational errors (e.g. statistical modelling, least squares adjustment of redundant data, covariance analysis and propagation); and blunders and gross errors (e.g. statistical tests for outliers and network design for reliability).

8. There are well developed techniques for deformation analysis.

9. Sets of target coordinates can be compared to theoretical geometric entities such as straight lines, planes, circles, cylinders, spheres etc.

Local three dimensional Cartesian coordinate systems are suitable for most close range surveys. Such a coordinate system has seven datum parameters: three translations, three rotations, and scale. If the coordinate frame is visualized as three mutually perpendicular rods welded together at a vertex, the location of the vertex in space fixes the three translation parameters. The orientation of the axes defines the three rotation parameters and, if one of the rods is of known length then the scale is fixed. Surveyors of course do not set up physical models of coordinate frames. The datum parameters are defined through a combination of coordinate and observational information.

For example, the coordinates of one reference target may be arbitrarily chosen to fix the translation parameters. One axis is usually aligned with the vertical direction as evidenced by the precise levelling bubble or vertical compensator in a level or theodolite. The orientation of the other two mutually perpendicular axes in the horizontal plane is arbitrary, but it may be convenient to make one axis parallel to the horizontal projection of the line between two reference targets. Finally, any measured distance between targets will determine scale. The set of constraints described so far is just sufficient to define the datum parameters and is called a set of minimal constraints. It is not a unique set; other combinations of coordinates and observations can yield minimal constraints.

Survey observation types include distances, azimuths, directions, zenith angles and height differences. An azimuth is an angle in a horizontal plane with respect to north. A direction is an angle in a horizontal plane with respect to the zero of a theodolite's horizontal circle. Zenith angles are measured in a vertical plane from the zenith down towards the target. Zenith angles can resolve two of the datum rotation parameters. An azimuth will fix the third rotation parameter. Both distances and height differences determine scale.

5. Deformation Analysis

Observations are subject to systematic errors, random errors, and gross errors (blunders). Systematic errors can be removed through calibration or special procedures. Random errors cannot be eliminated, but the magnitude of expected random errors can be reduced by averaging repeated observations. Redundant observations make it possible to check for blunders and, in general, improve the precision of adjusted coordinates.

Each observation gives one equation. To achieve a solution for the unknown coordinates, the number of observations must be at least equal to the number of unknowns and all points with unknown coordinates must be joined to the survey network by suitable observations. Survey networks are usually designed to be highly redundant - the number of observations greatly exceeds the number of unknown coordinates. As mentioned previously, redundancy improves the precision of the results and makes it possible to check for blunders.

The over-determined system of equations is solved by the method of least squares. This method, originated by C. F. Gauss in the early nineteenth century, has countless applications. Those who are familiar with, for example, least squares balancing, will recognize the form of the following equations:

$$\hat{\delta} = -[\, A^T C_l^{-1} A \,]^{-1} A^T C_l^{-1} w \tag{8}$$

$$C_{\hat{x}} = [\, A^T C_l^{-1} A \,]^{-1} \tag{9}$$

$$\hat{v} = A \hat{\delta} + w \tag{10}$$

where

$\hat{\delta}$	is the vector of corrections to original estimates of the unknown target coordinates
A	is the design matrix obtained by partial differentiation of each observation equation with respect to each unknown coordinate
C_l	is the variance-covariance matrix of the observations
w	is the vector of misclosures, f(x) - l
$C_{\hat{x}}$	is the variance-covariance matrix of the adjusted coordinates
$\hat{v}$	is the residuals vector. These are the small differences between the actual observations and the observations which would perfectly fit the adjusted coordinates. The nature of the least squares solution is to minimize the sum of the squares of the residuals.

Note from equation 15 that the precision of the adjusted coordinates is estimated from information about the observational precision, C_l, and the network geometry, A.

If there is sufficient redundancy in the network statistical testing can be done on the residuals to detect gross observational errors (also called blunders or outliers). The network adjustment must be repeated after blunders have been removed from the list of observations. Reliability, in surveying terminology, is the degree to which a network is self-checking against blunders. Measures of reliability were developed by W. Baarda (1967). For more details see Mackenzie (1985).

Correct solutions to these problems depend upon a mathematically rigorous treatment of all the measurements so that alignment changes and machinery deformations can be separated from measurement errors and possible movements of "stable" reference points. To explain how this is done, it is best to consider a casing deformation problem since it is the simplest from a mathematical point of view.

In a casing deformation problem we compare two sets of three-dimensional coordinates of target points located on the casing. The three-dimensional coordinates $\mathbf{x}_i$ and $\mathbf{x}_j$, with i and j denoting epochs, have been computed in separate adjustments of angular and distance measurements in a three-dimensional survey network. The adjustment results also include the following quantities:

Epoch i	Epoch j	
C_{x_i}	C_{x_j}	covariance matrix of coordinates
$\left(v^T C_l^{-1} v\right)_i$	$\left(v^T C_l^{-1} v\right)_j$	quadratic form of residuals

r_i r_j redundancy

The propagation of random errors in the angle and distance measurements into the three-dimensional coordinates is quantified by the covariance matrix of coordinates. The quadratic form of residuals, with v denoting the correction to each survey observation and C_l a diagonal matrix having each diagonal term equal to the standard deviations squared of the corresponding survey observations, represents the weighted corrections to the survey observations. The redundancy r is equal to the total number of observations in the network, less the total number of parameters computed, plus the rank defect (if any) in the survey network adjustment.

With the quantities defined above, one can perform a global test to determine if the coordinates determined in epoch i are the same as those determined in epoch j, i.e. to determine if the set of coordinate differences $(\mathbf{x}_j - \mathbf{x}_i)$ is due only to random errors in $\mathbf{x}_i$ and $\mathbf{x}_j$, and not actual movements. This test is called the global congruency test.

If one then assumes that there are no significant differences in coordinates, the following constraint model should hold:

$$\mathbf{d} = \mathbf{x}_j - \mathbf{x}_i = 0 , \ \mathbf{C}_d = \mathbf{C}_{x_i} + \mathbf{C}_{x_j} . \tag{11}$$

By using a standard Fisher test statistic for the variance factors of the unconstrained and constrained model, it can be decided whether or not significant deformations of the whole network have taken place between measurement epochs.

It is also possible to test for movements of groups of points. To do this a variance factor corresponding to a group movement is computed and tested against the quadratic form of the residuals, using the Fisher test. The required formulae for computing the group movement parameters and the corresponding variance factor are given in Gruendig et al. (1985).

One more problem remains in deformation analysis: the determination of possible movements of "stable" reference points. This is accomplished by testing the reference points for single point movements. To do this testing it is necessary that the reference points be included as variables in the adjustment rather than being fixed and removed from the adjustment. This can be done using an appropriate "inner constraints" or "free network" adjustment. If certain reference points have moved a significant amount, they are then treated the same as points on the deforming object. Mathematically, this means that the "inner constraints" are no longer applied to these points. A detailed treatment of "inner constraints" or "free network" adjustment, and the detection and removal of significantly moved reference points, is given in Biacs (1989).

Thus precision and reliability of a survey network can be estimated before the measurements are taken. The number and type of observations, the quality of the instruments, and the geometry of the network will be chosen so that the specified precision and reliability will be achieved.

6. Alignment Monitoring with an Electronic Theodolite System

Electronic theodolite systems are capable of determining three-dimensional point coordinates, with a precision of a tenth of a millimetre or better, at ranges up to ten metres. The aim of the present project is to apply such a system to the problem of monitoring alignment changes of rotating machinery during operation.

Theodolites are surveying instruments used to measure directions in a horizontal plane and zenith angles in vertical planes. A telescope equipped with cross hairs is mounted on a horizontal axis in a U-shaped bracket, the alidade, which can be turned about a vertical axis. With conventional optical-reading theodolites the instrument operator aims the cross hairs at a target and then reads internal glass angular scales with the aid of a microscope and optical micrometer. Directions and zenith angle standard deviations on the order of one arc second are attainable.

How does an optical jig transit differ from a theodolite? The most obvious difference is that jig transits do not have angular scales. The approach with jig transits is to position the optical axis on a reference line defined by other instruments or targets. Then offset distances are measured from the reference line. Auxiliary reference lines at right angles to the main reference line are set out with a pentaprism. Kissam (1962) is a major reference on the subject of optical tooling. In the preface to that book the statement is made:

"The subject of theodolites has been omitted chiefly because, in order to attain optical tooling accuracy with theodolites designed for surveying, such a comprehensive knowledge is required of their operation, construction, and inherent errors that to cover the subject adequately would increase the length of this book out of all proportion to the importance of theodolites in optical tooling."

Electronic theodolites have overcome many of the problems mentioned by Kissam. Ingenious electro-mechanical devices read angles at the touch of a button. See Cooper (1982) or Katowski and Schneider (1987). Systematic corrections can be applied automatically; data can be stored in a memory module, data can be sent out through a serial port to a data collector or micro computer. Most electronic theodolites employ some variation of the RS-232C serial communications standard.

The first applications of electronic theodolite systems were in the aerospace and automotive industries.Two or more theodolites and a microcomputer speed data collection and allow for real-time target positioning. In close range surveys the relative precision of distance observations is poor compared to the relative precision of the angular observations. Only one distance observation is needed to fix the network scale. Electronic theodolite systems have also been used for precise surveys of large structures such as dish antennae and atomic particle accelerators. See, for example, Wilkins (1989).

In alignment monitoring of rotating machinery, the rotating shafts are often not directly visible because of coupling covers. Targets then need to be fixed to the bearing housing or on the casing as close as possible to the shaft. Changes in the shaft position can be related to changes in the target positions by interpolation, by using additional information from proximitors in the bearing housing, or by using the target displacements as input to a finite element model.

If a shaft or other rotating part is visible, it may be possible to target the surface and determine target coordinates as the shaft rotates. The target will trace a circle in three-dimensional space, and by solving for the parameters of the best-fitting circle, one is determining the location and direction of the shaft axis.

Plotting point coordinates as a function of time is the simplest form of deformation analysis. More rigorous methods are described in the preceding chapter and indicate whether the calculated movements are statistically significant in light of the expected random measurement errors.

Design of survey networks around machinery can be difficult for the following reasons:

1. Lines of sight are often restricted by coupling covers, pipes, beams, columns,railings etc.
2. Instruments should be set up on a stable surface such as a concrete floor instead of a flexible steel grating.
3. Extra lighting may be required to ensure good accuracy of pointing on the targets.
4. Refraction will cause errors where lines of sight cross areas with a high temperature gradient.
5. Thermal radiation from very hot or cold objects can distort a survey instrument and its tripod.
6. The time available for gathering observations is limited, either because the targets of interest are moving, or because of other considerations. ("We want everything back together and running by ten o'clock.")
7. Preferably the instrument locations will not interfere with other maintenance activities.

As mentioned previously, the simplest deformation analysis is to compare target coordinates from two different epochs (instants in time). This approach is valid when the expected movements are large relative to the precision of the observations, and the datum is known to be stable. More rigorous deformation analyses are required if the expected movements are of the same magnitude as the random observational errors, or if there is uncertainty about the stability of the datum. Statistical tests are applied for global congruency of the network between epochs, localization of individual point movements, and localization of point group movements. The interested reader is referred to Biacs (1989) or Caspary (1989).

The mathematical model of a circle in three dimensional space is the link between target coordinates and rotation axis position; the model which follows was described in Bayly et al (1988). Any particular point on the surface of a rotating shaft follows a near-circular path. The rotation axis passes through the centre of the circle, and is normal to the plane of the circle. Thus if the mathematical parameters of the circle can be determined, the position and orientation of the rotation axis will also be known.

Mathematically, a circle in three dimensional space is modelled as the intersection of a plane with a sphere. If the plane passes through the centre of the sphere, the circle radius and the sphere radius are equal. The general algebraic equation of a plane is

$$ax + by + cz + d = 0 \ , \qquad (12)$$

where a, b, c and d are constant parameters and x, y, and z are point coordinates. This general form is not suitable for a least squares adjustment because, for any given plane, there would be an infinite number of solutions. Arbitrarily setting d = -1 will ensure a unique solution. The equation

$$ax + by + cz - 1 = 0 \qquad (13)$$

is adequate to represent any plane that does not go through the origin of the coordinate system. The equation of the sphere is

$$(x - x_0)^2 + (y - y_0)^2 + (z - z_0)^2 - r^2 = 0 \quad , \tag{14}$$

where r is the radius and x_0, y_0, and z_0 are the centre coordinates. Finally,

$$ax_0 + by_0 + cz_0 - 1 = 0 \tag{15}$$

constrains the centre of the sphere to lie in the plane of the circle. Equations 18, 19 and 20 thus comprise the algebraic mathematical model of a circle in three dimensional space. The coordinates x, y and z are treated as observables, while there are seven unknown parameters : a, b, c, x_0, y_0, z_0, and r. Equation 15 is written only once, but 13 and 14 are written once for every target observed. Three targets yield seven equations, sufficient for a unique solution. With n targets there are 2n + 1 equations and a redundancy of 2n - 6.

Software for the Industrial Alignment Project electronic theodolite system is written in the Turbo C language for computers which operate under MS-DOS. There are five main software modules:

1. The data collection module controls the interface, saves the raw observational data, performs preliminary data checks and creates an input file for the adjustment program.

2. The adjustment/pre-analysis module does a least squares solution for target coordinates, tests observational residuals for outliers, and estimates the precision of the adjusted coordinates.

3. The deformation analysis module differences coordinates between epochs and applies statistical tests for global network congruency, individual point movements and point group movements.

4. The form fitting module determines rotation axis position and direction from the parameters of a circle which best fits a set of target coordinates.

5. The real time positioning module calculates coordinates of an observed target using a previous solution for theodolite positions and orientations. It can also calculate directions and zenith angles from the present theodolite stations to any required point (setting out).

The electronic theodolite system being assembled under the auspices of the Industrial Alignment Project is based on two Wild T2002 theodolites and a Compaq LTE/286 lap top computer. As of May, 1990, the two theodolites and lap top computer have been acquired. The interface and software are being developed at the University of Calgary. A single channel interface was demonstrated at the Industrial Alignment Project Seminar in February, 1990. The multi-channel interface is approximately 90 per cent complete. The data collection and network adjustment programs are running but more features are to be added. A circle fitting program developed for a pocket computer (Bayly et al (1988)) will be translated to run on the lap top computer. The deformation analysis and real-time positioning programs have yet to be written.

Tests of the system at the University of Calgary will establish the attainable precision in favourable conditions - good lighting, unrestricted lines of sight, stable instrument locations, absence of vibration and refraction problems. Pre-analyses of close range networks indicate that coordinate standard deviations of a few tenths of a millimetre should be possible if the extent of the network is about ten metres. The next phase of testing will take place in the machine shop at Kadon Electro Mechanical Services Ltd. in Calgary. A shaker, accelerometers and vibration analyzers will be used to quantify the effect of vibration, at the theodolite and targets, on the precision of the observations. Circle fitting routines will be tested by targeting rotating components on lathes and milling machines. There will also be opportunities for experiments on the effects of refraction, and to test the deformation analysis and real-time positioning software.

The final phase of testing will be to use the system in one or more industrial case studies. An approach to alignment monitoring of an operating cement kiln is outlined below. It illustrates some of the principles relating to circle fitting and co-linear alignment.

Rotary kilns up to 150 m (500 ft) in length and 5 m (16 ft) in diameter are common in the cement industry. The kiln shell is fitted with thick steel tires at intervals of approximately 30 m (100 ft). Each tire runs on rollers mounted on an abutment or pier. Ideally these rollers are adjusted so that the tire centres are all on the theoretical kiln centre line, and the kiln does not have a tendency to shift in an axial direction.

The following is a typical alignment procedure for kilns which have been shut down and cooled. This method involves directing a laser beam along the theoretical centre line, removing some of the fire brick liner near each tire and tracing arcs from the inside of the kiln shell to find the tire centre. If the tire centre is too far away from the centre line defined by the laser beam, the support rollers are adjusted.

There would be obvious benefits in having an alignment procedure which could be done from the outside of the kiln while it was rotating. The rotation speed is about 2 RPM. The Industrial Alignment Project group is considering the following scheme (see Figure 5) :

1. Survey in a network of reference targets in stable ground beside the kiln. Coordinates of all targets will be in a local three dimensional Cartesian system. Due to the extent of the survey (100 m) and the precision being sought (on the order of 2 mm) corrections for earth curvature will be necessary.

2. Apply an adhesive target to the side of a tire.

3. Set up two theodolites in locations from which there is good visibility of the tire target. One theodolite will be equipped with an eyepiece laser.

4. Establish the theodolite station coordinates by taking observations to the benchmark targets.

5. Point the laser to hit the tire target once per kiln revolution. Point the second theodolite onto the laser spot. Store the zenith angles and horizontal directions. It is now possible to compute coordinates of one point on the circular path of the target.

6. Repeat step 5 at least two more times for different places on the target path - the more points that are positioned, the more accurate will be the circle parameter determination.

7. Repeat steps 2 to 6 for each tire. Now there will be enough information to compute coordinates of circle centres at each tire.

8. Decide on the required location for the kiln centre line. For example it might be defined by the centres of the first and last tires, or by the best-fitting line through all the tires, or by the centre line location from a previous epoch.

9. Calculate the offsets between the tire centres and their required positions. Make the necessary adjustments. Note that these offsets correspond to the vector h in the general co-linear alignment model, equations 4 and 5.

In conclusion, electronic theodolite systems appear to have potential for solving some difficult alignment monitoring problems. They are perhaps best suited for surveys involving a moderate number of targets, when results must be presented on site shortly after the observations have been completed. These types of systems were first used in the aerospace and automotive industries. Research undertaken as part of the Industrial Alignment Project will address practical problems such as vibration and refraction, and will explore a variety of applications, for example, rotating equipment alignment monitoring, machine tool alignment, and deformation surveys of piping and structures.

7. Parallel Alignment using Inertial Measuring Units (IMU)

Inertial technology employs a combination of accelerometer and gyroscope measurements to compute the position of the system and provide information on the attitudes of the inertial unit. If the inertial system is attached to some other system, usually a vehicle of some sort, one obtains the acceleration, velocity, and position as well as the roll, pitch and azimuth of the vehicle. In terms of rigid body motion, the translations and rotations of an object in space are completely defined.

Traditionally, IMU technology has been mainly utilized in navigation and geodesy for positioning and guidance. However the ability to recover the six degrees of freedom information described above means that it has a much wider range of applications. Inertial units have been used with considerable success in underground pipeline surveys (Porter et al, 1989), road profiling surveys (Lapucha et al, 1989) and analysis of the stability of mine shaft hoists (Martell and Wei, 1990) to name just a few examples. These are, of course, all dynamical applications. In a static environment such as we can expect to find in the majority of machinery alignment situations, inertial technology can be used to transfer an internally generated azimuth from one location to another. This can be applied to the parallel alignment problem .

This technique may be especially useful in situations where there are line of sight problems for traditional instruments, such as jig transits, since the IMU is totally self contained. It simply has to be moved from place to place without regard for line of sight connections.

It should be clearly stated at this point that by azimuth we usually mean the angle from north clockwise around to the reference axis of the inertial sensor block within the system. In fact, since we are really only interested in forcing two or more lines to be parallel to some initial reference line, without regard to true north, an arbitrary line on the *exterior* of the IMU can be chosen as a reference line i.e. as initial azimuth. This line can be projected in space and all other lines made parallel to it by simple distance-angle calculations.

The azimuth of the lines at each of the rollers are given by the ISS on the line defined by the laser. The offsets to each roller are measured and the azimuth of the axis of each of the rollers is computed. The difference in azimuths is directly the misalignments of the shafts.

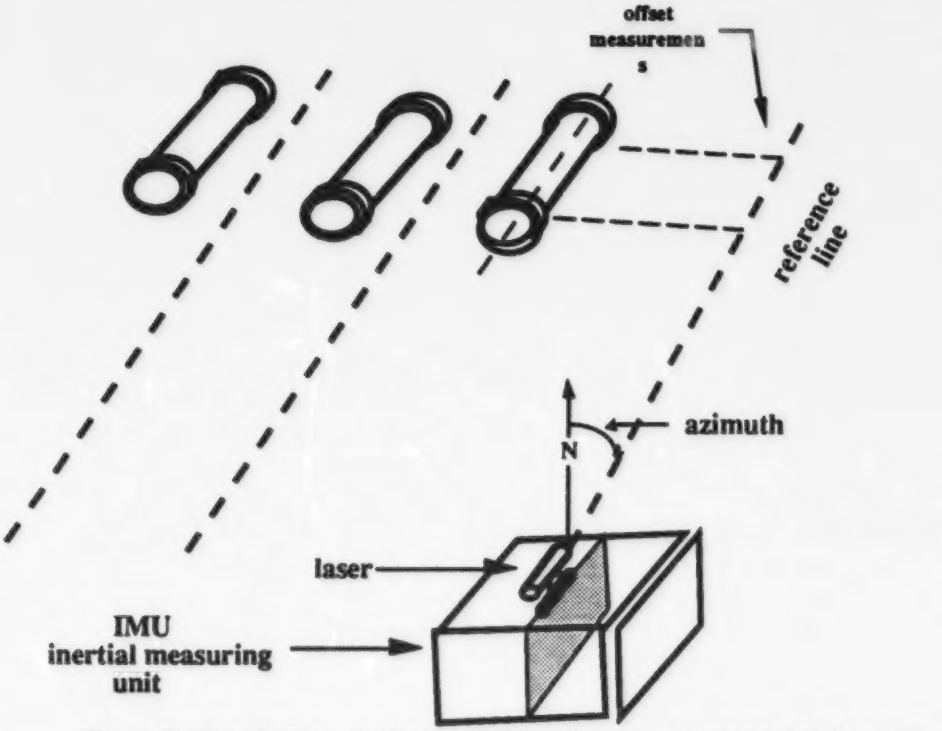

Figure 7: Use of a laser device mounted on the exterior of an inertial system

The system above portrays a configuration similar to the normal parallel alignment case - there are a number of offset lines set out by an optical device. The distances (offsets) from these lines are measured to the machine in question and the misalignments between each unit computed. However in the conventional case a baseline must be established to connect all the offset lines laid out, with the offsets usually being taken perpendicular to this baseline. The complication here lies in the necessity to maintain continuous lines of sight in areas which can normally be expected to be occupied by machinery. The inertial system has only to be transported from one location to another. It, in effect, carries the baseline with it as it is moved, without regard to the environment.

A major concern with inertial measuring units is the inherent tendency of the gyros to drift with time. This error tends to be dominated by an exponentially correlated bias, and in conventional ring laser gyro configurations a rather severe random walk introduced by dithering mechanisms used to prevent so-called lock-in of the contra-rotating light paths in the gyros. The concern then lies with the stability of the system azimuth over the period of the survey. For a static system an equation of the following kind may be used to describe the error growth of the azimuth with time.

$$\varepsilon_z = Ad_n + Bd_e + Cd_z + Db_e \tag{16}$$

where ε_z represents azimuth error, d_n, d_e, and d_z are constant gyro drifts in the north, east and vertical axes, and b_e is accelerometer bias in the east channel. A, B, C, D are time-dependent base functions which are composed of sinusoids governed by the two dominant natural frequencies of the system. These frequencies are the so-called Schuler rate of $1.235e^{-3}\ s^{-1}$ and the earth rate, $7.292e^{-5}\ s^{-1}$. The Schuler term has a period identical to that of an object in free-fall about the earth at sea-level (84 minutes), while the earth rate has a period of 24 hours. The detailed formulation can be found in Britting (1971).

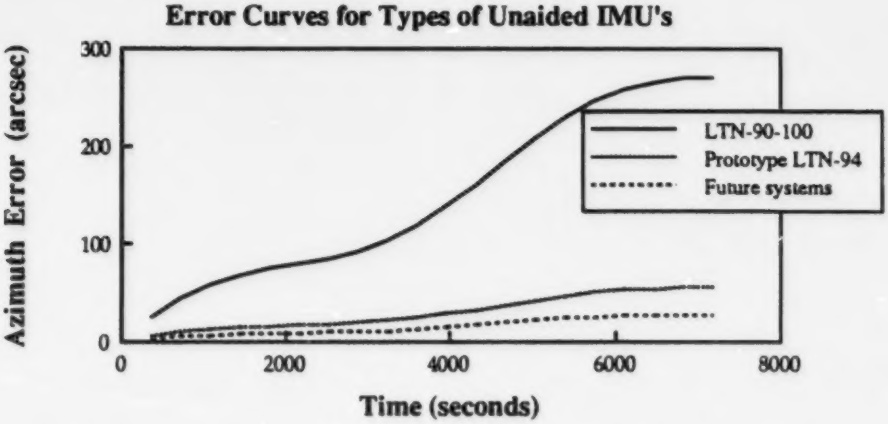

Figure 8: Azimuth error growth of ring laser gyro (RLG) IMU's. These error curves can be reduced considerably through external aiding techniques hence this is a worst case scenario.

In the figure above, the top curve displays the estimated azimuth error of a precise ring laser gyro as those contained in the LTN-90-100 IMU, used by the U. of C. The curve below is that of a prototype in use for about the last three years at Litton Industries, the LTN-94. Similar gyros are installed in each system, however the LTN-94 employs a rotating turntable rather than dither mechanism to prevent lock-in, decreasing noise in the gyro output by a factor of 5 to 10 (Matthews, 1989). The result is an error growth in the LTN-94 which indicates it might be used without external aiding for periods of up to one hour for most alignment purposes. This will almost certainly improve with production and research, and the third curve is a speculation based on this.

The LTN-90-100, on the other hand, will probably require external measurement updates to decrease the error curves indicated in the figure to levels acceptable for most industrial applications, say the 5 to 10 arc second region. Much of our present research in IMU technology focuses on this problem. Examples of updates to the system are external velocity measurements (zero, if you are stationary) and position updates from previously established points. However, velocity measurements are of little use in azimuth control. Position determination by other means could be used to improve the azimuth determination, although this may not be practical under field conditions.

The most promising techniques will probably be in field procedure which physically constrains the system to certain positions at the beginning and end of the survey. Any difference in azimuth would be due to drift, and corrections could be made to all measurements on this basis. Another idea would consist of rotating the system through 180 degrees to determine, by calibration procedures, the azimuth error on any given line. Another method being investigated is post-mission removal of the dither-induced noise frequencies by spectral techniques. The data, with noise so removed, would be re-processed and a new set of line azimuths determined. Still other techniques will be pursued in the future. However, it should be emphasized that the prototype inertial technology does exist which will handle the parallel alignment problem without updating and that this technology can be usefully employed in many other industrial applications besides the one described above.

8. Monitoring Casing Deformations by Digital Photogrammetry

For over a decade, photogrammetry has found increased application as a precise three-dimensional measuring tool in industrial and engineering areas. The use of photogrammetry can be attributed to the fact that it is non-contact, versatile and capable of delivering high precision. For example, photogrammetry has been employed for monitoring structures such as buildings, dams, antennae, aircraft and ships as well as other phenomena such as landslides. The application of photogrammetry to other deformation problems is natural considering its inherent attributes and previously found applications.

Photogrammetry employs various types of cameras for acquiring images from which measurements are made of recorded objects of interest. A camera can be considered in a manner similar to a theodolite except that the entire field of view of the optical system is employed rather than primarily the optical axis as in the case of theodolites. Traditionally film-based cameras have been used in photogrammetric surveys, although, digital cameras are finding increased usage as the resolution of digital cameras improves. However, the basic mathematical treatment of photogrammetric images for making measurements is the same regardless of the image medium (El Hakim, 1988).

The underlying mathematical models of photogrammetry are the collinearity equations or conditions. Simply stated, the collinearity equations assume that the object point, lens perspective centre and the corresponding image point all lie on a common straight line (see Figure 9).

The analytical form of the collinearity equations is given as follows:

$$x = x_p - \frac{r_{11}*(X-X^{o}) + r_{12}*(Y-Y^{o}) + r_{13}*(Z-Z^{o})}{r_{31}*(X-X^{o}) + r_{32}*(Y-Y^{o}) + r_{33}*(Z-Z^{o})} \tag{17}$$

$$y = y_p - \frac{r_{21}*(X-X^{o}) + r_{22}*(Y-Y^{o}) + r_{23}*(Z-Z^{o})}{r_{31}*(X-X^{o}) + r_{32}*(Y-Y^{o}) + r_{33}*(Z-Z^{o})} \tag{18}$$

where

x,y	are the photo coordinates
x_p,y_p	are the principal point coordinates

dx, dy	are additional parameters
f	is principal distance
r_{ij}'s	are elements of a three dimensional rotation matrix
X, Y, Z	are object space coordinates of point, and
X^o, Y^o, Z^o	are object space coordinates of perspective centre.

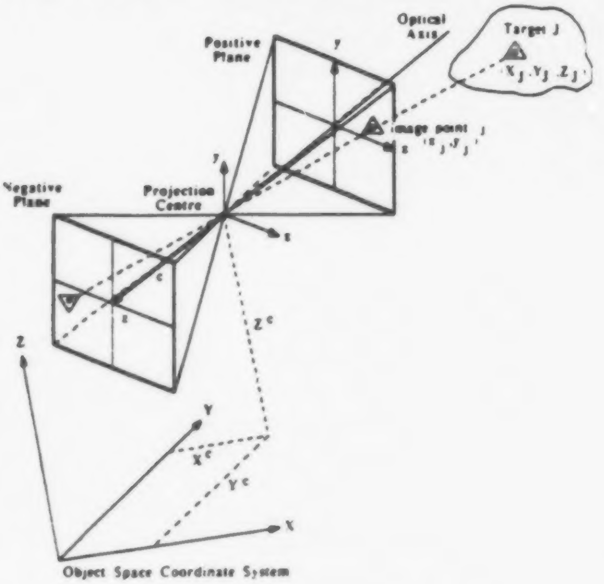

Figure 9: Imaging geometry.

In order to uniquely solve the collinearity equations a minimum amount of information is required concerning the datum related to the object space. This information can come in the form of control point coordinates or through the imposition of constraints. The choice of the datum defining information must be considered carefully in order to obtain meaningful results. In general, more information is available than is required to uniquely define the datum and, therefore, a procedure is required to solve the inconsistent equations. The method of least squares is the commonly employed to solve the overdetermined system of equations. Other forms of equations and constraints can conveniently be incorporated into a least squares solution if required. Some examples of these constraints are: distances between points, camera position and orientation and geometric constraints such as straight lines. Using the knowledge of the approximate target field, a preanalysis can be carried out for various camera configurations and observational accuracies. Once acceptable results are obtained the actual measurements can be carried out.

For most industrial applications described in previous sections, it is necessary to make measurements in a real - or near real - time manner. Film-based photogrammetry is no longer a viable method since the time required to process and measure the film can range from hours to days. Consequently, the use of digital imagery becomes more attractive since the need for film processing has been eliminated. In this case, the images are acquired using video cameras from which digital representations are sampled and stored. These resulting digital can be displayed on a video monitor or alternately numerically processed using a computer such as a PC. It is important to note, however, that the resolution of digital images is still inferior to that of film-based imagery and as such special post processing operations are required in order to achieve the most precise results possible. Accuracies of the order of 0.05 mm. for film based imagery have been reported in the literature (Brown, 1987).

Digital cameras are generally solid-state in nature and the most commonly used internal sensor is a charge coupled device (CCD). The use of CCD's is due to their high geometric accuracy during manufacturing and their geometric and sensitivity stability over time. A CCD sensor normally consists of an array of light sensitive elements referred to individually as picture elements or pixels. Each array is comprised of a certain number of rows and columns defining the active area of the sensor. Typical arrays range from 256 rows (vertical) by 576 columns (horizontal) up to 2024 rows by 2024 columns with higher resolutions being currently available. In addition, each pixel has a predefined number of bits for recording light intensity. The most commonly used number of bits assigned to each pixel is 8 which permits up to 256 grey levels to be recorded.

The ultimate objective of any photogrammetric survey is to obtain dimensional information concerning a particular object. This information is usually acquired in a discrete manner for selected points of interest. In most cases, the process of measuring objects using digital photogrammetric techniques should be as automated as possible in order to expedite the operation. Since the images are in a digital form certain image enhancement processes are possible and in many cases essential in order to localize the points of interest. The process of obtaining measurements of object points or targets involves three basic steps:1) detection, 2) recognition and 3) localization. By using uniquely shaped and well defined targets along with controlled lighting conditions and exposure settings each of these three forementioned steps can be simplified.

The detection procedure can be simply reduced to process whereby a circular convolutional low-pass filter is applied to the image such that filter window diameter is smaller than the expected target size. The resulting image after filtering should be relatively free of noise and other detail of little interest. The local maxima of the points remaining in the image are evaluated in an areawise fashion to ensure that they are indeed points and not lines, for example.

During the recognition process, targets are separated from other punctual information remaining in the filtered image. The use of well defined and uniquely shaped targets is essential for the efficient recognition of points of interest. Pattern recognition techniques, such as template matching, may be employed at this stage although the potential variations in shapes and sizes makes these procedures computationally intensive and often inappropriate. The use of controlled lighting in conjunction with highly reflective targets can greatly simplify this process. In the extreme case, images with only targets appearing would reduce the recognition problem to a trivial one. Images of this nature are of little use in future since all other points of potential interest would be lost.

The final process of localization is required to find the precise image coordinates of the targets to a sub-pixel level. In order to achieve these results, the targets must be designed such that cover several pixels on the image so that their shape and orientation can be used to precisely identify their centre.

Once the centres of all targets have been precisely located their pixel coordinates on each image on which they appear can be evaluated using the collinearity equations. The results of such an evaluation will include the camera location and orientation information, the coordinates of the object space targets and accuracy estimates for each of these estimated quantities. Real-time applications are particularly appropriate due to the well defined measurement epochs achievable with photogrammetry. As in the case of other surveying techniques (see section 4), the derived coordinate information can be used for comparing measurements for various epochs to determine whether any significant changes have occurred.

Conclusion

A unified mathematical model for machinery alignment is presented in this paper and the functional relationship between this model and different types of observables are outlined. The observables include relative displacements obtained from dial indicators or lasers, directions obtained from theodolites, and coordinate differences derived from digital cameras. The statistical treatment of actual measurements within this general framework is discussed and test statistics are reviewed which allow the separation of misalignments or deformations from purely stochastic effects.

The three systems specifically considered in this paper are a system of electronic theodolites, inertial survey systems, and a pair of digital cameras. Pre-analysis of the system outputs indicates that the accuracies required for the alignment of rotating machinery and machinery deformations can be achieved and that the systems offer advantages in flexibility and economy in a number of situations. Testing these systems for specific alignment cases is therefore the next step in the project. The alignment of a large lathe, rotating shafts and a rotating kiln are planned for this summer. Results from these tests will be used to fine-tune methods of analysis and operational procedures.

Acknowledgements

The support and cooperation of Nova Corporation of Alberta, Trans Canada Pipelines, Proctor and Gamble Cellulose, Alberta Gas Ethylene, Ipsco Inc., Lafarge Canada, Celanese Canada, Cominco Ltd, Alberta Natural Gas, Esso Resources, Petro Canada, and Amoco Canada in the above project is gratefully acknowledged. In addition we would like to thank Dr. Paul Kim of the National Research Council of Canada for support and encouragement.

References

Baarda, W. (1967). Statistical Concepts in Geodesy. Netherlands Geodetic Commision. Publications in Geodesy. New Series, Vol.2, No.5. Delft, The Netherlands.

Bayly, D.A., E.G.Anderson and S.J. Mugford (1988). Machinery Monitoring Surveys. Proceedings. Canadian Society for Civil Engineering Annual Conference, Vol. III:35-49, May 25-27, Calgary, Alberta.

Biacs, Z.F. (1989). Estimation and Hypothesis Testing for Deformation Analysis in Special purpose Networks. M. Sc. thesis, Department of Surveying Engineering Publication No. 20032, The University of Calgary, Calgary, Alberta.

Britting, K.R. (1971). Inertial Navigation Systems Analysis. Wiley Inter-Science, New York.

Brown, D.C. (1987). AutoSet, An Automated Monocomparator Optimized for Industrial Photogrammetry. Presented paper, Int Conf. and Workshop on Analytical Instrumentation. Phoenix, Arizona, November 1987.

Caspary, W. (1988). Concepts of Network and Deformation Analysis. Monograph 11, School of Surveying, The University of New South Wales, Kensington, N.S.W.

Cooper, M.A.R. (1982). Modern Theodolites and Levels. Granada, London.

Davis, R.E., F.S. Foote, J.M. Anderson, E.M. Mikhail (1981). Surveying: Theory and Practice. Mc-Graw Hill, New York.

El Hakim, S. F. (1988). Limiting Factors of Real-Time Image Metrology. Commision II, International Archives of Photogrammetry and Remote Sensing. Vol. 27, Part B2, Kyoto, Japan.

Gruendig, L., Neureither, M. and Bandorf, J. (1985). Detection and Localization of Geometrical Movements. Journal of Surveying Engineering, Vol. III, No 2, pp. 118-132.

Katowski, O. and A. Schneider (1987). Industrial Surveying. Wild Heerbrugg, Heerbrugg, Switzerland.

Kissam, P. (1962). Optical Tooling for Precise Manufacture and Alignment. McGraw-Hill, New York.

Lapucha, D., Schwarz, K.P., and Cannon, E. (1989) Precise Kinematic Positioning of a Mobile Road Inventory System. Report to the Institute for Transportation Studies, The University of Calgary.

Mackenzie, P.A. (1985). Design and Assessment of Horizontal Survey Networks. M. Sc. thesis, Department of Surveying Engineering Publication No. 20011, The University of Calgary, Calgary, Alberta.

Martell, H.E. and Wei, M. (1990). Application of Strapdown Inertial Surveyor in Determination of Hoist Skip and Mine Shaft Trajectory. To be presented at the International Symposium on Kinematic Systems in Geodesy, Surveying and Remote Sensing. Banff, Alberta. September, 1990.

Matthews, A. and Welter, H. (1989). Cost Effective, High-Accuracy Inertial Navigation. Navigation: Journal of the Institute of Navigation. Vol 36, No. 2, Summer 1989.

Mikhail, E.M. and F. Ackerman (1976). Observations and Least Squares. University Press of America, Lanham, Md.

Mikhail, E.M. and G. Gracie (1981). Analysis and Adjustment of Survey Measurements. Van Nostrand Reinhold, New York.

Porter, T.R., J.W.K.S. Smith, and Adams, J.R. Pipeline Inertial Geometry Pigging. Canadian Petroleum Association Colloquium V, Calgary, AlbertaOctober, 1989.

Wild-Leitz (1988). Wild Instruments on Line. Wild-Heerbrugg, Heerbrugg,Switzerland.

Wilkins, F.J. (1989). Integration of a coordinating system with conventional metrology in the setting out of magnetic lenses of a nuclear accelerator. M.Sc.E. thesis, Department of Surveying Engineering Technical Report No. 146, University of New Brunswick, Fredericton, N.B.

A COST EFFECTIVE ROTATING MACHINERY INFORMATION ACQUISITION AND ANALYSIS SYSTEM

STEVEN J. SABIN, BSEE, SALES ENGINEER

BENTLY NEVADA CANADA LTD.
NISKU, ALBERTA CANADA
T0C 2G0

ABSTRACT

The attached paper describes a low-per-point cost, computer-based machinery information acquisition and analysis system. The system is intended for use by plant maintenance personnel and minimizes the time and labour normally required for machine data collection in plant maintenance programs.

The innovative use of a single desktop computer allows data collection from up to 2040 machine points connected sequentially along a system cable. This architecture greatly reduces the per-point costs of transducers and installation and eliminates the need for local transducer power supplies.

The system minimizes maintenance costs by utilizing existing resources more efficiently and providing information allowing intelligent planning of maintenance shut-downs. The system gives plant managers, engineers, and maintenance supervisors immediate access to the status of all machinery.

KEYWORDS

Trendmaster™ 2000, Predictive Maintenance, Machinery Condition Monitoring, Machinery Data Acquisition, Machinery Maintenance, Machinery Data Collection, Machinery Condition Trending, Vibration Monitoring, Temperature Monitoring, Process Variable Monitoring, Vibration Spectrum, Rolling Element Bearings

ABOUT THE AUTHOR

Mr. Sabin is a Sales Engineer with Bently Nevada Canada Ltd. He obtained a Bachelor of Science degree in Electrical and Electronics Engineering from Oregon State University. He is an active member of IEEE, Tau Beta Phi, Eta Kappa Nu, Phi Kappa Phi, and is an Engineer-in-Training with APEGGA.

RÉSUMÉ

La communication ci-jointe décrit un système informatisé de saisie et d'analyse des données sur les machines peu coûteux. Le système est destiné au personnel de maintenance des usines et réduit au minimum le temps et la main-d'oeuvre normalement nécessaires pour la collecte des données sur les machines dans les programmes de maintenance des usines.

L'utilisation novatrice d'un seul micro-ordinateur permet de recueillir des données allant jusqu'à 2040 points de machines reliés séquentiellement par un câble. Cette architecture réduit considérablement le coût par point des transducteurs et de l'installation, tout en éliminant le besoin d'alimentation locale en courant électrique des transducteurs.

Le système minimise les frais de maintenance en faisant appel aux ressources disponibles de façon plus rationnelle et en fournissant des données qui permettent une planification intelligente des interruptions pour assurer la maintenance. Le système permet aux directeurs d'usine, aux ingénieurs et aux surveillants de la maintenance de s'informer sans délai de l'état de toutes les machines.

MOTS-CLÉS

Maintenance préventive, surveillance de l'état des machines, saisie des données sur les machines, maintenance des machines, collecte de données sur les machines, étude de la tendance de l'état des machines, surveillance des vibrations, contrôle de la température, contrôle des variables de procédé, spectre des vibrations, roulements.

BIOGRAPHIE

M. Sabin est ingénieur-vendeur chez Bently Nevada Canada Ltée. Il détient un B. Sc. en génie électrique et électronique de l'Université de l'Orégon (Oregon State University). Il est membre actif de l'IEEE, des "fraternités" Tau Beta Phi, Eta Kappa Nu, Phi Kappa Phi, et il fait un stage d'ingénieur à l'APEGGA.

INTRODUCTION

Given the need to be more competitive in the Global Market, increased throughput is a major concern. The goals of increased machine speeds and reduced downtime will put a greater emphasis on machinery health.

Implementation of vibration monitoring as part of a predictive maintenance program is an effective method to minimize machine downtime. This is evidenced by the large numbers of plants that have incorporated vibration monitoring as part of their maintenance programs. Two primary methods of vibration monitoring are presently used. The first employs continuous, dedicated monitors and transducers. While this can often be justified for large turbomachinery and other critical machines, it is almost never used on general purpose "balance of plant" type machinery as it requires large outlays of initial capital. The second method employs portable data acquisition instruments which require extensive commitments of labour. This paper presents an innovative new technology for data acquisition and analysis that drastically reduces the cost of a permanently installed rotating machinery information system.

PREVENTIVE VS. PREDICTIVE MAINTENANCE

The ideal goal of any maintenance program is to eliminate catastrophic machine failures while simultaneously maximizing the life and performance of the machine. In the past, most plants used running hours or a similar measure to determine maintenance intervals. In this way they sought to prevent machine failures by servicing the machine at regular, frequent intervals; hence, the name preventive maintenance. However, while frequent maintenance intervals reduce the likelihood of catastrophic failures, they do not eliminate them.

At first glance, this philosophy appears "safe" because it seeks to service a machine before problems develop. However, there are two intrinsic shortcomings in this approach. First, to improve safety, components are often run to only a fraction of their rated life and then replaced. This is inefficient. Second, this maintenance philosophy does not address the instances in which problems exist in either the component, the installation, or both. An incorrect installation or defective component can often cause a failure almost immediately after the "repaired" machine is put back in service. Failure of this type is sometimes referred to as "infant mortality". Thus, a preventive maintenance philosophy is not as safe an approach as at first appears. It cannot detect a defective component or installation; it can only "play the odds" with a machine and service it at intervals that make failure unlikely. The two goals of a maintenance program as mentioned above are seen to work against one another in a preventive maintenance program; i.e., improvements in extending maintenance intervals must be made at the expense of increased risk of a machine failure.

An approach to maintenance becoming more widely used is what is commonly called Predictive Maintenance. This philosophy can best be summarized by the phrase "if it ain't broke, don't fix it". More precisely, by monitoring the condition of a machine, maintenance intervals are determined by how the machine is running. This maximizes efficiency since a machine is not serviced until service is actually required. Many times the data collected for a machine is trended and degradation of components and performance can be easily identified. Decisions such as how much longer to run a machine before servicing are no longer guesswork. The data collected on a machine not only tells when maintenance is required, it is often useful in telling maintenance personnel what is wrong with a machine so they know where to look when the machine is opened up resulting in more efficient use of personnel.

Predictive maintenance has the added benefit of safety as the machinery is monitored periodically to detect problems. When there is a problem, maintenance is performed. Thus, predictive maintenance does not pit the goals of decreased downtime and increased safety against one another. Predictive maintenance has received wide acceptance in industry as a cost-effective and inherently safer practice.

HISTORY OF PREDICTIVE MAINTENANCE

In the past, predictive maintenance relied on the senses. Touch the machine and determine how much it is vibrating (figure 1) and how hot it is. Look at the machine and see if it is behaving normally. Smell the machine to detect product leaks, overheating, etc. Listen to the machine to detect problems in bearings, overloading, and so forth. A clipboard was checked appropriately and the machine was given a clean bill of health if the operator's senses could not detect any abnormalities. An obvious problem with these crude measurements was that problems were normally only apparent when they had progressed to the point of actually damaging the machine (figure 2).

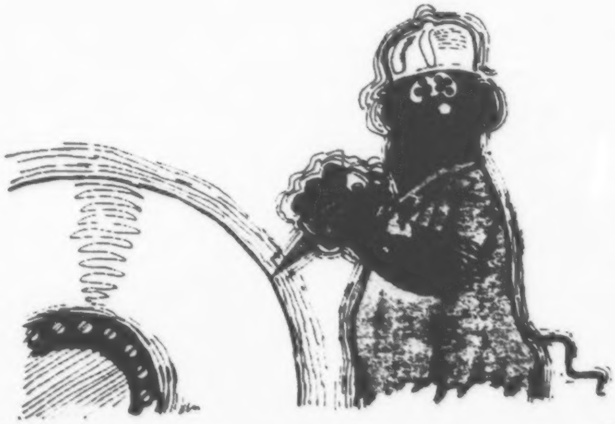

FIGURE 1.

As portable transducers became available to measure and quantify various machine conditions, the question "how is it running" could be answered much more objectively on general purpose machinery. Readings could be taken that were much more sensitive than simply "touch, look, smell, and listen". These readings could be hand logged and trends could be established as these readings changed from one measurement period to the next. With the advent of microprocessors came portable data collectors which would allow one to load a route into the data collector, stop and take readings at each point on the route, download the stored data from the data collection instrument into a desktop computer, and use the computer software to analyze and trend the collected data. The market has a number of fine offerings in the way of portable data collectors as the electronics industry continues to offer improvements in power, data storage, and speed in increasingly smaller packages (figure 3).

FIGURE 2.

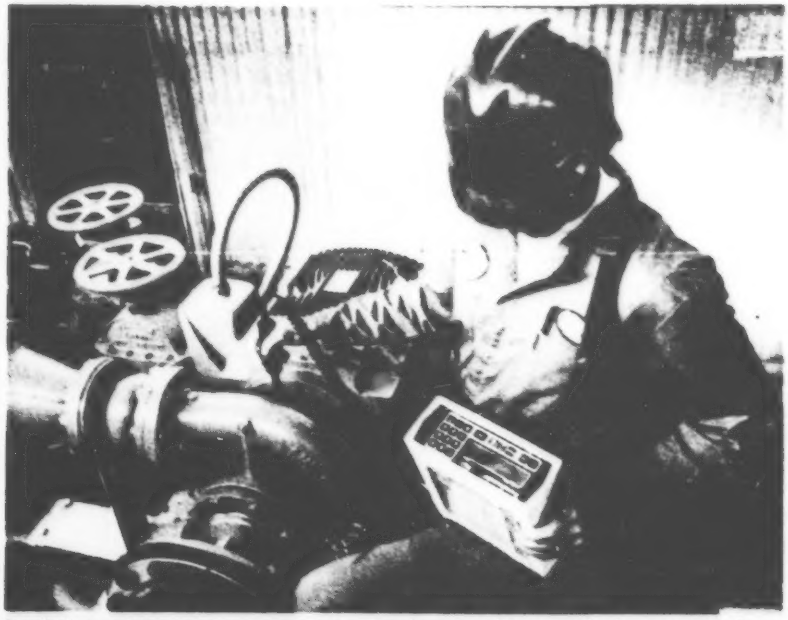

Predictive maintenance programs have greatly reduced lost production resulting from machine failure.

FIGURE 3.

However, predictive maintenance programs based on portable data collectors have several limitations as follows:

1) They require an extensive commitment of time and labour to collect data on all the points in a plant. While most data collectors are fairly simple to operate and do not require highly skilled labour in the data collection process, they do nevertheless require trained labour.

2) Some machines may be inaccessible due to physical or environmental constraints.

3) Portable data collectors often require working very near to (and sometimes on) operating machinery. This can be dangerous to the personnel taking the data and may dictate that a machine go unmonitored because readings simply cannot be taken safely.

4) It is seldom feasible to take readings more often than once a week. Much can happen to a machine between readings.

5) Some data collection instruments may not be approved for use in hazardous areas. Thus, extra labour (and extra cost) is required to accompany the data collection technician with an employee carrying a gas detector (sniffer) or other such safety apparatus when used in hazardous areas.

6) The accuracy of the data collected with hand-held transducers is dependent on positioning, pressure and angle of orientation among other factors.

As noted previously, the only other options available until now were to install permanent, continuous monitors or to adopt a preventive type of maintenance program. Neither of these is often economically justifiable. Clearly, the need for a new approach to predictive maintenance is required and it must address the following concerns:

1) Users are demanding more of their equipment and as such require more frequent and accurate data on machine conditions.

2) Maintenance programs must be as efficient as possible to remain competitive.

3) The total cost of implementing and operating a successful predictive maintenance program must be lower than other available options. The total cost must take into account the ongoing labour required for data collection.

A NEW, TECHNOLOGICALLY ADVANCED PRODUCT

Bently Nevada Corporation of Minden, Nevada has recently introduced a machinery information system called Trendmaster™ 2000 that fills the gap between portable data collection based programs and permanent, continuous monitoring. Figure 4 illustrates the elements of this permanently installed data acquisition and analysis system for general purpose machinery.

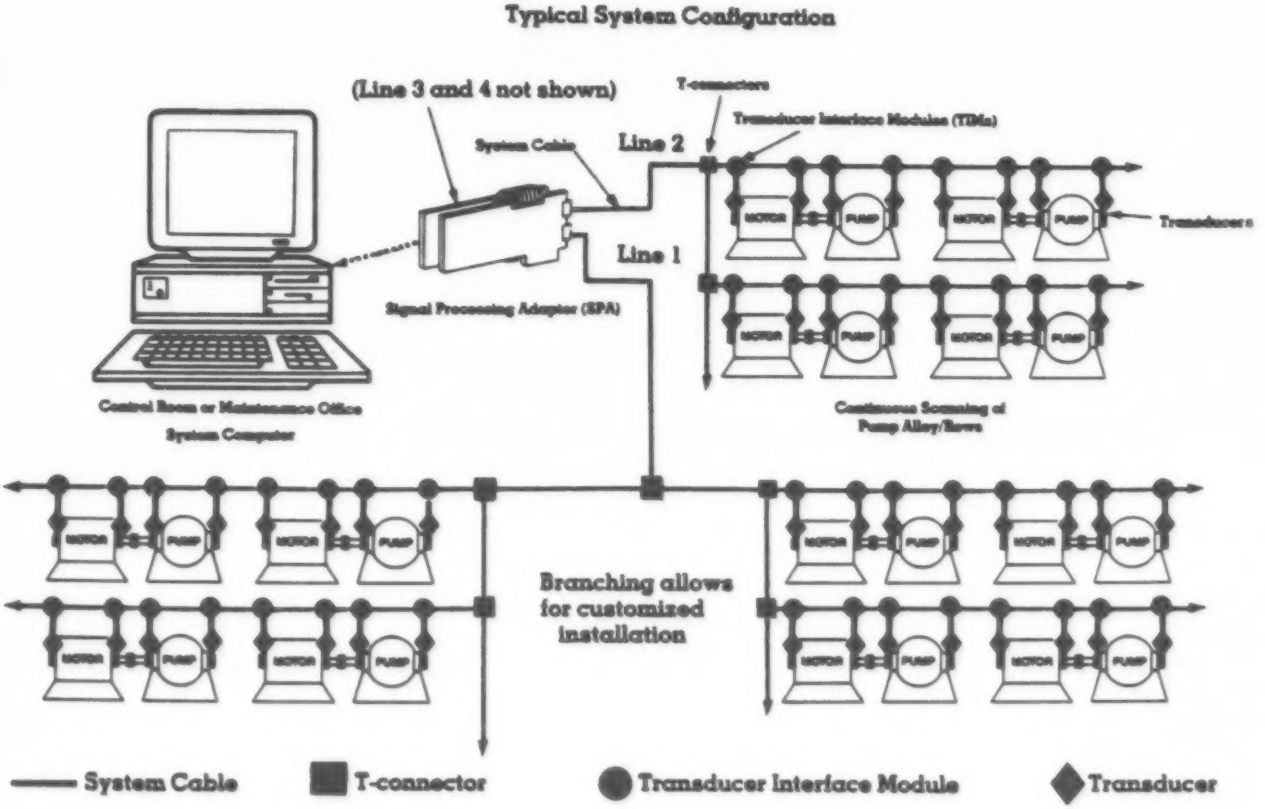
Typical System Configuration
(Line 3 and 4 not shown)
T-connectors
Transducer Interface Modules (TIMs)
System Cable
Line 2
Line 1
Transducers
MOTOR
PUMP
Signal Processing Adapter (SPA)
Control Room or Maintenance Office
System Computer
Continuous Scanning of
Pump Alley/Rows
Branching allows
for customized
installation
System Cable
T-connector
Transducer Interface Module
Transducer

FIGURE 4.

Unlike conventional systems which require a portable transducer to be carried from point to point, the Trendmaster™ 2000 uses low-cost permanently-mounted transducers on each point for which data is required. The computer automatically scans machine points to identify potential problems. In the serial scanning sequence, a single machine transducer point is energized, a reading is processed and the point is then powered down. This continues for each subsequent machine point in the system. Only one point is active at a time. The point reading is compared to user-defined alarm levels and if it exceeds a level, an indication is issued on the computer terminal. Audible as well as visual annunciation of an alarm condition is available to the user.

The system components and a short description of the features of each is as follows:

1) System Computer and Printer

   The computer must be dedicated as the system only collects data and provides alarm annunciation and machine information while the Trendmaster™ 2000 software is running on the computer. The required computer is an IBM-AT or compatible.

2) System Software

   The software allows configuration of the individual points in the system and allows these points to be placed in logical groups. Individual points as well as groups of points can be activated or deactivated as part of the active scanning loop. Alarm levels, scanning order, vibration filter corners, spectrum ranges, averaging, and windowing are among the many user configurable options. Trend files from 30 to 270 days with 1 day resolution are generated automatically by the system. Trends may be displayed which clearly show up to 4 user-defined alarm level setpoints and a cursor can be moved to read values at each point in the trend plot. Dynamic data can be stored weekly or monthly and spectra vs. time (waterfall) plots can be viewed which will show how the spectra for a point change at 1 week or 1 month intervals.

   Any two plots can be displayed on the same screen for comparison. This is an extremely powerful troubleshooting tool as the correlation between two points can become apparent and may signal the source of a problem. For example, increased vibration and decreased discharge flow through a centrifuge may indicate plugged nozzles. This condition might not be as readily apparent if the vibration and discharge flow trends are viewed separately.

   A spectrum of any vibration point may be viewed along with time-domain information and baseline data may be saved for future comparison to determine conditions such as bearing wear. The daily readings taken for each point may be viewed as well.

   A priority list allows up to 20 points to be scanned more frequently. This is particularly valuable when problem machinery is spotted and needs to be monitored more closely.

   The system annunciates visibly and audibly whenever an alarm condition occurs and alarm events are automatically logged in an alarm list that keeps the most recent 400 alarm events. A point may be configured to automatically store dynamic (waveform) data whenever an alarm condition is encountered as well. The system can display a point's status as OK, NOT OK (transducer or TIM problem), NO DATA (point inactive or TIM problem), ALARM 1, or ALARM 2.

Figure 5 shows several examples of the screens available.

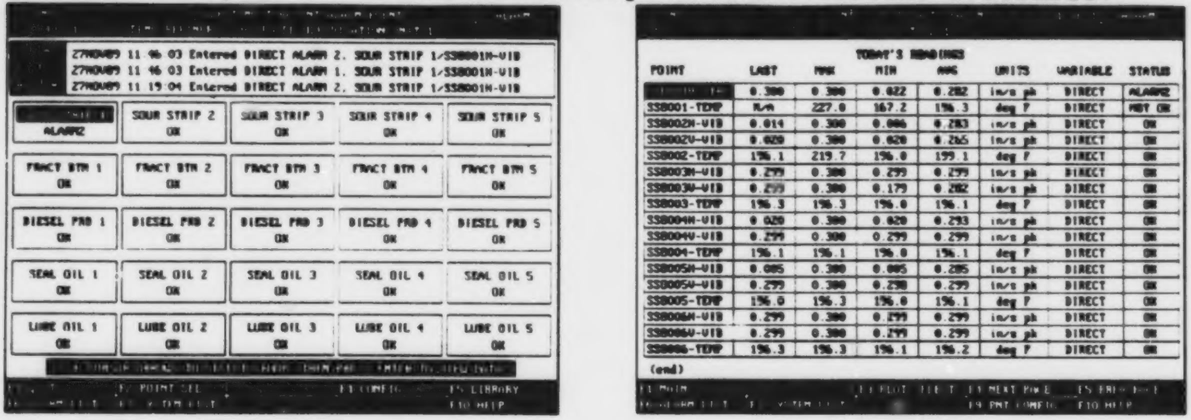

```
27NOV89 11 46 03 Entered DIRECT ALARM 2. SOUR STRIP 1/SS0001H-VIB
27NOV89 11 46 03 Entered DIRECT ALARM 1. SOUR STRIP 1/SS0001H-VIB
27NOV89 11 19:04 Entered DIRECT ALARM 2. SOUR STRIP 1/SS0001H-VIB
```

ALARM2
SOUR STRIP 2 OK
SOUR STRIP 3 OK
SOUR STRIP 4 OK
SOUR STRIP 5 OK
FRACT BTM 1 OK
FRACT BTM 2 OK
FRACT BTM 3 OK
FRACT BTM 4 OK
FRACT BTM 5 OK
DIESEL PRD 1 OK
DIESEL PRD 2 OK
DIESEL PRD 3 OK
DIESEL PRD 4 OK
DIESEL PRD 5 OK
SEAL OIL 1 OK
SEAL OIL 2 OK
SEAL OIL 3 OK
SEAL OIL 4 OK
SEAL OIL 5 OK
LUBE OIL 1 OK
LUBE OIL 2 OK
LUBE OIL 3 OK
LUBE OIL 4 OK
LUBE OIL 5 OK
F2 POINT SEL
F4 CONFIG
F5 LIBRARY
F10 HELP

TODAY'S READINGS

POINT	LAST	MAX	MIN	AVG	UNITS	VARIABLE	STATUS
[illegible]	0.300	0.300	0.022	0.282	in/s pk	DIRECT	ALARM2
SS0001-TEMP	N/A	227.0	167.2	196.3	deg F	DIRECT	NOT OK
SS0002H-VIB	0.014	0.300	0.006	0.283	in/s pk	DIRECT	OK
SS0002V-VIB	0.020	0.300	0.020	0.265	in/s pk	DIRECT	OK
SS0002-TEMP	196.1	219.7	196.0	199.1	deg F	DIRECT	OK
SS0003H-VIB	0.299	0.300	0.299	0.299	in/s pk	DIRECT	OK
SS0003V-VIB	0.299	0.300	0.179	0.282	in/s pk	DIRECT	OK
SS0003-TEMP	196.3	196.3	196.0	196.1	deg F	DIRECT	OK
SS0004H-VIB	0.020	0.300	0.020	0.293	in/s pk	DIRECT	OK
SS0004V-VIB	0.299	0.300	0.299	0.299	in/s pk	DIRECT	OK
SS0004-TEMP	196.1	196.1	196.0	196.1	deg F	DIRECT	OK
SS0005H-VIB	0.005	0.300	0.005	0.285	in/s pk	DIRECT	OK
SS0005V-VIB	0.299	0.300	0.298	0.299	in/s pk	DIRECT	OK
SS0005-TEMP	196.0	196.3	196.0	196.1	deg F	DIRECT	OK
SS0006H-VIB	0.299	0.300	0.299	0.299	in/s pk	DIRECT	OK
SS0006V-VIB	0.299	0.300	0.299	0.299	in/s pk	DIRECT	OK
SS0006-TEMP	196.3	196.3	196.1	196.2	deg F	DIRECT	OK

(end)

F1 MAIN
F9 PNT CONFIG
F10 HELP

Group Select

Point Select

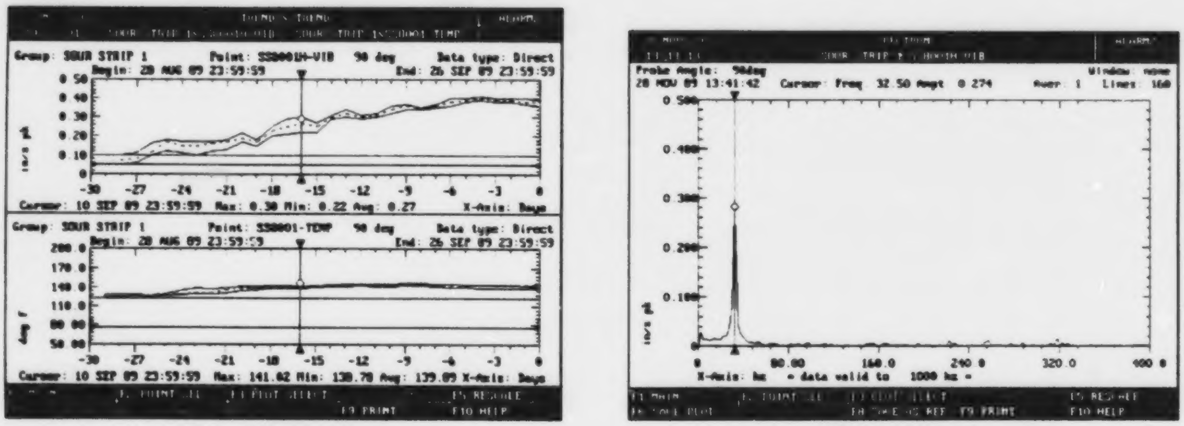

```
Group: SOUR STRIP 1          Point: SS0001H-VIB   90 deg        Data type: Direct
        Begin: 28 AUG 89 23:59:59                            End: 26 SEP 89 23:59:59
Cursor: 10 SEP 89 23:59:59  Max: 0.30 Min: 0.22 Avg: 0.27         X-Axis: Days
Group: SOUR STRIP 1          Point: SS0001-TEMP   90 deg        Data type: Direct
        Begin: 28 AUG 89 23:59:59                            End: 26 SEP 89 23:59:59
Cursor: 10 SEP 89 23:59:59  Max: 141.02 Min: 138.70 Avg: 139.89 X-Axis: Days
```

TREND VS TREND
ALARM
0.50
0.40
0.30
0.20
0.10
0
in/s pk
-30
-27
-24
-21
-18
-15
-12
-9
-6
-3
0
200.0
170.0
140.0
110.0
80.00
50.00
deg F
F9 PRINT
F10 HELP

```
Probe Angle:  90deg                                                Window: none
28 NOV 89 13:41:42   Cursor: Freq 32.50 Ampt 0.274            Aver: 1  Lines: 160
X-Axis: hz   = data valid to   1000 hz =
```

ALARM
0.500
0.400
0.300
0.200
0.100
in/s pk
0
80.00
160.0
240.0
320.0
400.0
F1 MAIN
F8 SAVE AS REF
F9 PRINT
F10 HELP

Trend Comparison

400 Line Spectrum

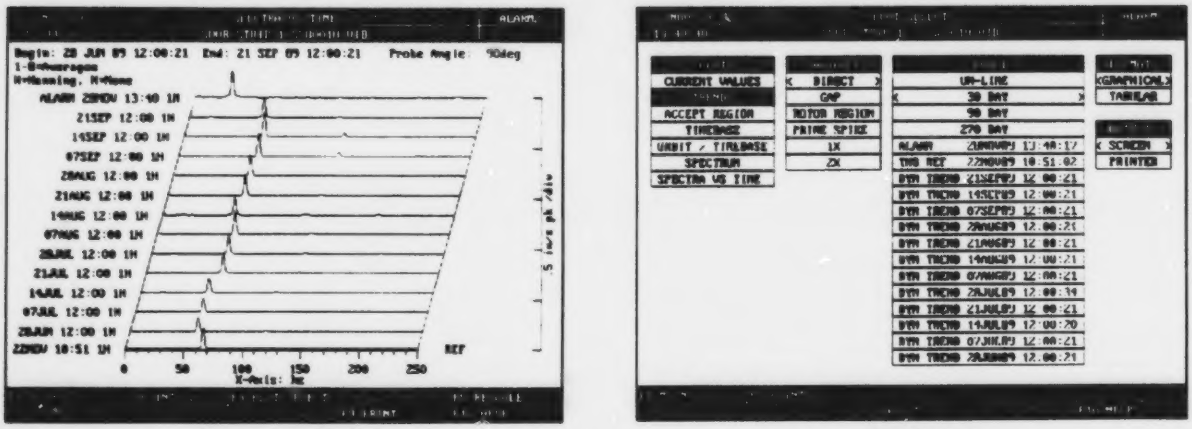

```
Begin: 28 JUN 89 12:00:21  End: 21 SEP 89 12:00:21   Probe Angle:  90deg
1-8=Averages
H=Hanning, N=None
```

ALARM
ALARM 28NOV 13:40 1N
21SEP 12:00 1N
14SEP 12:00 1N
07SEP 12:00 1N
28AUG 12:00 1N
21AUG 12:00 1N
14AUG 12:00 1N
07AUG 12:00 1N
28JUL 12:00 1N
21JUL 12:00 1N
14JUL 12:00 1N
07JUL 12:00 1N
28JUN 12:00 1N
22NOV 10:51 1N
REF
.5 in/s pk /div
0
50
100
150
200
250
X-Axis: hz
F9 PRINT
CURRENT VALUES
TREND
ACCEPT REGION
TIMEBASE
UNIT / TIMEBASE
SPECTRUM
SPECTRA VS TIME
< DIRECT >
GAP
ROTOR REGION
PRIME SPIKE
1X
2X
ON-LINE
< 30 DAY >
90 DAY
270 DAY
ALARM 28NOV89 13:40:17
TWO REF 22NOV89 10:51:02
DYN TREND 21SEP89 12:00:21
DYN TREND 14SEP89 12:00:21
DYN TREND 07SEP89 12:00:21
DYN TREND 28AUG89 12:00:21
DYN TREND 21AUG89 12:00:21
DYN TREND 14AUG89 12:00:21
DYN TREND 07AUG89 12:00:21
DYN TREND 28JUL89 12:00:34
DYN TREND 21JUL89 12:00:21
DYN TREND 14JUL89 12:00:20
DYN TREND 07JUL89 12:00:21
DYN TREND 28JUN89 12:00:21
<GRAPHICAL>
TABULAR
< SCREEN >
PRINTER
F10 HELP

Spectra vs Time

Plot Select

FIGURE 5.

3) Signal Processing Adapter (SPA)

The SPA consists of 2 standard AT sized expansion cards connected by a ribbon cable. One card handles analog signal processing and the other handles digital. The SPA is simply inserted in the expansion slots of the system computer. Each SPA can handle 4 lines containing 255 machine points each. The SPA controls the scanning protocol, transducer powering, and signal conditioning of the system. When installed in hazardous areas, the system architecture also eliminates the need for separate intrinsically safe barriers for each transducer.

Since only 1 transducer in each line is powered up by the computer at a time, at most 8 barriers would be required (1 for each line) on a full capacity system. This represents a significant savings in hardware and installation costs.

The scanning rate of the system depends on whether the point has been configured by the user as static (overall values) or dynamic (waveform data). The scanning rate is also dependent on things like filtering selected and rotational speed. Overall (unfiltered) vibration data takes about 1 second/point to gather.

4) System Cable

The system cable, which connects all points in a line to the system computer, is the communication line of the system. The cable connects machine points in a serial manner and can be in a continuous line or in a distributed "star" network through the use of T-connectors. The total length of cable in a single SPA line can be as much as 4000 feet. If greater distances are required, line extenders are available to significantly increase the line length allowed.

5) Transducer Interface Modules (TIM)

The TIM (figure 6) is the interface that connects a transducer to the system cable. Each TIM is given a unique address by setting an 8-position binary switch on the TIM. When addressed in the scanning cycle, the TIM and its associated transducer is powered. Until addressed, all TIMs and transducers are inactive. The TIM contains all the necessary conditioning circuitry for both power and signal.

Trendmaster 2000

The Transducer Interface Module (TIM) is a single channel unit that interfaces its corresponding transducer to the system.

FIGURE 6.

TIM design allows a number of mounting options including screws, tie-wrap, epoxy, or a 35mm DIN rail located by the machine or in an available NEMA 4X weatherproof housing (figure 7). TIMs are single channel units and one is required for each machine point. TIM's are available for a variety of transducer inputs.

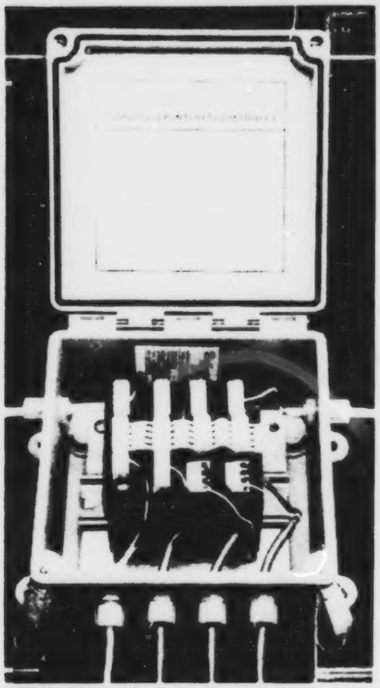

NEMA 4X housings capable of holding up to eight modules (TIMs) are available.

FIGURE 7.

6) Transducers

The system presently supports the following transducers:

- Velocity pickups
- RTDs
- Thermocouples
- Process variable 4-20 mA or 1-5 Vdc signals per ISA standard

Additional transducer types include proximity probes to allow such facilities as Keyphasor™ data, shaft orbit displays, and minute outer race deflection measurements on rolling element bearings. The Keyphasor™ capabilities will be especially useful to give phase as well as amplitude information on the vibration signal. The Keyphasor™ signal can also be used as a speed reference on variable speed machines to automatically adjust filter band ranges with changes in rpm of the machine.

APPLICATIONS

Before the possible uses of this system are examined, it is important to note that the system is designed to improve the efficiency of data collection and analysis in predictive maintenance programs. It is NOT intended as a continuous protection system for critical equipment. Intervals between readings may be as much as 30 minutes or more which is unsuitable for critical equipment protection and no relay facilities exist for automatic shutdown.

With the above in mind, the potential uses for the equipment are numerous and include among others:

- Paper machines (especially on the dry end where points are generally difficult if not impossible to get to with hand-held systems).

- "Pump Alleys" in refineries

- Industrial/Commercial HVAC systems

The system is ideal for any application where more frequent information on a large number of general purpose machines is required.

As mentioned previously, the system has only recently been introduced. As such, case histories are limited to our Beta test sites. One of these test sites provides an interesting aside.

A large casino/hotel complex near the Bently Nevada corporate offices and manufacturing facilities expressed interest in using the product as a beta test site on their HVAC equipment. One might be led to wonder why a casino would need such a thorough maintenance/information program. However, similar to an industrial plant, casinos are subject to "lost production". This can happen when ambient temperatures in the casino are too warm or too cool for the customers. It is known that the "window" of acceptable temperatures for keeping customers in the casino is quite narrow. Thus, temperatures in the casino must be tightly controlled; that means maintaining proper operation of their HVAC equipment. If not, "lost production" can easily amount to several hundred thousand dollars in the space of a few hours. The continuous information provided by the system is considered essential and the initial cost of the system can easily be recovered with a single machine save. The customer has attributed 3 machine saves to their system to date and are very pleased with the results they are getting.

BENEFITS

A typical predictive maintenance program for a plant might be as follows:

> Seven portable data collector instruments are used for gathering data on 4000 points at one week intervals.
> Two man-years of labour is necessary for collection and down loading of data each year. In addition, one-quarter of the the maintenance engineer's time is required. the estimated yearly cost of the program is over $150,000. The program is considered a success with estimated plant savings of $400,000 per year.

That's over $150,000 per year for collection and dumping of weekly data. The $400,000 savings is impressive but imagine the savings possibilities if the business area had access to automatically updated data every hour. The cost of monitoring this plant's 4000 points with two Trendmaster™ 2000 systems is easily and quickly paid back in two ways. First, it minimizes the ongoing labour required to gather weekly data. Second, the shorter intervals between readings allow problems to be caught much sooner than with weekly intervals. Thus, potentially damaging machine problems can be spotted much quicker and damage limited.

A quick summary of benefits includes:

- The system described in this paper is cost-effective, particularly when a large number of points are to be monitored.
- The system provides current and accurate information. Data is updated, stored, and trended automatically. This data is available to everyone in the plant from operators to managers to rotating equipment engineers. The right data for the right people is available all the time.
- The system is easily expandable. It is very easy to install and adding points is as simple as "dropping" another TIM and transducer off the system cable. No special termination of the system cable is required and more points can be added at the end or anywhere along the cable. One can start small and add more points easily and inexpensively.
- Because the system gathers the data automatically, your maintenance personnel can use their time for other duties. Thus, labour efficiency is improved.
- The trending capabilities of the system allow downtime to be predicted and scheduled. Expensive unplanned downtime is minimized.
- Machine condition and process variables can be monitored at frequent intervals and promptly corrected to give increases in product quality.
- Personnel are no longer required to be on or near operating machinery to gather data. Plant safety is increased as a result and data that may have previously been unattainable can now be monitored.
- The system is approved for use in hazardous areas (intrinsically sale).
- The system is continually being enhanced based on response from users. Additional transducer types, software upgrades, and remote access are just some of the many areas that will continue to evolve with this revolutionary new technology.

CONCLUSION

Permanently installed monitoring equipment on general purpose machinery such as pumps, compressors, motors, and centrifuges is now cost-effective. Machinery performance information is constantly available to the user as are the tools necessary to analyze the data. New technology and design has dramatically reduced the cost of this equipment and the time (and cost) required for installation. Plant maintenance personnel can now concentrate their efforts on solving identified machine problems instead of collecting data. This can lead to minimization of unplanned shutdowns and maintenance resource requirements, and ultimately to increased production, safety, and product quality.

REFERENCES

Muszynska A.; Laws, W.C.; "Periodic and Continuous Vibration Monitoring for Preventive/Predictive Maintenance of Rotating Machinery", presented at the ASME Winter Annual Meeting, Miami Beach, Florida, November 1985.

Harker, R.G.; Sandy, J.L.; "Rolling Element Bearing Monitoring and Diagnostic Techniques", presented at the Gas Turbine and Aeroengine Congress and Exposition, Amsterdam, The Netherlands, June 1988.

Applications Note, "Predictive Maintenance Through the Monitoring and Diagnostics of Rolling Element Bearings", Bently Nevada Corporation, June 1988.

Continuous Monitoring for Automated Predictive Maintenance

Craig Cantrell
Computational Systems Incorporated
Knoxville, Tennessee, U.S.A.

Abstract

The use of continuous monitoring for machinery surveillance is not a new concept. Many industries have used continuous monitoring systems for years to measure the vibration of critical machines. The systems monitored the overall vibration level and alarmed when the current level exceeded a preset limit. Most systems would provide automatic shutdown of the machine when the current vibration level exceeded a danger setpoint.

This type of monitoring system was designed to prevent catastrophic failure of the machine and provide a relative indication of the current machine condition. However, since no data storage was provided, when a shutdown occurred, data was not available for analysis to determine the cause of the shutdown or the extent of damage. An intensive manpower effort was required to perform the analysis and determine corrective maintenance.

With the onset of computer-based predictive maintenance during the past several years, many of these same industries now implement spectral-based periodic monitoring on a wide range of plant equipment. Predictive maintenance (PDM) using vibration frequency spectrum analysis has proven to be a very successful tool for fault detection and relative health indication of a machine. The success of these predictive maintenance programs has highlighted the deficiencies of continuous monitoring systems that only monitor overall vibration levels and has sparked the development of a new generation of continuous monitoring systems.

Biography

Craig Cantrell is the Product Manager of the Systems Product Line for Computational Systems Incorporated. He is a graduate of North Carolina State University with a Bachelors degree in Materials Engineering. He previously spent 6 years with the Tennessee Valley Authority in its nuclear power program.

RÉSUMÉ

La surveillance continue des machines n'est pas un idée nouvelle. Un grand nombre d'entreprises utilisent depuis des années des systèmes de surveillance continue pour mesurer les vibrations des machines les plus importantes. Ces systèmes sont conçus pour contrôler le niveau total des vibrations et pour donner l'alerte lorsque celui-ci dépasse les limites prévues. La plupart des systèmes sont pourvus de dispositifs d'arrêt automatiques qui se déclenchent lorsque le niveau des vibrations atteint le seuil dangereux.

Ce genre de système est conçu pour éviter les pannes catastrophiques et pour donner une certaine indication ponctuelle de l'état de la machine. Cependant, vu que ces systèmes n'étaient pas pourvus de mémoire, il n'existait aucune donnée permettant de déterminer et d'analyser les causes de l'arrêt ou l'étendue des dommages. Il fallait un effort d'analyse important, impliquant de nombreuses heures de travail, pour déterminer les causes du problème et prendre des mesures correctives nécessaires.

Depuis l'implantation , au cours des dernières années, des systèmes de maintenance préventive assistée par ordinateur, un grand nombre de ces mêmes entreprises fait maintenant appel, pour toutes sortes de machines, au contrôle périodique basé sur l'étude des spectres. La maintenance préventive à l'aide de l'analyse des spectres de fréquence des vibrations s'est avérée très efficace pour la détection des défectuosités ainsi que pour l'analyse de l'état général d'une machine. Le succès de ces programmes de maintenance préventive a mis en évidence les faiblesses des systèmes de surveillance continue qui ne contrôlent que les niveaux de vibration totaux et il a entraîné la mise au point d'une nouvelle génération de systèmes de surveillance.

BIOGRAPHIE

Craig Cantrell est directeur de la production des systèmes chez Computational Systems Incorporated. Il possède un baccalauréat en génie des matériaux de la North Carolina State University. Il a été à l'emploi de la Tennessee Valley Authority pendant 6 ans dans le cadre d'un programme de production d'énergie nucléaire.

Continuous Monitoring for Automated Predictive Maintenance

Key Features

The new generation of continuous monitoring systems are designed to support predictive maintenance and are based on the principles that are the backbone of successful PDM programs. The essential features of these new generation continuous monitoring systems include:

Computer-based hardware - The hardware of a continuous monitoring system should be based on computer technology. A computer-based system will maximize the speed, power and efficiency of the system functions. Setup and modification to the system monitoring configuration is almost effortless.

Frequency analysis - Frequency and time waveform analysis are proven techniques for evaluating the health of a machine. Frequency analysis provides the analyst with the information needed to accurately determine the cause of a developing problem. Frequency related defects (such as bearing faults, gear mesh problems, etc.) are detected much earlier using frequency analysis than using overall level monitoring.

The on-line system must have the capability of breaking the frequency signature into frequency bands that relate to specific component faults. The energy level within these faults is computed and compared to alarm limits for the earliest detection of developing machine faults.

Vibration and process signal measurement - The system must be capable of monitoring signals from a variety of transducer types. Correlation of vibration behavior with process parameters such as temperature and pressure is often critical to understanding the current health of a machine.

Automatic data screening/compression - A tremendous volume of data will be generated during routine data collection. The system must be equipped with an automated technique of data reduction so that only relevant data is permanently stored. This feature greatly reduces the manpower required for data analysis.

Alarm features - Automatic alarming features are necessary to support the detection and analysis of alarm events. Computer screen displays are necessary to identify the current status of the machines being monitored, alerting the operator to any alarms detected. When alarm events occur, data must be automatically captured and stored to aid the analysis of the machine fault. An alarm logging feature, such as an event list sent to a printer, is needed to record each alarm event and relevant information about the event. This feature enables the user to check on machine performance during periods when the monitoring system is not observed.

Permanent data storage - Both routine and alarm data should be permanently stored to support data diagnosis for predictive maintenance. Historical data is important as a record of previous machine performance and for use in detecting abnormal machine conditions.

Data diagnostic techniques - Software for data analysis is essential. When alarms occur, the collected data must be analyzed to identify the machine fault. Once the machine fault is known, corrective maintenance can be scheduled. A powerful software program that supports the analysis of frequency data is critical to the success of machine fault identification.

The software must also provide the ability to trend collected data. Trending of routine data will often identify the onset of a fault condition long before it reaches an alarm limit. The earlier the fault is detected, the more time is available for planning and scheduling the corrective maintenance.

Report generation - A report generation feature is necessary for developing summary reports of machine condition for routine reporting to plant management.

Flexibility of application - The system should be designed so that it can interface directly with shutdown monitoring systems or function as a stand-alone product. Many applications, such as turbine monitoring, require automatic shutdown of the machine as well as predictive maintenance continuous monitoring. Figure 1 illustrates the integration of a shutdown monitoring system with a predictive maintenance monitoring system. With this setup, the sensor signals from the machine are shared between the two systems eliminating the need to install duplicate sensors. Figure 2 depicts the predictive maintenance monitoring system connected directly to a machine.

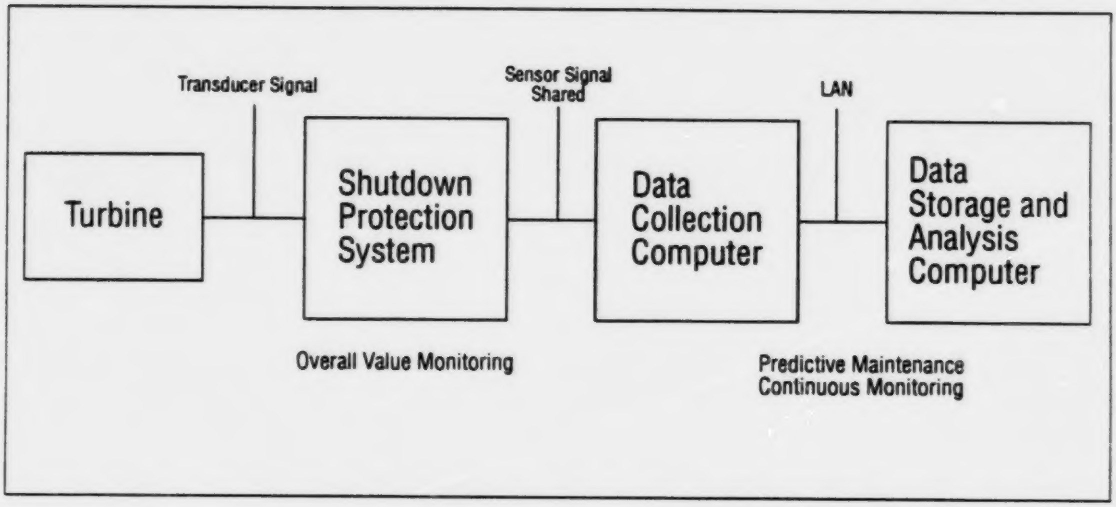
Transducer Signal
Sensor Signal Shared
LAN
Turbine
Shutdown Protection System
Data Collection Computer
Data Storage and Analysis Computer
Overall Value Monitoring
Predictive Maintenance Continuous Monitoring

Figure 1. Diagram illustrating interface of a shutdown protection system with PDM continuous monitoring system. Transducer signals are typically "shared" between the two systems, eliminating the need for duplicate sensor installation.

Distributed hardware - Figures 1 and 2 show a distributed monitoring hardware approach for the predictive maintenance monitoring system. Utilizing a distributed approach provides the ability to collect data at one computer while analysis, database management or reporting are performed on stored data at the other computer. Data collection is never interrupted unless halted by the user.

Transient Data Capture - Certain machines, such as turbines or compressors, often require data capture during startups and coastdowns to determine critical speed ranges. The data captured should be simultaneous for each input during the transient event. In addition to capturing the transient event, the data just preceding the event should be stored for post event analysis. This feature enables the analyst to review data leading up to the transient to better determine what event caused the machine trip. The PDM continuous monitoring system should have a transient data capture capability to support this machine analysis.

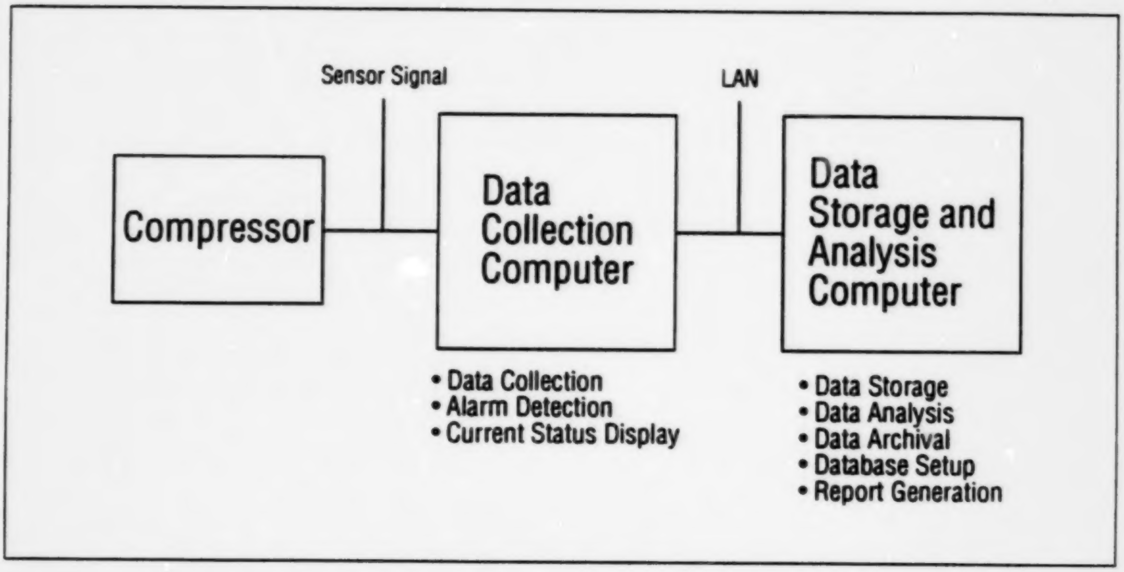
Sensor Signal
LAN
Compressor
Data Collection Computer
Data Storage and Analysis Computer
• Data Collection
• Alarm Detection
• Current Status Display
• Data Storage
• Data Analysis
• Data Archival
• Database Setup
• Report Generation

Figure 2. Typical PDM continuous monitoring system hardware illustrating the essential functions of the system and where they are performed.

System Cost/Benefit

When evaluating the use of a predictive maintenance continuous monitoring system, several factors should be considered. These factors include the system expense, the benefits derived and the selection of equipment to be monitored.

PDM continuous monitoring systems are not cheap, however, the payback from such a system can be enormous. The essential consideration when performing a cost/benefit analysis is to determine how much money can be saved through use of the system. By providing early detection of problems that would otherwise result in unscheduled downtime, the system should pay for itself quickly. Unscheduled downtime costs in most industries can be staggering. The savings from the prevention of just one unscheduled shutdown will often cover the system expense.

Equipment that is essential to the production process is a prime candidate for continuous monitoring. Machines such as turbines, compressors, paper machines, large motors, fans, pumps, etc. are typically instrumented with a predictive maintenance monitoring system. If one of these machines fails, the production process comes to a halt until the machine is back in operation.

Personnel safety is another consideration for using a predictive maintenance monitoring system. If the equipment is located in a hazardous environment, the risk to personnel is often too great for manual data collection. These situations include high temperature, high radiation or dangerous equipment operation areas. In each case, the dollars saved from reduced downtime and increased personnel safety far exceed the system expense.

Case Histories

The following are two examples of machine faults detected through the use of a PDM continuous monitoring system.

Example 1 - A major gulf coast ammonia producer uses the CSI MachineView Model 3100 PDM monitoring system to monitor the compressor trains (turbine and motor driven) of the plant's major processes. While performing trend analysis of turbine vibration data, the user noticed an intermittent high vibration on several sensors as shown in Figure 3. Based on the sensor locations, the problem was diagnosed as an intermittent rub. During the next maintenance outage, the turbine was investigated and found to have a warped wheel that caused the intermittent rub. Repair was made during the outage and the turbine returned to service. This is a good example of a machine fault that would probably have gone undetected unless monitored continuously since it was a periodic event.

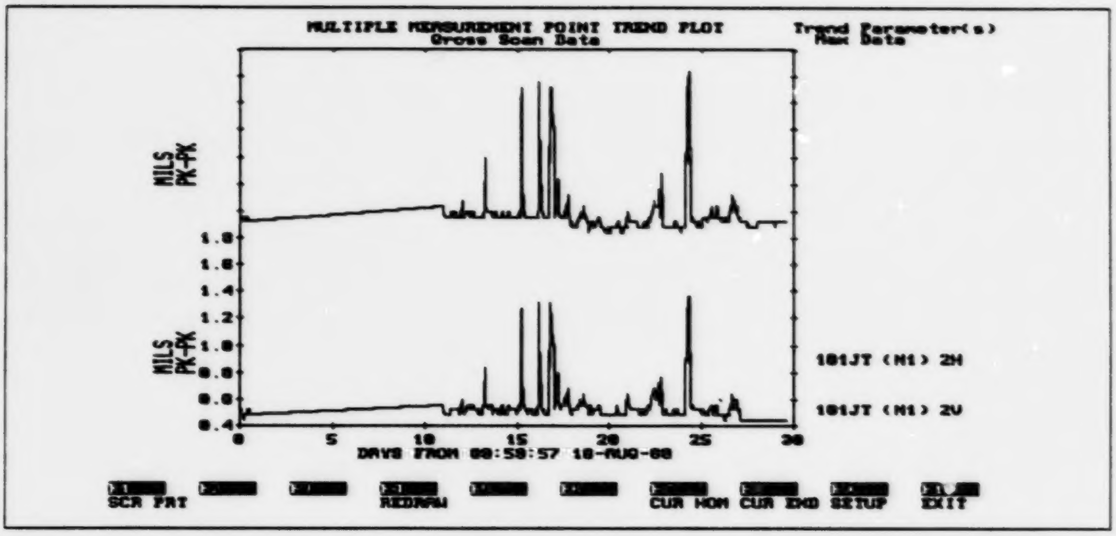
MULTIPLE MEASUREMENT POINT TREND PLOT
Gross Scan Data
Trend Parameter(s)
Max Data
MILS PK-PK
MILS PK-PK
1.8
1.6
1.4
1.2
1.0
0.8
0.6
0.4
101JT (M1) 2H
101JT (M1) 2V
0
5
10
15
20
25
30
DAYS FROM 09:58:57 10-AUG-88
SCR PRT
REDRAW
CUR HOM
CUR END
SETUP
EXIT

Figure 3. Vibration trend data showing intermittent high vibration resulting from turbine wheel rub.

Example 2 - A major southern newsprint paper manufacturer has installed a CSI MachineView Model 3100 system on his #5 newsprint paper machine. The system monitors bearings on major rolls, primarily in the press section of the machine. The monitoring system identified an increase in vibration of the granite roll bearing on the tending side of the machine. Figure 4 is a trend of the bearing outer race frequency vibration showing an increase in the vibration activity that indicated a bearing defect was developing. After following the degradation of the bearing for about two weeks, the paper machine was shut down and the bearing replaced. The machine was then put back in service. Figure 5 shows a multiple spectra plot of the frequency spectra taken three weeks before the repair, just prior to the repair and after the machine had restarted. Notice the significant decrease in vibration as a result of the repair. As a result of the system detection of the developing bearing failure, the maintenance staff was able to track the degradation and determine the appropriate time for repair. The actual repair downtime was minimized based on the advance notice of the problem.

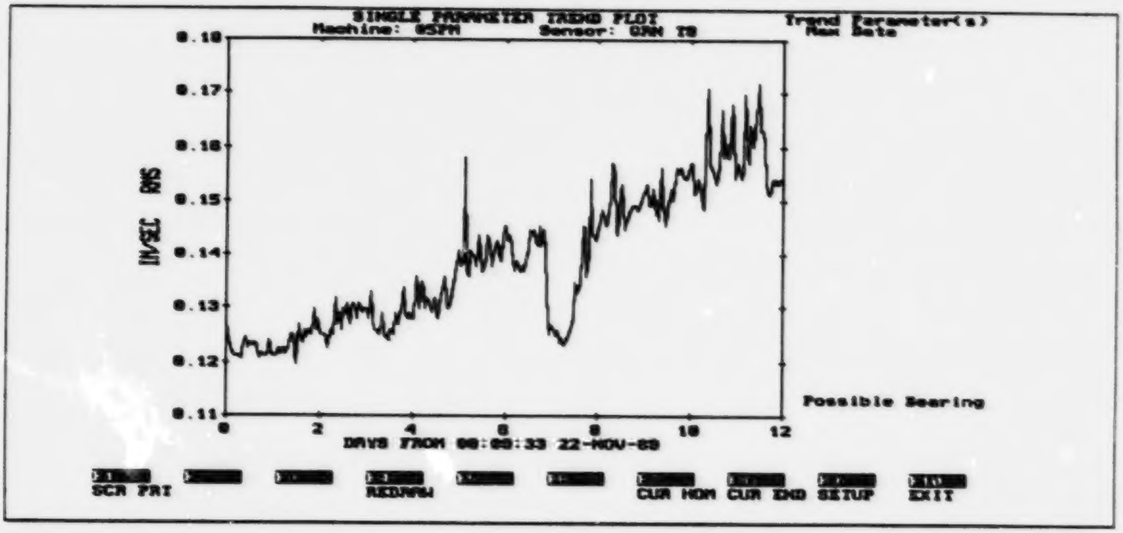

Figure 4. Granite roll bearing trend data showing significant increases in outer race vibration.

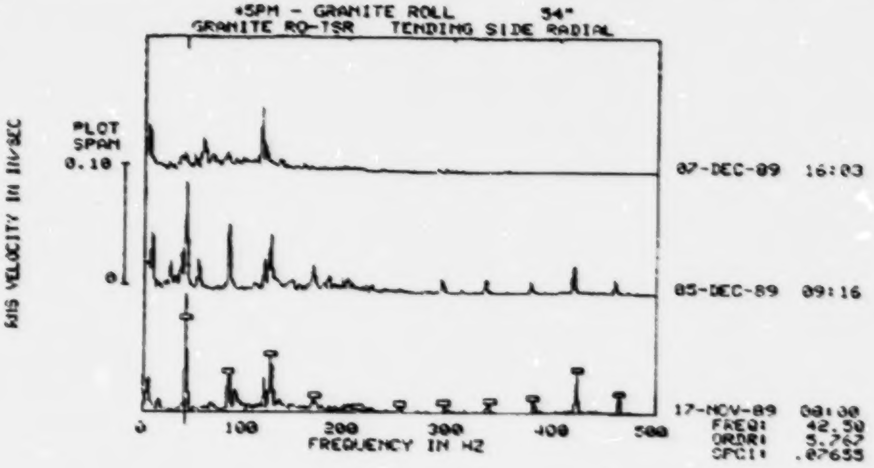

Figure 5. Multiple frequency signatures showing change in vibration as result of granite roll bearing replacement (Dec. 6).

Summary

Continuous monitoring systems that implement PDM techniques are becoming an integral part of the maintenance programs in many industries today. These systems are normally installed on machines critical to the production process or hazardous to plant personnel. Immediate payback on the investment in a monitoring system having the features discussed will be realized through increased machine efficiency and reduced plant downtime.

SESSION / SÉANCE 3

Machinery Fault Diagnosis and Expert Systems/
Diagnostic des défectuosités des machines et systèmes experts

LEAD PRESENTATION / PRÉSENTATION INAUGURALE

Development in Expert Systems with Application to Dynamic Problems in Rotating Machinery

by Rainer Nordmann and M. Keim

DEVELOPMENT IN EXPERT SYSTEMS WITH APPLICATION TO DYNAMIC PROBLEMS IN ROTATING MACHINERY

R. Nordmann, M. Keim
Department of Mechanical Engineering
University of Kaiserslautern, West Germany

ABSTRACT

In many technical processes rotating machinery is used in a wide range of different applications. These machines are expected to work securely and reliably. On one hand, there is a tendency to increase the specific power of the aggregate, which makes it more susceptible to vibration problems. On the other hand, the failure of one component can have significant financial impact for a company, not so much due to repair costs but because of production losses.

Therefore immediate help must be available if problems occur. As there are many influences which can contribute to the behavior of rotating machinery, usually experts have to be consulted in order to solve the problem. However, experts are rare and seldom quickly available at the specific location where they are needed. In such a case, the application of an expert system promises to assist operators or maintenance personnel with expert-level knowledge without a human expert being present personally.

This paper describes some basics about machinery maintenance and expert systems. It then gives an example of an expert system shell named MED2 and a knowledge base for TUrbo MAchinery-Diagnosis called TUMAD.

BIOGRAPHY

Rainer Nordmann completed his undergraduate and doctoral degrees in Mechanical Engineering in 1974 at the Technical University of Darmstadt in West Germany. He was an assistant professor in the Institute of Dynamics of Machines and became the head of the Machine Dynamics Laboratory in 1976. Since 1980 he has been the Professor of Dynamics of Machines and Control Theory at the Technical University of Kaiserslautern. His research group includes ten research assistants and fourteen student research assistants. In the past eight years, approximately twenty research projects have been carried out with funding from government agencies and several companies on topics such as forced and self-excited vibrations, modal and sensitivity analysis in rotor dynamics, dynamic behaviour of turbopump rotors, identification of seal and bearing coefficients, active magnetic bearings, dynamic behaviour optimization, and the development of expert systems for the diagnosis of rotating machines. He is very well known for this work and has published approximately sixty papers to date.

Marc Keim: Studies of Mechanical Engineering at the University of Kaiserslautern; Diploma in 1986; Started Research Work in the working group of Prof. Nordmann in January 1987; Employed with KSB (pump manufacturer) since December 1987; Special interests: Dynamics of Machines, Finite Elements, Expert Systems.

RÉSUMÉ

Les machines rotatives sont utilisées pour une foule d'applications différentes dans un grand nombre de procédés techniques et on s'attend à ce qu'elles fonctionnement continuellement sans problèbles. On a cependant tendance à augmenter la puissance spécifique de l'ensemble, ce qui le rend plus vulnérable aux problèmes de vibration; et si l'un des composants vient à faire défaut, l'impact financier sur la firme est généralement important, non pas tant à cause du coût des réparations que du manque à gagner.

Il faut donc pouvoir disposer sur le champ de l'assistance nécessaire en cas de défaut. Comme le comportement des machines rotatives peut être influencé par une multitude de facteurs, il faut habituellement consulter des experts pour trouver la cause du problème. Malheureusement les rares experts ne sont habituellement pas disponibles sans préavis et ils ne peuvent se rendre rapidement là où la situation l'exige. Dans un tel cas, les opérateurs ou le personnel d'entretien pourraient tirer profit de l'expertise de haut niveau d'un système expert qui les assisterait sans avoir recours à la présence physique d'un expert.

La présente étude décrit certains principes de base sur les systèmes experts et l'entretien des machines. Il donne comme exemple un système expert appelé MED2 ainsi qu'une base de données appelée "**TU**rbo **MA**chinery **D**iagnosis" ou TUMAD.

BIOGRAPHIE

Rainer Nordmann a obtenu ses diplômes de premier cycle et de doctorat en génie mécanique en 1974 à l'Université technique de Darmstadt, en Allemagne de l'Ouest. Il a été professeur adjoint à l'Institut de dynamique des machines et a été nommé directeur du Laboratoire de dynamique des machines en 1976. Depuis 1980, il est professeur de dynamique de machines et de théorie de la commande à l'Université technique de Kaiserslautern. Son groupe de recherche compte dix adjoints et quatorze étudiants. Au cours des huit dernières années, il a mené à bien une vingtaine de projets de recherche à l'aide de fonds d'organismes gouvernementaux et de plusieurs sociétés privées, dont les sujets furent variés: vibrations forcées et auto-entretenues, analyse modale et de sensibilité en dynamique des rotors, tenue dynamique des rotors de turbopompes, détermination de coefficients de joints et de roulements, roulements magnétiques actifs, optimisation de la tenue dynamique et mise au point de systèmes experts de diagnostic de machines tournantes, M. Nordmann jouit d'une grande réputation et a publié une soixantaine d'articles à ce jour.

Marc Keim a étudié le génie mécanique à l'université Kaiserslautern; diplômé en 1986, il a participé au groupe de travail du professeur Nordmann en janvier 1987; il est à l'emploi de KSB (un fabricant de pompes) depuis 1987. Ses champs d'expertise particuliers sont la dynamique des machines, les éléments finis et les systèmes experts.

DEVELOPMENT IN EXPERT SYSTEMS WITH APPLICATION TO DYNAMIC PROBLEMS IN ROTATING MACHINERY

R. Nordmann, M. Keim
Department of Mechanical Engineering
University of Kaiserslautern, West Germany

INTRODUCTION

In almost all areas of modern technics today machines with rotating components are used. Examples for this are turbines and generators for energy production, pumps for transporting liquid media, fans for conveying flue gas, compressors for compressing gaseous media and motors for driving systems. The operators expect these machines to work securely and reliably. Therefore especially dynamic stresses and resulting changing strains have to be heeded. Severe machinery vibrations can produce damages which normally lead to high economic losses because of production interrupt. In case of a failure of a turbomachine the reasons have to be found quickly and measures for reduction of the vibrations have to be initiated. Dynamic problems often are quite complicated and have several reasons (unbalance, instability of bearings and labyrinth seals, misalignment, cracks ...). Therefore, the knowledge and the experience of experts for vibrational issues will be necessary in order to solve these problems.

There is a tendency in mechanical engineering today to increase specific power and speed. For that reason the expected dynamic behavior has to be scrutinized already in the phase of design and construction. Highly advanced programs are available for calculating the vibrational properties for a given mechanical model. Good insight into the mechanisms that influence the vibrational behavior is necessary. Distribution of mass and stiffness of rotating parts and also the arrangement of bearings and seals have to be considered. Besides this, fluid–mechanical coupling effects in oil–lubricated bearings and seals, in labyrinth seals at the impeller and between the stages and last not least interactions between impeller and vaned diffuser change the dynamic behavior. The above mentioned effects were investigated experimentally and theoretically in quite a number of research projects.

With numerical predictions it is possible in some cases to achieve good correspondence with the later observed behavior of the real system. Nevertheless, quite often there is considerable disagreement in form of greater disturbing vibrations than calculated. In critical cases this can even lead to a shut down or a damage of the rotating machine. Reasons for these differences between calculation and real behavior can be:

- Wrong assumptions or neglecting of important mechanisms in the model,
- inaccurate input data for system parameters and load functions,
- changes in the dynamic properties of the system and/or in the dynamic loads during operation.

The last mentioned item e.g. could be changing clearances in journal bearings or seals, varying static preloads and temperatures leading to new eigenfrequencies and damping factors which possibly call forth instabilities. Increasing vibrations due to unbalance can be caused by vane failures, deposition or erosion at impellers, and by thermal influences.

These changes normally result in deterioration of the dynamic behavior. Vibrational amplitudes in rotating machinery should not exceed certain measures. Otherwise there is danger that the material is overstressed, clearances are enlarged or already existing cracks continue growing. Finally, increasing vibrations lead to severe damages even destructions and therefore losses of machines and production. To avoid this vibrational variations have to be recognized early in order to prevent damages by suited measures.

Because of the expectations for security, reliability, and availability it is necessary to use advanced methods of condition monitoring and failure diagnostics. Mechanical changes in a machine generally strongly influence the vibrational behavior of a machine. Therefore it is obvious to judge the condition of the machine by means of vibrational measurements (Figure 1).

A good condition monitoring and an effective failure diagnostic and therapy depend mainly upon three factors:

- Measurements: Sensors acquire diagnostic signals at appropriate points (Figure 1).
- Calculations: The signals are reduced to characterizing symptoms by using computer programs: Frequency analysis, Orbits, Eigenfrequencies, and so on.
- Experiences: The expert gathers the different informations of measurements and calculations. He analyses the dynamic behavior using his expert knowledge and experience. After the diagnosis of the reasons for the vibrations a suitable therapy will be suggested. At a real system this therapy has to be tested to find out whether additional or different measures have to be considered.

In case of a dynamic problem in a rotating machine usually a problem solution is found in a way as shown in Figure 2.

Because of the many mechanisms and effects that can lead to a failure of the machine an expert must know a lot of facts and rules. But with the many possibilities even an experienced specialist will have difficulties keeping a survey of everything that could have happened. Therefore tools are going to be developed to assist the expert in such areas. These tools are called expert systems because they should be able to simulate the knowledge of an expert (Figure 3).

Expert systems are appropriate when there are neither complete theories nor algorithms but mainly experiences, rules, or heuristics. In contrast to this conventional programs must have a fixed algorithm for treating any possible combination of input data otherwise the problem cannot be solved. In order to find a way around this situation it was a very important progress in expert system research when it was realized that a separation must take place between the knowledge about a problem and the way how to process this knowledge. The two components that emerge from this idea are called knowledge base and inference machine respectively (Figure 4).

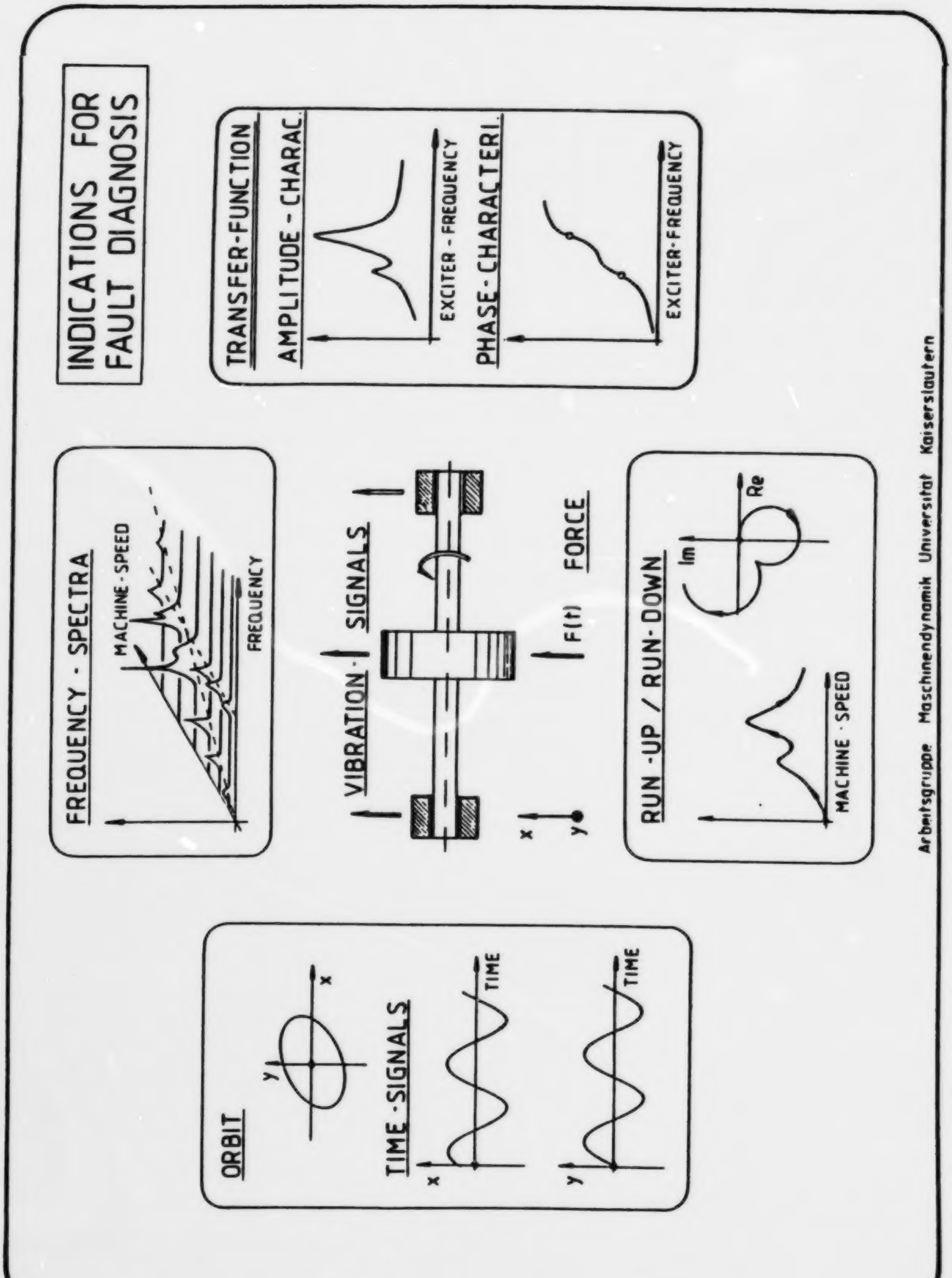
INDICATIONS FOR FAULT DIAGNOSIS
TRANSFER-FUNCTION
AMPLITUDE - CHARAC.
EXCITER - FREQUENCY
PHASE - CHARACTERI.
EXCITER - FREQUENCY
FREQUENCY · SPECTRA
MACHINE · SPEED
FREQUENCY
VIBRATION · SIGNALS
x
y
F(t)
FORCE
RUN-UP / RUN-DOWN
Im
Re
MACHINE · SPEED
ORBIT
y
x
TIME-SIGNALS
x
TIME
y
TIME
Arbeitsgruppe Maschinendynamik Universität Kaiserslautern

Figure 1: Indications for fault diagnosis

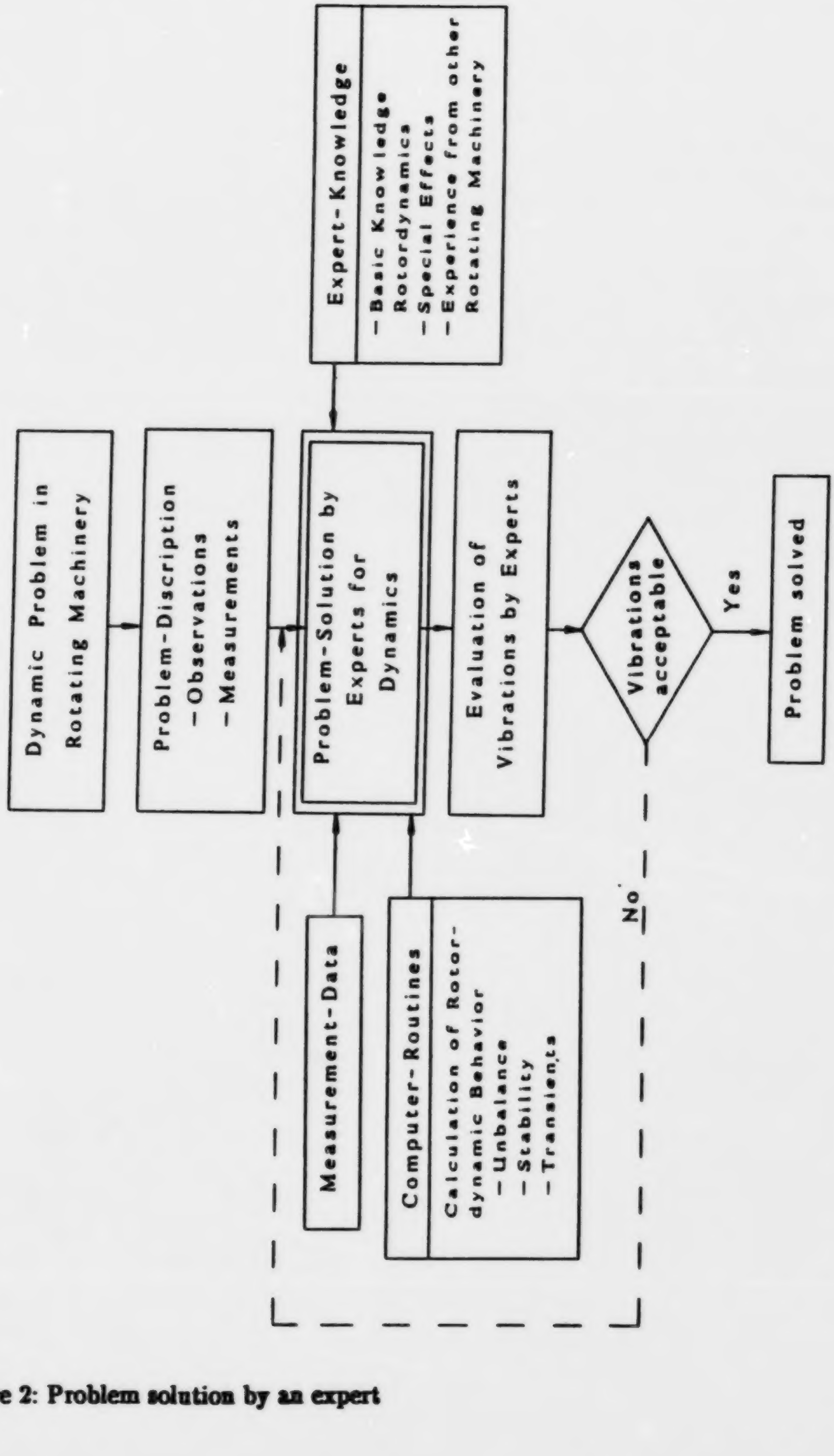
Dynamic Problem in Rotating Machinery
Problem-Discription
-Observations
-Measurements
Problem-Solution by Experts for Dynamics
Evaluation of Vibrations by Experts
Vibrations acceptable
Yes
Problem solved
No
Expert-Knowledge
- Basic Knowledge Rotordynamics
- Special Effects
- Experience from other Rotating Machinery
Measurement-Data
Computer-Routines
Calculation of Rotordynamic Behavior
- Unbalance
- Stability
- Transients

Figure 2: Problem solution by an expert

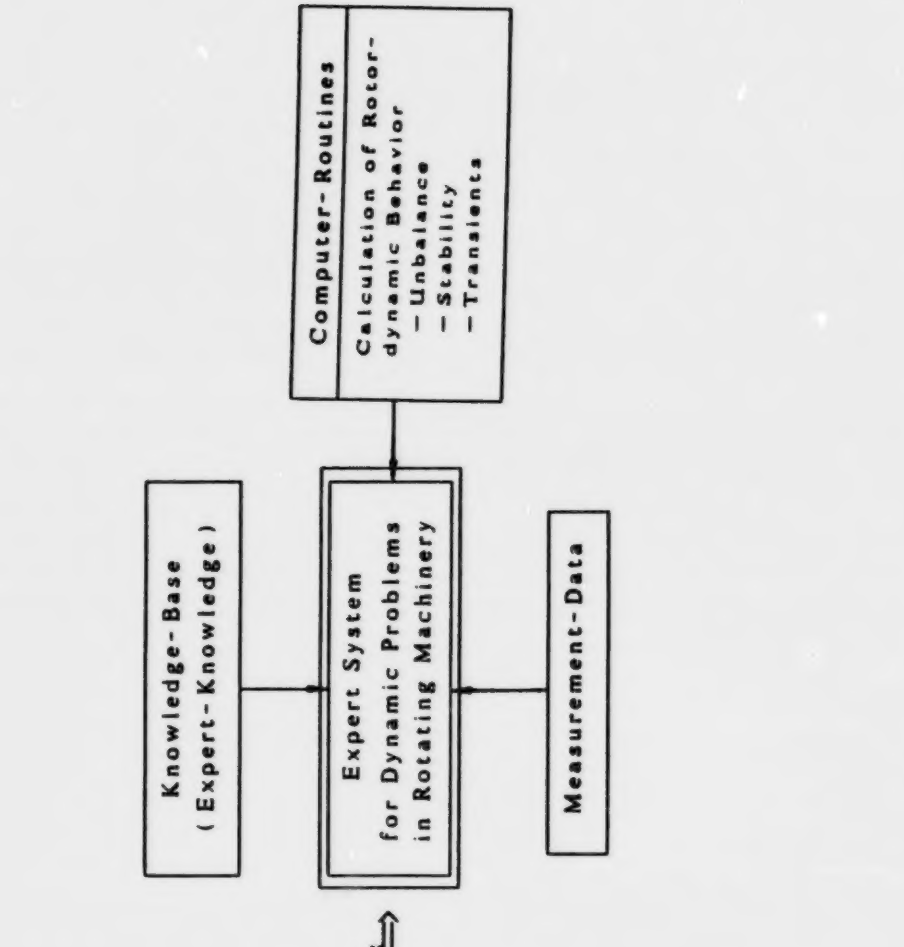
Dynamic Problem in Rotating Machinery
Problem-Discription
-Observations
-Measurements
Problem-Solution by Experts for Dynamics
Evaluation of Vibrations by Experts
Vibrations acceptable
Yes
No
Problem solved
Dialog
Knowledge-Base
(Expert-Knowledge)
Expert System
for Dynamic Problems
in Rotating Machinery
Measurement-Data
Computer-Routines
Calculation of Rotor-dynamic Behavior
— Unbalance
— Stability
— Transients

Figure 3: Problem solution by expert and expert system

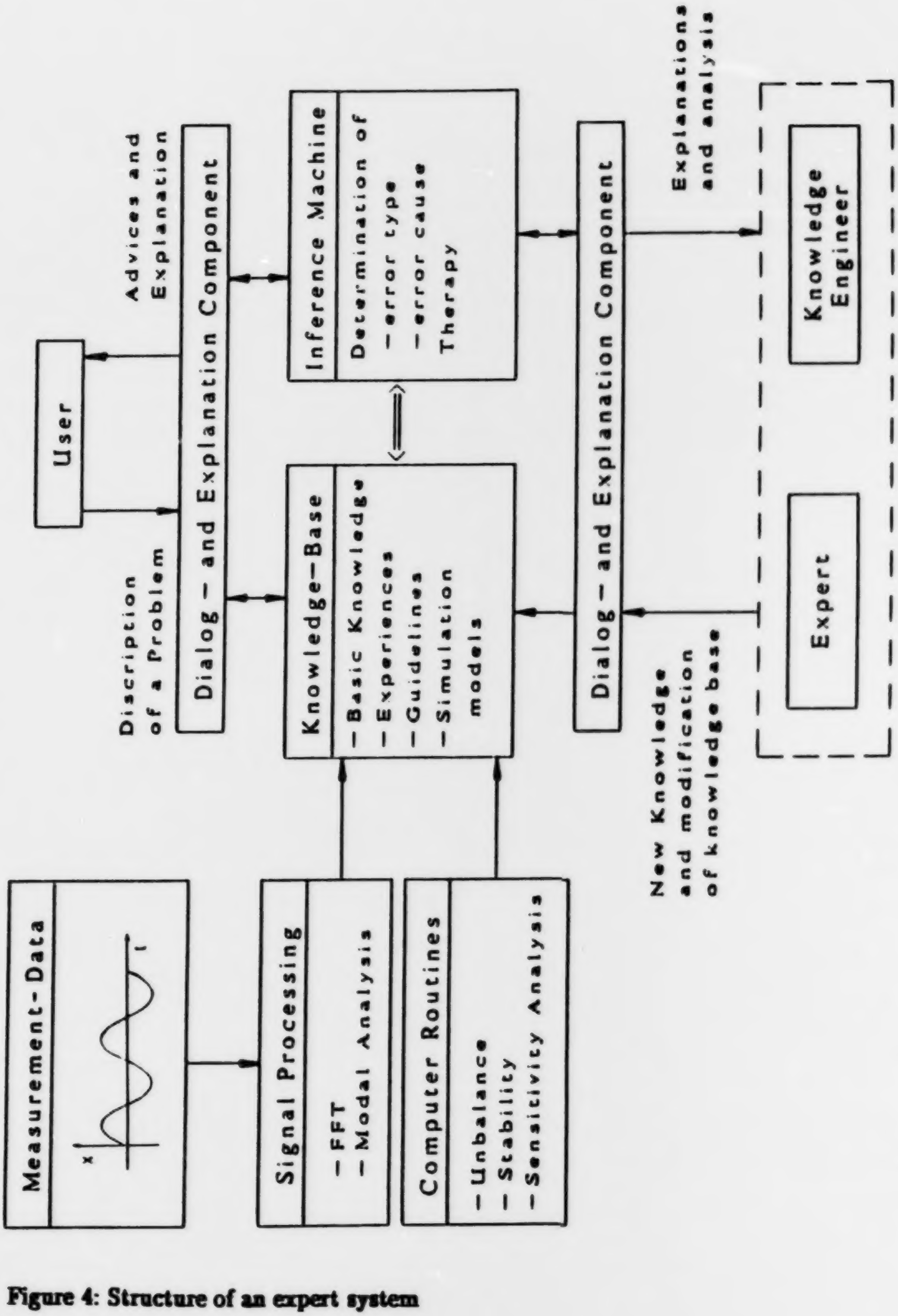
Measurement - Data
x
t
Signal Processing
– FFT
– Modal Analysis
Computer Routines
– Unbalance
– Stability
– Sensitivity Analysis
Discription of a Problem
User
Advices and Explanation
Dialog – and Explanation Component
Knowledge–Base
– Basic Knowledge
– Experiences
– Guidelines
– Simulation models
Inference Machine
Determination of
– error type
– error cause
Therapy
Dialog – and Explanation Component
New Knowledge and modification of knowledge base
Explanations and analysis
Expert
Knowledge Engineer

Figure 4: Structure of an expert system

The implications of this separation can be summarized as follows:

- Expert systems can be built with an empty knowledge base, then they are called tools (e.g. KEE, Babylon). If they are specialized on certain types of problems, like diagnosis, construction, planning, a.s.o., they are called shells (e.g. EMYCIN, KAS, MED2). In these cases the developer of an expert system can concentrate on the gathering and representation of the problem oriented knowledge and does not have to bother about dialog or explanation components. On the other hand he is restricted to the built–in features of the tool or shell.

- It seems reasonable that a knowledge base which is not mixed with specific knowledge about program processing is easier to modify or extend. The knowledge was made explicit and is accessible through a dialog component. That gives an advantage over "compiled" knowledge in conventional programs. Nevertheless, there are great differences between the various tools and shells on the market.

- Because of a humanlike representation of knowledge in the knowledge base, questions as "Why", "How", "What is" can be answered in a human like manner by displaying the pieces of knowledge that were used during the program run.

Figure 4 shows an expert system with its different components. In order to be able to use also conventional data processing programs, e.g. FFT or modal analysis, they are shown as addition to the knowledge base. In the diagnostic process it often will become necessary to use certain vibrational data out of measurements. Then these programs can be called by the knowledge base to calculate e.g. eigenvalues or amplitudes at specified frequencies and so on. These reduced data will be returned to the expert system for driving a diagnosis.

MED2: AN EXAMPLE FOR A RULE–BASED DIAGNOSTIC EXPERT SYSTEM SHELL

This chapter will introduce an expert system shell which uses rules for knowledge representation and is mainly intended for solving diagnostic problems. The shell's name is MED2, it is coded in Golden Common Lisp /5/ and is a development of the University of Kaiserslautern, Federal Republic of Germany /2,4/.

The diagnostic process can be described as the task to interpret given symptoms with regard to their cause. Symptoms can be observations, measurements, or experimental examinations. The cause behind the symptoms is called diagnosis and is obtained through the application of rules (Figure 5).

Symptoms and diagnoses in MED2

MED2 offers several types of objects like Questionsets, Manifestations (Symptoms), Pathoconcepts (Diagnoses), Derivatives (Therapies for Diagnoses), Rules, and some others. Figure 6 shows an example for a diagnosis.

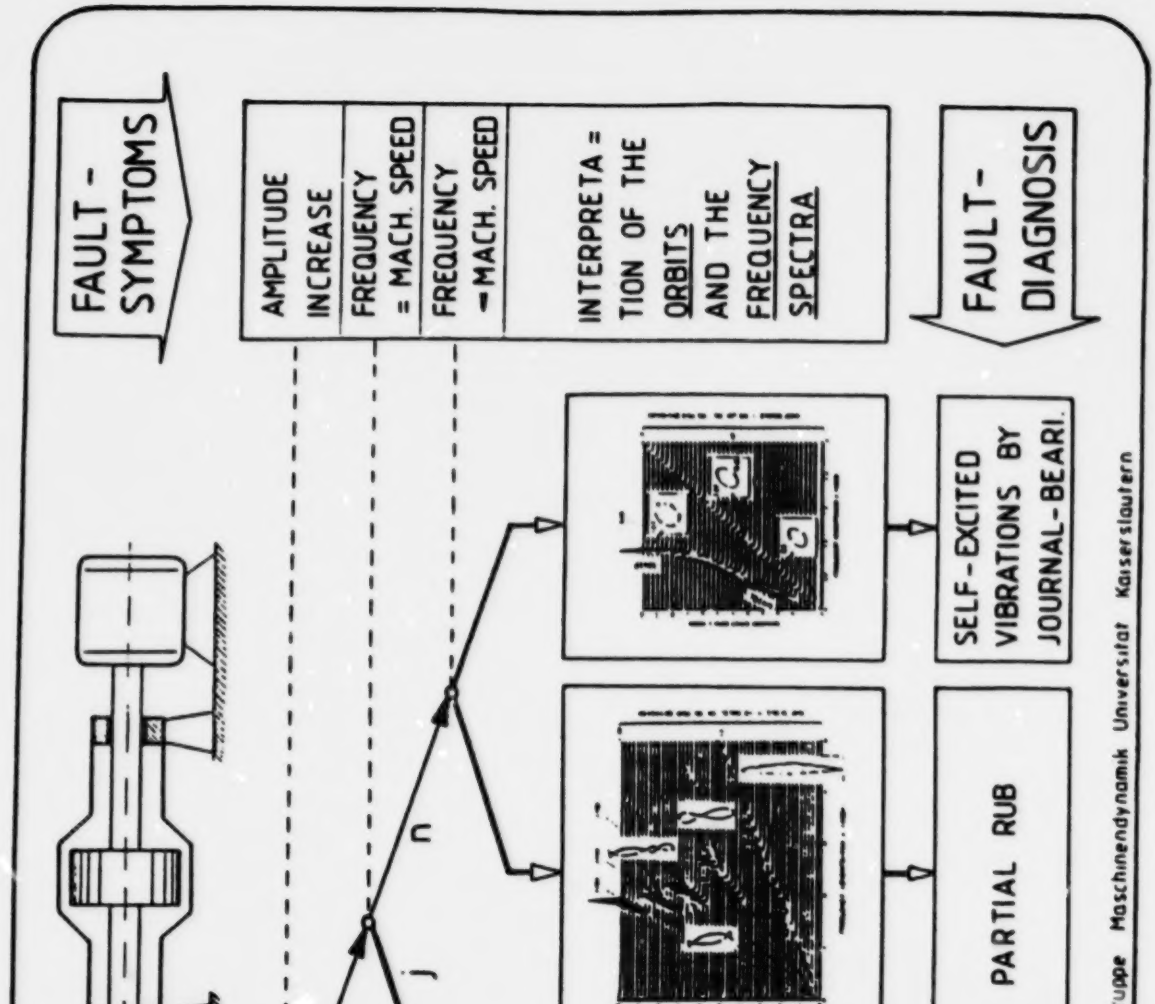
FAULT - SYMPTOMS
AMPLITUDE INCREASE
FREQUENCY = MACH. SPEED
FREQUENCY ≠ MACH. SPEED
INTERPRETA = TION OF THE ORBITS AND THE FREQUENCY SPECTRA
FAULT - DIAGNOSIS
n
j
j
n
MACHINE SPEED RPM
FREQUENCY CASCADE CPM
1X
GOOD CONDITION
UNBALANCE
PARTIAL RUB
SELF-EXCITED VIBRATIONS BY JOURNAL-BEARI.

Arbeitsgruppe Maschinendynamik Universitat Kaiserslautern

Figure 5: Fault matrix for rotordynamic problems

Diagnosis

NUMBER:	P xyz
NAME:	Oil–Whirl
TYPE:	Standard
CANDDIFFS:	Oil–Whip
CHILDREN:	Bearing–Whirl Seal–Whirl
APRIORI:	seldom
ATTENTION:	none
QSET:	–
POSSVARS:	–
DEFAULTVAR:	V xyz
COMMENT:	–

Figure 6: Representation of a diagnosis in MED2

The slots "NUMBER" and "NAME" are mandatory, the rest is optional.

- TYPE will be described in the chapter Inference Strategies.
- CANDDIFFS are diagnoses with similar symptoms as the displayed one and therefore can easily be confused with each other. MED2 offers special mechanisms to deal with those diagnoses (Differential–Diagnostic–Strategy).
- CHILDREN are more precise diagnoses which can be established using further knowledge. The idea is to build a hierarchy of diagnoses from general ones to individual ones.
- APRIORI describes the frequency of the diagnosis.
- QSET names additional questions that will be asked for, if the diagnosis has been established.
- DEFAULTVAR names the therapy that will be suggested by default.
- POSSVARS names additional therapies, one of which has to be selected, if DEFAULTVAR is not appropriate.

Rules

Using rules is the most commonly applied technique for representing knowledge in expert systems. They are most convenient to describe strategies or actions which have to be performed under certain conditions. The syntax is shown below:

Rule 1:

IF: Machine has sleeve bearing
AND vibration is 42 to 48 % of running frequency

THEN: suppose diagnosis is oil–whirl

The IF–part contains a set of "conditions" that have to be satisfied in order to fire the rule, that means to perform the "action" of the THEN–part. The last example showed that the action not necessarily has to be a "100 %–action". Here the diagnosis oil–whirl only could be stated with a certain probability which can be increased or decreased depending on other parameters of the machine. E.g. a heavy load on the bearings would decrease the oil–whirl likelihood.

There are numerous ways to express probability, e.g. with categories (positive, probable, possible ...), certainty factors, or points. In addition there are several theories /6,7,8/ how to combine single probabilities to an overall probability, but this is not part of this paper.

Rule 2:

IF: The machine is a pump
AND bearing type is unknown

THEN: assert bearing type is sleeve bearing

This rule manages incomplete knowledge by using default values if necessary facts are unknown. A rule in a diagnostic system then would connect observable or derived symptoms with a diagnosis (as shown in Rule 1).

Knowledge processing with rules

As an example on how the inference machine processes the contents of the knowledge base the mechanism of a rule–based expert system will be described below. Initially there is a set of known facts from the knowledge base or from a data base. The rules will be tested against these facts in the course of which there are two possibilities how this can happen.

Forward chaining

The facts can be used to test whether all conditions (if–parts) of a rule can be satisfied, in other words whether the rule can fire. The effect is that the action (then–part) of the rule establishes a new fact or alters an existing one, thereby affecting conditions of other rules. This technique is called forward chaining because of the "straight forward" process from already known facts to yet unknown final conclusions. Figure 7 shows a small example using the rules from the last chapter.

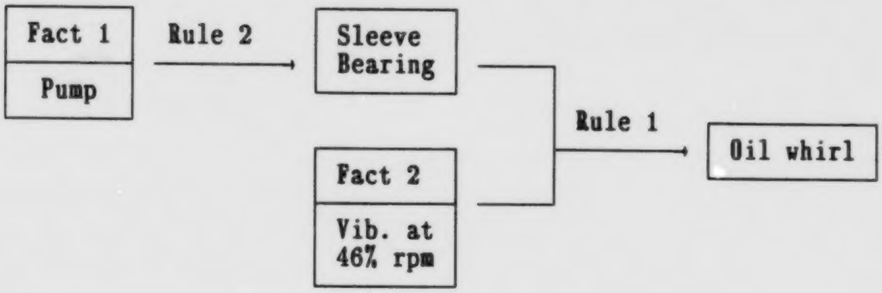

Figure 7: Forward chaining of rules

A major disadvantage in this approach is that, if there are many rules and facts to test against each other, the number of intermediate results can grow immensely, exceeding the computer's memory or the available time in which a solution has to be found.

Nevertheless, this mechanism is very useful e.g. in alarm conditions, i.e. if a newly derived fact requires immediate action, like stopping a machine or starting an emergency set.

Backward chaining

Suppose you had a goal which you wanted to examine using the rules in your knowledge base. Probably most of the facts that you know will lead to results which you are not interested in hence wasting lots of time, if you processed them in a forward chaining modulus.

Here it is more efficient to take the goal and look into all rules that have this goal in their conclusion (then–part) to see whether their conditions are satisfied. If so, the goal is established, if not, take the conditions as new sub–goals and proceed one step further "back". It becomes obvious, why this strategy is called backward chaining or goal driven knowledge processing. Figure 8 illustrates this with our little example:

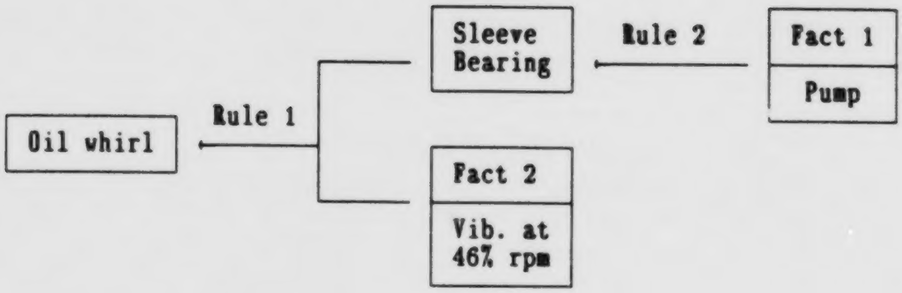

Figure 8: Backward chaining of rules

Oil–whirl is a suspected diagnosis, maybe because of an user input. Rule 2 could confirm this, Fact 2 is already known but the condition whether there are sleeve bearings in the machine is unknown. This could be confirmed by Rule 1, if its condition could be satisfied. That is the case, because Fact 1 is already known. Therefore the initial suspicion on oil–whirl can be confirmed.

The advantage over forward chaining is that only those rules are examined, that contribute to the interesting goal. Nevertheless, in large knowledge bases there might be a lot of "dead ends" where necessary facts to start the rule chain are missing maybe because of too little user input.

Many inference machines of commercial rule supporting expert systems are capable of combining both chaining mechanism to make use of the particular advantages.

Inference Strategies

The last chapter already introduced forward and backward chaining of rules. A skillful partition in forward– and backward–rules can effectively increase the system performance. A special mechanism in MED2 to further speed up the knowledge processing is the usage of "context diagnoses". An example will illustrate this: An oil–whirl will always occur at about 42 to 48 % of the running frequency of a rotor which has sleeve bearings. Suppose 10 % of the rules of a knowledge base would only support the oil–whirl probability. There might be symptoms like amplitude, location, and direction of vibration, but also operation conditions like load or temperature of bearings and so on which contribute to the oil–whirl probability. Now, if the only vibration signal were at running frequency, oil–whirl could not be the cause, so there would not be any need to take those rules into account. The same is true if there were neither seals nor sleeve bearings in the system.

To enable the expert system not to examine those rules it is possible to establish a diagnosis which is of the "context" type. In our example, a context–diagnosis "oil–whirl possibility" could be established if the vibration signal were at 42 to 48 % of running frequency and if the rotor had sleeve bearings. However, the system would not display this diagnosis, because there is not yet enough evidence. But now all rules concerning oil–whirl would be enabled to be matched against the symptoms, whereas rules e.g. for unbalance and other causes would not be examined. Figure 9 shows the syntax of a context sensitive rule in natural language for clarification

RULE xys:

NUMBER: R xyz
CONTEXT: Oil–whirl–possibility
CONDITION: Vibration is located in shaft or bearing
AND direction is radial
ACTION: confirm diagnosis "oil–whirl"

Figure 9: Example of a context sensitive rule in MED2

Of course, it would be possible to write the above shown "pre–conditions" into the condition parts of every affected rule, but that would not only blow up the knowledge base unnecessarily but also decrease the evaluation speed to a great extend. That is, because it is much faster for the inference machine to examine whether one context diagnosis is established than to examine whether one additional condition is satisfied. By the way, already three additional conditions would have to be examined in our example: Vibration–frequency, bearing–type, and seal–existence.

Explanation component

It was already stated, that an explanation from the expert system about its reasoning can be obtained from the knowledge it is reasoning about. Questions on "How did the system come to this conclusion" or "Why did it ask this question" can be answered particularly easy in rule–based systems. Here the chain of rules from the initial facts to the final conclusions can serve as an explanation. In addition, if it is possible to display them in a natural language like manner, they can also be understood by non–specialists of expert systems.

TUMAD: AN EXAMPLE FOR A TURBOMACHINERY DIAGNOSTIC EXPERT SYSTEM

Description of TUMAD

MED2 was used to build a knowledge base for diagnostic problems in rotating machinery, especially in turbomachinery. As a start, the well known diagnostic charts from Sohre /3/ were chosen as the knowledge source.

These charts connect 11 problem types and additionally 31 individual diagnoses with about 80 symptoms ranging from "Vibration Analysis" over "Operational Conditions" to "Installation". Figure 10 shows the first of these charts as an example. Numbers in the chart were found by statistical evaluation of numerous case histories and indicate percentages of cases showing above symptoms for causes listed in vertical column at left.

TUMAD, an expert system for TUrboMAchinery–Diagnosis, contains the contents of such charts in its knowledge base. The connection between symptoms and diagnoses by now has grown to over 2500 rules from which about 300 to 400 rules will fire in a typical diagnostic session. At present the knowledge base is in a redesign phase. This redesign will more strongly take into account the possibilities of context–diagnoses, differential–diagnoses and the ability to switch between forward and backward chaining. The goal is to reduce the total number of rules to allow further "extensions" on knowledge about vibration and frequency analysis. Secondly, the number of fired rules shall be reduced to speed up the diagnostic process.

An Example

The following example concerns a large turbomachinery set which had encountered severe vibration problems. The symptoms were entered following the order of Sohre's charts. They will be shown together with the corresponding output from TUMAD.

As for the "vibration analysis" the input was:

Predominant frequency of the spectrum:
Oil–whirl–frequency (42–48 % of running frequency)

- No suspicion of electrical origin of vibrations.
- Direction of predominant amplitude: *vertical*
- Location of predominant amplitude: *shaft*
- There was no possibility to have vibration–tests at varying speeds.

Figure 11 shows a complete list of suspected diagnoses. Intentionally none could be established so far, because there are more symptoms that must be entered in order to satisfy the so called "necessary conditions". This strategy was used to prevent that diagnoses will be established too early and in spite of too little evidence.

These charts are reproduced with the permission of Turbomachinery International Publications, Division of Business Journals, Inc., 22 South Smith Street, Norwalk, Connecticut, U.S.A. 06855, and may not be reproduced without its prior written permission.

SYMPTOMS AND DISTRESS MANIFESTATIONS

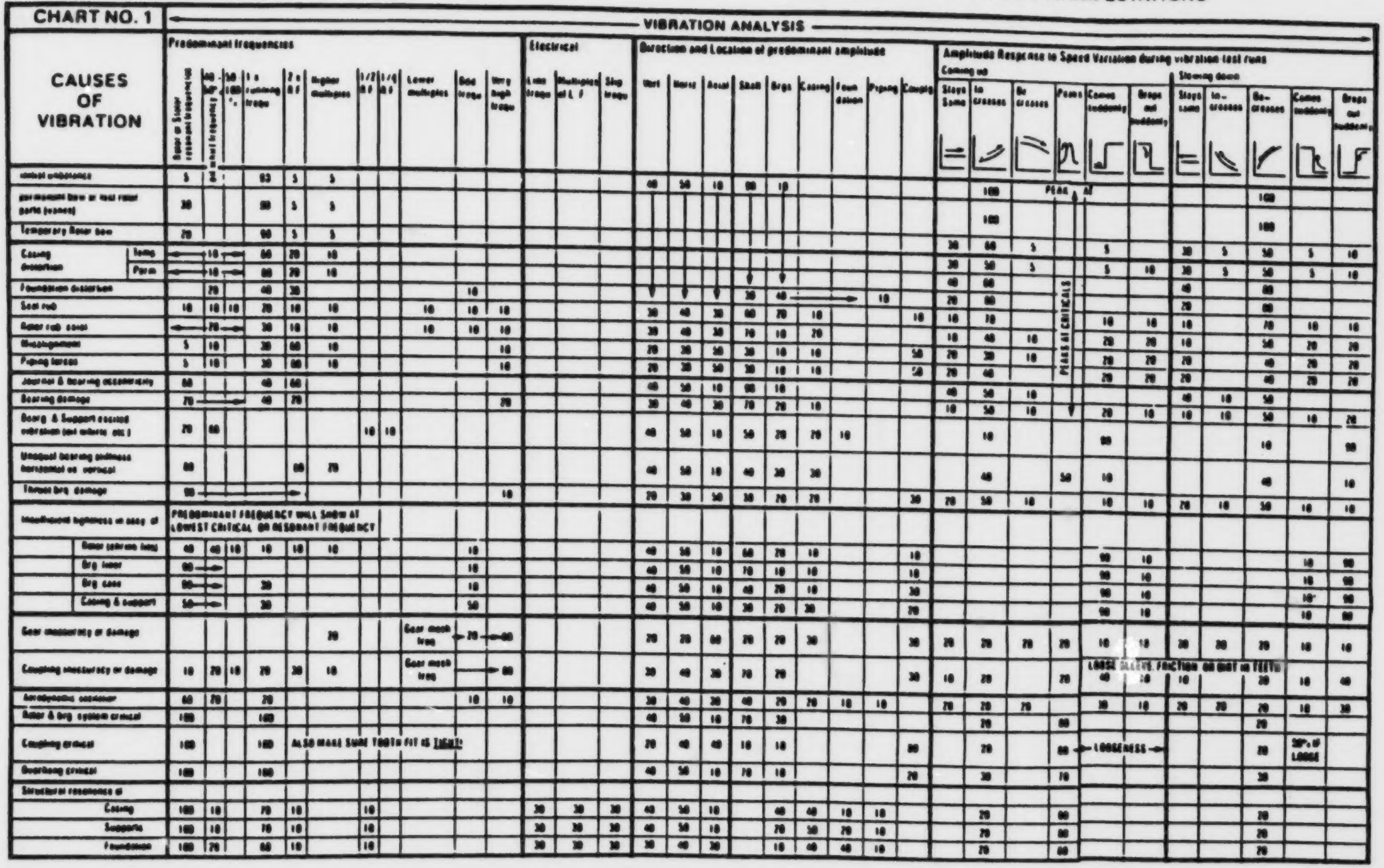
CHART NO. 1
VIBRATION ANALYSIS
CAUSES OF VIBRATION
Predominant frequencies
Electrical
Direction and Location of predominant amplitude
Amplitude Response to Speed Variation during vibration test runs
Coming up
Slowing down
PREDOMINANT FREQUENCY WILL SHOW AT LOWEST CRITICAL OR RESONANT FREQUENCY
PEAKS AT CRITICALS
LOOSENESS
ALSO MAKE SURE TOOTH FIT IS TIGHT!

Figure 10: Section of Sohre's chart No. 1

```
EXPLANATION—MODE OF MED2

suspected diagnoses and points (established beyond 41 points):

DRY_WHIRL                              10 points
RESONANT_VIBRATION                     10 points
CRITICAL_SPEED                         10 points
PIPING_FORCES                          10 points
CLEARANCE_INDUCED_VIBRATIONS           10 points
RESONANT_WHIRL                         10 points
OIL_WHIRL                              10 points
FRICTION_INDUCED_WHIRL                 10 points
VIBRATION_TRANSMISSION                 10 points
```

Figure 11: Suspected diagnoses after input of vibration analysis data

The "operational evidence" was entered as follows:

- Effect of operating conditions: *Vibration comes at full load*
- Effect of oil pressure and temperature variation: *Gets worse with decreasing temperature*
- Predominant radiated sound: *Unknown*
- History of machine: *Older than 10 years*
- Damage or distress signals: *Set out of alignment* and *Foundation settled or cracked.*

Figure 12 again shows the list of suspected diagnoses which could be reduced to a reasonable size.

```
EXPLANATION—MODE OF MED2

suspected diagnoses and points (established beyond 41 points):

FRICTION_INDUCED_WHIRL                 35 points
PIPING_FORCES                          25 points
DRY_WHIRL                              10 points
OIL_WHIRL                              10 points
PRESSURE_PULSATIONS                    10 points
```

Figure 12: Suspected diagnoses after input of operational evidence data

"Resonant Whirl" could be **established** and therefore is not in this list anymore. MED2 displays it in a separate window for **established** diagnoses to distinguish it from the merely **suspected** ones which have the lesser evidence.

The number of points can be interpreted as: possible (10 points), probable (25 and 35 points), and very probable (above 40 points). "Resonant Whirl" had been established with 55 points.

Further informations were entered about the foundation which had "loose sole plates" and was "shrunk". This did not alter very much, except for some weakly suspected diagnoses which were taken out of the working memory.

The result of the reasoning process is "Resonant Whirl" with a "very high probability". This diagnosis was correct, because the foundation of the turbomachinery set had a local resonant frequency which was excited by an oil–whirl vibration.

Extension of the Knowledge Base by Conventional Programs

Knowledge bases built upon diagnostic literature like the Sohre charts are quite general in nature. The relationships between symptoms and diagnoses shall cover a wide range of rotating machinery thereby being unspecific for special types of machines. To overcome this specific knowledge has to be entered which normally comes from human experts. However, the knowledge base still contains mainly "verbal" knowledge. As a result the expert system needs lots of keyboard input to describe the problem that shall be diagnosed.

Two extensions can provide more machine specific knowledge and a more automatic procedure for the diagnostic process. The first one is the incorporation of a data acquisition and condition monitoring system into the expert system. At present this is under development as an extension to TUMAD. Making use of a conventional program for data acquisition and reduction it will not be necessary anymore to enter vibrational date over keyboard. This reduces the amount of keyboard input as well as possible misunderstandings because of misinterpreted given answers to questions about the vibrational behavior.

Another extension is the simulation of the rotordynamic behavior by Finite Element Programs. Provided that machinery data are available a model can be built and calculations can be carried out with respect to eigenvalues, instabilities, unbalance responses, and so on. Figure 13 shows as an example the unbalance vibration amplitudes versus rotational speed of a boiler feed pump /9/. Normally there are several possibilities for the reason behind an observable behavior. E.g. an increasing amplitude of the vibration at running frequency could be caused by

- unbalance,
- thermal rotor bow because of temperature variations,
- a shift of an eigenfrequency letting the machine run into a resonance,
- a decrease of damping,
- a crack, and so on.

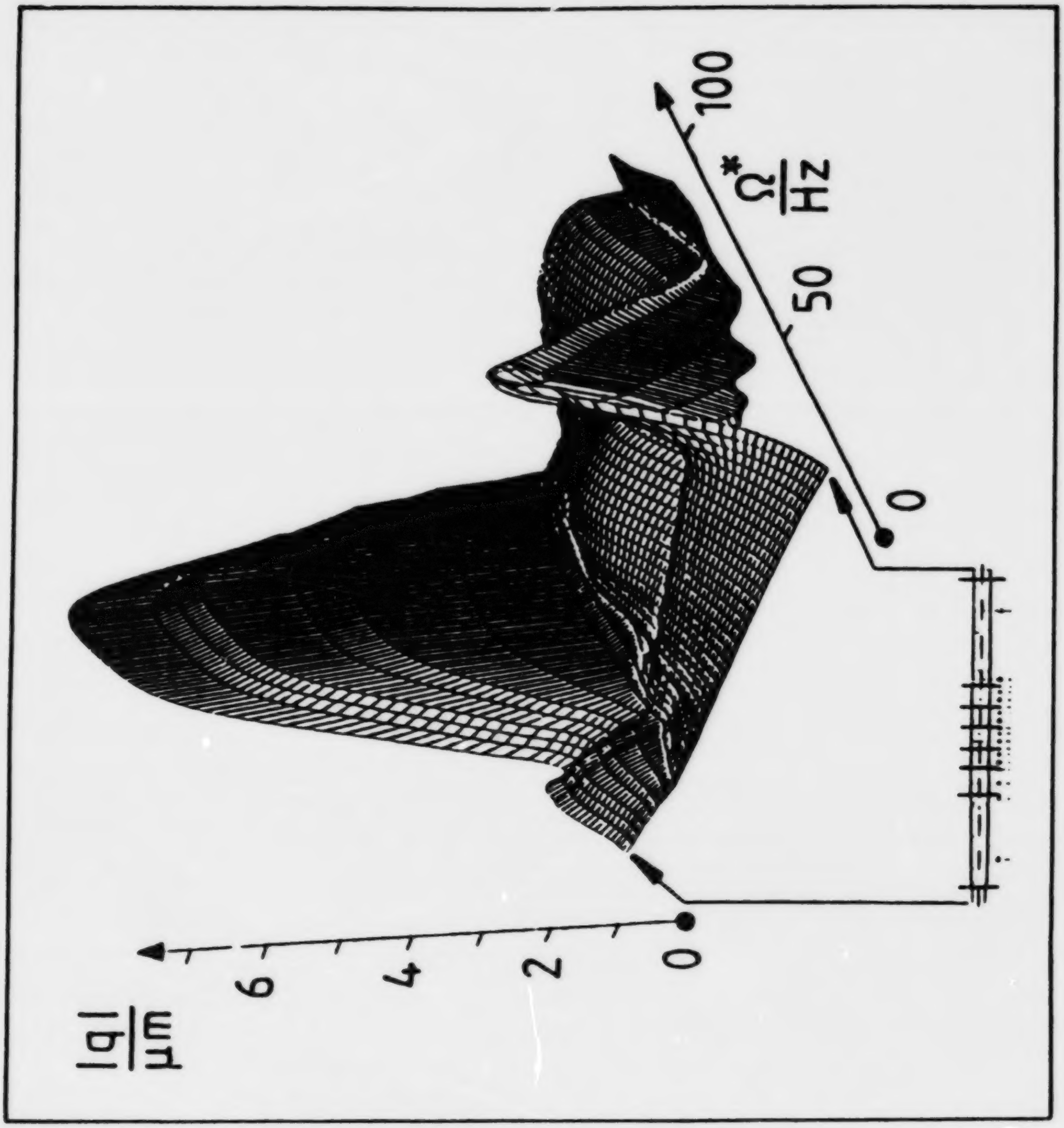

Figure 13: Unbalance vibration amplitudes versus rotational speed

With the help of rotordynamic calculations some conceivable causes will be excluded because the machinery or operating conditions speak against it. Although this procedure is standard in diagnosing rotordynamic problems by experts there are rare cases of combining such programs into expert systems /10/. The reason for this may be twofold:

- The expert system must be capable of interacting with a conventional program.
- The Finite Element Program must have reasonable runtime limits and yet take into account all relevant rotordynamic mechanisms otherwise important machinery responses will be neglected.

In his doctor's thesis Diewald describes a rotordynamic program, called TURBO /9/, that meets the above mentioned restrictions. However, so far there is no connection to an expert system. White /10/ shows good promise in connecting a rotordynamic simulation program to a knowledge based system for fault diagnosis in turbomachinery.

CONCLUSION

TUMAD is a diagnostic expert system for rotordynamic problems of turbomachinery. It runs on an IBM–AT or compatible and was developed with the diagnostic expert system shell MED2 /2,4/ which is implemented in Golden Common Lisp /5/. The knowledge base is built upon the Sohre charts /3/ which contain a statistical evaluation of turbomachinery problems. Several sets of test data, simulated ones as well as data from actual problems, could be diagnosed successfully so far.

In the future specific knowledge on vibration and frequency analysis will be added. The extension of connecting MED2 to a data acquisition and reduction system is under development. Further work has to be done to incorporate rotordynamic simulation programs which will assist the diagnostic process. Evaluation and testing of the knowledge base will be performed on the basis of available data from condition monitoring systems.

REFERENCES

/1/ Waterman, D.A.: A Guide to Expert Systems.
Addison–Wesley, 1986.

/2/ Puppe, Frank: Expertensysteme.
Informatik–Spektrum, 1986, Vol. 9, pp. 1–13.

/3/ Shore, J.S.: Turbomachinery Problems and their Correction.
Sawyer's Turbomachinery Maintenance Handbook, Vol. 2, Chapter 7, 1. Edition, Connecticut, USA, 1980.

/4/ Puppe, Frank: Diagnostisches Problemlösen mit Expertensystemen.
Informatik Fachberichte 148, Springer, Germany, 1987

/5/ Golden Common Lisp 286 Developer, Version 2.2
Gold Hill Computers, Cambridge, Massachusetts

/6/ Zadeh, L.A.: Role of Fuzzy Logic in Management of Uncertainty in Expert Systems.
Fuzzy Set and Systems, 1983

/7/ Gordon, J.; Shortliffe, E.: A Method for Managing Evidential Reasoning in a Hierarchical Hypothesis Space. AI–Journal 26, 323–357, 1985

/8/ Duda; Hart; Nilson : Subjective Bayesian Methods in Rule Based Systems.
Technical Note 124, SRI, 1984

/9/ Diewald, W.: Das Biegeschwingungsverhalten von Kreiselpumpen unter Berücksichtigung der Koppelwirkungen mit dem Fluid.
Fortschrittberichte VDI, Reihe 11, Nr. 121, 1989

/10/ White, M.F.; Steinebach, C.; Langas, P.M.: Vibex (Part 2): The Use of Rotordynamic Simulation as an Aid for Fault Diagnosis in Turbomachinery.
J.M. Montalvao e Silva and F.A. Pina da Silva (eds.), Vibration and Wear in High Speed Rotating Machinery, 773–781, Kluwer Academic Publishers, Netherlands, 1990

VARMINT
AN EXPERT SYSTEM FOR MACHINE MONITORING

Robert S. Reilly
Christopher A. MacPhail
Design Maintenance Systems Inc.
N. Vancouver, British Columbia
Canada V7M 3G8

ABSTRACT

A major part of the current generation of expert systems for maintenance is the process of consultation. In a consultative type expert system, the user supplies the facts needed by the knowledge base through a "question and answer" process. The information supplied by the user to the expert system leads the expert system to ask further questions, narrowing down the possible solutions to the maintenance problem. The results produced by this type of system can be insightful and valuable. However, the often lenghty consultation sessions can lead to, at best, a sporadic application of the expert system technology or, at worst a rejection of the technology entirely.

This paper describes the theoretical basis and practical implementation of a non-consultative expert system for the evaluation of the condition of rotating machinery. The goal of the **VARMINT** project ("Vibration Analysis for Rotating Machinery **INT**ernals") is to produce a system that will automatically perform sophisticated data analysis on vibration spectra and feed the results of the analysis to an inference engine. Most importantly, the operation of the system is to require little or no ingestion of information from the user. The user will query **VARMINT**, rather than **VARMINT** asking questions of the user.

BIOGRAPHIES

Robert S. Reilly is one of the founding partners of Design Maintenance Systems Inc. He possesses a bachelor's degree in Commerce from the University of British Columbia. He has developed several software products including a comprehensive oil analysis system and an innovative inventory management system.

Christopher A. MacPhail is a software engineer with Design Maintenance Systems Inc. He possesses a bachelor's degree in Computer Science and a technologist's diploma in Electrical Engineering. Over the last few years he has been involved in the software and hardware development of products ranging from fuel control systems to expert systems in vibration.

VARMINT
UN SYSTÈME EXPERT POUR LA SURVEILLANCE DES MACHINES

RÉSUMÉ

L'un des composants les plus importants de la présente génération des systèmes experts de maintenance est le procédé de consultation. Dans un système expert de type consultatif, c'est l'utilisateur qui fournit, par un procédé de questions et réponses, les informations requises par la base des données. Cette collecte de renseignements amène le système à poser d'autres questions, réduisant à chaque fois le nombre des solutions possibles aux problèmes d'entretien. Les résultats obtenus par ce genre de système peuvent être significatifs et précieux. Cependant, les sessions de consultations souvent longues peuvent aboutir, au mieux, à ce que la technologie soit appliquée de façon sporadique, ou, au pire, à ce qu'elle soit rejetée totalement.

Ce document décrit la base théorique et la mise en oeuvre pratique d'un système expert non consultatif pour évaluer l'état des machines rotatives. L'objectif du projet VARMINT (abbr. de "Vibration Analysis for Rotating Machinery INTernals) est de mettre au point un système qui pourra effectuer automatiquement l'analyse poussée des données sur les spectres de vibrations et introduire les résultats de ses analyses dans une machine à déduire. Objectif plus important encore, le système ne doit exiger aucune ou que très peu d'intervention de la part de l'utilisateur pour fonctionner. Celui-ci interrogera VARMINT, au lieu d'avoir à répondre aux questions de VARMINT.

BIOGRAPHIES

Robert S. Reilly est l'un des associés et fondateurs de Design Maintenance Systems Inc. Diplômé en commerce de la University of British Columbia, il a élaboré plusieurs logiciels dont un système complet d'analyse de l'huile et un système innovateur de gestion des stocks.

Christopher A. MacPhail est ingénieur en logiciels chez Design Maintenance Systems Inc. Il possède un baccalauréat en informatique et un diplôme de technicien en électrotechnique. Depuis quelques années, il participe à la mise au point de produits logiciels et matériels, allant des systèmes de commande de carburant aux systèmes experts d'étude des vibrations.

INTRODUCTION

One of the functions of the Fleet Systems Directorate of the Canadian Coast Guard (CCG) is to improve the quality of predictive maintenance tools available to fleet marine engineers. To this end, CCG has been equipping vessels with portable FFT spectrum analyzers and data collectors . The data collected by these units must be assessed by maintenance staff, who then determine machine health and formulate maintenance decisions.

As experienced personnel are not always available to interpret vibration data on all vessels, an intelligent tool is required to advise maintenance personnel and recommend action. Time-consuming consultative expert systems were considered inappropriate due to the operating constraints that apply to maintenance personnel when a CCG vessel is in operation. The envisioned tool was a PC-based expert system that could accept vibration spectral signatures and trend data, to provide recommendations concerning preventative maintenance scheduling, fault diagnostics and quality assurance.

The VARMINT project was initiated in June 1989. The stated objective of the project was to design a prototype expert system to analyze vibration signatures from shipboard rotating machines and provide recommendations on maintenance procedures [1]. The project was sponsored by the Fleet Systems Directorate of the Canadian Coast Guard and the Transport Development Centre. The contract was awarded to Design Maintenance Systems Inc. of North Vancouver, B.C., with a knowledge acquisition subcontract to MacDonald, Dettwiler Ltd. of Richmond, B.C.

THE VARMINT PROJECT

The scope of the VARMINT project covered the following areas:

1) Ship Selection
2) Shipboard Audit

3) Requirements Specifications
4) Platform Choice
5) Knowledge Acquisition
6) Software Design

1.) Ship Selection:
The first activity of the project was the choice of a vessel for on-going testing of the prototype. The vessel chosen was the CCGS Sir William Alexander. The Alexander is a Lloyds classification +100A1, a "Navaids Tender/Light Icebreaker". It was determined that the prototype would be installed on this ship for extensive testing upon completion of the programming and acceptance testing.

2.) Shipboard Audit:
An audit of all rotating machinery aboard the CCGS Sir William Alexander produced an extensive list of rotating machinery that needed to be covered, including:

a) Vertical pumps
b) Horizontal pumps
c) Hydraulic pumps
d) Compressors
e) Purifiers
f) Electric Motors
g) Winches
h) Fans
i) Turbochargers

The machine audit was carried out over the first six months of the project, and produced a comprehensive set of specifications [2].

a) Machine Technical Specifications
b) Machine Component Specifications
c) Vibration Parameters and Alarm Levels
d) Machine Component Defect Frequencies

3.) Requirements Specifications
The major criteria for the expert system software were laid out in the requirements specification phase of the project.

a.) Utilize the current data acquisition platform:

The Sir William Alexander already possessed an IRD 890 type data collector and an IRD 7090 data acquisition software. The VARMINT system makes use of this hardware and software, rather that replacing it with another method of collecting/storing vibration signatures. (See figure 1).

b.) Utilize readily available hardware:

The use of a PC based technology was deemed necessary. This enables the data acquisition software and the expert system to reside on the same platform. It also reduces the cost of moving the expert system to other ships in the fleet.

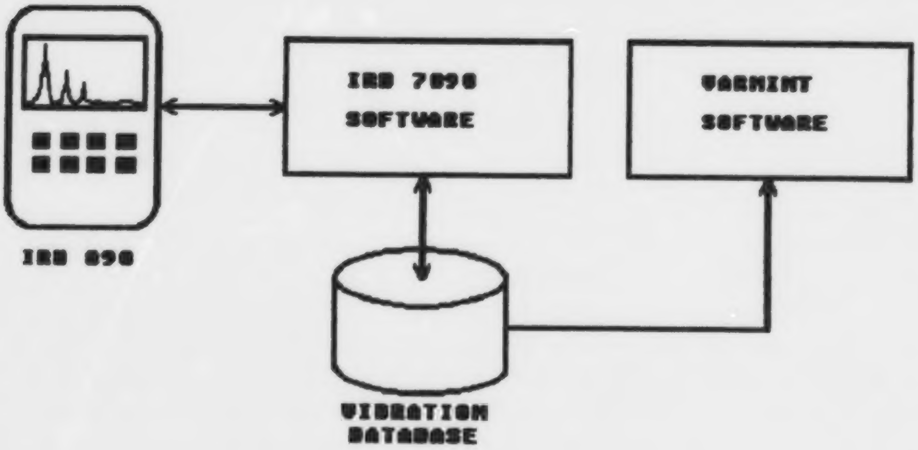

Figure 1 - VARMINT uses current database.

c.) Utilize all available analysis techniques:

The data analysis module of the VARMINT system is modelled after the types of analysis performed by human vibration experts. VARMINT acquires pertinent data not just from the current spectrum and overall vibration level, but by analyzing spectral components across the full set of available spectral history.

d.) User friendly interface:

VARMINT is designed to be used by shipboard marine engineers who possess varying levels of familiarity with both vibration analysis and computer systems. VARMINT is written with a complete windows type interface. All functions are available by operating a two-button mouse. The system has a complete machine modelling capability that develops graphic schematics of all machine trains on the system.

e.) Easily maintainable:

It is necessary that an engineer aboard ship should be able to alter the information that VARMINT maintains on the machines that are being analyzed. This will allow fine tuning of the system without programmer intervention. This will also allow the system to be moved to another ship with minimal programmer intervention. The VARMINT DATABASE module (VDBASE) allows the user to set a wide variety of trigger levels for each machine.

f.) Loggable results:

As the CCG vessel upon which VARMINT is based may be at sea for extended periods of time, it is important for the further development of the system that the maintenance personnel be encouraged to log the results of the VARMINT inferencing sessions and compare them with actual events. To this end, the system has a "tracking" subsection to allow users to log case histories and enter maintenance notes. The knowledge base and inference engine of the system have a full Explain and Justify feature to allow the user to inquire as to the reasoning used by the system to reach its conclusion.

The end result of the requirements analysis phase of the project was the Software Requirements Specification [3]. This report was used to set up the knowledge acquisition sessions and as the functional specification for software design and implementation.

4.) Platform Choice:
The Platform Choice was driven by the Software Requirements Specification and the first stages of the software design. The initial implementation decisions were as follows:

a) Hardware Platform:
The hardware platform chosen was an 80386 running at 20 MHz with a math coprocessor.
Hard Disk: A 135 MB ESDI type.
Display: VGA display with 16-bit VGA graphics card.

This configuration was deemed to be optimal both for development and operation of the expert system. The manufacturer selected was Olivetti.

b) Software Platform:
The software platform chosen was Microsoft Windows. The development languages chosen were Microsoft C and Actor (Whitewater Group). Actor, an object-oriented development language, was chosen for its ease of use. However, early in the implementation process it was determined that Actor was incompatible with our inference engine (see below). Also, the speed of the Actor code was unacceptable. The development team continued with C and the Microsoft Windows Software Development Kit. This combination proved to be both flexible and efficient.

c) Inference Engine:
The inference engine chosen was Nexpert by Neuron Data Ltd. This product has both an interactive development system which runs under Windows, and a protected mode runtime server which can be called by a host program. The VARMINT system delivered to the ship uses the runtime server.

The VARMINT system was implemented by Design Maintenance Systems Inc. from December 1989 to June 1990. The details of the platform choice are documented in the Platform Acquisition Document [4].

5.) Knowledge Acquisition:

The next two phases of the project, the Software Design and the Knowledge Acquisition were carried out in tandem. Knowledge acquisition was carried out on both a formal and informal basis. The knowledge engineer for the project interviewed a number of engineers aboard various Coast Guard vessels on both vibration analysis techniques and general shipboard maintenance practices. The formal knowledge acquisition involved several intensive interview sessions with the following experts:

a.) John Mitchell, President, Palomar Technologies International - a graduate of the Naval Academy at Annapolis and a recognized expert in the field of marine vibration analysis.

b.) Paul Y. Kim, Research Officer, National Research Council - an expert in tribology and the theoretical aspects of vibration analysis.

c.) Juris Buss, Marine Engineer, Design Maintenance Systems Inc. - a marine engineer with more than ten years experience in marine condition monitoring methods.

The knowledge acquisition sessions covered a wide variety of areas, including:

a) imbalance
b) misalignment
c) rolling element bearing wear
d) journal bearing wear
e) mechanical looseness
f) effects of cavitation
g) structural vibration
h) electric motor defects
i) resonant frequency effects
j) gearbox faults

The end result of the knowledge acquisition sessions was a Vibration Analysis Knowledge Acquisition document [5]. The information found in this document was further refined into the rules contained in the VARMINT knowledge bases.

6.) Software Design:

Two phases of the project, the Software Design and the Knowledge Acquisition were carried out in tandem. During the software design phase, Design Maintenance Systems Inc. software engineers specified system components down to the module level, detailing each modules function and interfaces with other modules. During the implementation phase, the modules were coded and tested to ensure they met their functional specifications. The high level modules defined in the Software Design Document [6] were:

a.) Machine Selection and Data Analysis -

User selects the machine to be analyzed. The system transforms overall readings, spike energy readings and spectra into "facts" to be input into the inference engine.

b.) Symptoms Analysis -

Facts input into the inference engine are examined and fault symptoms are generated. Fault symptoms look for changes in the overall readings or spectra that could indicate a change in machine state.

c.) Diagnosis Analysis -

Symptoms input into the inference engine are examined and fault diagnoses are generated. Diagnoses are the types of faults indicated by the symptom, ie imbalance, misalignment etc.

d.) Actions Analysis -

Diagnoses input into the inference engine are examined and recommended actions are generated. Actions are user tasks to rectify problems indicated by the Diagnosis Analysis.

e.) Explain/Justify -
Explanations and justifications for system outputs can be requested by the user. An explanation is a detailed description of a symptom, diagnosis or a recommended action. A justification lists the rules that were fired to produce the symptom, diagnosis or action.

g.) Logging Results -
The system has a "tracking" subsection to allow users to log case histories and enter maintenance notes. This module allows the user to record the results of a machine analysis for future perusal. Also, the user can enter free form text about the machine.

h.) Machine Modelling -
The user "models" the machine train to allow the system to analyze the machine automatically without user intervention during the inference. The model should be displayed graphically as a schematic.

The Software Design Document [6] was used as the main development document for the production of VARMINT code modules, just as the Knowledge Acquisition Document was used to produce rules.

THE VARMINT SYSTEM

VARMINT is a PC based expert system which determines machine condition by analyzing the vibration signals collected from that machine. The system utilizes the Microsoft Windows interface to create a user friendly, mouse driven environment. Some of the features of VARMINT are :

1) Individual and Batch Machine Analysis

2) Machine Modelling
3) Symptoms Produced by Statistical and Curve Fit Analysis on Data
4) Rule-Based Diagnosis of Problems
5) Rule-Based Recommended Actions
6) Full EXPLAIN and JUSTIFY of Symptoms, Diagnoses, and Actions
7) Graphic Machine Schematics

The VARMINT system runs under both Windows 2.1 and Windows 3.0. The system makes extensive use of the benefits of the Windows environment, such as

1) Integrated Graphics
2) MultiTasking Capability
3) Dynamic Data Exchange between programs
4) Resizable Windows and Icons

When the user first initiates VARMINT, he is presented with the main menu and introduction screen.

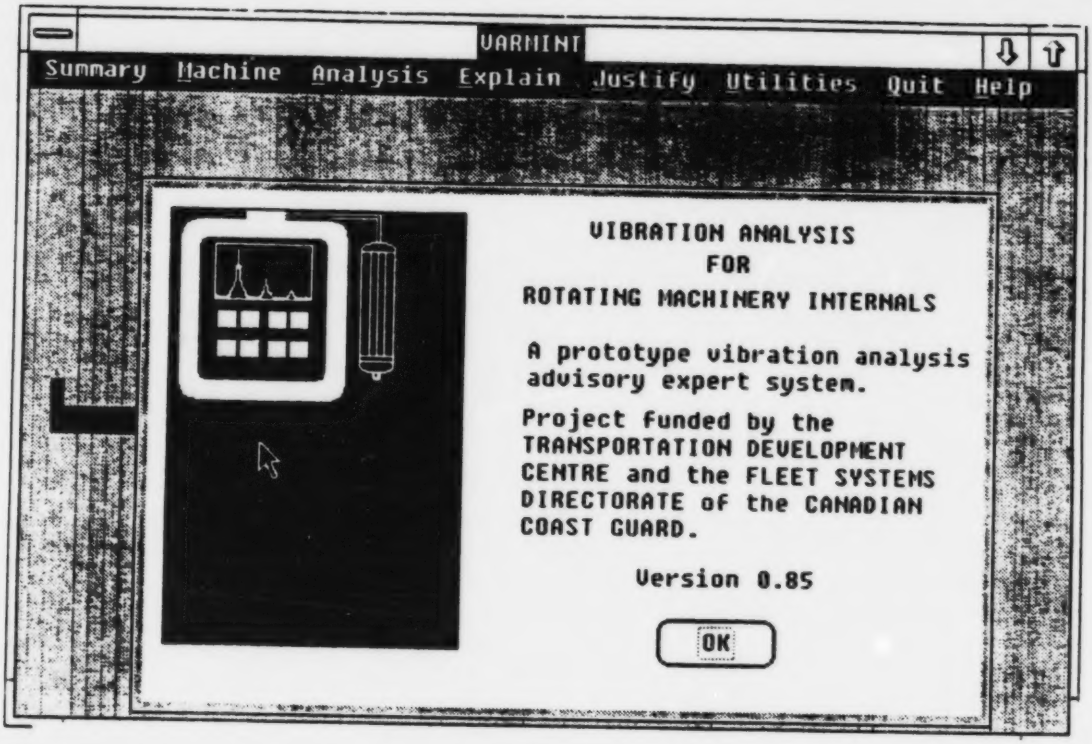
VARMINT
Summary Machine Analysis Explain Justify Utilities Quit Help
OK

VIBRATION ANALYSIS
FOR
ROTATING MACHINERY INTERNALS

A prototype vibration analysis advisory expert system.

Project funded by the TRANSPORTATION DEVELOPMENT CENTRE and the FLEET SYSTEMS DIRECTORATE of the CANADIAN COAST GUARD.

Version 0.85

VARMINT.1 - Opening Screen

1.) Individual Machine Analysis
Select a machine from the database of available machines. This database is set up using the VARMINT DATABASE system (VDBASE). The user selects a single machine for analysis .

VARMINT allows the user to select multiple machines for batch analysis and reporting. The user can also "pre-select" these machines and place them into a route for repeated batch processing.

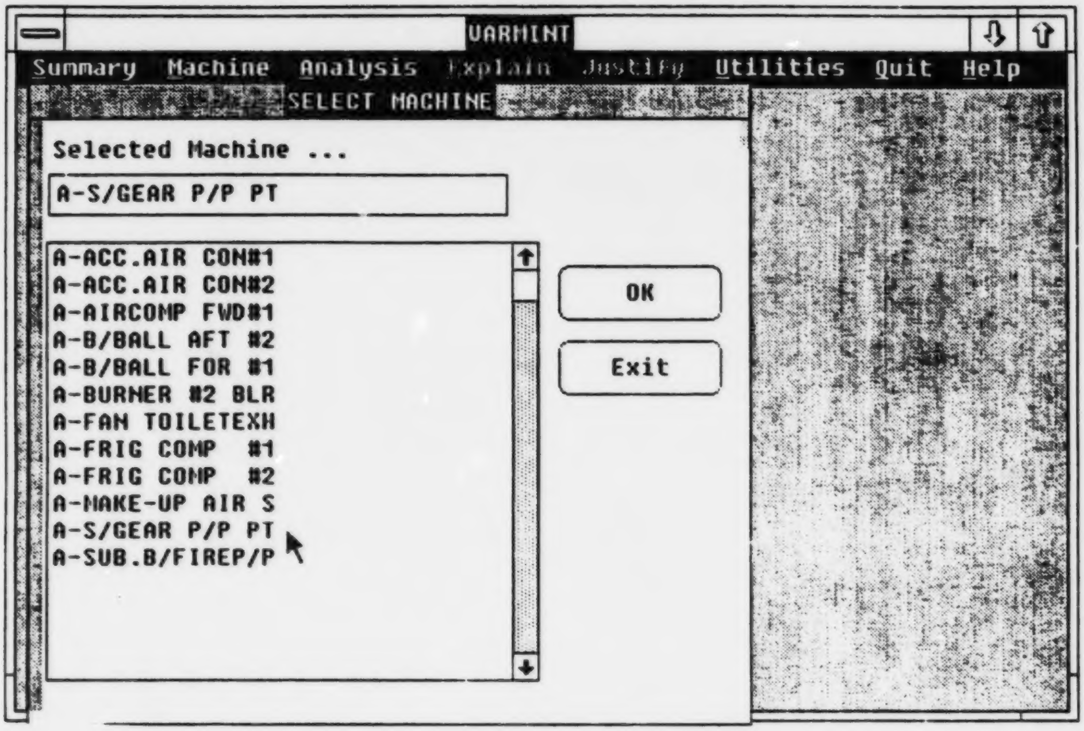
VARMINT
Summary
Machine
Analysis
Explain
Justify
Utilities
Quit
Help
SELECT MACHINE
OK
Exit

```
Selected Machine ...

A-S/GEAR P/P PT

A-ACC.AIR CON#1
A-ACC.AIR CON#2
A-AIRCOMP FWD#1
A-B/BALL AFT #2
A-B/BALL FOR #1
A-BURNER #2 BLR
A-FAN TOILETEXH
A-FRIG COMP  #1
A-FRIG COMP  #2
A-MAKE-UP AIR S
A-S/GEAR P/P PT
A-SUB.B/FIREP/P
```

VARMINT.2 - Select Machine for Processing

2.) Machine Modelling

Whether a machine is individually selected or part of a batch, the process of selection is consistent. The model of the machine is loaded from the VARMINT database. This model contains a number of components; each component in turn contains a number of points. This model (figure 2) contains the data needed for the machine to calculate bearing fault frequencies, gear mesh frequencies etc., as well as the amplitude alarm levels for these fault frequencies.

Upon completion of loading the information from the VARMINT database, the IRD 7090 database is accessed and the current and historical vibration data for the machine is loaded into the expert system.

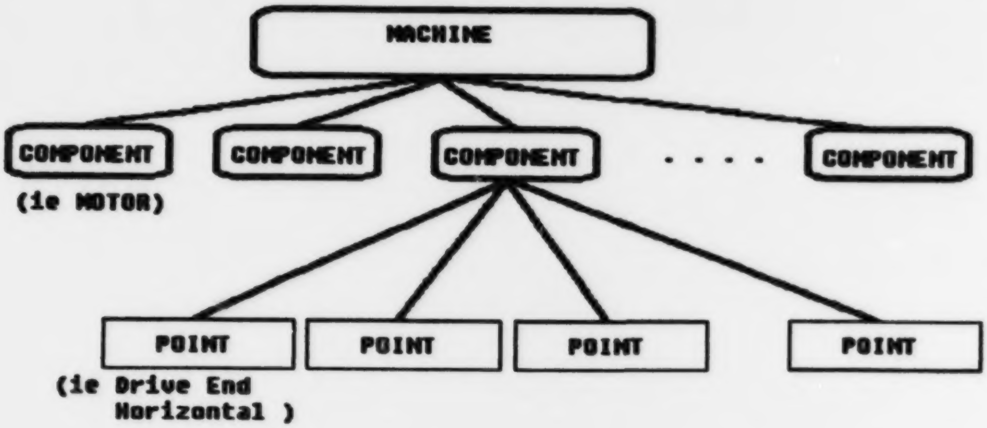
MACHINE
COMPONENT
COMPONENT
COMPONENT
. . . .
COMPONENT
(ie MOTOR)
POINT
POINT
POINT
POINT
(ie Drive End Horizontal)

Figure 2 - VARMINT has full machine modelling capabilities.

3.) Statistical/CurveFit Analysis on Data:

VARMINT uses much of the information that a vibration expert armed with a portable data collector can use - overall vibration trends, spike energy trends and waterfall spectral analysis (see figure 3).

Vibration information for VARMINT is, for each point of measurement, :

a) Overall vibration readings (0 - n);
b) Spike energy readings (0 - n);
c) Spectral histories (0 - n);

when n is a maximum storage depth set by the IRD 7090 software. n ranges from 1 to 26.

Each of the spectral histories is comprised of a number of lines of vibration information, each line representing an amplitude at a specific frequency. The information which is of interest to VARMINT is the 1X to 10X harmonics of the machine running speed, four energy bands covering the whole range of the spectrum, an overall value, and a spike energy value. For each of these, the mean and standard deviations are calculated. The current values are compared against absolute alarms levels, and against statistical thresholds based on the standard deviation.

For vibration analysis, absolute and statistical comparisons only provide some of the picture - it is also necessary to analyze the trend of the historical spectra for a particular point. The first step in this process is to "normalize" the waterfall of spectra to accomodate fluctuations in running speed. Once this has been achieved, the actual data points for a particular frequency can be isolated for curve fitting.

There are a number of exacting methods of performing curve fitting, (ie least squares, polynomial methods etc). But the VARMINT requirements are less demanding - we are interested in simulating an expert's "eyeball" assessment of a trend, by determining whether a series of data points form a flat line, a ramp with constant slope, a rapidly increasing upward curve, or a downward curve. Thus, an exact curve fit is not necessary, and a simpler approach would be more beneficial, not only conceptually, but also computationally.

Second order curve fitting for spectral and overall value trends in VARMINT are as follows:

1. Differentiate the series of line segments between the points in a piecewise continuous manner.

   $C_0 = ax^2 + bx + c;$
   $C_1 = 2ax + b;$

   Let m = 2a, slope of first-order curve;

2. If m = 0 (within a predetermined accuracy), then the original curve is first order with slope = b.

3. Else, m <> 0, and the original curve is second order.

In order to find the slope (m) and y-intercept (b) of the new curve, we must perform a linear curve fit to the set of data. Although the principle of least squares can be used, a simpler approach called the "three group method" [7], can be used to provide a fairly good estimate of the true straight line.

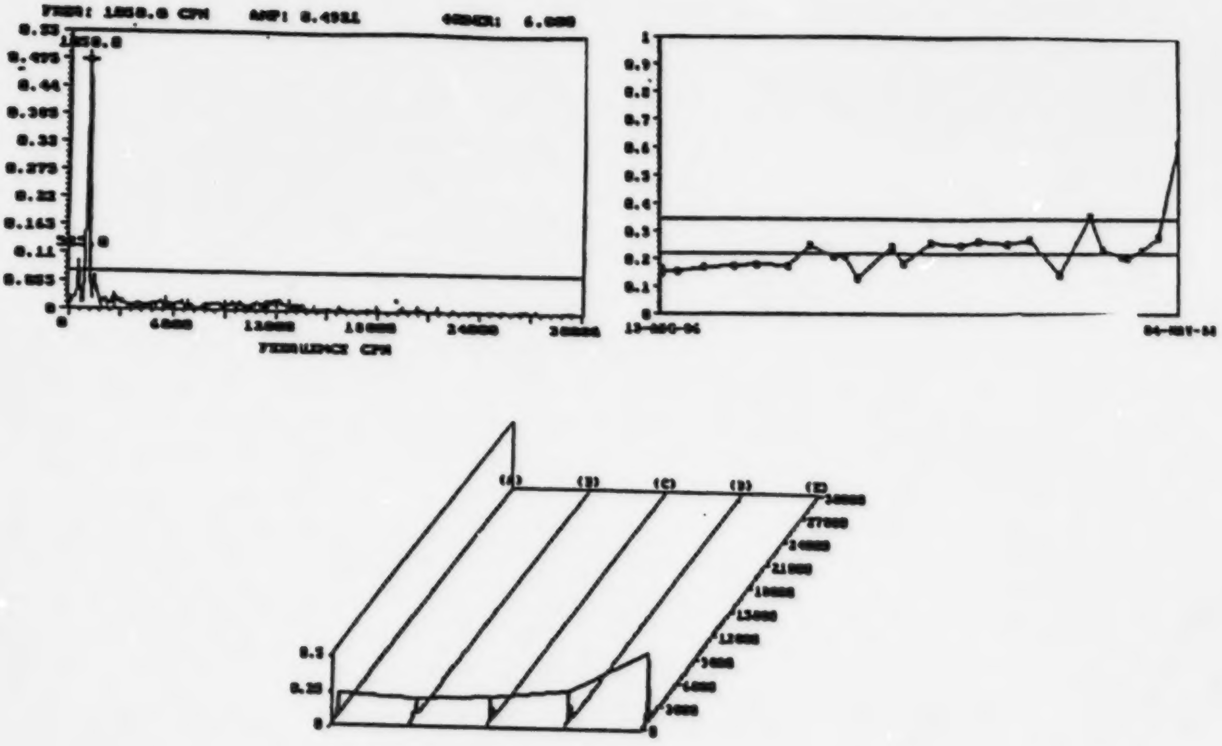

Figure 3 - VARMINT makes use of most of the available data.

Once all symptom data is processed, it is presented to the user as a series of one line summaries in a "list box". The user can scroll through the list box using the keyboard or the mouse. If the user wishes more extensive information on each symptom, he can select an individual symptom and ask for an explanation or justification (see below).

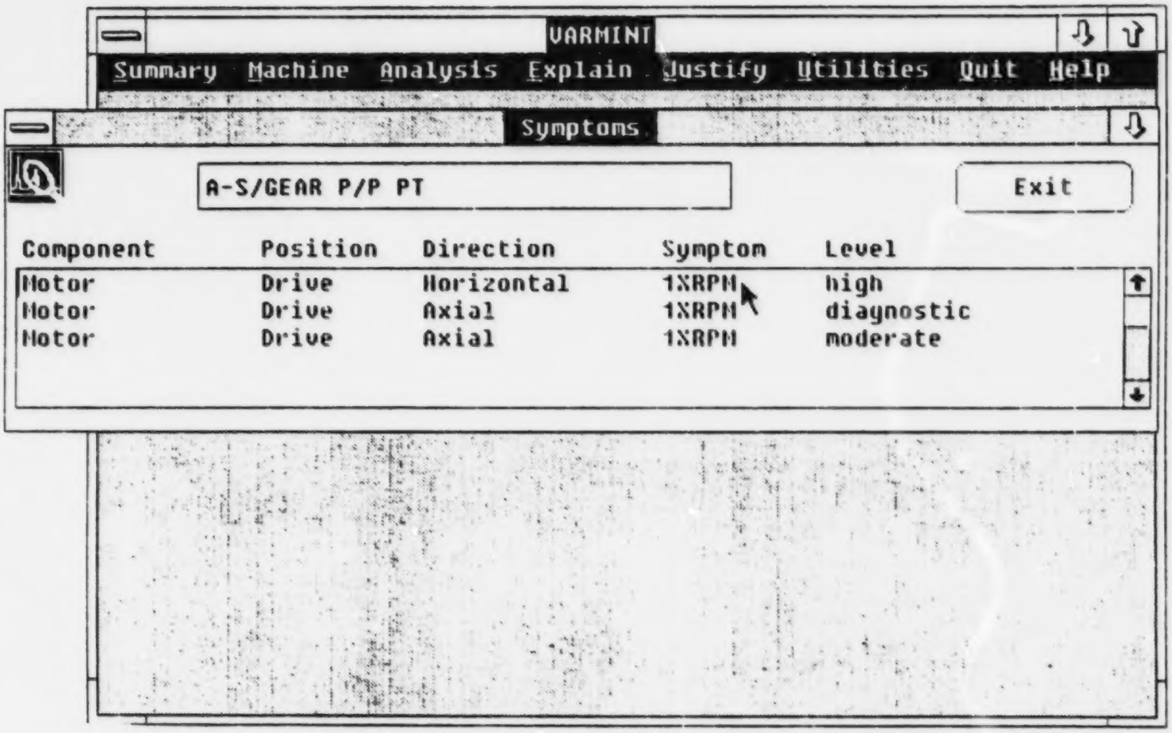
VARMINT
Summary Machine Analysis Explain Justify Utilities Quit Help
Symptoms
Exit

A-S/GEAR P/P PT

Component	Position	Direction	Symptom	Level
Motor	Drive	Horizontal	1XRPM	high
Motor	Drive	Axial	1XRPM	diagnostic
Motor	Drive	Axial	1XRPM	moderate

VARMINT.3 - Symptoms List Box

4.) Rule Based Diagnosis of Problems

The Diagnose module analyzes the selected machine's symptoms to come up with a set of fault hypotheses. Each of these hypotheses has a probability estimate and a severity level.

The careful design of the knowledge base structure for a nonconsultative expert system is a greater requirement than with consultative type expert systems. A larger proportion of rules are required to determine which of the (potentially many) available facts are pertinent. The knowledge bases tend to be larger and less obvious in their application than conventional knowledge bases.

The knowledge base of diagnostic rules is set up as a network of loosely linked "knowledge islands". The rules that link these islands enable the firing of other rules within the network - they determine the possibility that a fault hypothesis or set of hypotheses may be worth investigating. The rules within the islands generate conclusions about actual faults. (see figure 4).

This networking of rules increases the efficiency of a potentially very large knowledge base, as the vast majority of rules for a piece of equipment will be contained within islands that are not applicable for a given machine configuration or set of symptoms. The network structure of the knowledge base also increases the maintainability of the system, as the relationships between islands are explicit and the knowledge found within an island deals with one specific hypothesis, ie the possiblity of misalignment, coupling wear etc.

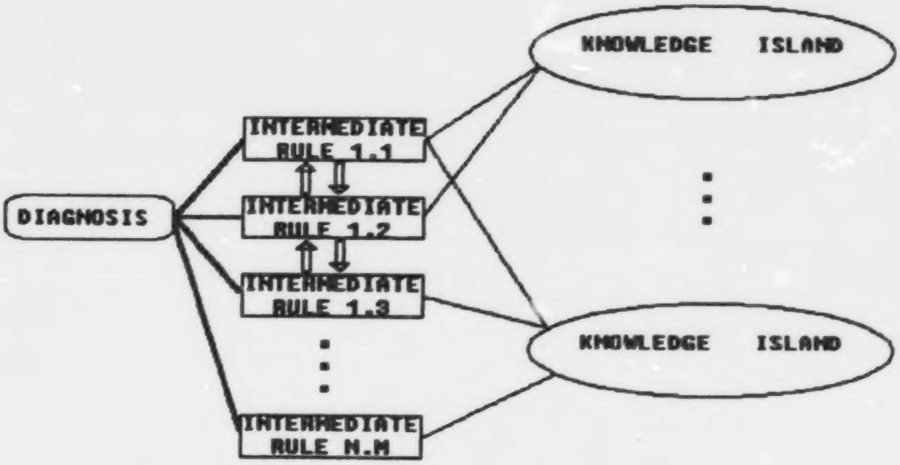
KNOWLEDGE ISLAND
INTERMEDIATE RULE 1.1
INTERMEDIATE RULE 1.2
INTERMEDIATE RULE 1.3
DIAGNOSIS
KNOWLEDGE ISLAND
INTERMEDIATE RULE N.M

Figure 4 - An interlinked networked rule base with "knowledge islands"

5.) Rule Based Recommended Actions

The Actions module maps hypothesized faults into one or more action recommendations, typically repairs or suggestions for further data collection and analysis. The urgency of the action is presented to the operator, as well as an estimated time to failure.

Symptoms, Diagnoses and Recommended Actions are presented to the user in the same style of list box.

6.) Explain and Justify

In each knowledge base in the system, each rule has associated text giving the reason behind the rule. Similarly, each conclusion reached by the knowledge base has associated text giving a complete description of the conclusion. (In VARMINT, symptoms, diagnoses and actions are referred to collectively as conclusions).

Whenever the operator desires greater detail about a conclusion, the system can produce an Explanation of the conclusion. If the operator is curious about the reasoning used to produce a conclusion, the system can produce a Justification, a list of the rules fired to produce the conclusion. The operator performs this action by selecting a conclusion with the mouse and then selecting Explain or Justify from the main menu.

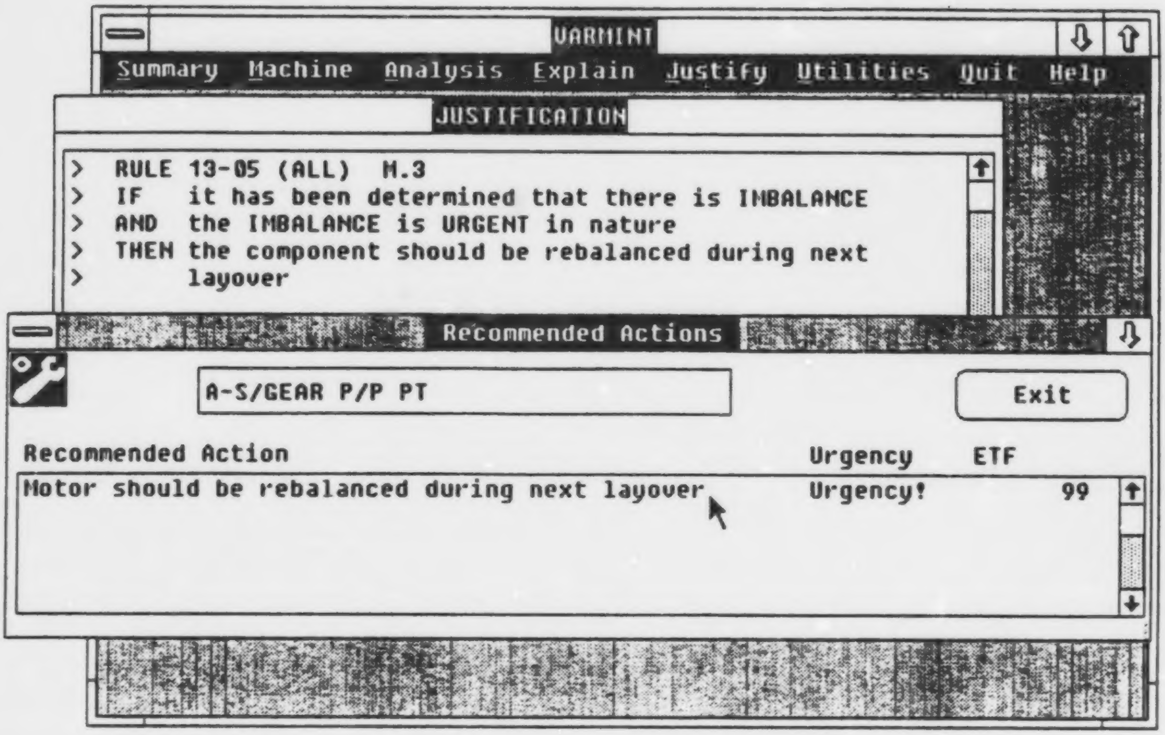
VARMINT
Summary Machine Analysis Explain Justify Utilities Quit Help
JUSTIFICATION

```
> RULE 13-05 (ALL)  M.3
> IF   it has been determined that there is IMBALANCE
> AND  the IMBALANCE is URGENT in nature
> THEN the component should be rebalanced during next
>      layover
```

Recommended Actions
Exit

A-S/GEAR P/P PT

Recommended Action	Urgency	ETF
Motor should be rebalanced during next layover	Urgency!	99

VARMINT.4 - Recommended Actions with Justification

7.) Machine Schematics

One of the best ways to present information to the operator is through the use of diagrams. The operator gets a better grasp of the relationship between the analysis results and the actual machine by having the results displayed in a schematic format.

To this end, VARMINT has had a schematic modelling subsystem added to the inference engine. It is expected that in future editions of VARMINT, much of the information currently available will be accessible through the schematic model, allowing the user to query the state of a machine by simply selecting a machine component with the mouse. This functionality will require a further study.

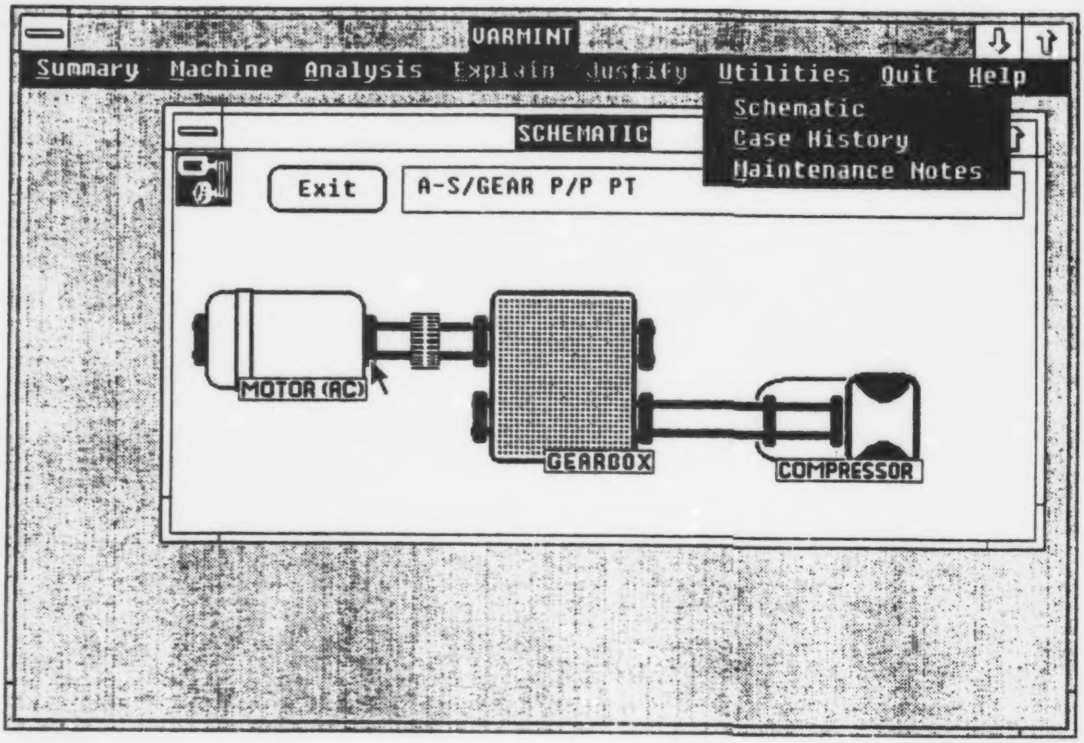
VARMINT
Summary
Machine
Analysis
Explain
Justify
Utilities
Quit
Help
Schematic
Case History
Maintenance Notes
SCHEMATIC
Exit
MOTOR (AC)
GEARBOX
COMPRESSOR

A-S/GEAR P/P PT

VARMINT.5 - Machine Schematic

8.) The Advantages/Disadvantages of Windows-based Systems

VARMINT has been designed and implemented as a Windows application. It takes advantage of Windows' inherent benefits, such as a consistent graphics interface, resizable/moveable windows, and the ability to reduce any window to an icon for easy manipulation by the user.

VARMINT also takes advantage of Windows' multitasking capability. This allows other programs to be run simultaneously with VARMINT. (see VARMINT.6) We have only begun to scratch the surface of the practical benefits of this capability. For example, we envision using Windows' Dynamic Data Exchange (DDE) capability to transfer VARMINT results directly to word processors, spreadsheets or , most importantly, directly to Windows-based maintenance management systems.

Another Windows advantage is simply that once you have learned the operation of one Windows-based program, all other Windows-based programs have the same user interface. The job of learning various systems becomes greatly reduced.

The disadvantage of Windows is simply one of utilizing resources. VARMINT requires an 80386 based computer to run with acceptable speed. This requirement will become less noticeable over time as hardware continues to drop in price relative to performance.

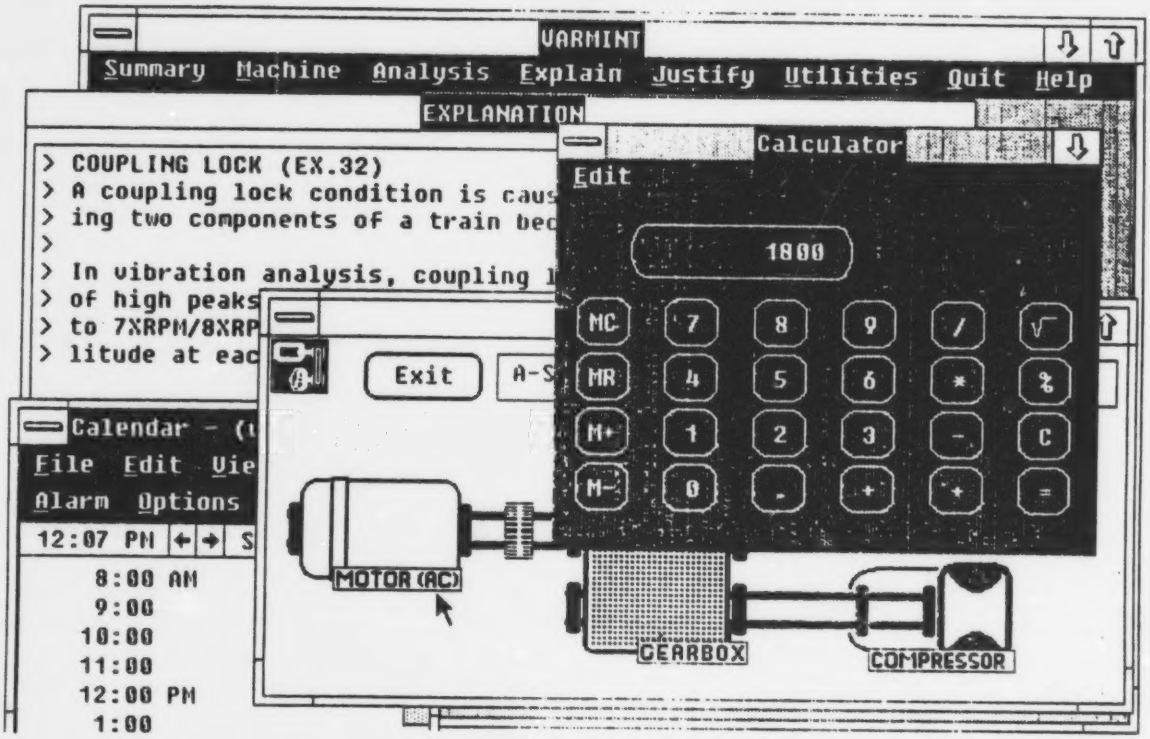
VARMINT
Summary
Machine
Analysis
Explain
Justify
Utilities
Quit
Help
EXPLANATION
Calculator
Edit
1800
MC
7
8
9
/
√
MR
4
5
6
*
%
M+
1
2
3
-
C
M-
0
.
+
+
=
Exit
A-S
Calendar - (u
File
Edit
Vie
Alarm
Options
12:07 PM
S
8:00 AM
9:00
10:00
11:00
12:00 PM
1:00
MOTOR (AC)
GEARBOX
COMPRESSOR

```
> COUPLING LOCK (EX.32)
> A coupling lock condition is caus
> ing two components of a train bec
>
> In vibration analysis, coupling l
> of high peaks
> to 7XRPM/8XRP
> litude at eac
```

VARMINT.6 - Using Windows' Multitasking Capabilities

CONCLUSIONS

Expert systems are becoming valuable tools for maintenance operations in industry. In this paper, the process of developing a non-consultative type expert system has been described. Some of the numerical and inferencing techniques required to analyze vibration data have been reviewed . Our conclusion, after having undertaken this project, is that an automated expert system requires an extensive machine modelling capability, sophisticated data analysis and a set of carefully designed knowledge bases. The Windows environment is beneficial to the operator, both for ease of learning and ease of use.

REFERENCES

[1] Transportation Development Centre T8200-8-8548/01
Statement of Work
Expert System for Vibration Analysis of Ship Machinery

[2] Buss, Juris
"Machine Audit on the 'Sir William Alexander'"
prepared for T8200-8-8548/01, November 1989

[3] Bult, Timothy, Reilly, Robert S.,
"Software Requirements Specification"
prepared for T8200-8-8548/01, November 1989

[4] Bult, Timothy, Reilly, Robert S.
"Platform Selection, Vibration Analysis Expert System"
prepared for T8200-8-8548/01, November 1989

[5] Bult, Timothy
"Vibration Analysis Knowledge Acquisition rev. 7.2"
prepared for T8200-8-8548/01, April 1990

[6] Bult, Timothy, Reilly, Robert S., MacPhail, Christopher A.
"VARMINT Software Design Description"
prepared for T8200-8-8548/01, December 1989

[7] Lyon, Arthur J., Ph.D.
"Dealing with Data"
1970, Pergamon Press Ltd.

[8] Schlitz, Richard L.
"Accuracy in Determining Rolling Element Forcing Frequencies"
Proceedings of the First International Machinery Monitoring and Diagnostics Conference, 1989

[9] Neuron Data Inc.
"Nexpert Object Fundamentals"
Neuron Data Inc, 1987, 1988

[10] Parsaye, Kamran, Chignell, Mark,
"Expert Systems for Experts"
John Wiley and Sons, Inc., 1988

FIELD EXPERIENCE IN VIBRATIONAL BEHAVIOUR OF 2 STAGE, CENTRIFUGAL PUMPS

M.M. Osman and B. Alavi

Ontario Hydro
700 University Avenue H13
Toronto, Ontario
M5G 1X6

ABSTRACT

This paper is on the vibration behaviour of 2 stage, double volute centrifugal pumps. Recent experience with this type of equipment has shown sensitivity to mechanical vibrations caused by fluid forces acting at the blade passing frequencies. Clearances between stationary and rotating parts seem to have an important effect on this dynamic behaviour. Pump unbalance and misalignment tend to have less influence on the vibration levels than changes to these clearances and pump operating conditions.

The information given includes vibration specification, data obtained from shop tests, routine commissioning measurements and results of a comprehensive diagnostic program carried out when high vibrations were deleted at site. The recorded high vibrations are associated with blade passing frequencies. Levels up to 20 mm/sec, 0-pk on the pump bearings were measured at low flow conditions. Vibration levels and spectra at high frequencies (up to 50 kHz) were also taken. Examples of the many vibrations and vibro-acoustic measurements including the results of the application of spectral analysis and correlation techniques are presented.

KEYWORDS

Boiler feed pump vibrations, blade passing frequencies, hydraulic effects.

BIOGRAPHIES

As a senior Design Specialist, Dr. Moustafa M. Osman's current activities/interests are :

» Trouble shooting of vibration and noise problems for heavy equipment, especially centrifugal pumps (horizontal and vertical) and combustion turbines.
» Industrial noise control in the work place and the environment.
» Determination of in-situ equipment vibration limits for commissioning and monitoring purposes.
» Pedictions for rotor dynamic behaviour using computer software, e.g. unbalance response, critical speeds, stability.
» Active cancellation of noise and vibration in industrial environment.

B. Alavi, Ph.D., is a Design Engineer in the Noise and Vibration Control Unit of Ontario Hydro since 1988. He received his Bachelor's, Master's and Ph.D. degrees in Mechanical Engineering from the University of Leeds in England. Prior to joining Hydro, he worked as a Senior Development Engineer at British Oxygen Company (UK) where he was a member of the design team responsible for design and development of a wide range of high speed axial flow compressors. Dr. Alavi's field of expertise is in the areas of vibration analysis and control and bearing desing.

RÉSUMÉ

Le présent document porte sur le comportement vibratoire des pompes centrifuges bicellulaires à double volute. Certains faits ont récemment démontré que ce type de pompe est très sensible aux vibrations mécaniques qui sont engendrées lorsque la fréquence des forces fluides est la même que celle du passage des aubes. Ce comportement dynamique semble dépendre fortement du jeu entre les pièces fixes et les pièces rotatives. Le déséquilibre et le mauvais alignement des pompes semblent avoir moins d'impact sur le niveau des vibrations que les changements de jeux ou de conditions de fonctionnement.

Les renseignements donnés comprennent des caractéristiques vibratoires, des données obtenues lors d'essais en atelier, des mesures normales de mise en service ainsi que les résultats d'un programme complet de diagnostic exécuté lorsque des vibrations importantes ont éte décelées. Les niveaux de vibration élevés enregistrés sont reliés aux fréquences de passage des pales. Des niveaux atteignant jusqu'à 20 mm/sec, amplitude sur les roulements des pompes ont été enregistrés dans des conditions de débit minimum. Des niveaux de vibrations et des spectres à hautes fréquences (jusqu'à 50 kHz) ont aussi été enregistrés. Plusieurs mesures vibratoires et vibro-acoustiques comprenant des résultats d'analyses spectrales et de techniques de corrélation sont aussi données.

MOTS CLÉS

Vibrations des pompes d'alimentation de chaudière, fréquences de passage des pales, effets hydrauliques.

BIOGRAPHIES

Spécialiste principal en conception, le docteur **M.M. Osman** s'occupe des domaines suivants:

- diagnostic de problèmes vibratoires et acoustiques du matériel lourd et plus spécialement des pompes centrifuges (horizontales et verticales) et des turbines à combustion;
- contrôle des bruits industriels dans les lieux de travail et l'environnement;
- établissement sur place des limites vibratoires du matériel pour la mise en service et le contrôle;
- prédictions du comportement dynamique des rotors à l'aide de logiciels, par exemple réponse de déséquilibre, vitesses critiques, stabilité;
- élimination du bruit et des vibrations dans l'industrie.

Le docteur **B. Alavi** est ingénieur d'études à l'Unité de contrôle du bruit et des vibrations d'Ontario Hydro depuis 1988. Il a obtenu son baccalauréat, sa maîtrise et son doctorat en génie mécanique à l'Université de Leeds en Angleterre. Avant de se joindre à l'équipe d'Ontario Hydro, il a travaillé comme ingénieur principal de mise au point pour la compagnie British Oxygen (Royaume-Uni) où il était membre de l'équipe responsable de la conception et du développement d'une vaste gamme de compresseurs axiaux à grande vitesse. Les spécialités du docteur Alavi sont l'analyse et le contrôle des vibrations et la conception des roulements.

FIELD EXPERIENCE IN VIBRATIONAL BEHAVIOUR OF 2 STAGE, CENTRIFUGAL PUMPS

M.M. OSMAN AND B. ALAVI

ONTARIO HYDRO
Mechanical & Equipment Engineering Department
Noise and Vibration Control Unit
700 University Avenue
Toronto, Ontario M5G 1X6

1.0 INTRODUCTION

This paper is primarily on field experience with 2-stage centrifugal pump mechanical vibration and some of the diagnostic techniques used to address high vibration level problems. Many recent studies including work sponsored by EPRI addressed this issue from design point of view [1,2]. In this study emphasis is on the measurement techniques that can be used to identify the causes of the problem. Also presented is information and data related to pump specification, shop and commissioning tests.

The reported experience reflects the perceived opposing demands for high hydraulic efficiency and low pump vibration. As the trend for larger MW per unit increased, the quest for higher pump efficiency became attractive to the utilities. Consequently, pump designers/manufacturers strived to achieve maximum performance at the expense of other design parameters, namely pump dynamics and vibrational behaviour at partial loads. The 2-stage centrifugal design, Figures 1 and 2, with its relatively short rotor and high efficiency at or near full load makes it an attractive choice from the manufacturer point of view. The drawbacks of such designs from vibrational behaviour were not apparent until the last decade or so; in particular the relationship between suction flow conditions and pump vibration levels at partial loads.

2.0 BACKGROUND

Recent experiences with such centrifugal pumps at Ontario Hydro indicate certain points:

- At shop tests where the suction conditions are near ideal, the vibrational behaviour appears to cause no concern. An expected increase in the vibration level at low flows is evident but the amplitude of vibrations and other hydraulic parameters (NPSH test) do not cause concern.
- When pumps are shipped to site, where the main difference is the piping configuration with more bends and elbows, a net deterioration in the vibration levels at all flow conditions is evident. This deterioration is most noticeable at the pump bearings in the horizontal direction.
- Extended operation at low flows results in potential or actual damage, mostly at the inlet or the first stage impeller, thus indicating a possible relationship to suction conditions.
- Some of the remedial actions taken included improved suction conditions, staggered vanes for the double inlet first stage impeller, different number of vanes and angular location for first and second stage impellers, a v-shaped notch across the tip of the first stage impeller, under filing of first stage

impeller vanes and increased tip clearances between the impellers and the volute.

3.0 MEASUREMENTS AND DATA

Many measurements are taken for different pumps at various times. Due to the potential for vibration problems, attention is given to the equipment vibration limits at the time of specification and procurement. Figure 3 shows the bearing vibration specification as given in a tender document and that offered by a manufacturer. Note the difference in radial and axial levels in the manufacturer's units at BEP (best efficiency point). Also to be noted the expected deterioration in vibration levels at the low flows.

A significant amount of data are generated, only selected samples are given here to illustrate the techniques adopted at Ontario Hydro.

3.1 SHOP VS. SITE TESTS

In an attempt to avoid problems at site and/or costly remedial action, shop tests are required. However, experience has shown that low vibration levels at the shop do not seem to guarantee trouble-free vibration behaviour at site. In one particular case, the site driver is shipped for the pump shop test and mounting arrangement is taken into account in analyzing the data which included vibration levels and spectra covering all frequencies of interest; the generated information do not show any problem and indicate a well damped behaviour even at low flows; however at site the same pumps show high vibration levels.

Samples showing the overall vibration levels at the shop are given in Figures 4 and 5 under low flow (recirculation) and near full flow conditions while Figures 6 and 7 show the results from the site test under similar conditions.

3.2 COMMISSIONING/EARLY OPERATION

Typically during this period, the pumpsets are operated for extended periods under low flow conditions, an NPSH test and system flushing are also performed. Overall vibration levels are taken on the bearing in three directions for various flow conditions. The horizontal component seems to be the highest, especially at the low flows. Most of the vibration seem to be concentrated around the blade passing frequencies in comparison to other components at one time the rpm and its harmonics. Figure 8 shows the amplitude of the blade passing frequencies as measured on the pump bearings for different flow conditions in the horizontal and vertical directions.

Based on the fact that the main difference between the shop and site test is primarily the piping configuration, modifications to the inlet piping is tried with the objective of improving the suction flow conditions. A longer straight inlet piping section and a flow separator at the closest elbow to the pump are introduced. The results of this exercise are presented in Figure 9.

3.3 DIAGNOSTICS

A number of extensive vibration, pressure pulsation and vibro-acoustic measurements are performed to identify the cause of high vibration problem. First a structural vibration test is conducted to investigate the possibility of a coincidence between the natural frequencies of the main mechanical components of the pumpset bearings, etc. and any critical operating frequencies such as blade passing, etc. Also important is to check that no rotor critical frequency is near the operating frequency or its multiples.

A comprehensive diagnostics test that includes bearing vibration, pressure pulsation at the suction and vibro-acoustic measurements to investigate the relationship(s) between pump suction hydraulics and pump mechanical behaviour is performed. Excerpts from the results of this diagnostic test are given in Figures 10 to 14. Examples of the application of spectral analysis techniques are shown in Figures 15 to 18.

Finally endurance test by operating the pump under low flow conditions can be a very useful tool to examine the possibility of damage to pump internals, provided, of course, that time and cost would permit.

4.0 ANALYSES AND CONCLUSIONS

The data gathered and the analyses conducted identify certain points which can be used as guidelines to rectify the problem and assist in developing better future designs. It must be recognized that the presented analyses and conclusions are limited in scope to the pumpset/installations surveyed. However, the applied diagnostic techniques can be universally applied.

4.1 ANALYSES

Examination of the various data produced and in particular results of the diagnostics test indicates the following:

- The dominant pressure pulsations appear at rotating speed and its multiples, also at its blade passing frequencies.
- At very low flow rates, high pulsations are apparent at low frequencies. This is believed to be generated by internal flow recirculation.
- The intensity of the pulsations decreases with increase in flow rate, as one may expect.
- The coherence functions show that there is no coherence between the cavitation pulsations and the bearing vibrations.
- As expected the vibro-acoustic levels increase with decrease in flow rate, there is indication of high vibro-acoustic activity near the pump inboard bearing and the second stage pump casing.
- There seems to be a strong coherence between the flow pulsations and bearing vibration at the blade passing frequencies including a possible cause and effect between the inlet flow condition and bearing vibration.

4.2 CONCLUSIONS

Based on the various test results and the above analyses, the following conclusions can be reached:

- High bearing vibrations is related to flow conditions at the suction and is sensitive to low flow rates.
- The lip clearances between the stationary and rotating parts have an influence on the amplitude of the vibrations, they also affect the pump performance.
- The main cause of high vibrations seem to be recirculation of the flow especially at the eye of the impeller.
- Suction pipe modification appear to have little effect on reducing the high vibration levels.
- It seems that among the various pump internals design that influence high vibrations, the first stage impeller is the most important.

References:

[1] EPRI Feed Pump Hydraulic Performance and Design Improvement, Vol. 1 and Vol. 2, March 1982

[2] Ingersoll-Rand Pump Technology Seminar - Toronto, May 1990

Acknowledgement:

The authors would like to thank Quang-Chieu Chau for the preparation and presentation of the graphs and table that follow.

TABLE 1: MEASUREMENT LOCATIONS FOR VIBRO-ACOUSTIC AND PRESSURE PULSATION READINGS

INLET NOZZLE VIBRATION	CHANNEL 1
PUMP-CASE 1ST STAGE VIBRATION	CHANNEL 2
PUMP-CASE 2ND STAGE VIBRATION	CHANNEL 3
DISCHARGE NOZZLE VIBRATION	CHANNEL 4
I/B BEARING HORIZONTAL VIBRATION	CHANNEL 5
I/B BEARING AXIAL VIBRATION	CHANNEL 6
I/B BEARING VERTICAL VIBRATION	CHANNEL 7
O/B BEARING HORIZONTAL VIBRATION	CHANNEL 8
O/B BEARING AXIAL VIBRATION	CHANNEL 9
O/B BEARING VERTICAL VIBRATION	CHANNEL 10
INLET PRESS PULSATION (FLUSH)	CHANNEL 11
INLET PRESS PULSATION (STANDPIPE)	CHANNEL 12
MAGNETIC VIBRO-ACOUSTIC-SUCTION	CHANNEL 13
MAGNETIC VIBRO-ACOUSTIC-DISCHARGE	CHANNEL 14

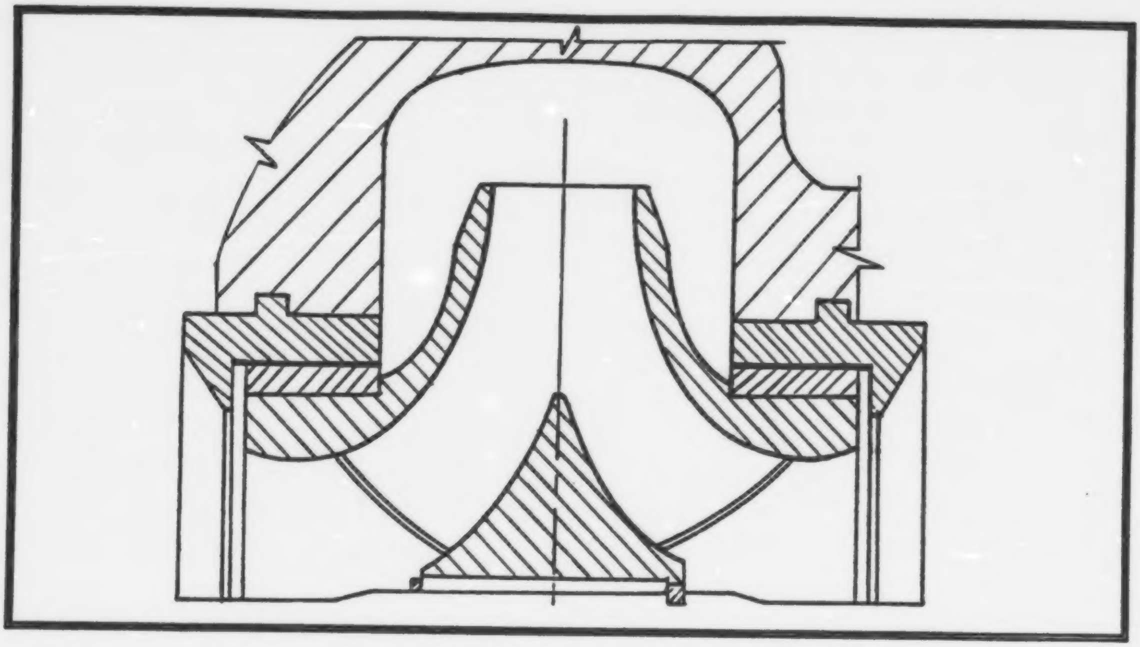

FIGURE 1: CENTRIFUGAL PUMP DOUBLE INLET, FIRST STAGE

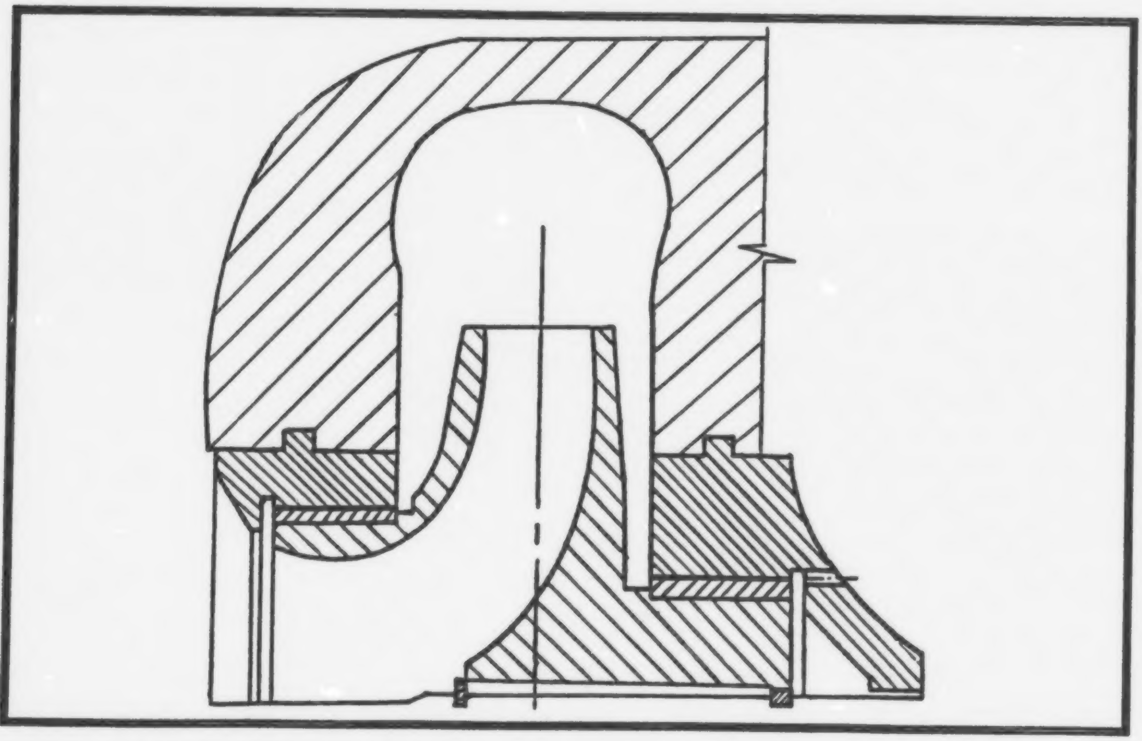

FIGURE 2: CENTRIFUGAL PUMP SINGLE DISCHARGE, SECOND STAGE

Vibration Limits VS Flow

Measured at Bearing Housing

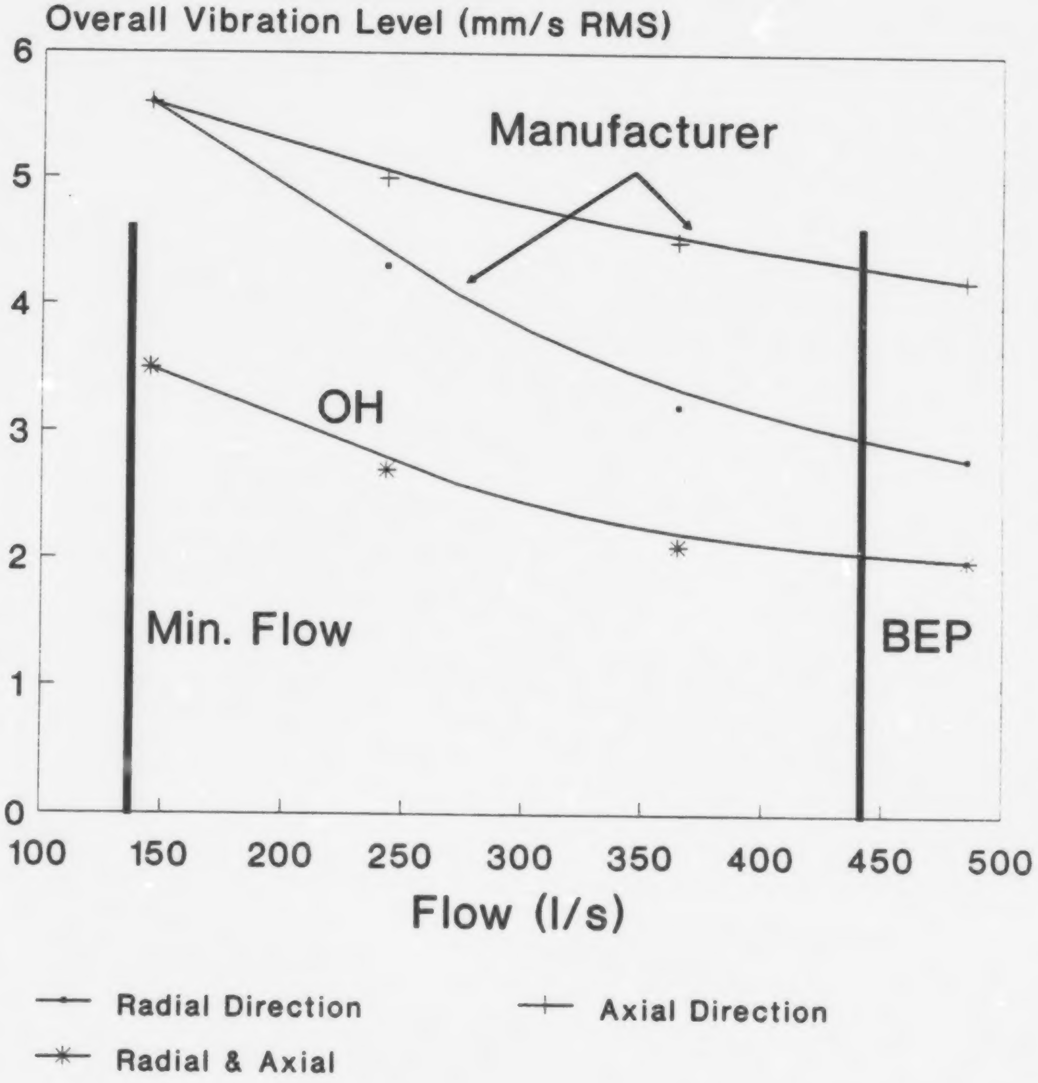

FIGURE 3

Pump Vibration Levels

Shop Tests

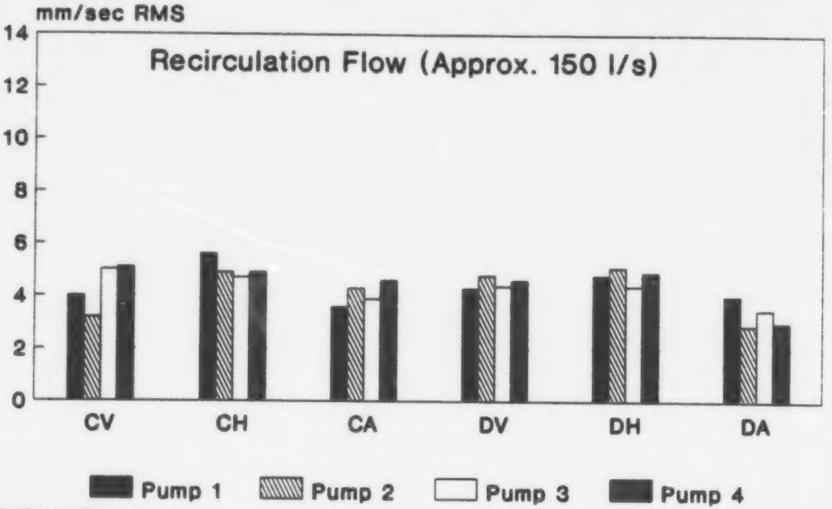

FIGURE 4

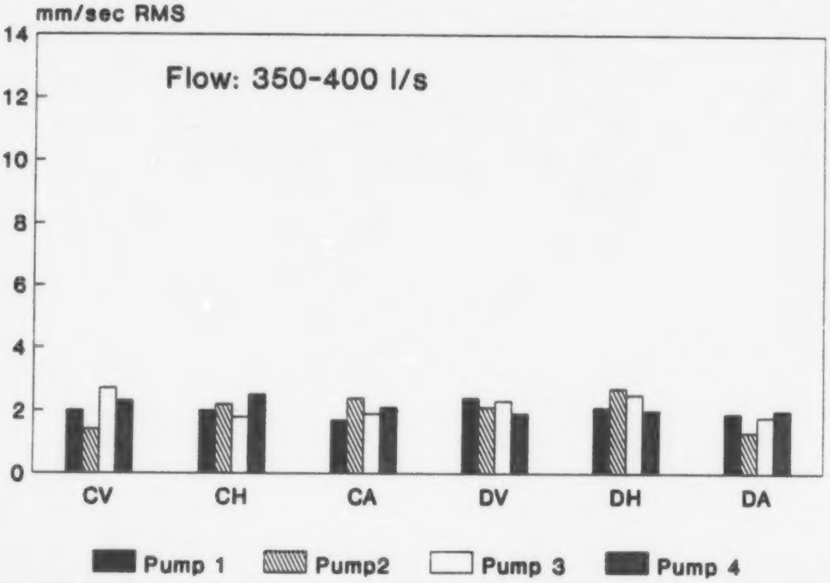

FIGURE 5

C- Inboard Bearing; D- Outboard Bearing;
V- Vertical; H- Horizontal; A- Axial

Pump Vibration Levels

Site Tests

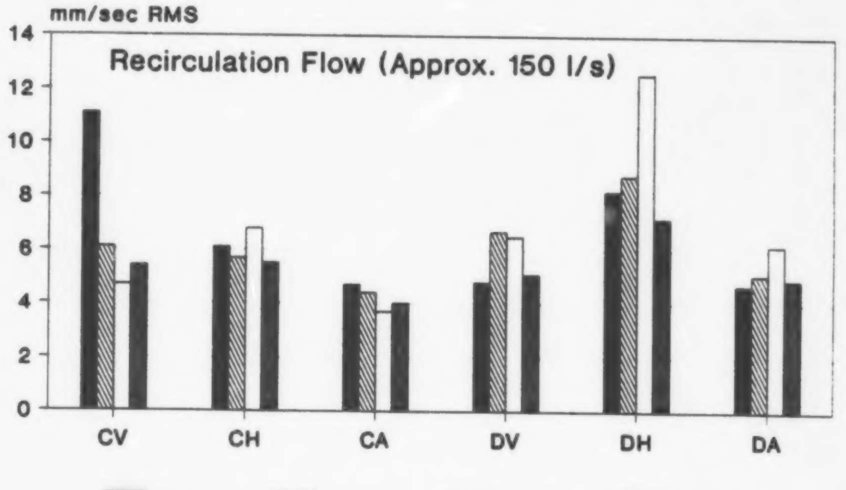

FIGURE 6

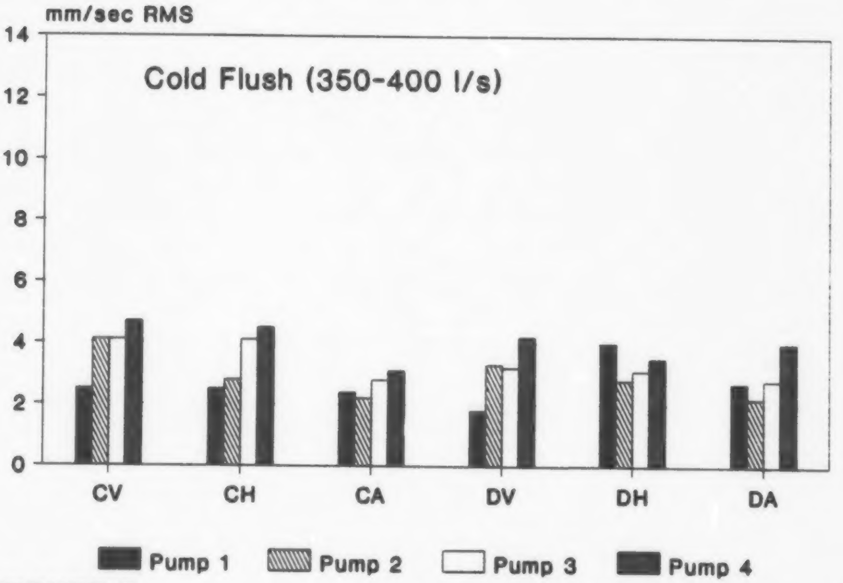

FIGURE 7

C- Inboard Bearing; D- Outboard Bearing;
V- Vertical; H- Horizontal; A- Axial

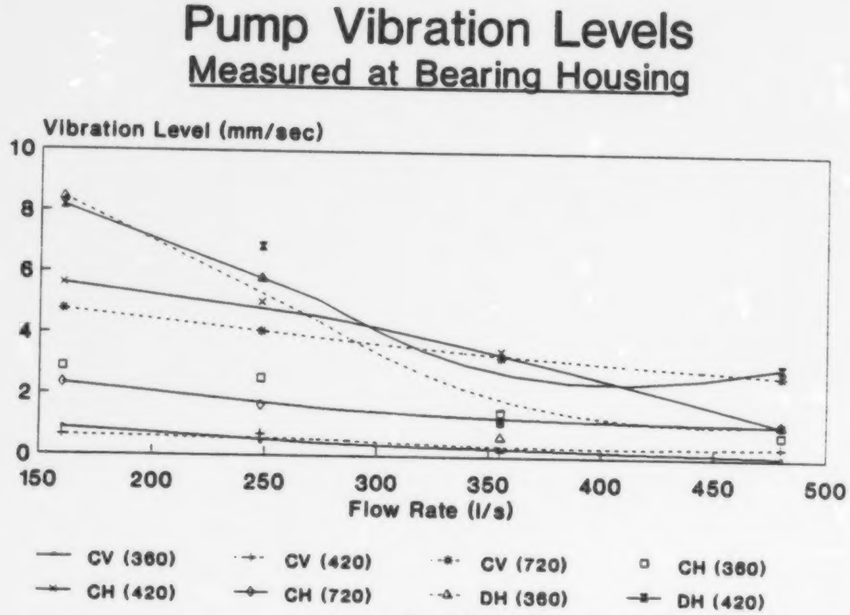

FIGURE 8

C- Inboard Bearing; D- Outboard Bearing;
V- Vertical; H- Horizontal

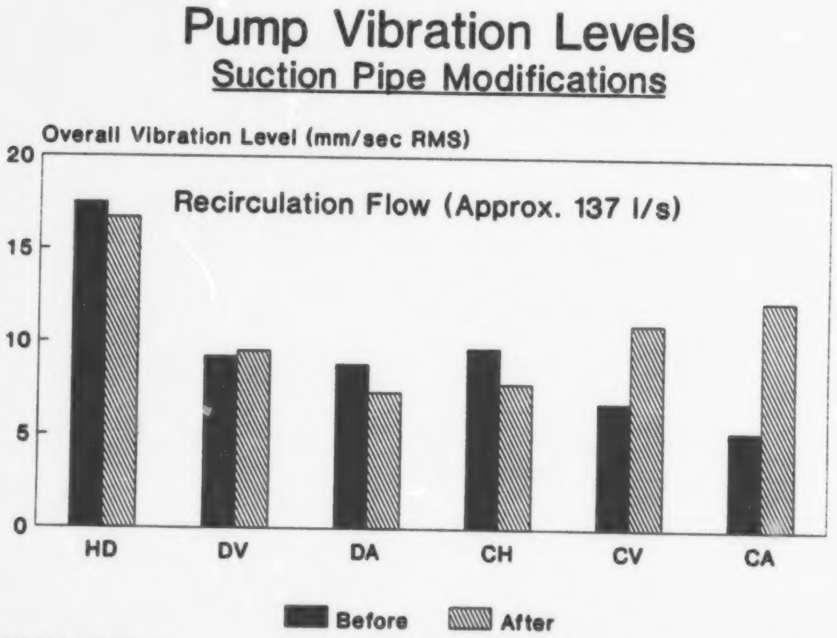

FIGURE 9

C- Inboard Bearing; D- Outboard Bearing;
V- Vertical; H- Horizontal; A- Axial

Vibro-acoustic Results

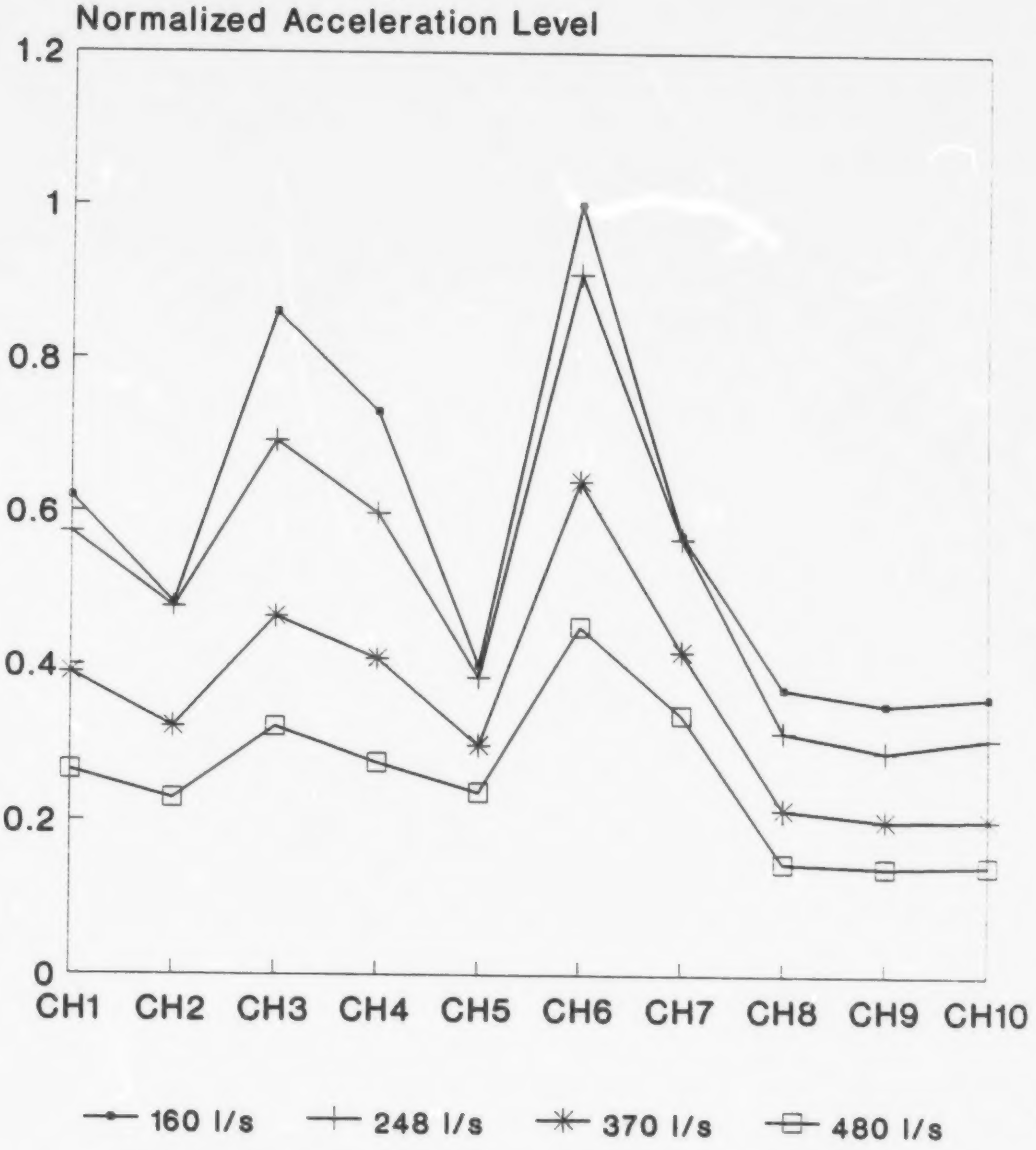

FIGURE 10

Up to 50 KHZ

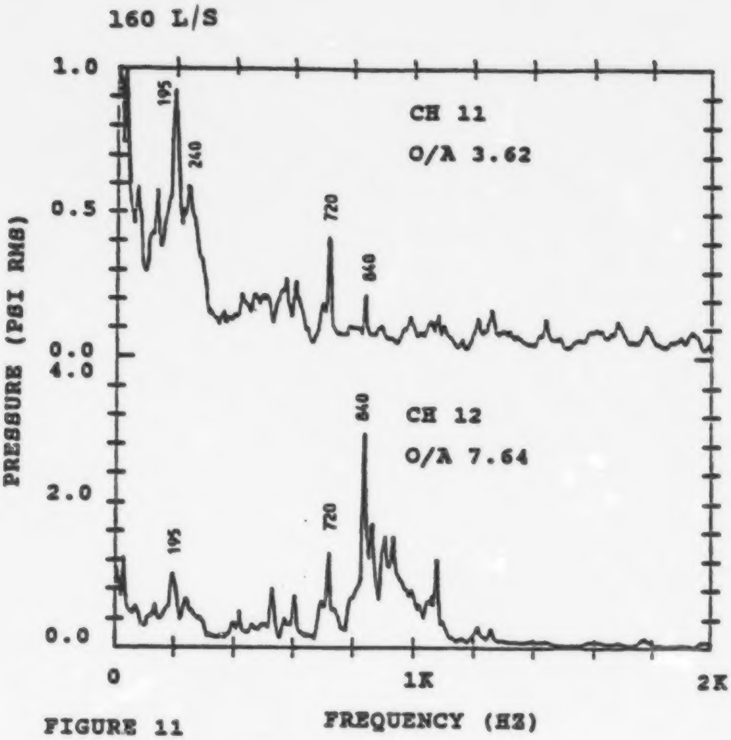

FIGURE 11

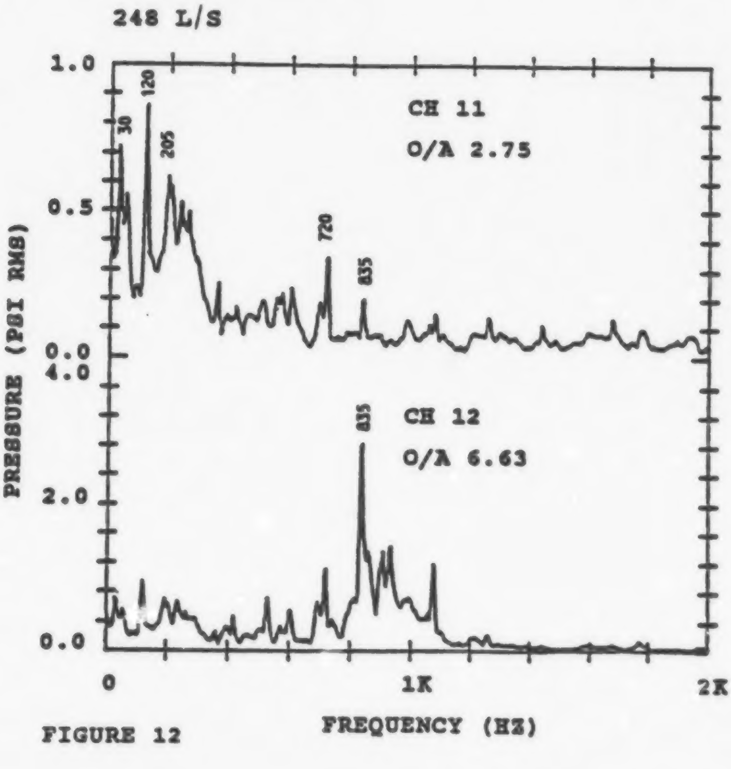

FIGURE 12

357 L/S

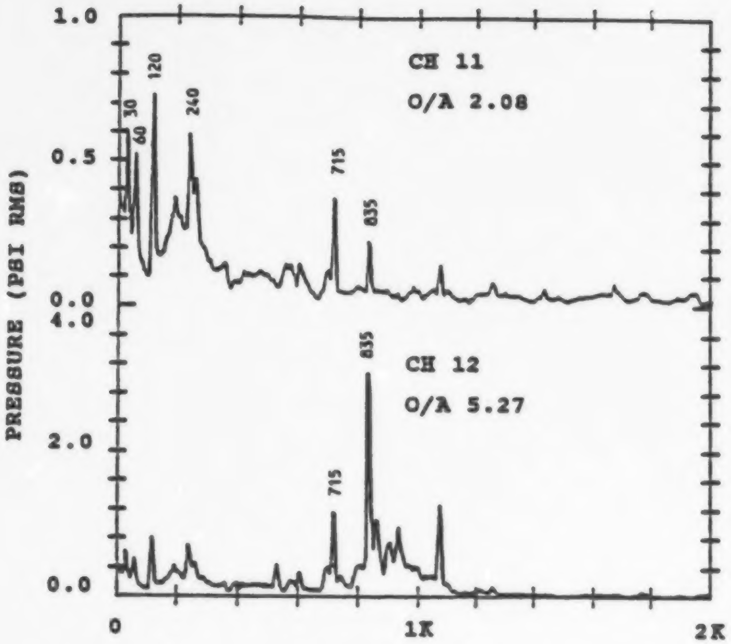

FIGURE 13

480 L/S

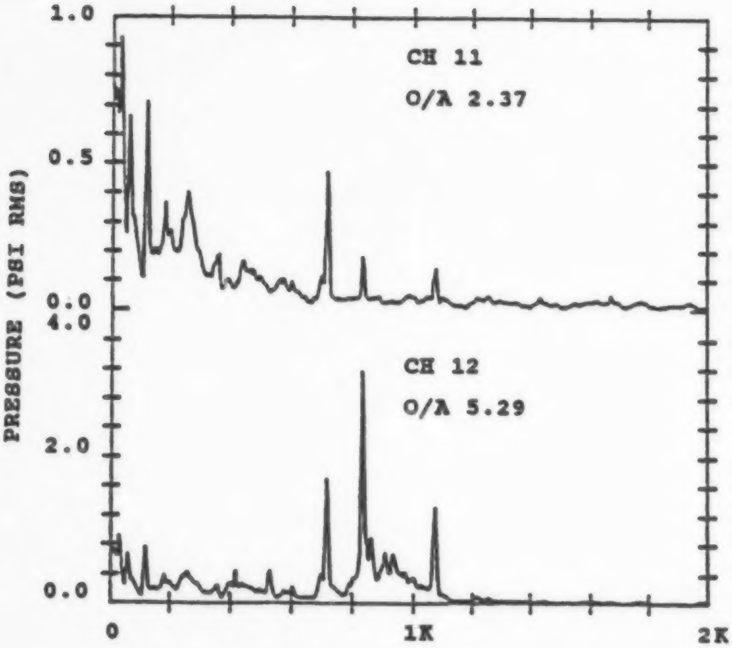

FIGURE 14

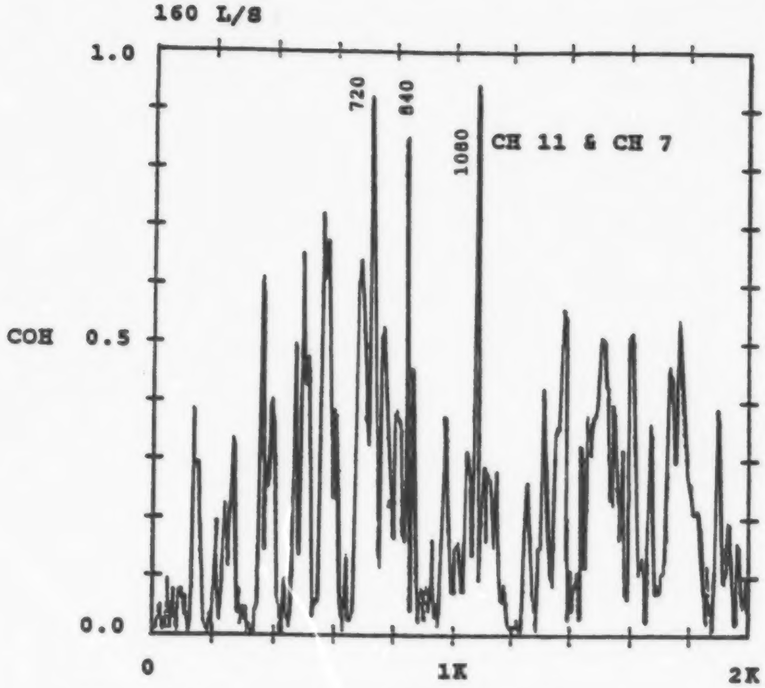

FIGURE 15

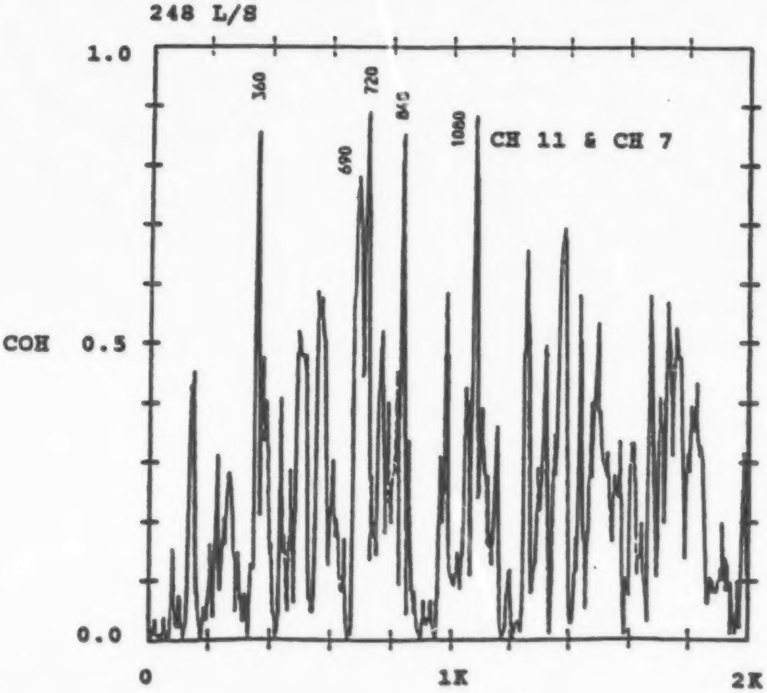

FIGURE 16

COHERENT OUTPUT POWER CH7/CH11 (m/s*s)/PSI

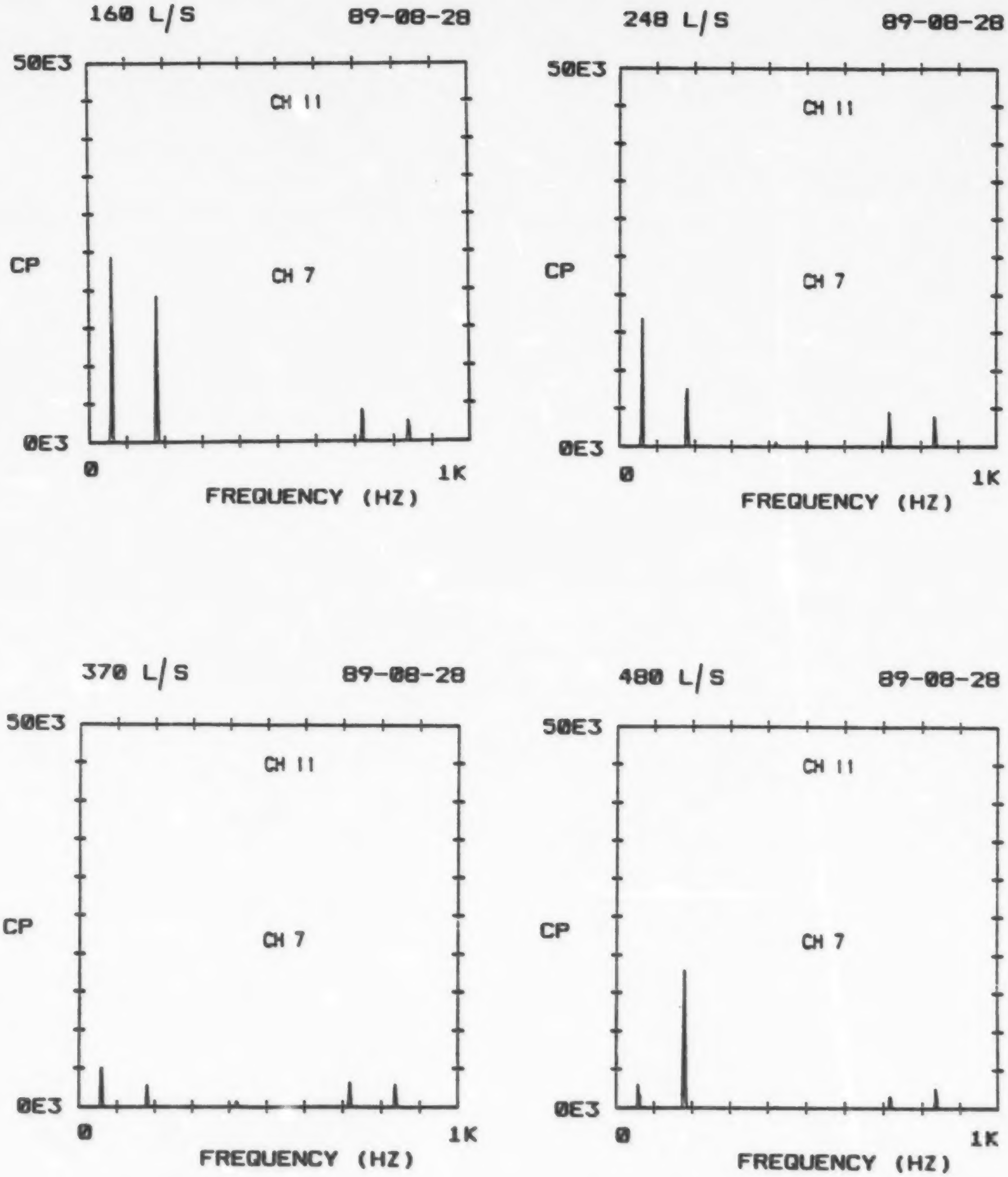

FIGURE 17

COHERENT OUTPUT POWER CH8/CH11 (m/s*s)/PSI

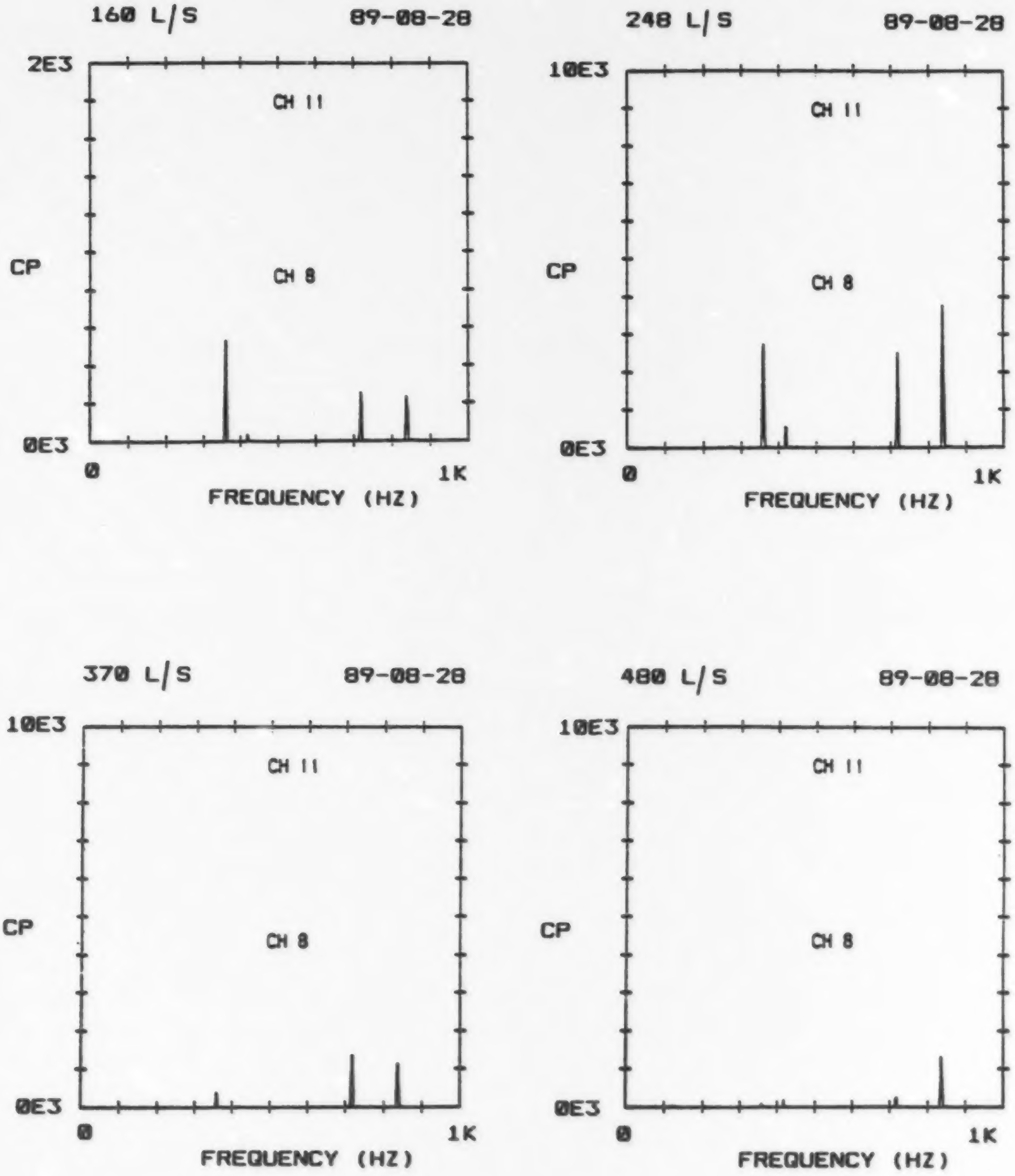

FIGURE 18

UPDATE ON MACHINERY VIBRATION STANDARDS

Stewart Maxwell
Ontario Hydro
700 University Avenue
Toronto, Ontario
M5G 1X6

ABSTRACT

Five members of the Machinery Dynamics Sub-Committee are part of a Canadian Advisory Committee to the Standards Council of Canada on vibration of machines. Canada is a participating member of the International Organization for Standardization (I.S.O.) through this working group.

The group represents Canada's interests in the revision of existing standards and in the formulation of new Standards. The working group is presently active on Standards for measurement and evaluation of vibration on rotating and non rotating parts of vertical and horizontal machines from 500MW and on vertical and horizontal hydraulic machines.

KEY WORDS

Vibration, Standards, Rotating Machines, Standards Connexe (S.c.), International Standards (I.S.O.)

BIOGRAPHY

Stewart Maxwell is Section Head of Machine Dynamics in Ontario Hydro's Central Production Services Division. With over 25 years experience in the field of vibration analysis and balancing, his current major area of responsibility is the provision of services to nuclear and thermal generating stations in the diagnosis and control of vibration in rotating equipment. He is a registered Professional Engineer in the Province of Ontario, a Director of the Vibration Institute and Chairman of the Canadian Advisory Committee of the ISO (International Standards Organizations) on Vibration of Machines.

RÉSUMÉ

Cinq membres du Sous-comité de la dynamique des machines font partie d'un Comité consultatif canadien auprès du Conseil canadien des normes sur la vibration des machines. Le Canada est un des membres participant de l'Organisation internationale de normalisation (I.S.O.) par l'entremise de ce groupe de travail.

Le groupe représente les intérêts du Canada pour la révision des normes existantes et la formulation de nouvelles normes. Le groupe de travail étudie présentement les normes de mesurage et d'évaluation des vibrations des composants rotatifs et non rotatifs des machines verticales et horizontales de plus de 500 MW et des machines hydrauliques verticales et horizontales.

MOTS CLÉS

Vibration, normes, machines rotatives, Standards Connexes (S.c.), normes internationales (I.S.O.)

BIOGRAPHIE

Stewart Maxwell est le chef de la Section de la dynamique des machines de la Division des services centraux et de la production d'Ontario Hydro. Il a plus de 25 ans d'expérience dans le domaine de l'analyse des vibrations et de l'équilibrage et ses principales responsabilités actuelles sont la fourniture de services aux centrales nucléaires et thermiques en matière de diagnostic et de contrôle des vibrations sur les machines rotatives. Il est ingénieur enregistré dans la province de l'Ontario, directeur de l'Institut des vibrations et président du Comité consultatif canadien auprès de l'ISO (Organisation internationale de normalisation) sur la vibration des machines.

UPDATE ON MACHINERY VIBRATION STANDARDS

Introduction

Five members of the Machinery Dynamics Subcommittee (MDSC) are part of a Canadian Advisory Committee (CAC) to the Standards Council of Canada (SCC), on the International Organization for Standards (ISO). Specifically, on Technical Committee 108 (TC 108), Subcommittee 2, Working Group 1 (SC2/WG1). The Working Group has the title "Vibration of Machines." The actual "abbreviation" of the committee title is, therefore, CAC/SCC/ISO/TC 108/SC2/WG2 - "Vibration of Machines," but it is known as the MDSC, Standards Working Group. The Working Group is a participating member of the ISO and represents Canada's interests in the revision of existing Standards and in the formulation of new Standards.

There are six areas of Standards activity on which to report progress since the last MDSC seminar in September 1988. These are:

1.0 Rationale for the Use of ISO - 1940 Balance Quality of Rigid Rotors.

2.0 ISO 7919 Parts 1, 2, 3 and 4 - Measurement of Vibration on Rotating Shafts.

3.0 ISO 7919 Part 5 - Vibration of Hydraulic Machines.

4.0 ISO 2372 Parts 1, 2 and 3 - Measurement of Vibration on Non-Rotating Parts.

5.0 ISO 2372 Part 6 - "Reciprocating Machines."

6.0 Priorities for Future Parts of ISO 7919 and ISO 2372.

1.0 Rationale for the Use of ISO - 1940

At the last MDSC Seminar in Calgary, September 1988 a discussion workshop was held in which areas of concern were voiced from the floor. One of the recurring topics was the situation regarding Canadian Vibration Standards. In particular, there was criticism of ISO 1940 in that the majority of people that were balancing rotors during maintenance or after repair work, found that they could easily balance to one-half of the ISO Standard or to an even lower tolerance. This had resulted in loss of credibility for the ISO Standard and the various speakers asked why the Standard was not tightened, since this would be easily achieved.

In response to this concern, I met with the Chairman and members of the relevant ISO committee last year.

The ISO response is that the ISO Standard - 1940, was produced for production line type balancing of newly manufactured parts. An extensive survey was made to determine at what point further balance refinement became uneconomical as a trade off between production costs and operating life/reliability. The present Standard represents the point at which no increased life or reliability is considered to result from further balance refinement.

However, in the case where repair work or maintenance work of a given rotor is concerned, other factors apply. In this work, because of wear of other components of the machine, the effects of tear down, tooling errors and reassembly errors, it is considered prudent to indeed balance to (say) one-half the ISO Standard, or even lower. In such cases also, the additional effort involved in balance refinement is a far smaller proportion of the job cost than in the case of new production work where no allowance for wear, etc, need be made.

Possibly this explanation may not satisfy all of the those who brought this up at the last seminar. However, it should be noted that ISO Standards include input from all member countries and represent their valid experience. Some countries have detailed statistics to support their submissions and the Standard that eventually evolves represents a consensus of all members' experiences. It is worth noting here that ISO Standards are reference guidelines and not firm specifications.

2.0 STATUS OF ISO 7919 Parts 1, 2, 3 and 4

"Mechanical Vibration of Non-Reciprocating Machines - Measurement on Rotating Shafts and Evaluation."

The first four parts of this Standard have now been issued as Draft International Standards (DIS). This means that the work of the technical working group is complete and the documents are waiting for final ratification by the ISO Council in Geneva.

These documents have the following titles:

ISO 7919 - "Mechanical Vibration of Non-Reciprocating Machines - Measurement on Rotating Shafts and Evaluation"

Part 1 - General Guidelines

Part 2 - Guidelines for Large Land-Based Turbine Generator Sets

Part 3 - Guidelines for Coupled Industrial Machines

Part 4 - Guidelines for Gas Turbines

Canada participated actively in the formation of these Standards and voted for their acceptance. The MDSC Standards Working Group has recommended that they be adopted as Canadian Standards.

An important feature of the new Standard is the concept for classifying vibration criteria in "severity zones." In the past, criteria had been defined where operation was deemed "good," "satisfactory," "unsatisfactory" and "unacceptable."

In the new Standards, emphasis is placed on the definitions of the zones themselves and not on the zone boundaries. Although there has to be boundaries between the zones, these are not as rigid as before, as can be seen from the zone definitions.

Zone A - The vibration of newly commissioned machines would normally fall within this zone.

Zone B - Machines whose vibration falls within this zone are considered acceptable for long-term operation.

Zone C - When vibration values are recorded within this zone, it is common practice to initiate alarms which provide a warning that remedial action is required.

Generally, the machine may be operated for a limited period at these values until a suitable opportunity arises for remedial action to be taken.

Zone D - When vibration values are recorded which are in excess of the upper values for Zone C, it is common practice to initiate a "trip." Vibration values that fall into this zone are considered to be of sufficient severity to cause damage.

For a full appreciation of the philosophy of the new Standards, the complete text of ISO/DIS/7919 should be consulted.

The criteria for ISO/DIS/7919 Parts 2, 3 and 4 are shown in Figures 1, 2 and 3.

Figure 1

Criteria for ISO/DIS/7919/2

Recommended Values for Maximum Shaft Relative Displacement (S_{pk-pk}) for Large Steam Turbine Generator Sets at Zone Boundaries

Values in Micrometres peak-to-peak

Zone Boundary	Shaft Rotational Frequency r/min			
	1,500	1,800	3,000	3,600
	Maximum Shaft Relative Displacement			
A/B	100	90	80	75
B/C	200	185	165	150
C/D	320	290	260	240

Recommended Values for Maximum Shaft Absolute Displacement (S_{pk-pk}) for Large Steam Turbine Generator Sets at Zone Boundaries

Values in Micrometres peak-to-peak

Zone Boundary	Shaft Rotational Frequency r/min			
	1,500	1,800	3,000	3,600
	Maximum Shaft Absolute Displacement			
A/B	120	110	100	90
B/C	240	220	200	180
C/D	385	350	320	290

Figure 2

Criteria for ISO/DIS/7919/3

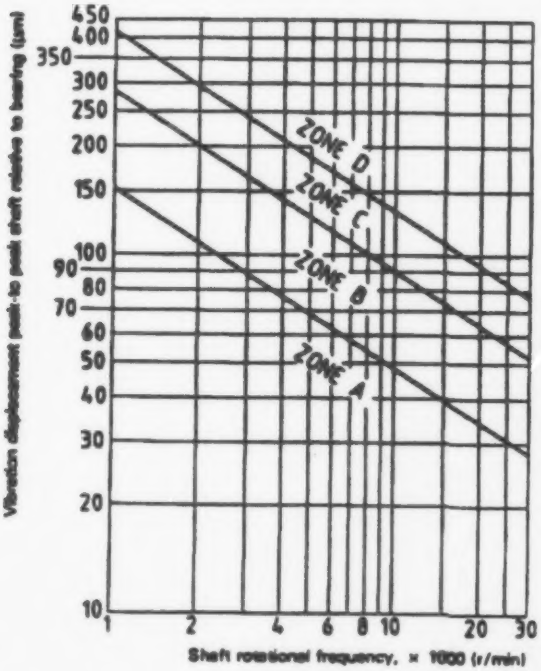

Recommended values of maximum relative displacement (S_{pk-pk}) as a function of the maximum service speed for coupled industrial machines

Figure 3

Criteria for ISO/DIS/7919/4

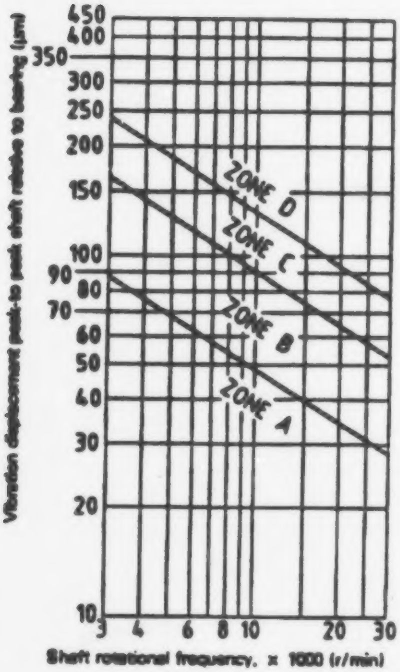

Recommended values of maximum relative displacement ($S_{pk - pk}$) as a function of the maximum service speed for gas turbines

3.0 STATUS OF ISO 7919 Part 5 - HYDRAULIC MACHINES

This Standard is still in an early draft stage. It will cover vertically and horizontally mounted machines from 120 - 3,600 Rev/min and > 1 MW. Canada is active in the preparation of this Standard. Henri Day of Hydro-Quebec is the Canadian representative on the Working Group and he has had significant input to the present working draft on behalf of Canada.

4.0 STATUS OF THE MAJOR REVISION OF ISO 2372

The title of the new ISO 2372 is: Mechanical Vibration - Measurements on Non-Rrotating Parts and Evaluation.

Part 1 of the Standard - General Guidelines has progressed to the "Committee Draft" (CD) stage. (This was formerly known as a (DP) draft proposal.) This means that it is out of the hands of the technical working group and is proceeding through the ISO parent committee stages towards ratification.

Part 2 of this document - "Guidelines for Large Land-Based Steam Turbine Generator Sets in Excess of 50 MW" is in its sixth draft version and is in the process of voting for acceptance as a CD. Canada coauthored this part of the Standard with the USA.

This part of the Standard has been written to replace Class III and IV machines of ISO 2372 and ISO 3945.

The main changes in the new Standard are:

(1) Consistency with and complementary to the shaft vibration standard for the same class of machine (ISO 7919/2).

(2) Emphasis on the classification of severity zones.

(3) A single set of criteria for 1,500/1,800 rev/min and a second set for 3,000/3,600 rev/min, only.

(4) The criteria for the 1,500/1,800 rev/min and the 3,000/3,600 rev/min speeds are not related by constant velocity.

(5) Criteria are provided in units of peak velocity and peak-to-peak displacement in addition to RMS velocity.

The proposed new criteria are shown in Figures 5, 6 and 7.

ISO 2372/2 Severity Zone Boundary Values

Figure 5

Evaluation Zone Boundaries Based on
Bearing Housing/Pedestal Vibration Velocity - (mm/sec RMS)

Vibration Velocity (RMS)

Zone Boundary	Shaft Rotational Speed (RPM)	
	1,500/1,800	3,000/3,600
A/B	2.6	3.8
B/C	5.3	7.5
C/D	8.3	11.9

Figure 6

Evaluation Zone Boundaries Based on
Bearing Housing/Pedestal Vibration Velocity - (mm/sec PEAK)

Vibration Velocity (0 - PEAK)

Zone Boundary	Shaft Rotational Speed (RPM)	
	1,500/1,800	3,000/3,600
A/B	3.7	5.3
B/C	7.4	10.6
C/D	11.8	16.8

ISO 2372/2 Severity Zone Values

Figure 7

Evaluation Zone Boundaries Based on
Bearing Housing/Pedestal Vibration Displacement - (micrometers PK-PK)

Vibration Displacement (PEAK-PEAK)

Zone Boundary	Shaft Rotational Speed (RPM)	
	1,500/1,800	3,000/3,600
A/B	45	30
B/C	85	60
C/D	135	95

Note: The values in Figures 6 and 7 are derived from Figure 5 by assuming the vibration consists of a sinusoidal component at shaft rotational frequency.

The new criteria were arrived at based on current world-wide practice and values acceptable to users and manufacturers in North America. A second consideration was that the criteria have a rational relationship to ISO 7919 Part 2. These considerations were consistent with the divergence from constant velocity that was required to eliminate the intolerably high equivalent displacement values, at 1,500/1,800 rev/min that were a problem in ISO 2372/3945.

Again, the complete document should be reviewed to correctly interpret the criteria and understand the rationale of the new Standard.

Revision of ISO 2372 Part 3

This revision deals with machines in the range of power from 300 kW - 50 MW. This part is in draft form but will conform to the general guidelines of the revised ISO 2372 Part 1. It will have vibration criteria governed by displacement at low frequencies and acceleration at high frequencies, with velocity dominant over a mid frequency range. The change over frequencies will be determined from the size of the machine.

(6) Reciprocating Machines

Work has begun on a Standard for reciprocating machines. The work is at an early stage and Canada is not involved in the working group. This work had originally been Part 6 of ISO 2372, but some current opinion is that those machines are so different, that a separate Standard will be required.

(6) Priorities for Future Parts of ISO/7919 and ISO/2372

The following is a partial list of machine groups under consideration and in process. The order of priority has not yet been fixed.

Proposed Future Parts of ISO 7919 and ISO 2372

Machine Group	Document Number	Example of Equipment	Status
Horizontal and vertical driven machines (< 50 MW) 120 - 15,000 RPM	2372/3	Turbine/motor driven generators, feedpumps compressors	In process
Reciprocating machines	2372/6 (or new Standard)	Engines for diesel generator sets. Marine propulsion and auxiliary engines	In process
Vertically and horizontally mounted hydraulic machines (120 - 3,600 RPM) > 1 MW	7919/5	Turbines, pumps	In process
Gas turbine sets	2372/4	Same as 7919/4	New
Aircraft engine derivative gas turbine sets	2372/8	Small/medium sized gas turbine generators	New
Large, low speed equipment	2372/9	Paper mills, cooling tower fans, rolling mills	New

The Standards Working Group of the MDSC would welcome comments on the above list and on this progress report. If anyone wishes to propose a standard category or a priority based on their experience, please contact any member of the MDSC.

VIBRATION TROUBLESHOOTING OF TWO HELICOPTER MAIN GEARBOXES

F. Dubé

Engine Laboratory
National Research Council Canada
Montreal Road, Ottawa, Canada
K1A 0R6

Laboratoire des moteurs
Conseil national de recherches Canada
Chemin Montréal, Ottawa, Canada
K1A 0R6

Abstract

Vibration analysis techniques were used to troubleshoot two Sea King helicopter main gearboxes displaying the same unusual vibration characteristics. These techniques can be grouped in three general categories, time averaging, spectrum analysis and gear analysis. Time averaging and gear analysis were carried out using a Mechanical Systems Diagnostic Analyzer (MSDA) while spectrum analysis was done using a spectrum analyzer. Each technique provided complementary information contributing to the solution of the problem.

The vibration problem was identified as a 2890 Hz tone synchronous with the input shafts of the gearboxes and equal to nine times their rotational speed. This paper describes the approach taken to identify the source of the problem along with the analysis techniques used.

Key words

helicopter, transmission, gearbox, vibration analysis, signal processing.

Biographical notes

François Dubé is a research officer at the Engine Laboratory of the National Research Council of Canada. He is presently engaged in research on condition monitoring of mechanical systems, particularly gas turbine engines and helicopter transmissions, using advanced vibration analysis techniques. He obtained a mechanical engineering Bachelor degree and a Master degree from Laval University. He is a member of the American Helicopter Society and of the Association of Professional Engineers of Ontario.

DÉPANNAGE DE VIBRATION DE DEUX BOÎTES DE TRANSMISSION D'HÉLICOPTÈRE

RÉSUMÉ

Des techniques d'analyse de vibration ont été utilisées pour le dépannage de deux boîtes de transmission principales d'hélicoptère Sea King présentant la même caractéristique vibratoire insolite et non-identifiée. Ces techniques peuvent être groupées en trois catégories, la moyenne en temps, l'analyse spectrale et l'analyse des engrenages. Le "Mechanical Systems Diagnostic Analyzer (MSDA)" fut utilisée pour l'analyse en temps et l'analyse des engrenages, tandis qu'un analyseur de fréquence a été employé pour l'analyse spectral. Chaque technique fournit de l'information complémentaire contribuant à la résolution du problème.

Le problème de vibration fut identifié comme étant une fréquence de 2890 Hz synchrone avec les arbres d'entrés des boîtes de transmission et égale à neuf fois leur vitesse de rotation. Cette publication décrit l'approche utilisée pour identifier la source du problème ainsi que les techniques d'analyse employées.

MOTS CLÉS

Hélicoptère, boîte de transmission, analyse de vibration, traitement de signaux.

NOTES BIOGRAPHIQUES

François Dubé est un agent de recherche employé au laboratoire des moteurs du conseil national de recherches du Canada. Il fait présentement de la recherche sur la surveillance du comportement des systèmes mécaniques, notamment appliquée aux turbines à gaz et aux boîtes de transmission d'hélicoptère, en employant des techniques avancées d'analyse de vibration. Il a obtenu un baccalauréat et une maîtrise en génie mécanique de l'université Laval. Il est membre de l'American Helicopter Society et de l'association des ingénieurs professionnels de l'Ontario.

VIBRATION TROUBLESHOOTING OF TWO HELICOPTER MAIN GEARBOXES

INTRODUCTION

As part of the acceptance test procedure, repaired or overhauled main gearboxes (MGB) from the Canadian Forces CH124 Sea King helicopter are required to meet specified vibration level criteria. The vibration generated by the gears and shafts of the main gearbox power train (see Fig. 1) needs to be below amplitude limits at specific frequencies related to important components. The vibration is measured with an accelerometer mounted on the ring gear, in a plane perpendicular to both the input and main rotor shafts, and the signal is processed with an analyzer that produces the vibration signature of the tested gearbox.

Two gearboxes, designated MGB "A" and MGB "B" in this paper, generated vibration energy at 2890 Hertz, a frequency not identified to be related to any component of the gearbox and consequently not usually monitored. Because of the maintenance history of gearbox "A", it was determined that a potential vibration problem existed within the two gearboxes. This paper presents the approach and techniques used to troubleshoot this peculiar problem.

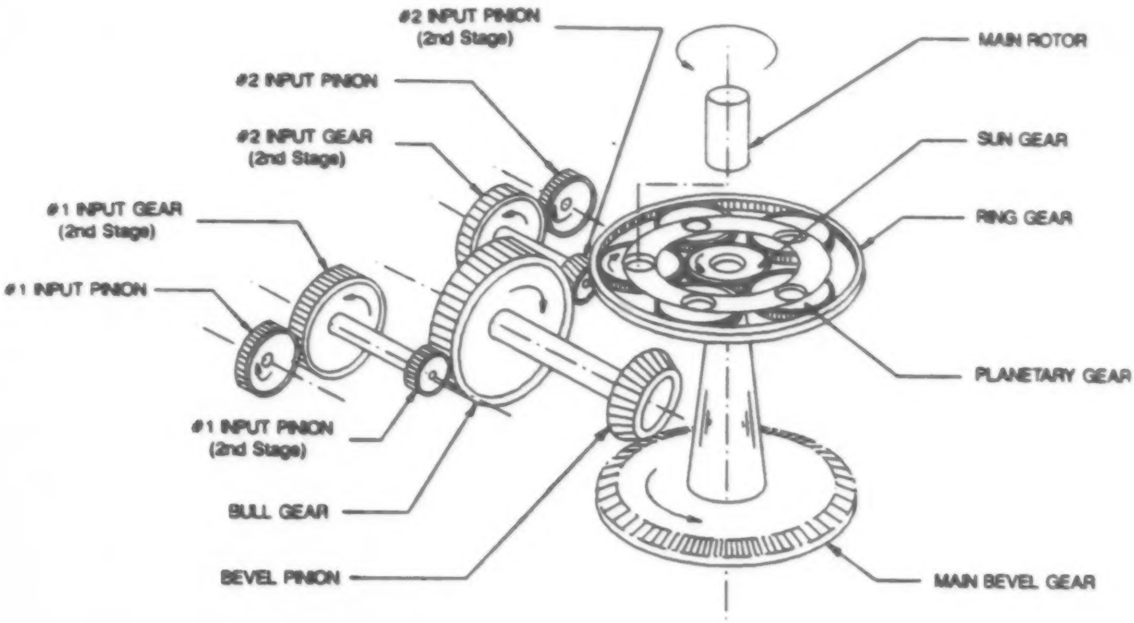
#2 INPUT PINION (2nd Stage)
MAIN ROTOR
#2 INPUT PINION
#2 INPUT GEAR (2nd Stage)
SUN GEAR
#1 INPUT GEAR (2nd Stage)
RING GEAR
#1 INPUT PINION
PLANETARY GEAR
#1 INPUT PINION (2nd Stage)
BULL GEAR
BEVEL PINION
MAIN BEVEL GEAR

Figure 1. Diagram of the Sea King MGB power train.

MAINTENANCE LOGBOOK REVIEW

The first step was to research all the previous vibration signatures from other MGBs tested on the same test stand and under the same operating conditions. It was determined that, although measurable vibration levels at the 2890 Hz tone were occasionally present, their magnitudes were considerably less than those measured in the present cases. The 2890 Hz tone magnitudes of all other MGBs tested before were less than 0.5 g and were not listed in the ten highest peaks of the frequency spectrums. On the other hand, for gearboxes "A" and "B", the magnitudes of the 2890 Hz tone were the fourth most dominant of their vibration signature with levels of 3.7 g and 4.8 g respectively.

Gearbox "A"

The gearbox "A" maintenance logbook indicated that the gearbox had been overhauled in 1988. The vibration measurements taken during the acceptance run showed that, while the amplitudes of all monitored frequencies were within limits, the 7.2 g vibration level measured at the 2890 Hz tone was abnormal. After several unsuccessful maintenance actions to rectify this situation, the gearbox was released for installation in an aircraft, providing that oil debris and vibration levels be closely monitored. After 282.3 hours of operation, MGB "A" was removed from the helicopter, due to metallic particles found in the filters, and sent back to the contractor for repair. The technical investigation revealed that the cage of one of the bearings supporting the bull gear and bevel pinion shaft was cracked and worn. The gearbox was repaired, but the 2890 Hz tone was still significant on the vibration signature taken after the repair.

Gearbox "B"

Gearbox "B" was removed because of metal contamination (chip light indication) in 1988 and sent to the contractor for overhaul. It was found that the source of the contamination was a helical input gear with a broken tooth. After rebuild, the vibration signature obtained during the acceptance run was very similar to MGB "A" signature. Thus it was decided to wait the results of the troubleshooting carried out by NRC before undertaking any action.

VIBRATION MEASUREMENTS

The two gearboxes were instrumented with nine accelerometers and one phase lock tachometer for further data acquisition. The accelerometers were installed on the gearbox housing at locations were a direct path to internal shaft support existed. They were installed at the following locations; two near each input in the axial and lateral axes, two on the ring gear in the vertical and lateral axes, two on the bottom cap in the vertical and axial axes, and one on the accessories housing in the axial axis. The tachometer was installed on the tail take off shaft producing a one per rev signal.

The gearboxes were tested following the procedure used during a normal acceptance test run and the vibration signals were recorded on a 14 channel tape recorder having the capability to record signal from DC to 50 kHz. Measurements were taken at two operating conditions: 750 and 1500 kilowatts total input power at a main rotor shaft speed of 206 rpm.

SIGNAL ANALYSIS

The signals were analyzed at NRC using the Mechanical Systems Diagnostic Analyzer (MSDA) and a Spectral Dynamic spectrum analyzer model SD380. The MSDA was used for data acquisition, time averaging and gear analysis, and the SD380 was used for spectrum analysis and zooming.

Time averaging

Synchronous time averaging was used to determine if the 2890 Hz tone was related to any particular shaft in the gearbox. First, using only the vibration signal from the accelerometer mounted on the ring gear in the lateral axis, time averages of the vibration signal, sampled over 256 rotations of the shaft, were obtained for each rotating shaft of the power train. It was found that the unidentified vibration was synchronous only with the input shafts of the gearboxes. As the use of a single accelerometer did not allow to differentiate between the two inputs, the same process was applied to the accelerometers mounted on each input.

The time signals from each MGB "A" input are shown in Figures 2 and 3. The amplitude of the 2890 Hz tone from the #2 input was 19.7 g versus 3.6 g from the #1 input. For MGB "B" the situation was similar but for the reverse input, the #1 input 2890 Hz amplitude was 22.0 while it was 4.4 for the #2 input.

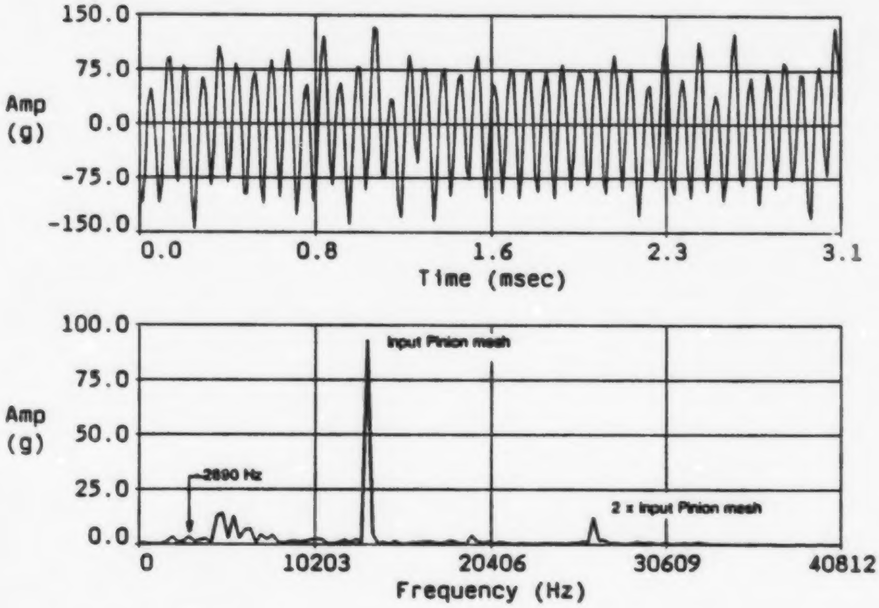

Figure 2. Time averaged signal and FFT spectrum of MGB "A" #1 input vibration.

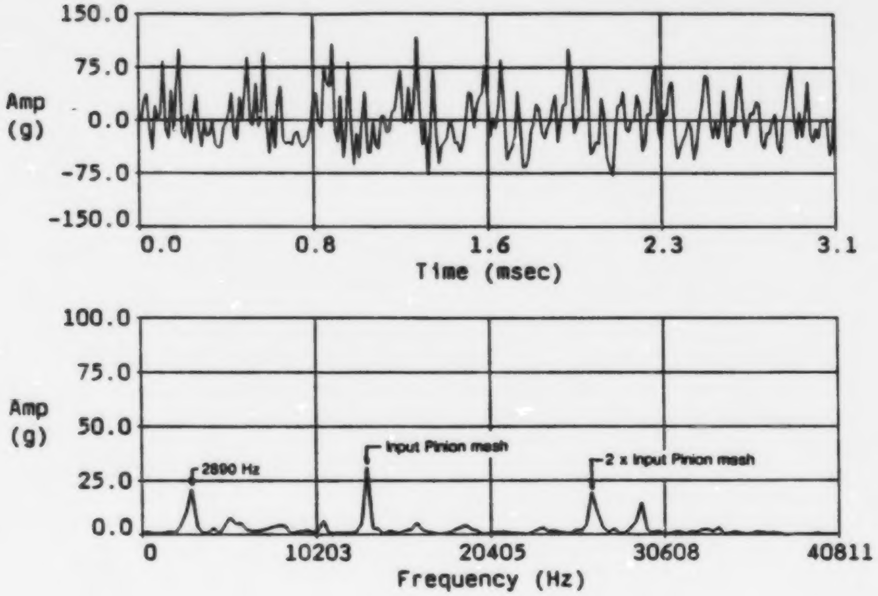

Figure 3. Time averaged signal and FFT spectrum of MGB "A" #2 input vibration.

The synchronous time averaged signal from each shaft were analyzed, abnormalities were observed with the time signals from MGB "A" #2 input 1st and 2nd stage, as well as for MGB "B" #1 input 1st and 2nd stages. Figures 4 and 5 show the time averaged signals of the 2nd stages of MGB "A" #1 and #2 input respectively. Generally a good pair of gears produces a vibration signal where the meshing frequency is dominant and the time averaged signal has a sinusoidal shape. The signals from the MGB "A" #1 input pinion (Figure 2) and of #1 input 2nd stage (Figure 4) are representative of vibration signals produced by good gears. Figures 3 and 5 display time signals that are irregular and quite different from the corresponding #1 input 1st and 2nd stages signals.

Another significant characteristic of the vibration signals related to MGB "A" #2 input was the relatively high level of the second harmonic of the input pinion meshing frequency. The presence of a strong second harmonic is usually related to misalignment. Furthermore, the first and second harmonics of the #2 input pinion mesh was modulated by the 2890 Hz tone as manifested by the sidebands in the frequency display of Figure 2. Similar characteristics were also observed for MGB "B".

Analysis of the time averaged signals allowed the identification of the 2890 Hz tone as being the ninth harmonics of the input shaft frequency. Also it was determined that its source resided with the #2 input of MGB "A" and with the #1 input of MGB "B".

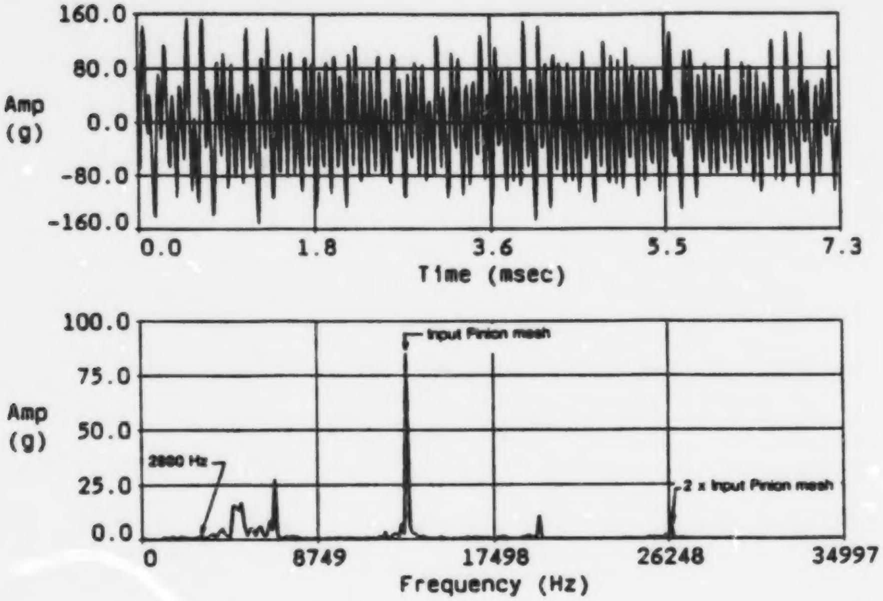

Figure 4. Time averaged signal and FFT spectrum of MGB "A" #1 input 2nd stage vibration.

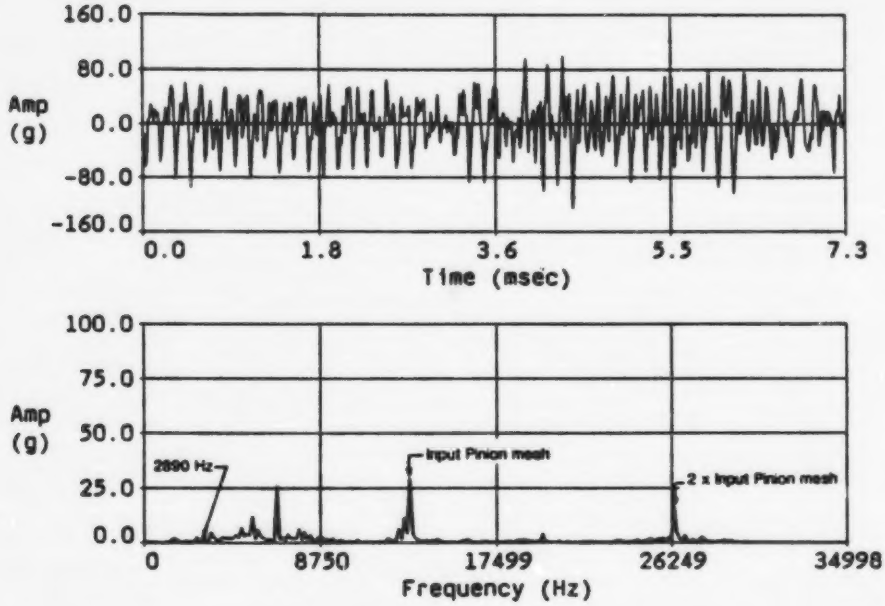

Figure 5. Time averaged signal and FFT spectrum of MGB "A" #2 input 2nd stage vibration.

Spectrum analysis

In order to confirm the indications provided by the synchronous time averaging analysis, the vibration signals from the inputs of the two gearboxes were analyzed using spectrum averaging.

As seen in Figure 6, the 2890 Hz tone was a significant peak for the #2 input of MGB "A". Its amplitude was almost 6 time higher than for input #1 which was a clear indication that the source of this tone was related to the #2 input. The #2 input zoom spectrum of Figure 7 contains strong 321.2 Hz sidebands on each side of the 2890 Hz tone. These sidebands are the rotational speed of the input shafts.

The vibration behaviour of MGB "B" was similar to MGB "A" as seen in Figure 8. In this case the 2890 Hz was predominant for the #1 input with its amplitude being 5 times higher than the #2 input. Here the 321.2 Hz were also present but less significant. The main characteristic of MGB "B" vibration, which was not significant for MGB "A", was the very high level (104 g) of the #1 input second harmonic of the input pinion meshing frequency shown in Figure 9. The sidebands on both sides indicate that the modulation generated by the 2nd stage input shafts (137.2 Hz) was more important than the one from the first stage.

The analysis of the vibration signals, obtained through spectrum averaging and zooming, indicated that the problem resided with the #2 input of MGB "A" and the #1 input of MGB "B". This confirmed the assessment done using time averaging and provided supplementary information indicating that the MGB "B" #1 input 2nd stage could also be at fault.

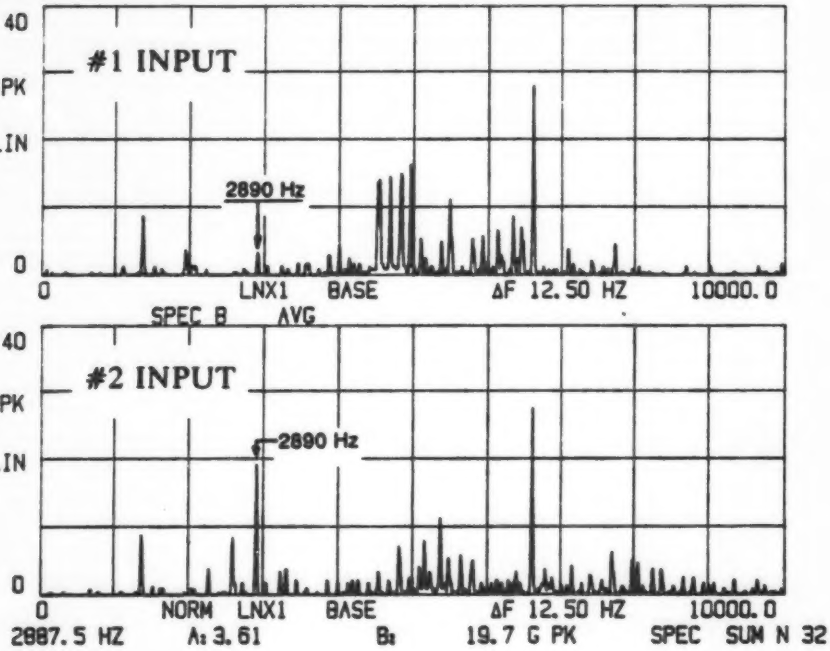

Figure 6. Frequency of MGB "A" #1 and #2 inputs, 0-10000 Hz.

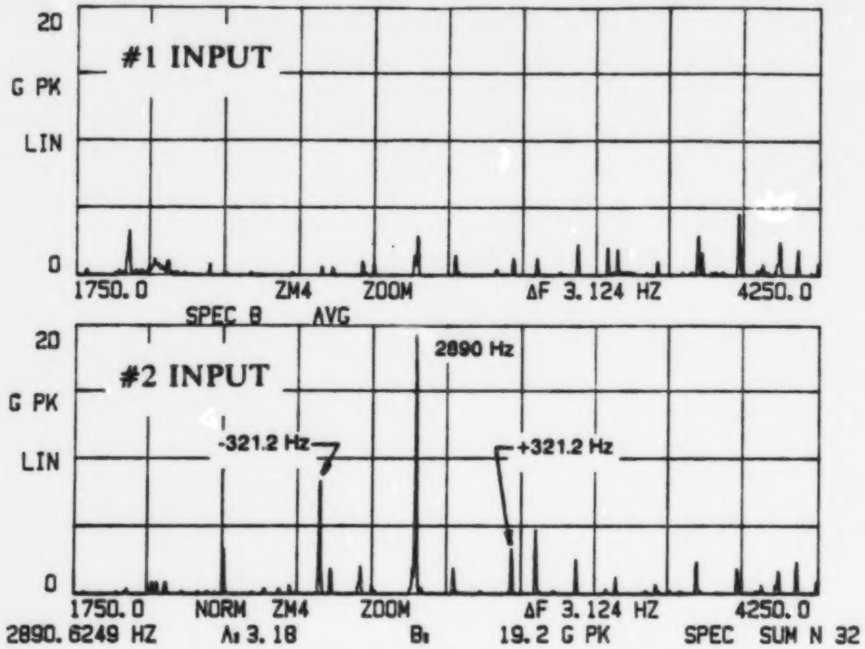

Figure 7. Zoom spectra of MGB "A" #1 and #2 inputs, 1750-4250 Hz.

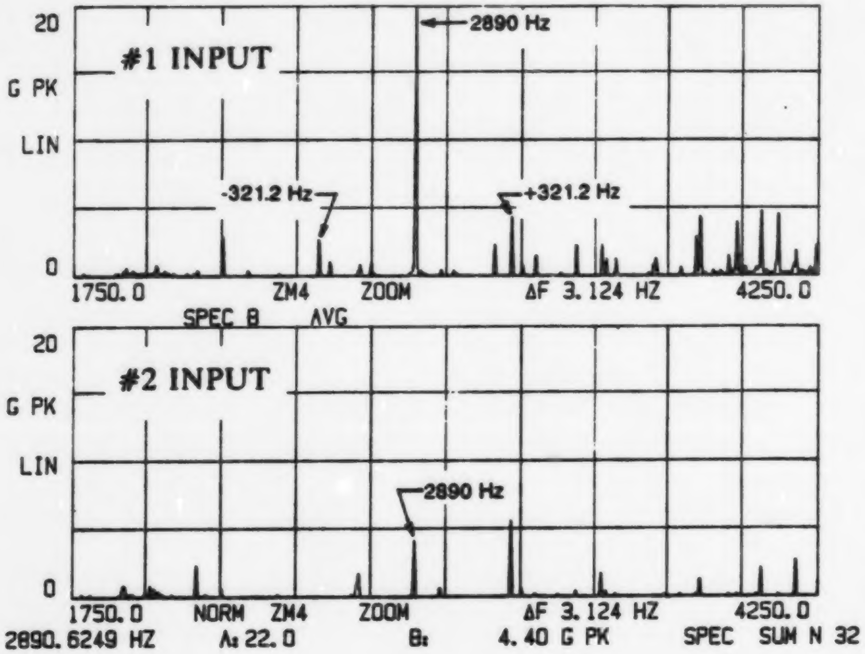

Figure 8. Zoom spectra of MGB "B" #1 and #2 inputs, 1750-4250 Hz.

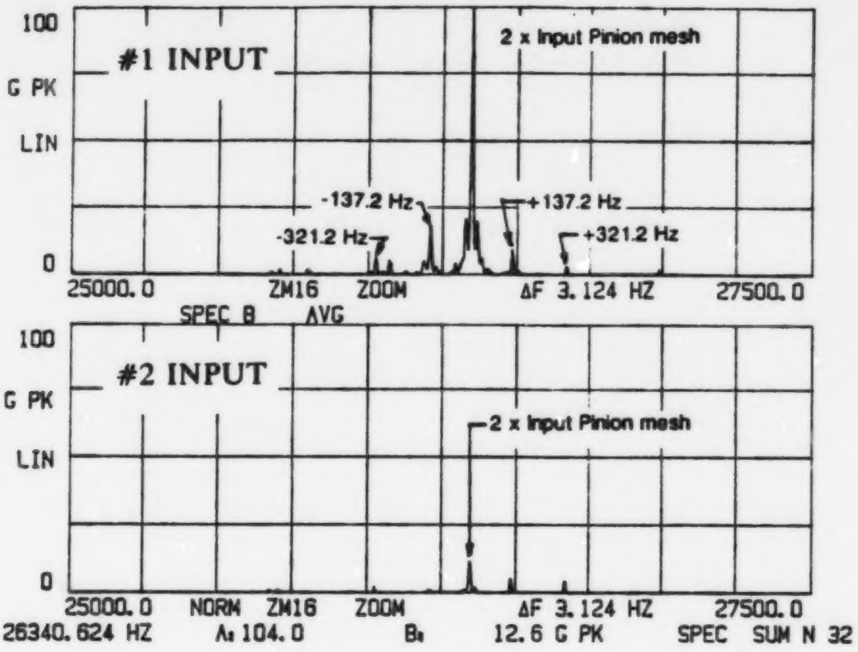

Figure 9. Zoom spectra of MGB "B" #1 and #2 inputs, 25000-27500 Hz.

MSDA data analysis

The Stewart Hughes Limited gear analysis software package SGAV, which runs on their Mechanical Systems Diagnostic Analyzer (MSDA), was used to assess the gears of the power train (Figure 1). This analysis package is based on synchronous time averaging of the vibration signal and reduces the complex signals to some significant numbers. Some of the numbers calculated by SGAV are for monitoring purposes and require baseline data. The other numbers, called Figure of Merits (FM) numbers, provide diagnostic information by extracting characteristic features of the vibration signal related to individual faults. The FM numbers, used for the evaluation of the two gearboxes, along with a description of their usage are listed in Table 1.

As there was no baseline data available, only the numbers based on the signature pattern analysis were used to assess the gears. The results of the MSDA analysis of MGB "A" and MGB "B" are listed in Tables 2 and 3 respectively. The values outside the limits applicable to each FM numbers are underlined, and the values close to the limits are in parentheses.

Four of the five FM numbers indicating faults in MGB "A" were related to the #2 input. Both FM3 numbers for the two stages of the #2 input are outside the FM3 band-limit (0.95 - 1.05). This parameter is usually affected by faults not related to the gear. It is usually sensitive to faults such as structural parametric excitation, instability within journal bearings or critical speed vibration. The FM1A number exceeding the limit for the #1 input pinion (2nd stage) is due to the very low level of the mesh frequency vibration. As the FM1A number is the ratio of the signal modulation to the mesh frequency level, a relatively low modulation of the signal can appear significant.

Table 1. Gear analysis parameters

FM NUMBER	DESCRIPTION	USAGE
FM1A-B	• Measure of the low frequency amplitude modulation in the vibration signature. • Ranges from 0 (no modulation) to 1.0. • Should be less than 0.1, a danger exist if it is greater than 0.5.	Gear alignment, location, eccentricity.
FM1A	• Measure of the amplitude modulation in a narrow-band (±2 sidebands of the mesh frequency). • Same limits as for FM1A-B.	Same as FM1A-B.
FM3	• Ratio of the zero-crossing count of the signal average to the extracted meshing frequency waveform. • Acceptable if between 0.95 and 1.05, serious if less than 0.6.	Drive faults, parametric excitation such, as system resonance, instability in journal bearings.
FM4A	• Kurtosis (4th statistical moment) of the residual gear signature. • The residual is obtained by removing all discretely identifiable tones within a gear averaged spectrum. • Sensitive to clearly defined impulsive events. • Acceptable if less than 3.5, dangerous if above 4.0.	Tooth damage.
FM4B	• The ratio of the standard deviation of the residual signature to that of the original vibration signature. • A measure of the distributed surface noise. • Acceptable if less than 0.5, rising to 1.0 as damage increases.	Wear faults.

Table 2. MSDA results for MGB "A".

Gear	FM1A-B	FM1A	FM3	FM4A	FM4B
#1 Input pinion	0.01	0.01	1.00	2.66	0.28
#2 Input pinion	0.07	0.12	0.80	2.97	(0.45)
#1 Input (2nd stage)	0.02		0.99	2.83	0.37
Gear		0.02			
Pinion		0.67			
#2 Input (2ND STAGE)	0.03		0.75	2.97	(0.43)
Gear		0.28			
Pinion		0.30			
Bull gear	0.03	0.21	1.00	3.11	0.21

The MSDA results for MGB "B", presented in Table 3, are less conclusive than for MGB "A". Seven FM numbers were outside the limits, three of them were related to the #1 input, three to the #2 input, and the other to the bull gear. The two FM1A numbers above the limits were caused by the very low vibration level of the mesh frequency and thus not judged significant. There were four FM3 numbers outside the limits, as the two input shafts are linked together through the bull gear, it was estimated that the four indications were caused by a single fault. This same fault could have also caused the FM4B number related to the #2 input pinion to exceed the limit. Two other numbers were closed to their respective limits, both were related to the #1 input pinion (2nd stage).

Table 3. MSDA results for MGB "B".

Gear	FM1A-B	FM1A	FM3	FM4A	FM4B
#1 Input pinion	0.07	0.04	0.63	3.38	0.31
#2 Input pinion	0.12	0.04	0.62	2.72	0.64
#1 Input (2nd stage)	(0.41)		0.68	3.10	(0.49)
Gear		0.15			
Pinion		0.77			
#2 Input (2nd stage)	0.08		1.00	3.08	0.30
Gear		0.09			
Pinion		0.52			
Bull gear	0.04	0.26	1.11	2.90	0.34

MAINTENANCE ACTIONS

The maintenance actions carried out on the two gearboxes were governed by different factors such as parts availability and the requirement to supply a serviceable gearbox for aircraft installation as soon as possible. As there was no fault indication with MGB "A" #1 input components, the #1 input 1st stage and 2nd stage shafts and gears of MGB "A" were installed in MGB "B". New #1 and #2 input components were installed in MGB "A". On the acceptance test, the vibration levels of both gearboxes were acceptable which indicated that the vibration troubleshooting carried out had been successful. Though the parts removed were inspected and no visual fault was found that could explain the vibration problem.

CONCLUDING REMARKS

Different vibration analysis techniques were used to troubleshoot an unusual vibration problem affecting two Sea King main gearboxes. The techniques allowed to identify specific components in each gearbox as the probable source of the problem. The unusual vibration was not present after the replacement of these components which shows that the findings of the troubleshooting procedure were correct.

The use of several analysis techniques to troubleshoot a problem increases the confidence level in the findings and reduces the possibilities of making a wrong assessment.

ACKNOWLEDGEMENTS

This work has been carried out for the Director of Maritime Aircraft Engineering and Maintenance of the Department of National Defence.

REFERENCES

1. Randall, R.B. *Frequency Analysis*. Bruel & Kjær, September 1987.

2. Stewart R.M. *Some Useful Data Analysis Techniques for Gearbox Diagnostics*. Application of Time Series Analysis, ISVR, University of Southampton, Sept 1977.

3. Nicks, J.E. and Krishnappa, G. *Evaluation of Vibration Analysis for Fault Detection Using a Gear Fatigue Test Rig*. Proceedings of the Institution of Mechanical Engineers, First International Conference, Gearbox Noise and Vibration, 1990-5, pp. 165-172.

4. Dubé, F. *CH124 Helicopter Main Transmission Vibration Analysis Review*. Institute of Mechanical Engineering, National Research Council, Ottawa, Ontario. Report no. CTR-ENG-023 (to be published).

CONDITION MONITORING OF BORING TOOLS

Z. Reif, M. Mailloux and S. Prsa

Department of Mechanical Engineering
University of Windsor
Windsor, Ontario N9B 3P4

ABSTRACT

Market trends of recent years, particularly in the automotive industry, have significantly increased the need for improvements in productivity and product quality. In untended manufacturing the most important results are achieved by the use of machine condition monitoring with predictive maintenance systems. One of the most common causes of machine downtime on transfer lines and F.M. systems is tool damage and to a lesser extent tool wear. From previous work it was determined that vibration, as the sensing medium, produced best results, particularly with drills, in detecting these faults.

In order to expand the scope of the general investigation, a feasibility study was carried out to determine if a similar approach could be used with boring tools. Several boring tools were operated until completely worn. At regular intervals the degree of wear of the tool was measured and the vibration recorded. Subsequent analysis indicated that a definite relationship existed between the degree of wear and the resulting changes in vibration. Although the results were not as good as those obtained with drilling, several changes in procedure were indicated which are likely to produce improvements.

Keywords: Boring, Tool Condition Monitoring, Machine Diagnostics

---

Dr. Zygmunt Reif is a Professor in the Department of Mechanical Engineering at the University of Windsor. He has received his B.Sc. (Eng.) and Ph.D. degrees in Mechanical Engineering from the University of London and he is registered as a Professional Engineer in the Province of Ontario. His principal fields of research are machinery vibration and noise.

Mr. Mark Mailloux and Mr. Steve Prsa have recently obtained the B.A.Sc. degree in Mechanical Engineering from the University of Windsor and are employed in industry as Mechanical Engineers.

RÉSUMÉ

Face aux tendances observées sur le marché au cours des dernières années, en particulier dans le domaine de l'industrie de l'automobile, il devient de plus en plus nécessaire d'améliorer la productivité et la qualité des produits. En fabrication automatisée, cela implique principalement la surveillance du comportement des machines à l'aide de systèmes de maintenance préventive. L'endommagement des outils et, dans une moindre mesure, l'usure des outils constituent l'une des principales causes d'interruption des machines sur les chaînes-transferts et sur les systèmes à modulation de fréquence. Des travaux antérieurs ont montré que les vibrations constituaient le meilleur indice du comportement des outils, en particulier des perceuses.

Afin d'étendre la portée du projet de recherche, nous avons réalisé une étude de faisabilité dans le but de déterminer s'il serait possible d'appliquer une méthode similaire aux outils de forage. Nous avons ainsi utilisé plusieurs outils de forage jusqu'à usure complète. A intervalles réguliers, nous avons mesuré le degré d'usure de l'outil et les vibrations. Une analyse subséquente des résultats a montré qu'il existait effectivement une relation entre le degré d'usure et les changements observés dans les vibrations. Les résultats n'étaient pas aussi bons que ceux obtenus avec les perceuses, mais ils nous ont permis de proposer plusieurs modifications dans les méthodes employées susceptibles d'entraîner une amélioration de la productivité.

MOTS CLÉS: forage, surveillance du comportement des outils, diagnostics des machines.

BIOGRAPHIE

Monsieur Zygmunt Reif est professeur au Département de génie mécanique de l'université de Windsor. Il a obtenu son baccalauréat (génie) et son doctorat en génie mécanique à l'université de London et il détient le titre d'ingénieur professionnel de la Province de l'Ontario. Ses domaines de recherche principaux sont les vibrations et le bruit des machines.

Monsieur Mark Mailloux et Monsieur Steve Prsa ont récemment obtenu leurs baccalauréats en sciences appliquées à l'université de Windsor et ils travaillent actuellement comme ingénieurs en mécanique dans l'industrie.

INTRODUCTION

Market trends of recent years, particularly in the automotive industry, have imposed requirements for significant improvements in productivity and product quality. These factors, together with the continuing expansion of automation, have stimulated the development and application of preventive and predictive maintenance systems in the manufacturing industry. The best potential for cost reductions exists in its metal removing sectors. The corresponding definitions of machinery diagnostics and prognostics are also often used. Although a clear definition does not exist, preventive maintenance is predominantly based on periodic measurements, which are generally performed manually at daily, weekly and even monthly intervals. Maintenance decisions are based on magnitudes of results. Predictive maintenance, on the other hand, depends predominantly on continuous measurements under computer control. Maintenance decisions are made in this case on the basis of magnitudes, trends or patterns of results. Both types have their preferred areas of application, where best results are produced within the prevailing operational and cost constraints. Although the general trend is towards increasing computer control and the application of expert systems, there will always be a place for manual procedures.

The application of condition monitoring procedures provides in most cases sufficient information to detect developing failures of essential machine components. This permits extension of the useful life of the component and it reduces significantly the probability of a catastrophic failure. The most important aspect is the corresponding decrease of machine downtime and improvements in the general management of maintenance. Cost studies(1) indicate in most cases significant reductions and a pay-back period for the expense of installing such systems of only a few months.

Condition monitoring is currently practiced, at various levels of sophistication, predominantly in the power and process industries, where machinery generally operates at constant speeds and loads in a relatively benign environment. Application of these procedures to manufacturing with automated machinery is more difficult but potentially more rewarding. This is particularly true with machining systems, of which transfer lines are the most important examples, since this type accounts for the majority of metal removing work in North America. Transfer lines consist of several automatic machine tools, sometimes as many as fifty, which are interconnected by a common guideway. Workpieces are moved in a continuous stream sequentially from one machining station to the next, until all cutting is completed. For example, internal combustion engine blocks enter a transfer line system as rough castings at once end and leave it completely machined at the other end at a rate of approximately two hundred units per hour. The process is completely untended and the mode of operation is cyclic with continuous changes in motion and load. The working environment is very hostile, requiring almost complete enclosure by safety guards. The value of production can be more than $30,000 per hour and the average downtime is around 25%. It is predominantly caused by unexpected component failures with bearing and tools being the main contributors. Even a partial reduction of the downtime has the potential of significant decreases of operating cost and thus corresponding improvements of productivity.

Condition monitoring is based on measurements of an appropriately selected physical property of the system, which is often referred to as the sensing medium. Although several, widely differing properties are used, in applications to machining systems vibration is emerging as the preferred medium. It has a wide scope of application, the transducers are relatively small and robust, it can be applied to on-line monitoring, and perhaps most importantly it can provide simultaneously information on the condition of several vital components. A large number of descriptors, such as for example maximum value, rms average, crest factor, several properties of the frequency spectrum, cepstrum, variance, Kurtosis, acoustic emission, etc. Vibration transducers are compact, robust and relatively inexpensive. In many respects, condition monitoring with vibration is the old "screwdriver-to-the-ear" method which is made respectable by the application of electronics and computer control.

The results presented in this paper are part of a general project to determine the basic relationships between the deteriorating condition of essential machine tool components and the resulting changes of vibration. The measurements are taken from the main structure, as near to the cutting area as permitted by the operating constraints. Although the primary objective is application to transfer lines, the results are useful for general metal cutting applications.

TOOL CONDITION MONITORING

Although tool condition monitoring is not yet fully developed, several methods are already in use. Most are based on measurements of power, force, torque and vibration(2,3,4,5,6,7). One of the most promising approaches is the use of piezo-electric films in the tool holder.

Output data from sensors can provide information on the degree of wear and damage of tools. In untended manufacturing the latter is more important. At present most methods are fairly good at detecting serious tool damage, but are generally far less effective in determining the degree of wear. On transfer lines, however, it is common practice to change all tools after each working shift. This results in significant under-utilisation, but it reduces the incidence of machine downtime due to unexpected tool deterioration. It is a management decision, which is based on relative costs.

The results produced with vibration as the sending medium are at least as good as those obtained with other methods. In addition there are several other advantages. Vibration transducers are relatively small and inexpensive. They are also more robust and can be very easily and quickly mounted and replaced. Perhaps most importantly, in many applications to transfer lines, the extension of the monitoring functions of an existing system to include tool wear and damage, requires only the addition of appropriate software to the control computer.

MEASUREMENTS WITH BORING TOOLS

Investigation of tool condition monitoring by means of vibration were extended, after studies of drilling and turning, to boring, which is one of the major metal cutting functions employed on transfer lines. The results presented here were obtained from an initial feasibility study to evaluate corresponding dynamic conditions and to determine the best measuring procedures.

From previous work it was established that a single vibration transducer, which was mounted on the structure near the tool, provided generally satisfactory output data for monitoring the condition of tools, bearings of the tool spindle, power drive components and even for some general operating properties, such as for example rotational unbalance. It was also shown that measurement of vibration acceleration produced best results. This was partly due to the greater sensitivity to developing damage in higher frequency regions, where potential masking effect of other machinery vibration was negligible, and also due to the relatively small size of accelerometers. One of the most important operational impediments on transfer lines is a very restricted space in the working zone. Therefore, displacement or velocity transducers, because of their relatively larger size, could not be used as sensors in the majority of applications.

A standard lathe with a special tool post and holder, was used for the measurements. A HSS tool with a relatively short and integral bar was clamped in the horizontal holder on which accelerometers were mounted. Workpieces were cut in 70 mm length from cylindrical bar stock of 4340 cold drawn alloy steel and were predrilled concentrically to 6.5 mm dia. This choice of workpiece was predominantly determined by availability; large numbers of such specimen were left over after previous drilling tests. Although relatively small boring tools had to be used, these specimen were satisfactory in most other respects.

In all tests the workpieces were rotated and the tool was stationary. The depth of cut, surface speed and feed were selected to be within recommended values. At regular intervals the vibration acceleration was recorded and tool wear was measured by means of a travelling microscope along the rake and relief faces. Rake face measurements were difficult to perform and were generally inconsistent because of pitting and edge built-up. Best results were obtained with the relief face, therefore these measurements were used for evaluating the final results.

Accelerometers were attached to the tool holder in the vertical and horizontal directions. Locations of these transducers were varied in preliminary cutting tests to determine best vibration response. During the actual cutting test sequences their output was recorded at regular intervals in the time and frequency domains. An FFT analyser was used for this purpose and for the following analysis.

DISCUSSION OF RESULTS

Figure 1 shows the vibration acceleration frequency spectra of one boring tool at different levels of wear. The lowest characteristic corresponds to a nearly new tool and the highest to the almost completely worn condition. Well defined changes in magnitudes of the spectrum at increasing wear are evident. The general shape, however, remains essentially unaltered. Modal analysis, which was performed on the tool-holder-post system(8), produced dominant natural frequencies at 750, 1850 and 3000 Hz. The three main peaks of Figure 2 are located approximately at these frequencies, which suggests that the vibration response, which is excited by the cutting forces, depends predominantly on the structural properties of the tool head assembly. Similar results were obtained with the drilling experiments, where it was initially expected that the vibration of the relatively slender and flexible tool would predominantly influence the spectrum.

In the feasibility study only three tools were tested. The corresponding results of the magnitude of the major peak in the spectrum, centered at 3000 Hz, against normalised tool wear, are shown in Figure 2. Normalised wear was obtained by dividing each wear measurement by the maximum value, which was determined at the end of the tool wear range. In all previous testing of other types of tools it was found that a significant variability in endurance existed between nominally identical new tools. The application of normalised wear resulted in originally somewhat scattered graphs to coincide more closely and exhibit a well defined trend, as can be seen in Figure 4. Although in Figure 2 a general increase of vibration with wear is evident, it is not as good in respect of changes of magnitudes and trends as that obtained for example with drills, Figure 4. There are two main reasons for this. Firstly, the measurement of wear in this case was less consistent because of greater geometric complexity of the cutting edges. In addition, the boring tools were of relatively low quality, which resulted in rapid wear without a clear condition of failure. Thus the choice of the common denominator, which as the measured value at maximum wear, was not clearly defined and likely to be inconsistent. Also corresponding results obtained for drills were slightly better, but a significant improvement was achieved by the application of statistical descriptors, such as standard deviation which is shown in Figure 4. A comparison of three descriptors is shown in Figure 3 for one of the tools. It is evident that measurement of peak amplitude of the frequency spectrum produces best results.

As mentioned previously well defined conditions of failure were not achieved. it is very likely that chipping or breaking of the tool would produce similar and well defined changes in vibration acceleration as those shown for a drill in Figure 5.

CONCLUSIONS

Although the results obtained in this feasibility study were not outstanding, sufficient evidence for a good condition monitoring potential is present. Significant improvements can be achieved by refining and extending the experimental and evaluating procedures. In particular, larger and better quality tools, and the application of statistical analysis to the data, are likely to produce best results. Also, because of the equipment used in this case, measurements were only made in the range 0-10 KHz. As was shown in drilling experiments, best results were obtained in the 10 KHz to 20 KHz. Thus an extension of the measuring range has the potential of further improvements.

REFERENCES

1. Reeves, C.W., Vibration Monitoring on Chemical Process Plant - the Justification, Proceedings of the 2nd International Conference on Condition Monitoring, London, England, May 1988, pp. 1-15.

2. Stockline, L.E., New Developments in Tool Condition Inspection Systems, Proceedings of the 1987 Eastern Manufacturing Technology Conference, Springfield, Massachusetts, November 1987, Vol 2, pp. 179-196.

3. Beyer, P.J., Tool Condition Sensor for Automated Manufacturing, Proceedings of the 1987 Eastern Manufacturing Technology Conference, Springfield, Massachusetts, November 1987, Vol 4, pp. 206-226.

4. Suzuki, I., Inasaki, I. and Koshimizu, S., Acoustic Emission Detection of Cutting Tool Chipping, Proceedings of the 1987 Eastern Manufacturing Technology Conference, Springfield, Massachusetts, November 1987, Vol 1, pp. 197-216.

5. Kuhbauch, P. and Quante, F., A New System for Tool Wear and Failure Monitoring in Multispindle Drilling Heads, VDI Berichte Nr. 644, 1987 Proceedings of the 5th International Symposium on Technical Diagnostics, Paderborn, F.D.R., October 1987, pp. 275-282.

6. Kincaid, H.R., Machine Tool Action Monitoring Systems, Proceedings of the 10th Machinery Dynamics Seminar, N.R.C., Calgary, September 1988, pp. 349-372.

7. Moore, T.N. and Pei, J., The Determination of Milling Cutter Tool Condition Using Vibration Signals, Proceedings of EAM 90, Kingston, 1990, pp. 297-302.

8. J. Miller, Modal Analysis of Machine Tools, Senior Project Report, Department of Mechanical Engineering,University of Windsor, 1990.

9. Reif, Z., Lau, H.K., Monitoring the Condition of Drills by Means of Vibration, Proceedings of the 7th International Modal Analysis, Las Vegas, February 1989, pp. 1022-1027.

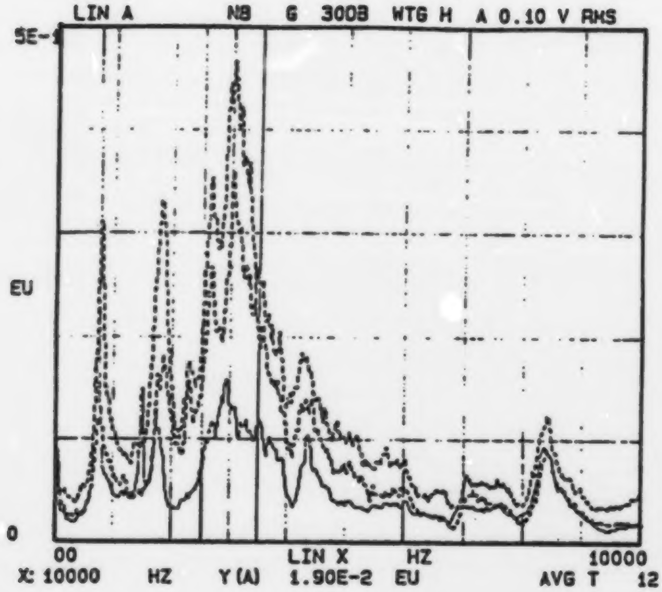

Fig. 1. Changes of Frequency Spectrum of Acceleration with Progressing Tool Wear

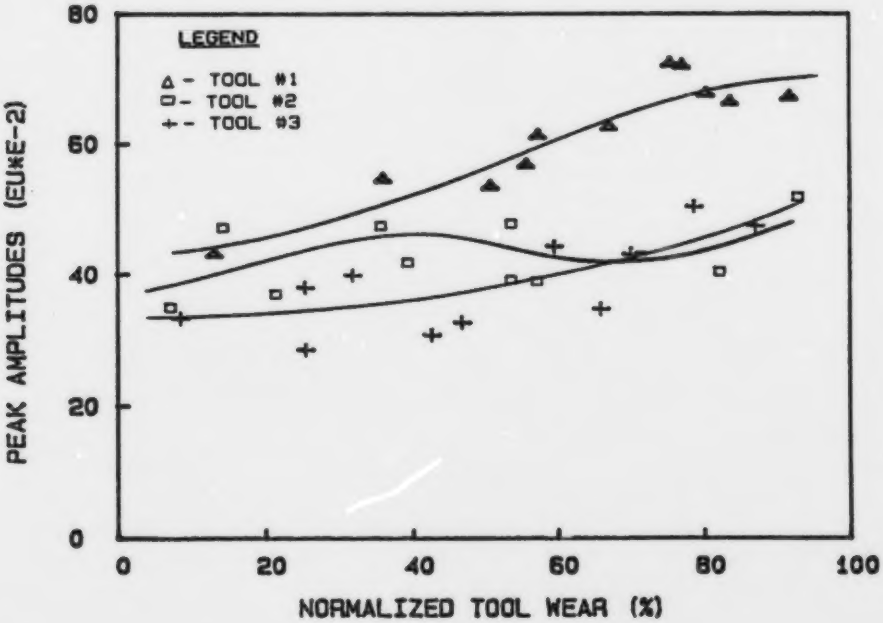

Fig. 2. Acceleration Levels in Major Frequency Bandwidth

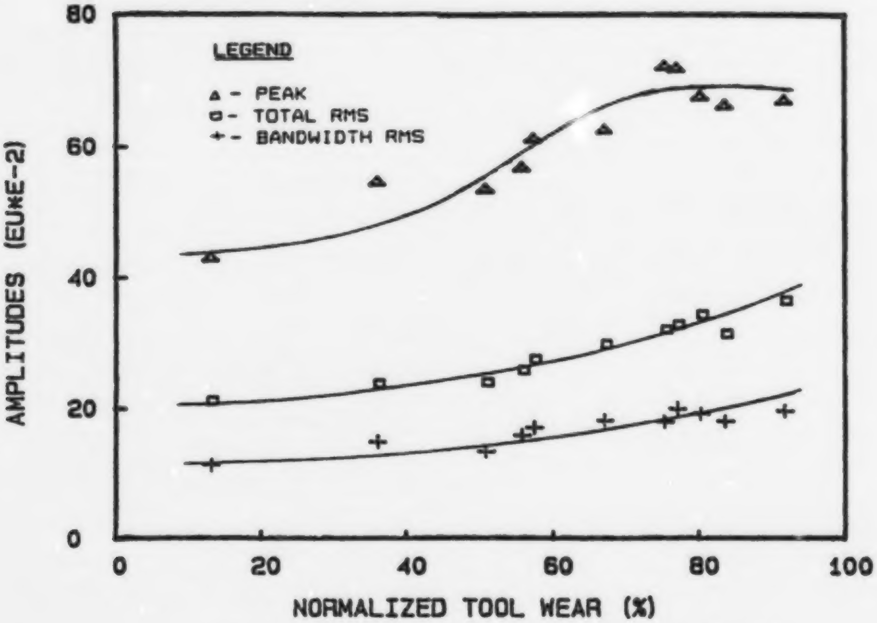

Fig. 3. Variation of Acceleration Levels with Normalised Tool Wear

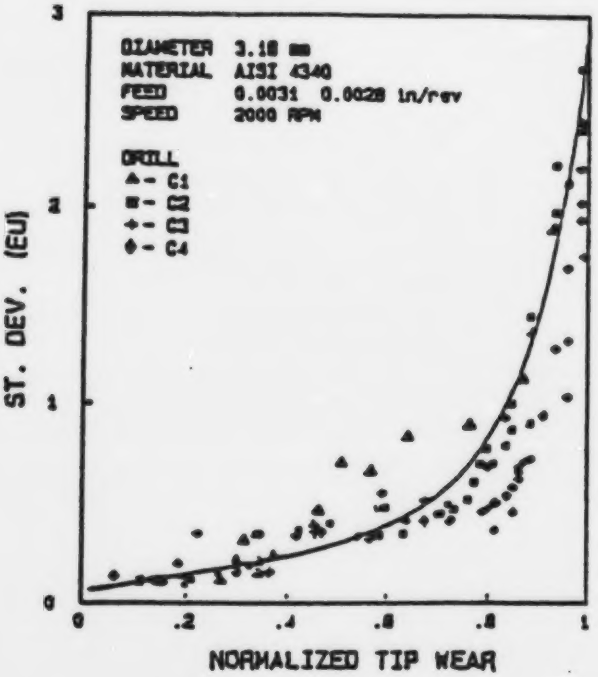

Fig. 4. Variation of Standard Deviation with Drill Wear

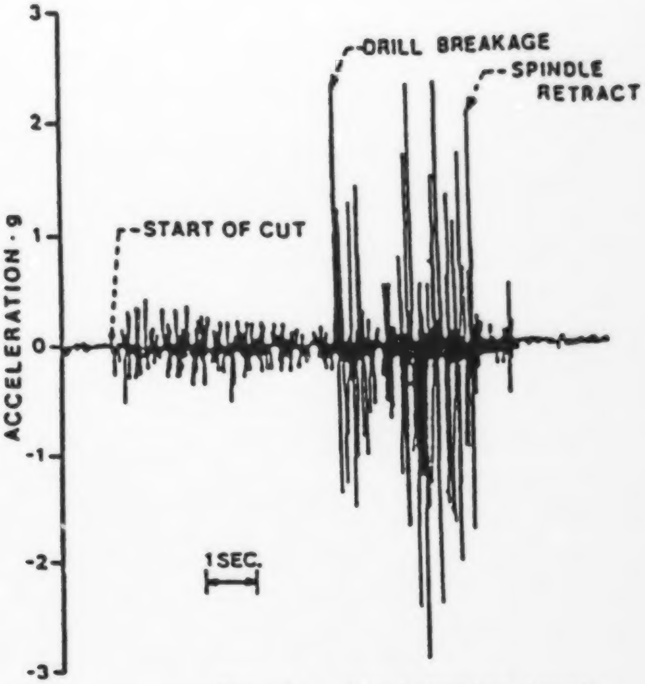

Fig. 5. Acceleration Levels for Drill Breakage

AUTHOR INDEX

INDEX DES AUTEURS

PAGE

Alavi, B. 247
Amini, A. 15

Bayly, D.A. 150

Cantrell, C. 190
Chapman, M.A. 150
Craggs, A. 48, 64
Czompo, J. 150

Dubé, F. 278

Eckert, W.F. 48
Eshleman, R.L. 40

Gibbs, J.R. 150

Hancock, R.C. 133
Howes, B.C. 56

Jardine, A.K.S. 99

Keim, M. 201

Loewen, T. 110
Lund, J.W. 3

MacPhail, C.A. 223
Mailloux, M. 291
Martell, H.E. 150
Masterson, S.G. 56
Maxwell, A.S. 265
Mugford, S.J. 150

Nordmann, R. 201

Osman, M.M. 247

Perricone, F. 110
Prsa, S. 291

Reif, Z. 291
Reilly, R.S. 223

Sabin, S.J. 176
Sankar, T.S. 15
Schwarz, K. P. 150

Taylor, A.G. 64
Teskey, W.F. 150

MACHINERY DYNAMICS SUBCOMMITTEE
MEMBERSHIP PROFILE

PROFIL DES MEMBRES DU
SOUS-COMITÉ DE LA DYNAMIQUE DES MACHINES

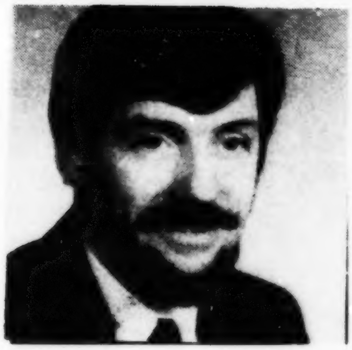

Chairman/Président

Professor Robert J. Rogers
Department of Mechanical Engineering
University of New Brunswick
Fredericton, New Brunswick
E3B 5A3

Telephone: (506) 453-4513
Fax: (506) 453-5025

Bob Rogers has been a member of the MDSC since 1981 and was elected chairman in 1988. As a mechanical engineering professor at the University of New Brunswick since 1977, Bob has taught courses in kinematics, dynamics, machine design, finite elements and vibration analysis. Besides his research into heat-exchanger tube vibration and impact, Bob has a keen interest in machinery vibration. In 1980 he did a machinery vibration survey for the Canadian Electrical Association. Bob Rogers and Paul Kim recently completed the MDSC educational and industrial surveys. Bob is currently building a geared torsional vibration apparatus which will be modelled using a finite element program.

Secretary/Secrétaire

Dr. Paul Y. Kim
Tribology and Mechanics Laboratory
Institute for Mechanical Engineering
National Research Council Canada
3650 Wesbrook Mall
Vancouver, BC
V6S 2L2

Telephone: (604) 666-1053
Fax: (604) 666-7203
Telex: 04-55141

Paul Y. Kim is a research officer at the Tribology and Mechanics Laboratory, Institute for Mechanical Engineering, National Research Council, Vancouver, Canada. He is secretary and a member of the Machinery Dynamics Subcommittee, and is engaged in research in Machinery Dynamics including rotor dynamics, machinery health monitoring, and flexible rotor balancing. Paul Kim and Bob Rogers are conducting MDSC's nation-wide survey on Machinery Dynamics Activities at Canadian Universities, Colleges, and Industries. Eventually, this will be sought to be used as a part of basic data for recommendations for related national policies on Machinery Dynamics in Canada.

Mr. Yves Caron
Structures and Dynamics
Pratt & Whitney Canada Inc.
1000 Marie-Victorin
Longueuil, Québec
J4G 1A1

Telephone: (514) 677-9411
ext. 7153
Fax: (514) 647-7652/3

Yves Caron works at Pratt & Whitney Canada where he supervises a group of specialists dealing with the dynamics of small gas turbine engines. His interests cover rotor dynamics, gear system vibrations, rotor balancing and the monitoring of engine vibrations. His activities include the development and application of new analytical methods and design criteria, vibration testing of engines, engine installations and development rigs. He currently manages a research program on rotor stability.

Dr. Anthony Craggs
Department of Mechanical Engineering
University of Alberta
Edmonton, Alberta
T6G 2G8

Telephone: (403) 492-4517
Fax: (403) 492-2200

Dr. Anthony Craggs received his Ph.D. degree from the Institute of Sound and Vibration Research, University of Southampton in 1969. Presently a Professor of Mechanical Engineering at the University of Alberta, where he teaches in Machine Dynamics and Acoustics. His current interests are in the fields of computer modelling and in particular with the application of the finite element method to shaft dynamics and duct acoustics. Most recently a major project has been completed in which a computer program was developed for modelling large generator sets as an aid to their balancing. Presently his work is proceeding on methods of refining the computer model to give better agreement with test data.

Mr. Brian Howes
Beta Machinery Analysis Limited
1615 - 10th Avenue SW, Suite 300
Calgary, Alberta
T3C 0J5

Telephone: (403) 245-5666
Fax: (403) 245-3257

Mr. Brian Howes is Chief Engineer, involved with training and field troubleshooting of machinery problems throughout North America.

Current company activities include analysis of piping systems, balance sensitivity testing on large electric motors, failure analysis and re-design of a gearbox, startup checks on large reciprocating compressor installations, and field analysis at startup of large industrial gas turbines

Mr. A. Stewart Maxwell
Ontario Hydro, A8H2
700 University Avenue
Toronto, Ontario
M5G 1X5

Telephone: (416) 592-4267
Fax: (416) 592-7066

Stewart Maxwell is Technical Superintendent of Machine Dynamics in Ontario Hydro's Central Production Services Division. With over 25 years experience in the field of vibration analysis and balancing, his current major area of responsibility is the provision of services to nuclear and thermal generating stations in the diagnosis and control of vibration in rotating equipment. He is a registered Professional Engineer in the Province of Ontario, a Director of the Vibration Institute, Deputy Chairman of the Machinery Dynamics Sub-committee, and Chairman of the Canadian Advisory Committee to the ISO (International Standards Organization) on Vibration of Machines.

Dr. Tom Moore
Department of Mechanical Engineering
Queen's University
Kingston, Ontario
K7L 3N6

Telephone:	(613) 545-2582
Fax:	(613) 545-6300

Dr. Tom Moore is an Associate Professor of Mechanical Engineering at Queen's University, Kingston. Dr. Moore's research interests include the development of diagnostic techniques for use in automated, predictive maintenance systems; the analysis, prediction, and reduction of machine tool cutting noise; and the dynamic analysis of machine structures using experimental modal analysis techniques.

Mr. Stephen Rowland
Hymac Limited
2995 Le Corbusier
Laval, Québec
H7L 3M3

Telephone:	(514) 337-4750
Fax:	(514) 687-4774

RESUME NOT AVAILABLE

Mr. Harindra D. Samarasekera
Toyo Pumps North America Corporation
171 West Esplanade, Suite 200
North Vancouver, BC
V7M 1A1

Telephone:	(604) 988-7187
Fax:	(604) 988-2493

Mr. Harindra Samarasekera is presently Chief Engineer at Toyo Pumps North America Corporation. Prior to the present appointment he was the Chief Mechanical Engineer at Bingham International Inc., a technically advanced manufacturer of pumps. Before his tenure at Bingham, he was employed as a Rotating Equipment Engineer in a petroleum refinery. During the last two years, he has also been a consultant to Trans Mountain Pipe Line Ltd. Mr. Samarasekera has extensive experience and knowledge of pumps and pumping systems. He has gained this experience in the past seventeen years working as a Designer, Consultant and a Trouble Shooter. Mr. Samarasekera has published several papers on the subject of pumps, specifically on Vibrations, Cavitation and Pressure Pulsations. He has a Masters degree and a Bachelors degree in Mechanical Engineering. He is also a Professional Engineer of the province of British Columbia and a member of ASME and CSME. Mr. Samarasekera has been a member of the Machinery Dynamics Sub-committee since 1983.

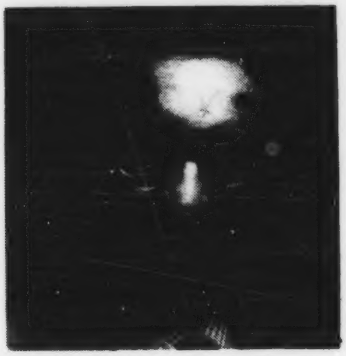

Dr. T.S. Sankar
Department of Mechanical Engineering
Concordia University
1455 de Maisonneuve West
Montréal, Québec
H3G 1M8

Telephone:	(514) 848-3130
Fax:	(514) 848-3494

Dr. T.S. Sankar is a full Professor in the Department of Mechanical Engineering at Concordia University and was the Chairman of the Department during 1976-1987. Dr. Sankar is internationally recognized for his research in the area of mechanical systems with special emphasis on dynamics, reliability, vibrations, robotics, and composite materials. He holds major research grants from the Governments of Canada and Quebec, as well as numerous industrial grants and contracts. He has supervised 26 M.Eng. and 10 Ph.D. these and has authored over 250 scientific papers in referred journals and major conferences. Presently the Senior Vice President of the Canadian Society of Mechanical Engineering, he holds executive positions in many learned societies including the ASME technical committees and the commissions of the International Federation for the Theory of Machines and Mechanisms. He was the past Chairman of the Machinery Dynamics Sub-committee during 1984 to 1987.

Alternate for/Suppléant de
T.S. Sankar

Dr. Rama B. Bhat
Department of Mechanical Engineering
Concordia University
1455 de Maisonneuve West
Montréal, Québec
H3G 1M8

Telephone: (514) 848-3137

Dr. Rama B. Bhat is a Professor of Mechanical Engineering at Concordia University. His research interests are in Rotor Dynamics, Random Vibrations, Modal Testing and Structural Acoustics. He has been a consultant to SPAR Aerospace Ltd., in the area of Structural Acoustics. He is an alternate member of the Canadian Machinery Dynamics Sub-committee of the National Research Council Canada. His work on "Programming Structured Synthesis System" won him a NASA Award for creative development and technical innovation. His research on vibration of beams and plates using beam characteristic orthogonal pollynomials developed by him, have been singled out to be an original and unique contribution.

Alternate for/Suppléant de
A.S. Maxwell

Dr. Moustafa M. Osman
Mechanical & Equipment Engineering Department
Ontario Hydro, H13
700 University Avenue
Toronto, Ontario
M5G 1X6

Telephone: (416) 592-4988
Fax: (416) 592-2009

As a senior Design Specialist, Dr. Moustafa M. Osman's current activities/interests are : Trouble shooting of vibration and noise problems for heavy equipment, especially centrifugal pumps (horizontal and vertical) and combustion turbines. Industrial noise control in the work place and the environment. Determination of *in-situ* equipment vibration limits for commissioning and monitoring purposes. Predictions for rotor dynamic behaviour using computer software, e.g. unbalance response, critical speeds, stability. Active cancellation of noise and vibration in industrial environment.

Alternate for/Suppléant de
B. Howes

Mr. D.N. Schuh
1615 - 10th Avenue SW
Suite 300
Calgary, Alberta
T3C 0J5

Telephone:	(403) 245-5666
Fax:	(403) 245-3257

Mr. Schuh is the President of Beta Machinery Analysis Ltd., with new product and services development as one of his major technical roles.

Development of new techniques to inspect reciprocating engines and compressors without disassembly is a current major effort.

Current company activities include analysis of piping systems, balance sensitivity testing on large electric motors, failure analysis and re-design of a gearbox, startup checks on large reciprocating compressor installations. And field analysis at startup of large industrial gas turbines.